EINDHOVEN UNIVERSITY OF TECHNOLOGY

Dendrimers in action : structure, dynamics and functionalization of poly(propylene imine) dendrimers

Citation for published version (APA):
Bosman, A. W. (1999). *Dendrimers in action : structure, dynamics and functionalization of poly(propylene imine) dendrimers*. [Phd Thesis 1 (Research TU/e / Graduation TU/e), Chemical Engineering and Chemistry]. Technische Universiteit Eindhoven. https://doi.org/10.6100/IR523548

DOI:
10.6100/IR523548

Document status and date:
Published: 01/01/1999

Document Version:
Publisher's PDF, also known as Version of Record (includes final page, issue and volume numbers)

Please check the document version of this publication:

• A submitted manuscript is the version of the article upon submission and before peer-review. There can be important differences between the submitted version and the official published version of record. People interested in the research are advised to contact the author for the final version of the publication, or visit the DOI to the publisher's website.
• The final author version and the galley proof are versions of the publication after peer review.
• The final published version features the final layout of the paper including the volume, issue and page numbers.

Link to publication

General rights
Copyright and moral rights for the publications made accessible in the public portal are retained by the authors and/or other copyright owners and it is a condition of accessing publications that users recognise and abide by the legal requirements associated with these rights.

• Users may download and print one copy of any publication from the public portal for the purpose of private study or research.
• You may not further distribute the material or use it for any profit-making activity or commercial gain
• You may freely distribute the URL identifying the publication in the public portal.

If the publication is distributed under the terms of Article 25fa of the Dutch Copyright Act, indicated by the "Taverne" license above, please follow below link for the End User Agreement:

www.tue.nl/taverne

Take down policy
If you believe that this document breaches copyright please contact us at:

openaccess@tue.nl

providing details and we will investigate your claim.

Download date: 04. Oct. 2023

Dendrimers in Action

Structure Dynamics and Functionalization of Poly(propylene imine) Dendrimers

Tonny Bosman

Dendrimers in Action

Structure, Dynamics, and Functionalization of
Poly(propylene imine) Dendrimers

Dendrimers in Action

Structure, Dynamics, and Functionalization of Poly(propylene imine) Dendrimers

PROEFSCHRIFT

ter verkrijging van de graad van doctor aan de Technische Universiteit Eindhoven, op gezag van de Rector Magnificus, prof.dr. M. Rem, voor een commissie aangewezen door het College voor Promoties in het openbaar te verdedigen op vrijdag 18 juni 1999 om 16.00 uur

door

Anton Willem Bosman

geboren te Nijmegen

Dit proefschrift is goedgekeurd door de promotoren:

prof.dr. E.W. Meijer
en
prof.dr. D.A. Tomalia

Copromotor:
dr.ir. R.A.J. Janssen

This research has been financially supported by the Council for Chemical Sciences of the Netherlands Organization for Scientific Research (CW-NWO).

Cover design: Tonny Bosman, Ben Mobach

Druk: Universiteitsdrukkerij, Technische Universiteit Eindhoven.

CIP-DATA LIBRARY TECHNISCHE UNIVERSITEIT EINDHOVEN

Bosman, Anton W.

Dendrimers in action: structure, dynamics and functionalization of poly(propylene imine) dendrimers / by Anton W. Bosman.- Eindhoven: Technische Universiteit Eindhoven, 1999
Proefschrift. - ISBN 90-386-2561-8
NUGI 813
Trefwoorden: dendrimeren / supramoleculaire structuren / nanostructuren
Subject headings: dendrimers / supramolecular structures / nanostructures

die Chemie allein macht es nicht...

H. Ringsdorf

Ik schrijf mijn eigen lied...

A. Hazes

in *"Zij gelooft in mij"*

Aan mijn ouders

Voor Anke

Table of Contents

Chapter 1 About Dendrimers **1**

1.1 Introduction 2
1.2 The Purity of Dendrimers 2
1.3 The Physical Behavior of Dendritic Molecules 6
1.3.1 Localization of End Groups in Dendrimers 6
1.3.2 Dendrimers versus Linear Macromolecules 12
1.3.3 Lower versus Higher Generation Dendrimers 14
1.3.4 The Behavior of Dendrimers on Surfaces and in Amphiphilic Materials 16
1.4 Aim and Scope of the Thesis 21
1.5 References and Notes 23

Chapter 2 Soft-Core Dense-Shell Dendrimers **29**

2.1 Introduction 30
2.2 Topological Trapping of Functionalities in the Dendritic Box 31
2.2.1 Charge Transfer with the Dendritic Box 31
2.2.2 Photosensitizer in the Dendritic Box 35
2.2.3 Concluding Remarks 40
2.3 Perforated Dendritic Box 40
2.3.1 Preparation of DAB-*dendr*-(NH-*t*-BOC-Gly)$_n$ 41
2.3.2 Hydrogen Bonding in Solid State 43
2.3.3 Hydrogen Bonding in Solution 44
2.3.4 Host–Guest Interactions of DAB-*dendr*-(NH-*t*-BOC-Gly)$_{64}$ versus DAB-*dendr*-(NH-*t*-BOC-L-Phe)$_{64}$ 46
2.3.5 Concluding Remarks 48
2.4 Overall Conclusions 49
2.5 Experimental Section 50
2.6 References and Notes 53

Chapter 3 Nitroxyl-Functionalized Dendrimers **57**

3.1 Introduction 58
3.2 Synthesis 59
3.3 EPR Spectroscopy 61
3.4 IR Spectroscopy 67
3.5 Influence of Spacer Length on Biradicals 69
3.6 Conclusion 71
3.7 Experimental Section 72
3.8 References and Notes 73

Chapter 4 Metallodendrimers **77**

4.1 Introduction 78
4.2 Poly(propylene imine) Dendrimers as Polyvalent Ligands 80
4.2.1 Cu(II)-complexes 80
4.2.2 Zn(II)-complexes 86
4.2.3 Ni(II)-complexes 86
4.3 Catalysis 88
4.3.1 Azide-binding by Cu(II)-dendrimers 88
4.3.2 Ester Hydrolysis with Zn(II)-dendrimers 89
4.4 Separation based on Nanoscopic Size 91
4.4.1 Nanofiltration 92
4.4.2 Metal Absorption 93
4.4.3 Reversible Azide-Binding 95
4.4.4 Ester Hydrolysis in Membrane Reactor 96
4.5 Conclusions 98
4.6 Experimental Section 98
4.7 References and Notes 100

Chapter 5 Biomimicry with Dendrimers **105**

5.1 Introduction 106
5.2 Multi-Copper Hemocyanine Model 107
5.2.1 Synthesis and Metal-Binding Properties DAB-*dendr*-$(PY2)_n$ 108
5.2.2 Binding of Cu(I) and O_2 by DAB-*dendr*-$(PY2)_{32}$. 112
5.2.3 Concluding Remarks 114
5.3 Non-Covalent and Covalent Dendritic Multi-Porphyrin Arrays 114
5.3.1 Non-Covalent Multi-Porphyrin Assemblies 115
5.3.2 Covalent Multi-Porphyrin Assemblies 119
5.3.3 Concluding Remarks 123
5.4 Conclusions 123
5.5 Experimental Section 125
5.6 References and Notes 129

Summary **133**

Samenvatting **135**

Curriculum Vitae **137**

List of Publications **139**

Dankwoord **141**

About Dendrimers*

1

Abstract: *The esthetically appealing structures of dendrimers have attracted the interest from many different disciplines of science. In this chapter the literature on some controversial issues in dendrimer research is reviewed, aiming at an enhanced insight into the purity of dendrimers and their conformational behavior. The translation of dendrimer properties into functional materials, is the scope of the subsequent chapters.*

* Part of this work has been published: Bosman, A. W.; Janssen, H. M.; Meijer, E. W. *Chem. Rev.* **1999**, *99*, xxxx.

1.1 Introduction

Ideally, dendrimers are perfect monodisperse macromolecules with a regular and highly branched three-dimensional architecture. Dendrimers are produced in an iterative sequence of reaction steps, in which each additional iteration leads to a higher generation material. The first example of an iterative synthetic procedure towards well-defined branched structures has been reported by Vögtle,[1] who named this procedure a "cascade synthesis". A few years later, in the early 1980s, Denkewalter patented the synthesis of L-lysine-based dendrimers.[2] The patents describe structures up to high generations, however, except for size exclusion chromatography (SEC) data,[3] no detailed characteristics of the materials are given.

The first dendritic structures that have been thoroughly investigated and that have received widespread attention are Tomalia's PAMAM dendrimers[4] and Newkome's "arborol" systems.[5] Both dendrimers are constructed divergently, implying that the synthesis is started with a multifunctional core molecule and is elaborated to the periphery. At a later date and on the basis of the original work of Vögtle,[1] divergently produced poly(propylene imine) dendrimers have been reported by Mülhaupt[6] and de Brabander.[7] Today, these poly(propylene imine) dendrimers are commercially available. In 1990, Fréchet introduced the convergent approach towards dendrimers.[8] In convergent procedures, the synthesis is started at the periphery and elaborated to the core. Fréchet's aromatic polyether dendrimers are easily accessible and have been studied frequently, not only by the Fréchet group but also by other researchers. Finally, Moore's convergently produced phenylacetylene dendrimers[9-11] are the last of the five classes of dendrimers, reported up to high generations, that are studied in detail and most known. Additionally, many other types of interesting, valuable, and esthetically pleasing dendritic systems have been developed,[12] and thus, a variety of dendritic scaffolds has become accessible with defined nanoscopic dimensions and discrete numbers of functional end groups.

Many of the intriguing properties of dendrimers as well as their syntheses and possible applications are discussed in excellent books and reviews that have been published by various experts in the field.[12-19] In this chapter, studies are highlighted that contribute to a better understanding of the properties of dendrimers and studies that offer insight into the possibilities for and the limitations of the use of dendritic materials. Some of these studies relate to three somewhat controversial issues. First, one can question the perfection of higher generation dendrimers. In the divergent synthetic approach, for example, several hundred reaction steps have to be conducted on the same molecular fragment to obtain higher generation species. Second, the conformational behavior of dendrimers is an issue of debate, giving rise to the following

questions: Are the end groups in dendrimers pointing outward or are they severely backfolded? Do dendrimers always have a globular shape or can this shape be highly distorted? Are cavities present inside the dendrimer? Is it possible to obtain site isolation in the core? How do the physical properties of dendrimers change at higher generations and how do these physical properties relate to those of linear analogues?

1.2 The Purity of Dendrimers

Two conceptually different synthetic approaches for the construction of high-generation dendrimers exist: the divergent approach and the convergent approach. Both approaches consist of a repetition of reaction steps, each repetition accounting for the creation of an additional generation. The two methodologies have their own characteristics, and therefore, the perfection of the final dendritic product is related to this synthetic approach.

In the divergent synthesis, the dendrimer is grown in a stepwise manner from a central core, implying that numerous reactions have to be performed on a single molecule. Consequently, every reaction has to be very selective to ensure the integrity of the final product. For example, an average selectivity of 99.5% per reaction will, in the case of the synthesis of the fifth generation poly(propylene imine) dendrimer (64 amine end groups; 248 reactions, see Scheme 1.1), only result in $0.995^{248} = 29\%$ of defect-free dendrimer. Since every new generation of divergently produced dendrimer can hardly be purified, the presence of a small number of statistical defects cannot be avoided. Bearing this in mind, the divergent synthesis can be seen as the "macromolecular approach" towards dendrimers: the purity of the dendrimers is governed by statistics. The reality of statistical defect structures is also recognized in the iterative synthesis of polypeptides or polynucleotides on a solid support (the Merrifield synthesis),[20] so the knowledge gathered in this field should be considered when the perfection of dendritic structures is discussed.

In the convergent approach, the difficulty of many reactions that have to be performed on one molecule has been overcome by starting the synthesis of these dendrimers from the periphery and ending it at the core. In this fashion, a constant and low number of reaction sites is warranted in every reaction step throughout the synthesis. As a consequence, only a small number of side products can be formed in each reaction, and therefore, every new generation can be purified (although the purification of higher generation materials becomes increasingly troublesome). Thus, convergently produced dendrimers, which can be seen as dendrimers prepared in an "organic-chemistry approach", can be defect-free.

The characterization of dendrimers is rather complex due to the size and symmetry of these macromolecules. Various NMR techniques (^{1}H, ^{13}C, ^{15}N, ^{31}P), elemental analyses, and chromatography techniques (HPLC, SEC) are widely used, but these techniques cannot reveal small amounts of impurities in, especially, higher generation dendrimers.[21] Fortunately, recent progress in ESI (electrospray ionization) and MALDI (matrix-assisted laser desorption ionization) mass spectrometry allows for an in-depth analysis of dendrimers. ESI-MS has been used to identify the imperfections in both poly(propylene imine)[22] and poly(amidoamine) dendrimers (PAMAM).[23] Both of these dendrimer types are made via a divergent synthesis and are very suitable for electrospray ionization due to their polar and basic nature.

All generations of poly(propylene imine) dendrimers with either amine or nitrile end groups have been analyzed with ESI-MS to quantitatively determine the importance of various side reactions.[22] In the approach followed, all possible side reactions have been grouped in two different pathways that describe the formation of defect structures on going from one amine generation to the next (Scheme 1.1). One pathway accounts for incomplete cyanoethylations and retro-Michael reactions, the other pathway accounts for intramolecular amine formations (cyclizations).[24] With the ESI-MS spectra of all five generation poly(propylene imine) dendrimers at hand, the significance of both pathways has been calculated using an iterative computing process. Thus, every MS spectrum has been simulated. The simulation indicates a polydispersity (M_w/M_n) of 1.002 and a dendritic purity of ca. 23% for the fifth generation poly(propylene imine) dendrimer. Since the perfect structure is the dominant species in the final product, it seems more appropriate to discuss the mixture in terms of dendritic purity than in terms of polydispersity (the dendritic purity is defined as the percentage of dendritic material that is defect-free).

ESI-MS studies on PAMAM dendrimers indicate defect structures arising from retro-Michael additions and intramolecular lactam formations (Scheme 1.2).[23] For a fourth generation PAMAM dendrimer (48 end groups), a polydispersity of 1.0007 has been reported.[23]

MALDI-MS studies on other divergently produced higher generation dendrimers (i.e., Newkome-type dendrimers[25–27] and carbosilanes[28–31]) have also shown the presence of small numbers of imperfect structures. Metallodendrimers that have been studied with L-SIMS,[32] MALDI-MS,[33] and ESI-MS[34,35] are of lower generations, and consequently, these materials hardly contain defect structures, even though these materials have been produced in a divergent approach.

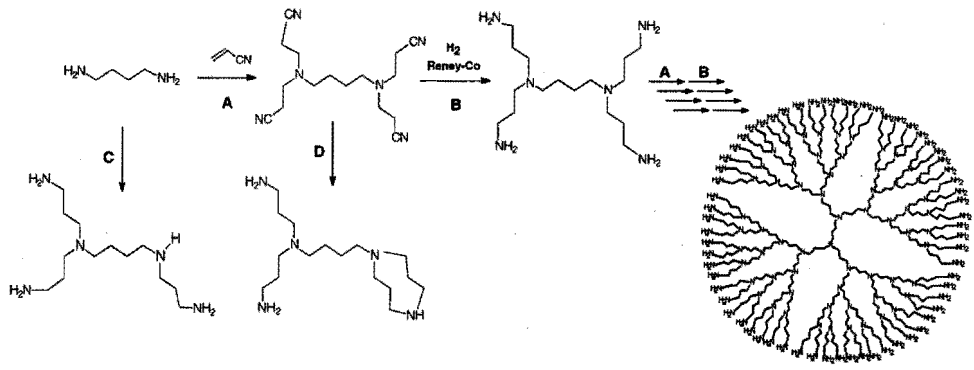

Scheme 1.1: *The synthesis of poly(propylene imine) dendrimers (reactions A and B) and alternative, unwanted reaction paths C and D. Path C illustrates "missed" Michael additions (either by an incomplete cyanoethylation or by a retro-Michael reaction). Path D illustrates unwanted cyclization reactions. Paths C and D describe defect reactions on going from one amine generation to the next.*[22]

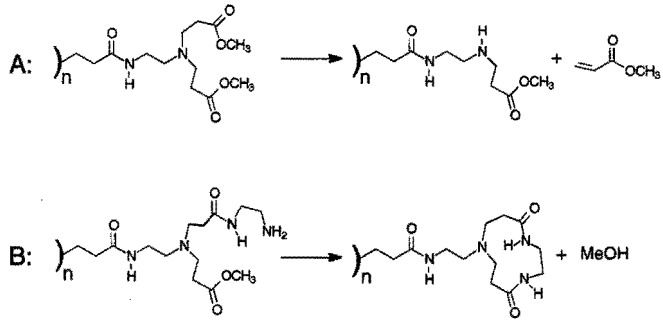

Scheme 1.2: *Unwanted reactions in the PAMAM-synthesis: retro-Michael reactions (A) and lactam formations (B).* [23]

Dendrimers synthesized via the convergent approach can be produced nearly pure, as confirmed by MS data. MALDI mass spectra of Fréchet-type dendrimers display very limited amounts of impurities.[36] Moore's phenylacetylene dendrimers have also been investigated with MALDI-MS.[37] For a dendrimer with a mass of 39 969 D, almost no impurities have been detected.[10] ESI-MS data on carboxylate-terminated phenylacetylene dendrimers subscribe the high degree of purity that can be attained for these dendrimers.[22]

The detailed mass studies that have been devoted to the characterization of dendrimers indicate the most important difference between both synthetic methodologies at hand. The "polymeric nature" of the divergent approach results in an accumulating number of statistical defect structures for every next generation. The

defects are the result of the many reactions that have to be performed on the same molecular fragment. Furthermore, almost no possibilities exist for the purification of intermediate generations. The exponential growth in the number of reactions to be performed on higher generations, makes it virtually impossible to produce perfect dendrimers of generations beyond five or six. For instance, the average selectivity of 99.5% per reaction leads to a dendritic purity of 29% for a fifth generation poly(propylene imine) dendrimer and yields purities of 0.995^{504} = 8.0% for the sixth generation and only 0.995^{1016} = 0.6% for the seventh generation. Virtually no perfect structures will be present in even higher generation materials. The "organic nature" of the convergent approach results in defect-free dendrimers due to the limited number of reactions performed on the same molecule on going from one generation to the next. Additionally, it is possible to purify intermediate generations.

The—in the end—small differences in structural features of the divergently produced structures on one hand and the convergently synthesized structures on the other are not expressed in differences in overall properties of these two classes of dendrimers (for example, all investigated dendrimers show a maximum in the intrinsic viscosity as a function of their molecular weight). Therefore, dendrimers, regardless the way in which they have been prepared, can indeed be considered as the synthetic macromolecules with the most defined or most perfect primary structure known today.[13]

1.3 The Physical Behavior of Dendritic Molecules

On paper, dendrimers are usually drawn in a highly symmetrical fashion. The molecular structure is displayed with all tiers—having the characteristic algorithmic growth pattern—pointing outward, the end groups are invariably located at the surface, and the overall picture suggests that the dendrimer is a spherical entity. Of course, the typical architecture of a dendrimer has consequences for its physical behavior and logically research in the last decade has sought to reveal the true nature of dendrimers, not only regarding their appearance but also regarding their physical characteristics.

The first part (1.3.1) in this section deals with the studies on the localization of the end groups in dendritic systems. Such studies are of relevance since many of the proposed uses of dendrimers rely on the availability of the large amount of neighboring end groups (for modification, as active ligands, etc.). Related topics concern the density profiles in dendrimers and the limits of perfect dendrimer growth, and these subjects are also addressed. Further key issues in this section relate to the deviating properties of dendrimers as compared to their linear macromolecular counterparts (1.3.2) and encompass the transition in physical properties when a sequence of dendrimer generations is considered (1.3.3). Finally, numerous studies have dealt with amphiphilic

dendrimers and with the behavior of dendrimers on solid or fluid surfaces (1.3.4). These studies have revealed unexpected conformational features of dendritic molecules.

1.3.1 Localization of End Groups in Dendrimers

Theoretical Calculations. One of the first reports in which the position of end groups in dendrimers is considered, has been published by de Gennes and Hervet.[38] The authors have used a self-consistent field model in which the monomers of each generation are assumed to be fully elongated and in which the end groups of the dendrimer are grouped in concentric circles around the core. The model indicates that dendrimers can grow freely up to a certain—predictable—limiting generation. It also shows that the core of the dendritic molecule has the lowest density.

Numerical calculations using the kinetic growth model of Lescanec and Muthukumar predict a monotonic decrease in density on going from the center of the dendrimer to its periphery.[39] As a consequence, the ends of the branches are not positioned at the surface but are severely backfolded. Qualitatively similar results have been obtained from Monte Carlo simulations that have been performed by Mansfield and Klushin.[40] A molecular dynamics (MD) study of Murat and Grest shows that the importance of backfolding of the chains increases with generation (moreover, this study has shown a strong correlation between the solvent polarity and the mean radius of gyration).[41] Finally, Boris and Rubinstein have used a self-consistent mean field model (SCMF) to describe flexible dendrimers. The model predicts that the density is the highest in the core and shows that the end groups are distributed throughout the volume of the dendrimer (Figure 1.1).[42]

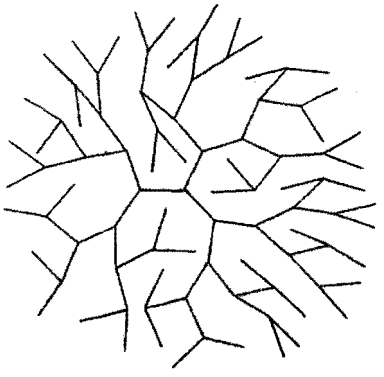

Figure 1.1: *Schematic representation of a backfolded trifunctional fifth generation dendrimer according to Boris and Rubinstein.*[42]

Studies on specific dendrimers have first been reported by Naylor et al., who have performed MD simulations on PAMAM dendrimers.[43] More detailed MD studies have been performed by Miklis et al.[44] and by Cavallo and Fraternali,[45] both on poly(propylene imine) dendrimers functionalized with *N-t*-BOC-L-phenylalanine. The investigation of Cavallo and Fraternali indicates that some backfolding of the terminal amino acids occurs, but not to such an extent that the dendrimer core is completely filled, resulting in a low-density region inside the higher generation dendrimers. In addition, the authors have found an increasing inter end group interaction on going from the first to the fifth generation.

MD studies on poly(propylene imine) dendrimers with amine end groups have recently been performed with two different force fields representing a good and a bad solvent.[46] Both force fields produce a certain degree of backfolding, being more pronounced for the force field representing a bad solvent. Monte Carlo simulations on dendritic polyelectrolytes by Welch and Muthukumar show a dramatic change in dendrimer conformation depending on the ionic strength of the solvent.[47] The investigated polyelectrolytes are topological analogues of poly(propylene imine) dendrimers. At high ionic strength, backfolding of the end groups takes place and a "dense core" dendritic structure is formed. At low ionic strength, the multiple charges in the dendrimer force the molecule to stretch out resulting in a "dense shell" structure (Figure 1.2).

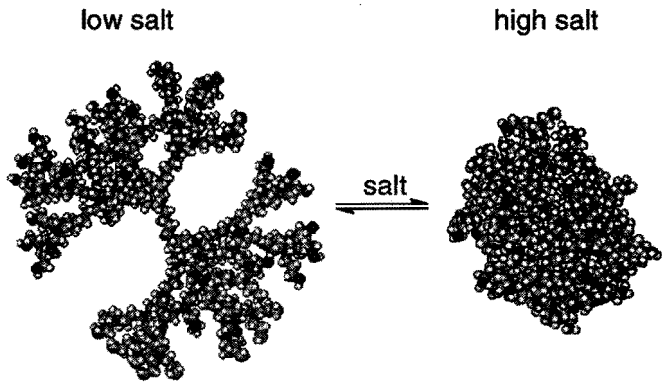

Figure 1.2: *The occurrence of a dense shell (left) or a dense core conformation (right) of poly(propylene imine)dendrimers is dependent on the ionic strength of the solution (picture kindly provided by B. Coussens, DSM, The Netherlands).*

Almost all aforementioned computational investigations predict backfolded branches in dendritic structures (the only exceptions being the study by de Gennes and Hervet and, to some extent, the work of Cavallo and Fraternali). Backfolding is an

important process in most models, because the conformation of the tiers is mainly determined by repulsive monomer–monomer excluded volume interactions and by the entropic energy penalty for the swelling of the dendrimer. In the next paragraph, experimental data will show that the importance of backfolding is dependent on the actual dendritic structure. Attractive secondary interactions between the end groups, for example, can effect the conformations of branches significantly, thereby notably reducing backfolding.

Experimental studies. The polyether dendrimers synthesized by Fréchet et al. (for a typical example see Figure 1.4 top) have been investigated in detail to establish the possibilities for backfolding in these molecules. One of the first studies by Mourey et al. uses an experimental set-up in which size exclusion chromatography is coupled to differential viscometry.[48] The hydrodynamic radii, calculated from the measured intrinsic viscosity, increase approximately linearly with the dendrimer generation. Additionally, a maximum in the intrinsic viscosity as a function of molecular weight is found. Both of these trends are in qualitative agreement with the model of Lescanec and Muthukumar,[39] implying that the end groups can be found throughout the dendrimer volume.

Rotational-echo double-resonance (REDOR) NMR studies on Fréchet-type dendrimers by Wooley et al. have shown that backfolding also takes place in the solid state.[49] The authors have found that the radial density for a fifth generation polyether dendrimer decreases monotonically with increasing distance from the center of mass. In addition, Gorman et al. have measured the spin lattice relaxation (T_1) in polyaryl ether dendrimers with a paramagnetic core.[50] The data reveal that the end groups are close to the core of the molecule. Recently, the hydrodynamic volumes of Fréchet-type dendrimers with rubicene cores have been determined by fluorescence depolarization measurements.[51] Qualitatively, this study has given the same results as those obtained by Mourey et al. (i.e., the end groups are backfolded).[48] In addition, the study has indicated that the hydrodynamic volume of the investigated dendrimers appears to be temperature independent, whereas this volume is strongly influenced by the solvent. The dendrimers are collapsed in poor solvents, while in a theta-solvent a more open dendritic structure exists.[51]

The previous examples of polyaryl ether dendrimers are built up from flexible non-interacting units. Percec et al. have produced polyaryl ether dendrimers with pendant perfluorinated[52] or perhydrogenated[53] aliphatic chains. The dendrimers assemble in the solid state in such a way that segregation between the dendritic wedge and the end groups takes place. The segregation is apparent from X-ray diffraction data and transmission electron microscopy (TEM) measurements.[54] Recently, Stühn et al.

have observed similar phase separation phenomena in carbosilane dendrimers with perfluorohexyl groups on the periphery.[55] In contrast to the dendrimers with the noninteracting units discussed before, all these segregated systems do not exhibit backfolding.

The conformational behavior of PAMAM dendrimers has been studied with several techniques. SEC in combination with intrinsic viscosity measurements has been used to obtain the hydrodynamic radii of the PAMAM dendrimers.[13,56,57] The authors conclude that the acquired data are in agreement with the de Gennes model, i.e., the PAMAM dendrimers have a hollow core and a densely packed outer layer. ^{13}C NMR relaxation studies on PAMAM dendrimers by Meltzer et al. have indicated no dramatic change in chain dynamics up to the nineth generation.[58] The measurements show that chain motion is most rapid near the termini of the molecule and is slower in the interior. It has been concluded that the branches are backfolded to some extent to relieve the steric crowding on the dendritic surface. These conclusions have been confirmed in a subsequent ^{2}H NMR study by the same authors on various generation PAMAMs labeled with deuterium.[59] Small-angle X-ray scattering (SAXS) measurements on PAMAM dendrimers have not given clear-cut results.[60] For the higher generations (M_w > 50 000), the overall density appears to be independent of the generation. These data do not exclude any postulate: the terminal groups can reside on the dendrimer surface, but backfolded arrangements are also possible. Additional results from a small-angle neutron-scattering (SANS) study on a deuterium-labeled seventh generation PAMAM dendrimer indicate that the end groups are preferably positioned at the exterior of the molecule.[61]

End group modification of PAMAMs with naphthalenediimide anion radicals affords molecules that show strong π–π stacking interactions between the modified end groups.[62] The stacking is apparent from near-infrared spectroscopy measurements. Comparable results have recently been obtained with amido-ether dendrimers functionalized with oligothiophenes on the periphery.[63] In the case of these dendrimers, backfolding is presumably prohibited by intramoleculair end group interactions.

Various studies have been devoted to the hydrolyzed "half-generation" PAMAM dendrimers. These molecules have a poly(amido amine) dendritic core that is surrounded by a shell of carboxylate end groups (Figure 1.3 left). The picture of a unimolecular anionic micelle is supported by various photophysical measurements (data on pyrene fluorescence,[64] steady state $Ru(bpy)_3^{2+}$ quenching,[65] and dynamic $Ru(phen)_3^{2+}$ quenching[66] have been disclosed) and by ESR measurements (Cu(II),[67] nitroxides,[68] and Mn(II)[69] have been used as probe molecules). Unimolecular micellar systems based on dendrimers have also been reported by Newkome et al. Alkane[70] or polyamide[71] cores

and carboxylate or amine end groups have been employed. Both SEC and two dimensional diffusion-ordered NMR-spectroscopy (DOSY) have shown that the hydrodynamic radii of the polyamide dendrimers strongly depend on the pH of the solvent.

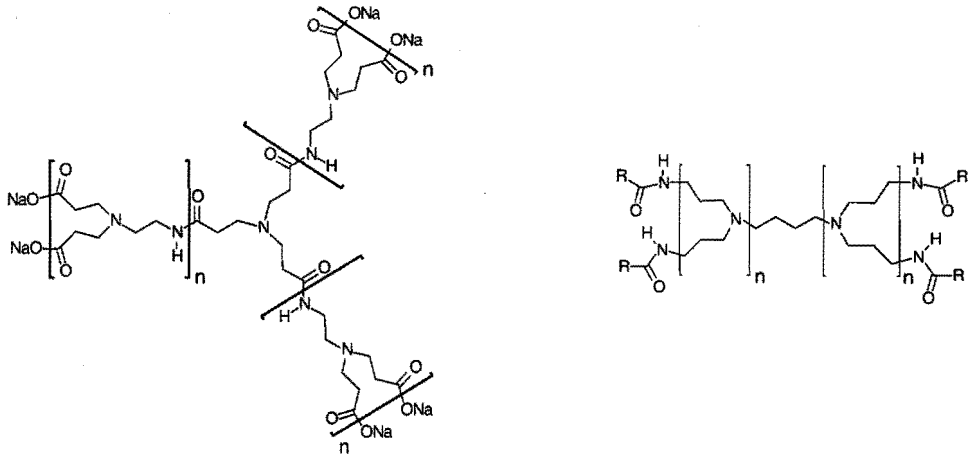

Figure 1.3: *Half-generation PAMAM dendrimer (left) and amide-functionalized poly(propylene imine) dendrimer (right); n denotes dendrimer generation.*

Scherrenberg et al. have recently investigated poly(propylene imine) dendrimers with both nitrile and amine end groups using viscosimetry and SANS measurements.[46] Independent of the nature of the end group or the solvent used, the authors have found a linear relationship between the radius of the dendrimer and its generation number. This linear dependency correlates with the results of the molecular dynamics study by Murat and Grest.[41] Hence, poly(propylene imine) dendrimers are flexible molecules with a relatively homogeneous density distribution, implying that the end groups must be backfolded to some degree. Another SANS study on amine terminated poly(propylene imine) dendrimers has shown that the molecules tend to stretch when the amines are protonated.[72] These data reflect and confirm the flexible character of poly(propylene imine) dendrimers.

Various studies have been performed on poly(propylene imine) dendrimers that have been amidated (these materials are abbreviated by the formula DAB-*dendr*-(NHCO–R)$_n$; Figure 1.3, right).[73] The fifth generation poly(propylene imine) dendrimer modified with *N*-*t*-BOC protected phenylalanine, the so-called "dendritic box" (DAB-*dendr*-(NH-*t*-BOC-L-Phe)$_{64}$), has been shown to have a rigid shell consisting of *t*-BOC-protected amino acids.[74] The soft-interior hard-exterior configuration is confirmed by

spin lattice (T_1) and spin-spin (T_2) carbon relaxation measurements,[74] and by the absence of optical rotation in this system.[75,76] The rigidity of the shell is thought to originate from the many possibilities for intramolecular hydrogen bonding between the amides or the carbamates in the end groups.

Reviewing the cited reports, the localization of the end groups of dendrimers depends critically on the structure of the dendrimer in question. The flexible nature of most known dendrimers usually implies that the end groups are found throughout the dendrimer volume. Thus, the voids inside the dendrimer are filled up to a certain extent. However, when the end groups can communicate with each other via secondary interactions such as π–π interactions, electrostatic repulsions, hydrogen-bonding interactions or hydrophobic effects, the dendritic terminal units will assemble at the periphery, thereby precluding backfolding.

1.3.2 Dendrimers versus Linear Macromolecules

When dendrimers in solution are considered, the occupied volume of a single molecule increases cubically with generation, whereas its mass increases exponentially (assuming a spherical shape for the dendrimer). This typical "growth" pattern of dendritic molecules determines their solution properties and makes these properties deviate from those of linear molecules, especially at higher molecular weights. The intrinsic viscosity is a physical parameter for which such a deviation has been measured. In contrast to linear polymers (that obey the Mark–Houwink–Sakurada equation), the intrinsic viscosity of dendrimers is not increasing with molecular mass but reaches a maximum at a certain dendrimer generation (for polyaryl ether,[48] poly(propylene imine),[7] and PAMAM dendrimers,[13] these maxima have been reported).[77] Also in the solid state, the growth pattern of dendrimers determines their physical characteristics. In general, it is believed that a gradual transition in overall shape, from a more extended arrangement for lower generation dendrimers to a compact and approximate globular shape for higher generation dendrimers,[43] causes the deviation in physical behavior of dendrimers from those of linear macromolecules.

In the next part, various studies are surveyed in which the behavior of dendritic molecules is compared to the behavior of linear polymers or oligomers that are compositionally related. Until now, only one study has dealt with the comparison of dendrimers with their linear isomers, having exactly the same number of repeat units and end group functionalities.[78] This study by Hawker et al. is the only investigation in which the influence of molecular architecture on physical properties is addressed absolutely. The reason for the absence of more of such studies can be found in the

synthetic inaccessibility of the linear isomers (usually, the dendritic isomers can be produced far more easily).

Fréchet et al. have studied several physical properties of polyether and polyester dendrimers.[79] The increase in glass transition temperature (T_g) of the dendrimers levels off at higher molecular weights, a phenomenon that is also observed for the linear analogues. For linear polymers in general, a leveling off of the T_g increase has been known for a long time, and this effect is explained by the declining influence of the end groups and the role of the entanglement molecular weight. Dendrimers have more end groups at higher masses, but, as opposed to linear macromolecules, dendrimers are not significantly entangled. The absence of entanglements in the higher generation materials is described in a study on the melt viscosities of polyether dendrimers,[80] and a rheologic study on PAMAM dendrimers.[81] In another study by the same authors, it appears that the melt viscosity is a physical parameter that is very dependent on the type of end group in the dendrimer.[82]

Miller et al. have compared the solubilities of 1,3,5-phenylene-based dendrimers with those of oligo-*p*-phenylenes.[83] Although *m*-phenylenes would have been more appropriate linear analogues, the study shows that the dendrimers have an enhanced solubility. Similar results have been obtained by Fréchet et al. who have compared dendritic polyesters with their linear counterparts.[84] In contrast to the linear polyesters, the dendrimers are soluble in a vast range of organic solvents. The authors also note a marked difference in reactivity: the debenzylation of the polyesters via catalytic hydrogenation on Pd/C is only possible for the dendritic structures. Differences in solubility and reactivity have also been found between poly(propylene imine) dendrimers with nitrile end groups and poly(acrylonitrile). The nitrile dendrimers are soluble in various organic solvents, whereas their linear analogues are crystalline and only soluble in very polar solutes such as dimethylformamide and concentrated sulfuric acid. Due to this limited solubility, the catalytic hydrogenation of poly(acrylonitrile) is not possible, while dendritic polynitriles are easily hydrogenated.[7,85] For all these cases, the observed differences in solubility and reactivity have been attributed to the globular architecture of the dendrimers and the accessibility of the end groups of the dendrimer.

The uniqueness of dendritic architectures has been shown in an elegant study by Hawker et al. in which polyether dendrimers are compared with their linear isomers (Figure 1.4).[78] Especially the fifth and sixth generation dendrimers display differing features when compared to their structural isomers. The hydrodynamic volume of the fifth generation polyether dendrimer is approximately 30% smaller than that of its linear analogue. The difference is ascribed to a more compact—backfolded—globular structure of the dendrimer. In addition, the fifth generation dendrimer is completely

amorphous (a T_g of 42 °C is recorded) and is soluble in a variety of organic solvents, whereas the linear analogue is highly crystalline and poorly soluble in THF, acetone, and chloroform. The Hawker investigation solidly confirms that the physical behavior of dendrimers is different from that of linear polymers, and equally important, it shows that dendrimers need to have a certain size to display significantly different physical behavior. The next section concentrates on additional studies in which dendrimers of various generations have been compared.

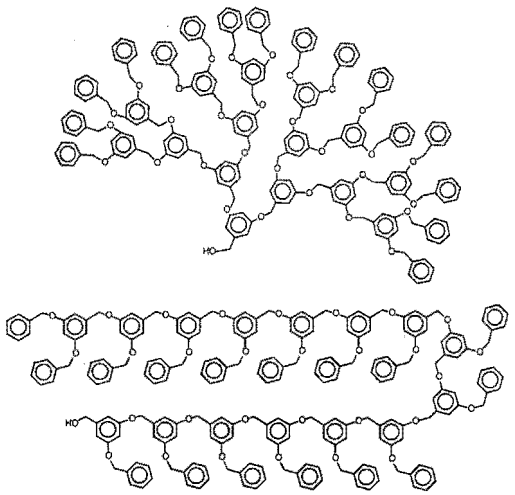

Figure 1.4: *The fourth generation polyaryl ether dendrimer (top) and its linear isomer (bottom).*[78]

1.3.3 Lower versus Higher Generation Dendrimers

As noted earlier, the intrinsic viscosity of dendrimer solutions drops at a certain generation number. The differences in physical behavior between low and high generation materials within a homologous sequence of dendrimers have been revealed in numerous other studies as well. Usually, photoactive probes have been used in these studies.

Fréchet et al. have attached the solvatochromic probe 4-(*N,N*-dimethyl)-1-nitrobenzene to the focal point of various generations of polyether wedges.[86] In low polarity solvents and on the basis of measured chromophoric shifts, a distinct transition in the polarity of the dendritic interior is observed on going from the third to the fourth generation. For the higher generations, the micro-environment of the chromophore is highly polar (comparable to the polarity of DMF as determined with the π^* scale[87]). The study indicates that the higher generation Fréchet dendrimers must have a closed and

compact structure in order to severely limit the influence of the solvent on the probe (i.e., the core environment). In contrast with the study by Fréchet, Zimmerman et al. have concluded that the polarity of the interior of a polyether dendrimer is either apolar or controlled by the solvent.[88] The authors have based this conclusion on hydrogen-bonding studies using a naphthyridine core. The discrepancy between both studies can be explained by the different physical parameters that have been considered (solvent polarizability versus H-bonding), by the different immediate surroundings of the probes, and by the fact that Zimmermann et al. have investigated four generations, whereas Fréchet has considered two additional bulkier generations.

Phenylacetylene dendrimers with a *p*-dimethoxybenzene moiety at the focal point have been made by Moore et al.[89] The maximum in fluorescence of a charge-transfer state in the dendrimer shows an anomalous shift for the fifth and sixth generation. Remarkably, a substantial shift in the fluorescence maximum can also be induced when pentane instead of hexane is used. Apparently, not only the solvent polarity but also the size and shape of solvent molecules are important factors in these kind of probe studies.

PAMAMs and poly(propylene imine) dendrimers also display transitions in their physical behavior when a sequence of generations is considered. Investigations on saponificated half-generation PAMAM dendrimers using various photophysical probes indicate a transition in dendrimer appearance on going from generation 3.5 to 4.5.[64,65] Spin relaxation data (T_1 and T_2 measurements) on a series of *N*-*t*-BOC-L-Phe-terminated poly(propylene imine) dendrimers[74] and hyper-Raleigh scattering (HRS) measurements on such dendrimers with 4-(dimethylamino)phenyl carboxamide end groups[90] show, in both cases, a transition in physical behavior around the fourth generation.

Spin relaxation data (T_1) of Fréchet-type dendrimers with porphyrin[91] or azobenzene cores[92] show a distinct transition between generation three and four, resulting in unique photophysical behavior for the higher generation materials. In the azobenzene systems, photoisomerization has been reported by using low energy photons (i.e., infrared irradiation), whereas in the porphyrin system a very efficient energy transfer from the dendron subunits to the porphyrin core takes place.

Poly(propylene imine) dendrimers of various generations have been grown from amine terminated polystyrene chains (PS–NH_2) with narrow molecular weight distributions.[93] Aggregation of these PS-*dendr*-$(NH_2)_x$ amphiphiles in water has been studied by various characterization techniques (monolayer experiments, pyrene probe fluorescence experiments, dynamic light scattering (DLS), conductivity and TEM measurements), showing that the morphology of the aggregates is determined by the

size (generation) of the dendritic head group. As the head group becomes more bulky, the aggregates change their shape from inverted micelles, to vesicles and rodlike structures, and finally to spherical micelles. These observations are in line with Israelachvili's theory on the assembly of surfactant molecules.[94] The next section focuses on other amphiphilic dendrimers that have been investigated. Additionally, the behavior of dendrimers on surfaces will be discussed.

1.3.4 The Behavior of Dendrimers on Surfaces and in Amphiphilic Materials

Transmission electron microscopy (TEM) studies have been performed on unimolecular carboxylate-terminated micelles with either PAMAM[13,56] or alkane frameworks[70]. The PAMAMs of Tomalia have been studied with cryo-TEM using the sodium cations as contrast agents. For a 4.5 generation PAMAM dendrimer, spherical structures are visible with diameters varying from 80 to 100 Å. The structures have been assigned to individual molecules. Newkome et al. have visualized alkane dendrimers with 36 carboxylate end groups. When tetramethylammonium counterions are used, spherical monomolecular structures are visible with sizes of around 30 Å. When the carboxylic acids are used as end group, aggregated structures are observed that probably are caused by intermolecular H-bonding. Using TEM, Newkome et al. have also observed aggregates formed by second generation polyols.[95] Recently, amine-terminated PAMAMs (of generations five to ten) stained with sodium phosphotungstate have been investigated with TEM.[96] The dendrimers are spherical with radii that are consistent with SAXS-data (from 4 nm for generation five up to 15 nm for generation ten). The tenth generation dendrimer has also been investigated with cryo-TEM in vitrified water, revealing a polyhedral shape for these molecules. Noninterpenetrating ordered aggregates have been observed, the formation of which can be suppressed to some extent by adding HCl. This is probably due to protonation of the termini resulting in electrostatic repulsions between separate molecules. Accordingly, close-packed aggregates can be obtained in dilute NaCl solutions in which charges are shielded efficiently.

Various types of metallodendrimers form monomolecular spherical structures on solid surfaces. Majoral et al. have used high-resolution TEM to visualize different generations of gold-containing polyphosphine dendrimers.[97] Dendrimers of generation three, four, five, and ten (theoretical number of Au sites: 24, 48, 96, and 3072, respectively) give isolated spheres with diameters of 60 ± 5, 75 ± 5, 90 ± 5, and 150 ± 5 Å, respectively. Van Veggel et al. have reported on spherical aggregates of palladium-

containing dendrimers that have been studied using AFM.[98] The second generation metallodendrimers have a radius of 15–20 nm and a height of 4.2 nm.

Carbosiloxane dendrimers with trimethylsilyl end groups have been visualized with scanning force microscopy (SFM).[28] On a glass substrate, single dendritic molecules are observed with globular shapes and diameters in the order of 3 nm (Figure 1.5a). The materials have a strong tendency to coagulate; therefore, in addition to monomolecular structures, clusters, and even droplets are also visible. Complete wetting of a mica surface has been observed for carbosilane dendrimers modified with hydroxyl end groups.[99] The wetting is attributed to the preferential adsorption of the hydroxyl groups to the mica surface. Modification of the substrate with a semifluorinated coating results in dendrimer droplets on the surface.

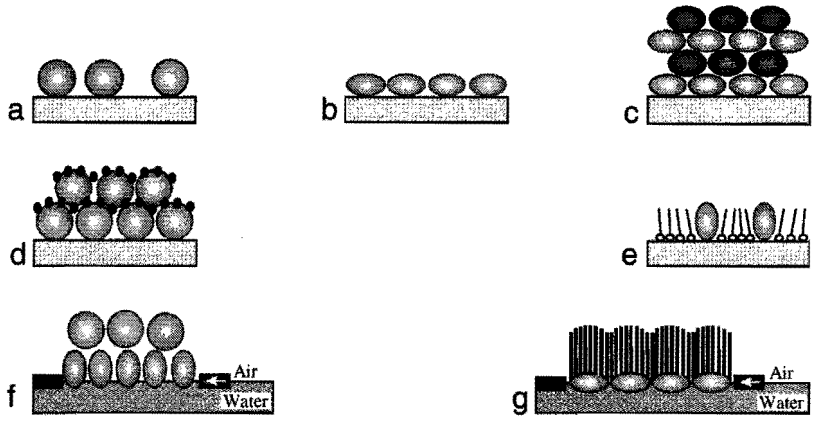

Figure 1.5: *Schematic representation of the different modes of adsorption of dendrimers on surfaces: (a) adsorbed noninteracting dendrimers;[28] (b) adsorbed dendrimers with surface-interacting end groups;[99–102] (c) interacting multilayer dendrimer films;[100] (d) multilayer dendrimer films with ionic shielding;[103] (e) mixed monolayer;[105] (f) compressed dendrimer Langmuir bilayer;[107,108] (g) dendrimer Langmuir monolayer.[110]*

The assembly of dendrimers in monolayers or multilayers on solid surfaces has been discussed in several studies. The previously mentioned hydroxyl-terminated carbosilanes organize in monolayers with thicknesses of approximately half the expected (theoretical) values.[99] Apparently, strong deformation of the surface-bound dendrimers takes place (Figure 1.5b). Tsukruk et al. have observed the deformation of PAMAMs in monolayers on silicon surfaces.[100] The PAMAMs are collapsed and highly compressed along the surface normal, resulting in flattened, disklike structures (Figure 1.5b). To explain the observed deformation, electrostatic interactions between the terminal cationic functional groups and the activated (negatively charged) substrate are assumed. Monolayers of carboxylated PAMAMs on positively charged surfaces also give

flattened structures.[101,102] Compression of dendrimers is also observed in multilayer films of oppositely charged PAMAMs ($-NH_3^+$ and $-CO_2^-$ termini).[100] In this case, electrostatic interactions between the layers cause the compression (Figure 1.5c). Watanabe and Regen have illustrated that deformation resulting from electrostatic interactions can be prevented by using a low molecular weight shielding agent. The authors have used Pt(II) salts that are located between adjacent dendrimer layers, thereby shielding the electrostatic interactions (Figure 1.5d).[103]

Interestingly, the deformation of dendrimers on surfaces has been predicted by Mansfield in a Monte Carlo study.[104] The investigation considers the adsorption of dendrimers on a surface at different interaction strengths. The calculations show a flattening of the dendrimer shape with increasing adsorption strengths. As reflected in the "phase diagram" (Figure 1.6), the mode of adsorption of the dendrimers is dependent on adsorption strength and on the generation number (higher generation dendrimers have more interaction sites per molecule, and therefore, these dendrimers have a better chance to be adsorbed).

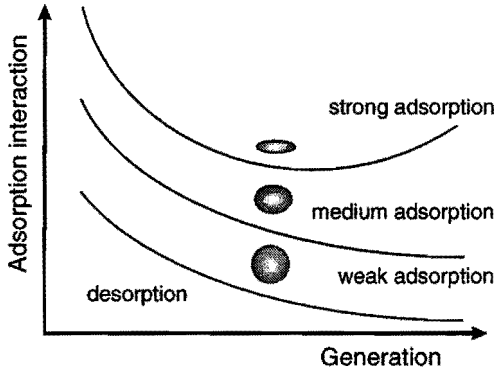

Figure 1.6: *A "phase diagram" that shows how the shape of dendrimers in adsorbed monolayers depends on the strength of the adsorption interaction and the dendrimer generation. The data are based on calculations by Mansfield.*[104]

An interesting type of deformation has been found by Crooks et al.[105] Monolayers of PAMAMs adsorbed on a gold surface flatten due to multiple Au–amine interactions, but subsequent submission of alkanethiols to the surface results in a mixed monolayer in which the PAMAMs acquire a prolate configuration due to the shear exerted by the thiols (Figure 1.5e). The shear originates from the stronger thiol–Au interaction as compared to the amine-Au interaction. If the adsorption time of the dendrimer monolayer is rather short (45 s instead of 20 h), exposure to hexadecanethiol results in

piling up of the dendrimers to vacate the surface in favor of the thiols.[106] Eventually, this leads to complete desorption of the dendrimers from the surface.

The assembly of dendritic molecules on the air-water interface has been investigated by several authors. White et al. have investigated polyether wedges with a benzylic alcohol function at the core.[107,108] For generations one to four, the dendrimers behave as classical surfactant molecules in a Langmuir trough. The isotherms of generations five and six, however, indicate nonsurfactant behavior, once more reflecting the deviating properties of higher generation dendrimers. Compression of the fourth generation polyether dendrimer results in the formation of a stable bilayer. In this bilayer, the dendrimers are compressed laterally with respect to the surface normal, producing an ellipsoidal shape which is twice as high as broad (Figure 1.5f). Neutron reflectivity studies on analogues with perdeuterated end groups indicate that the terminal benzyl groups are located at the top of the lower layer.[108] More stable monolayers were formed when oligo(ethylene glycol) tails were used as core-functionality.[109]

Poly(propylene imine) dendrimers functionalized with hydrophobic alkyl chains (palmitoyl chains or alkyloxyazobenzene chains) assemble in stable monolayers at the air-water interface.[110] In the assemblies, the dendrimers adopt a cylindrical, amphoteric shape, in which the ellipsoidal dendritic moiety acts as a polar headgroup and the alkyl chains arrange in a parallel fashion to form an apolar tail (Figure 1.5g). This representation is based on the observation that the molecular area of a dendritic molecule increases linearly with the number of end groups in this molecule. Additionally, the observed molecular area corresponds to the area occupied by one hydrophobic chain, in an all-trans arrangement, times the number of hydrophobic chains in one molecule. When poly(propylene imine) dendrimers with pendant adamantyl or *N-t*-BOC-L-Phe end groups are spread on the air-water interface, a non-linear dependency of the molecular area with generation is found and stable monolayers are not formed.

Amphiphilic PAMAM dendrimers comparable in design to those reported for the poly(propylene imine) dendrimers[110] have been studied on the air-water surface by Tomalia et al.[111] The PAMAMs with aliphatic end groups of varying lengths (6, 8, 10, and 12 carbon atoms) also display the linear behavior between the molecular area at the compressed state and the number of end groups per molecule. Tomalia et al. explain their findings in a model in which the lower generations are asymmetric like the poly(propylene imine) dendrimers, while the higher generations act as hydrophobic spheroids floating on the air–water interface. Since no indication for the latter behavior is found, it is proposed here that also the amphiphilic PAMAM dendrimers of high

generations, when disposed on air–water interfaces, are highly distorted with all aliphatic end groups pointing upwards.

In addition to the Langmuir–Blodgett (LB) studies, the aggregation in water of the palmitoyl and alkoxyazobenzene-functionalized poly(propylene imine) dendrimers has been studied.[110] At a pH of 1, vesicle-type structures are observed as evidenced by (cryo) TEM micrographs, dynamic light scattering (DLS) data, X-ray diffraction results and osmometry measurements. In the aggregates, the dendrimers are thought to have similar conformations as those observed at the air–water surface. The hydrophilic protonated dendritic component faces the water, while the aliphatic chains are packed in a parallel fashion to form an apolar bilayer. Within this assumption, the axial ratio is calculated at 8:1 for the highest dendrimer generation (the axial ratio is defined as the ratio between both characteristic distances in an ellipse). Thus, the dendritic head group has a flattened, far from globular, ellipsoidal shape.

Strong deformation from a spherical shape is also observed in liquid crystalline (LC) dendrimers. Attachment of a mesogenic unit to the dendrimer periphery results in a deformation of the dendritic core in order to align the LC units. Cylindrical conformations are found for LC-modified carbosilane[112] and poly(propylene imine) dendrimers (Figure 1.7a),[113] having cyanobiphenyl and 3,4-bis(decyloxy)benzoyl end groups respectively. In contrast, severe flattening of the dendritic core is observed in cyanobiphenyl-functionalized poly(propylene imine) dendrimers (Figure 1.7b),[114] comparable to the deformation observed for amphiphilic poly(propylene imine) dendrimers in monolayers or vesicles.[110]

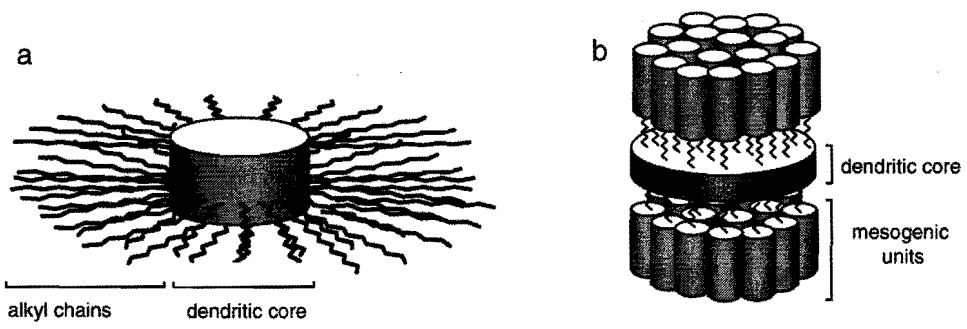

Figure 1.7: *Proposed models for the conformation of poly(propylene imine) dendrimers bearing mesogenic groups in (a) hexagonal columnar phases[113] and (b) smectic layered phases.[114]*

The phenylacetylene dendrimers prepared by Moore et al. are distinguished from other dendrimers by their rigidity. The authors describe them as "shape persistent" and

"dimension persistent".[10] The shape persistency has been confirmed by electron microscopy and diffraction measurements on the first and second generation phenylacetylene dendrimers.[115] However, even these rigid dendrimers can be deformed to "pancake"-shaped structures, when LC behavior is induced by modifying the outer functionalities with oligoethylene glycol chains.[116] Columnar discotic liquid crystalline phases are observed for these materials. Similar molecular organization has been found for stilbenoid dendrimers.[117]

In reality, dendrimers do not necessarily behave as might be expected from a simple representation on paper. Most dendrimers possess flexible branches that can adopt different conformations, implying that the end groups can fold back into the interior of the molecule. More surprisingly, the flexibility in dendritic molecules—even in bulky higher generation dendrimers—allows that these molecules can adopt shapes that are far from globular. Such shapes are only observed when dendrimers are exposed to "external stimuli", i.e., secondary interactions that force the dendrimers into specific supramolecular arrays. Flattened dendritic structures have for example been found in monolayers and in LC materials.

It has firmly been established that specific properties can only be expected from higher generation dendrimers. In this respect, the drop in intrinsic viscosity for higher molecular weight dendrimers has frequently been mentioned, although other properties also change for higher generation dendrimers (see for example the simple and elegant study by Hawker et al.[78]).

1.4 Aim and Scope of the Thesis

More than 10 years after the initial reports on the syntheses of dendritic macromolecules, many characteristics of these macromolecules have been revealed. The development of advanced mass spectrometry techniques (ESI-MS, MALDI-TOF MS) has enabled researchers to exactly determine the purity of dendrimers. Thus, it has been confirmed that dendrimers are synthetic macromolecules that are almost monodisperse and previously unattainable polydispersities well below 1.01 are common for dendrimers. Theoretical and experimental data have clearly shown that dendrimers are highly flexible molecules. The conformational flexibility brings about many initially unexpected properties, e.g., the end groups can be severely backfolded, the interior of a dendrimer is able to expose itself to the environment, and huge distortions of the overall dendritic shape are possible under specific experimental circumstances. Finally, it has been established that higher generation dendrimers show deviating properties, not only in relation to their lower generation analogues but also when compared to linear and compositionally similar oligomers or polymers.

Today, research on dendrimers is not only focused on disclosing aberrant or special features of dendrimers but considerable effort is also invested in the development of applications for dendrimers. Dendritic molecules have been tested in supramolecular polymer chemistry, in medicinal chemistry, and in catalysis.[118] Soon dendrimers might be used in new devices, since it can be expected that highly defined molecules with precise submicron dimensions will be of relevance for those active in the emerging fields of bio- and nanotechnology. Additionally, research on dendritic materials is facilitated by the circumstance that, nowadays, a few types of thoroughly studied dendrimers are either commercially available or easily accessible. Thus, it has become possible to broaden the potential of these materials even further. Consequently, the research described in this thesis concerns the modification of poly(propylene imine) dendrimers with different functionalities, that all make use of the unique features of the dendritic framework in order to explore the added-value of the dendrimer architecture.

In Chapter 2, dendrimers are used to physically entrap guest-molecules by the construction of a dense shell around a flexible dendrimer ("the dendritic box"). In this way, the guests show typical characteristics due to the dendritic micro-environment. In addition, the structure of the shell has been modified and investigated both in solution (IR and NMR spectroscopy) and in the solid state (X-ray diffraction), to obtain a more flexible system. These studies indicate that the presence of hydrogen bonds between the end groups is of utmost importance. In order to get more insight into the dynamic behavior of poly(propylene imine) dendrimers, these dendrimers have been functionalized with pendant stable nitroxyl radicals, as described in Chapter 3. EPR spectroscopy reveals that the flexibility of nitroxyl functionalized dendrimers is related to both temperature and nature of the solvent. These dependencies can be attributed to the presence of a network of H-bonds in the periphery of the molecule.

In Chapter 4, the dendrimers are used as nano-scaffolds for several metal-ions like Cu(II), Ni(II) and Zn(II). These metal-ions are bound by the end groups of the poly(propylene imine) dendrimers. The highest generation dendrimer binds 32 metal-ions, and has nanometer dimensions. This makes it possible to use membrane-filtration to isolate the metallodendrimer from the solution, opening the way to use these dendrimers for continuous metal extraction, sensor-applications and catalysis, as shown in this chapter.

Finally, functionalized poly(propylene imine) dendrimers are used in Chapter 5 to mimic the multivalency present in many biological systems using the highly branched architecture of the dendrimers. The first example consists of a Cu(I)-modified dendrimer which is able to bind multiple molecules of dioxygen. Therefore, this

multivalent dioxygen complex may be seen as a model for oxygen binding by hemocyanine assemblies, the oxygen-carriers in mollusks and arthropods. In the second example, the poly(propylene imine) dendrimers are used as scaffold to assemble multiple porphyrins, both in a covalent and noncovalent way. The covalent assemblies show intramolecular electronic interactions between the porphyrin end groups in the excited state, thereby mimicking the light harvesting of the natural LH2 system, which is responsible for capturing and storing light-energy in photosynthetic bacteria.

1.5 References and Notes

1. Buhleier, E. W.; Wehner, W.; Vögtle, F. *Synthesis* **1978**, 155-158.
2. Denkewalter, R. G.; Kolc, J.; Lukasavage, W. J. U.S. Pat. 4,289,872, Sept. 15, 1981. Denkewalter, R. G.; Kolc, J.; Lukasavage, W. J., U.S. Pat. 4,360,646, Nov. 23, 1982. Denkewalter, R. G.; Kolc, J.; Lukasavage, W. J., U.S. Pat. 4,410,688, Oct. 18, 1983.
3. Aharoni, S. M.; Crosby, C. R., III; Walsh, E. K. *Macromolecules* **1982**, *15*, 1093–1098.
4. Tomalia, D. A.; Dewald, J. R.; Hall, M. J,; Martin, S. J.; Smith, P. B. *Preprints of the 1st SPSJ International Polymer Conference*; Soc. Polym. Sci. Japan, Kyoto, 1984, 65. Tomalia, D. A.; Baker, H.; Dewald, J. R.; Hall, M.; Kallos, G.; Martin, S.; Roeck, J.; Ryder, J.; Smith, P. *Polym. J. (Tokyo)* **1985**, *17*, 117–132. Tomalia, D. A.; Baker, H.; Dewald, J. R.; Hall, M.; Kallos, G.; Martin, S.; Roeck, J.; Ryder, J.; Smith, P. *Macromolecules* **1986**, *19*, 2466–2468.
5. Newkome, G. R.; Yao, Z.-Q.; Baker, G. R.; Gupta, K. *J. Org. Chem.* **1985**, *50*, 2003–2004.
6. Wörner, C.; Mülhaupt, R. *Angew. Chem., Int. Ed. Engl.* **1993**, *32*, 1306–1308.
7. De Brabander-van den Berg, E. M. M.; Meijer, E.W. *Angew. Chem., Int. Ed. Engl.* **1993**, *32*, 1308–1311.
8. Hawker, C. J.; Fréchet, J. M. J. *J. Am. Chem. Soc.* **1990**, *112*, 7638–7647. Hawker, C. J.; Fréchet, J. M. J. *J. Chem. Soc., Chem. Commun.* **1990**, 1010–1013.
9. Moore, J. S.; Xu, Z. *Macromolecules* **1991**, *24*, 5893–5894. Xu, Z.; Moore, J. S. *Angew. Chem., Int. Ed. Engl.* **1993**, *32*, 246–248.
10. Kawaguchi, T.; Walker, K. L.; Wilkins, C. L.; Moore, J. S., *J. Am. Chem. Soc.* **1995**, *117*, 2159–2165.
11. Moore, J. S. *Acc. Chem. Res.* **1997**, *30*, 402–413.
12. Newkome, G. R.; Moorefield, C. N.; Vögtle, F. *Dendritic Molecules: Concepts, Syntheses and Perspectives*; VCH: Weinheim, Germany, 1996.
13. Tomalia, D. A.; Naylor, A.; Goddard, W. A., III *Angew. Chem., Int. Ed. Engl.* **1990**, *29*, 138–175.
14. Tomalia, D. A.; Hedstrand, D. M.; Wilson, L. R. In *Encyclopedia of Polymer Science and Engineering*, 2nd ed.; Kroschwitz, J. I., Ed.; Index Volume; Wiley: New York, 1990; pp. 46–92.
15. Fréchet, J. M. J. *Science* **1994**, *263*, 1710–1715.
16. Tomalia, D. A.; Durst, H. D. *Topics Curr. Chem.* **1993**, *165*, 193–313.
17. Ardoin, N.; Astruc, D. *Bull. Soc. Chim. Fr.* **1995**, *132*, 875–909.
18. Fréchet, J. M. J.; Hawker, C. J.; Gitsov, I.; Leon, J. W. *J. Macromol. Sci., Pure Appl. Chem.* **1996**, *A33*, 1399–1425.
19. For an review on phosphorus- and silicon-based dendrimers, see: Gudat, D. *Angew. Chem., Int. Ed. Engl.* **1997**, *36*, 1951–1955.
20. Solomons, T. W. G. *Organic chemistry*, 6th ed.; Wiley: New York, 1996; p. 1169.
21. For a typical example, see: Pesak, D. J.; Moore, J. S.; Wheat, T. E. *Macromolecules* **1997**, *30*, 6467–6482.
22. Hummelen, J. C.; van Dongen, J. L. J.; Meijer, E. W. *Chem. Eur. J.* **1997**, *3*, 1489–1493. Here, a complete description and discussion of the ESI-MS measurements on the DAB-dendrimers is presented. For more (technical) details, the reader is referred to this article.
23. Kallos, G. J.; Tomalia, D. A.; Hedstrand, D. M.; Lewis, S.; Zhou, J. *Rapid Commun. Mass Spectrom.* **1991**, *5*, 383–386. Schwartz, B. L.; Rockwood, A. L.; Smith, R. D.; Tomalia, D. A.; Spindler, R. *Rapid*

Commun. Mass Spectrom. **1995**, *9*, 1552–1555. Dvornic, P. R.; Tomalia, D. A. *Macromol. Symp.* **1995**, *98*, 403–428. Tolic, P. T.; Anderson, G. A.; Smith, R. D.; Brothers, H. M., II; Spindler, R.; Tomalia, D. A. *Int. J. Mass Spectrom. Ion Proc.* **1997**, *165/166*, 405–418.

24. The hydrogenation proceeds quantitatively, provided the appropriate reaction conditions are chosen. Remarkably, ESI-MS analysis of material obtained by interrupting the hydrogenation of a poly(propylene imine) dendrimer has revealed the presence of only two products: fully converted dendrimer and completely unreacted starting material. This "all-or-nothing" reaction can be explained by assuming that the nitrile dendrimer is fully hydrogenated before it is released from the surface of the Raney Co catalyst.
25. Dandliker, P. J.; Diederich, F.; Gross, M.; Knobler, C. B.; Louati, A.; Sanford, E. M., *Angew. Chem., Int. Ed. Engl.* **1994**, *33*, 1739–1742.
26. Dandliker, P. J.; Diederich, F.; Gisselbrecht, J.-P.; C. B.; Louati, A.; Gross, M. *Angew. Chem., Int. Ed. Engl.* **1995**, *34*, 2725–2728.
27. Mattei, S.; Walliman, P.; Kenda, B.; Amrein, W.; Diederich, F. *Helv. Chim. Acta.* **1997**, *80*, 2391–2417.
28. Lorenz, K.; Mülhaupt, R.; Frey, H.; Rapp, U.; Mayer-Posner, F. J. *Macromolecules* **1995**, *28*, 6657–6661.
29. Sheiko, S. S.; Eckert, G.; Ignat'eva, G.; Muzafarov, A. M.; Spickermann, J.; Räder, H. J.; Möller, M. *Macromol. Rapid Commun.* **1996**, *17*, 283–297.
30. Wu, Z.; Biemann, K. *Int. J. Mass Spectrom. Ion Proc.* **1997**, *165*, 349–361.
31. Krska, S. W.; Seyferth, D. *J. Am. Chem. Soc.* **1998**, *120*, 3604–3612.
32. Lau, R. L. C.; Chan, T.-W. D.; Chan, I. Y.-K.; Chow, H.-F. *Eur. Mass. Spectrom.* **1995**, *1*, 371–380.
33. Bodige, S.; Torres, A. S.; Maloney, D. J.; Tate, D.; Kinsel, G. R.; Walker, A. K.; McDonnell, F. M. *J. Am. Chem. Soc.* **1997**, *119*, 10364–10369.
34. Moucheron, C.; Kirsch-De Mesmaeker, A.; Dupont-Gervais, A.; Leize, E.; van Dorsselaer, A. *J. Am. Chem. Soc.* **1996**, *118*, 12834–12835.
35. Huck, W. T. S.; van Veggel, F. C. J. M.; Reinhoudt, D. N. *Angew. Chem., Int. Ed. Engl.* **1996**, *35*, 1213–1215. Huck, W. T. S.; Prins, L. J.; Fokkens, R. H.; Nibbering, N. M. M.; van Veggel, F. C. J. M.; Reinhoudt, D. N. *J. Am. Chem. Soc.* **1998**, *120*, 6240–6246.
36. Leon, J. W.; Fréchet, J. M. J. *Polym. Bull.* **1995**, *35*, 449–455. Pollak, K. W.; Sanford, E. M.; Fréchet, J. M. J. *J. Mater. Chem.* **1998**, *8*, 519–527.
37. Walker, K. L.; Kahr, M. S.; Wilkins, C. L.; Xu, Z.; Moore, J. S. *J. Am. Soc. Mass Spectrom.* **1994**, *5*, 731–739.
38. De Gennes, P. G.; Hervet, H. *J. Phys., Lett. Fr.* **1983**, *44*, L351–L361.
39. Lescanec, R. L.; Muthukumar, M. *Macromolecules* **1990**, *23*, 2280–2288.
40. Mansfield, M. L.; Klushin, L. I. *Macromolecules* **1993**, *26*, 4262–4268.
41. Murat, M.; Grest, G. S. *Macromolecules* **1996**, *29*, 1278–1285.
42. Boris, D.; Rubinstein, M. *Macromolecules* **1996**, *29*, 7251–7260.
43. Naylor, A. M.; Goddard, W. A., III; Kiefer, G. E.; Tomalia, D. A. *J. Am. Chem. Soc.* **1989**, *111*, 2339–2341.
44. Miklis, P.; Çagin, T.; Goddard, W. A., III *J. Am. Chem. Soc.* **1997**, *119*, 7458–7462.
45. Cavallo, L.; Fraternali, F. *Chem. Eur. J.* **1998**, *4*, 927–934.
46. Scherrenberg, R.; Coussens, B.; van Vliet, P.; Edouard, G.; Brackman, J.; de Brabander, E.; Mortensen, K. *Macromolecules* **1998**, *31*, 456–461.
47. Welch, P.; Muthukumar, M. *Macromolecules* **1998**, *31*, 5892–5897.
48. Mourey, T. H.; Turner, S. R.; Rubinstein, M.; Fréchet, J. M. J.; Hawker, C. J.; Wooley, K. L. *Macromolecules* **1992**, *25*, 2401–2406.
49. Wooley, K.L.; Klug, C. A.; Tasaki, K.; Schaefer, J. *J. Am. Chem. Soc.* **1997**, *119*, 53–58.
50. Gorman, C. B.; Hager, M. W.; Parkhurst, B. L.; Smith, J. C. *Macromolecules* **1998**, *31*, 815–822.
51. De Backer, S.; Prinzie, Y.; Verheijen, W.; Smet, M.; Desmedt, K.; Dehaen, W.; De Schryver, F. C. *J. Phys. Chem. A* **1998**, *102*, 5451–5455.
52. Percec, V.; Johansson, G.; Ungar, G.; Zhou, J. *J. Am. Chem. Soc.* **1996**, *118*, 9855–9866.
53. Balagurusamy, V. S. K.; Ungar, G.; Percec, V.; Johansson, G. *J. Am. Chem. Soc.* **1997**, *119*, 1539–1555.

54. Hudson, S. D.; Jung, H.-T.; Percec, V.; Cho, W.-D.; Johansson G.; Ungar, G.; Balagurusamy, V. S. K. *Science* **1997**, *278*, 449–452.
55. Stark, B.; Stühn, B.; Frey, H.; Lach, C.; Lorenz, K.; Frick, B. *Macromolecules* **1998**, *31*, 5415–5423.
56. Tomalia, D. A.; Hall, V. B.; Hedstrand, D. M. *Macromolecules* **1987**, *20*, 1167–1169.
57. Dubin, P. L.; Edwards, S. L.; Kaplan, J. I.; Mehta, M. S.; Tomalia, D. T.; Xia, J. *Anal. Chem.* **1992**, *64*, 2344–2347.
58. Meltzer, A. D.; Tirrell, D. A.; Jones, A. A.; Inglefield, P. T.; Hedstrand, D. M.; Tomalia, D. A. *Macromolecules* **1992**, *25*, 4541–4548.
59. Meltzer, A. D.; Tirrell, D. A.; Jones, A. A.; Inglefield, P. T. *Macromolecules* **1992**, *25*, 4549–4552.
60. Prosa, T. J.; Bauer, B. J.; Amis, E. J.; Tomalia, D. A.; Scherrenberg, R. *J. Polym. Sci. B* **1997**, *35*, 2913–2924.
61. Amis, E. J., Topp, A., Bauer, B. J., Tomalia, D. A. *Polym. Mater. Sci. Eng.* **1997**, *77*, 183–184. Amis, E. J., Topp, A., Bauer, B. J., Tomalia, D. A. submitted for publication in *J. Am. Chem. Soc.*
62. Duan, R. G.; Miller, L. L.; Tomalia, D. A. *J. Am. Chem. Soc.* **1995**, *117*, 10783–10784. Miller, L. L.; Hashimoto, T.; Tabakovic, I.; Swanson, D. R.; Tomalia, D. A. *Chem. Mater.* **1995**, *7*, 9–11.
63. Miller, L. L.; Kunugi, Y.; Canavesi, A.; Rigaut, S.; Moorefield, C. N.; Newkome, G. R. *Chem. Mater.* **1998**, *10*, 1751–1754.
64. Caminati, G.; Turro, N. J.; Tomalia, D. A. *J. Am. Chem. Soc.* **1990**, *112*, 8515–8522.
65. Moreno-Bondi, M. C.; Orellana, G.; Turro, N. J.; Tomalia, D. A. *Macromolecules* **1990**, *23*, 910–912.
66. Gopidas, K. R.; Leheny, A. R.; Caminati, G.; Turro, N. J.; Tomalia, D. A. *J. Am. Chem. Soc.* **1991**, *113*, 7335–7342.
67. Ottaviani, M. F.; Bossmann, S.; Turro, N. J.; Tomalia, D. A. *J. Am. Chem. Soc.* **1994**, *116*, 661–671.
68. Ottaviani, M. F.; Cossu, E.; Turro, N. J.; Tomalia, D. A. *J. Am. Chem. Soc.* **1995**, *117*, 4387–4398.
69. Ottaviani, M. F.; Montalti, F.; Romanelli, M; Turro, N. J.; Tomalia, D. A. *J. Phys. Chem.* **1996**, *100*, 11033–11042.
70. Newkome, G. R.; Moorefield, C. N.; Baker, G. R.; Saunders, M. J.; Grossman, S. H. *Angew. Chem., Int. Ed. Engl.* **1991**, *30*, 1178–1181.
71. Newkome, G. R.; Young, J. K.; Baker, G. R.; Potter, L. A.; Cooper, D.; Weis, C. D.; Morris, K. F.; Johnson Jr., C. S. *Macromolecules* **1993**, *26*, 2394–2396. Young, J. K.; Baker, G. R.; Newkome, G. R.; Morris, K. F.; Johnson Jr., C. S. *Macromolecules* **1994**, *27*, 3464–3471.
72. Ramzi, A.; Scherrenberg, R.; Brackman, J.; Joosten, J.; Mortensen K. *Macromolecules* **1998**, *31*, 1621–1626.
73. DAB stands for diaminobutane, referring to the core molecule that is used. The poly(propylene imine) dendrimers reported by Mülhaupt[6] have been produced starting from NH_3.
74. Jansen, J. F. G. A.; de Brabander-van den Berg, E. M. M.; Meijer, E. W. *Science* **1994**, *265*, 1226–1229.
75. Jansen, J. F. G. A.; Peerlings, H. W. I.; de Brabander-van den Berg, E. M. M.; Meijer, E. W. *Angew. Chem., Int. Ed. Engl.* **1995**, *34*, 1206–1209.
76. Peerlings, H. W. I.; Meijer, E. W. *Chem. Eur. J.* **1997**, *3*, 1563–1570.
77. The maximum has been made plausible by analyzing the mentioned growth pattern of dendrimers. The volume of a dendrimer proceeds by first approximation with n^3, whereas the mass proceeds with 2^n (n = the generation number). The intrinsic viscosity [η] is expressed in volume per mass and the quotient of the foregoing volume and mass functions indeed displays a maximum.[15,18]
78. Hawker, C. J.; Malmström, E. E.; Frank, C. W.; Kampf, J. P. *J. Am. Chem. Soc.* **1997**, *119*, 9903–9904.
79. Wooley, K. L.; Hawker, C. J.; Pochan, J. M.; Fréchet, J. M. J. *Macromolecules* **1993**, *26*, 1514–1519.
80. Hawker, C. J.; Farrington, P. J.; Mackay, M. E.; Wooley, K. L.; Fréchet, J. M. J. *J. Am. Chem. Soc.* **1995**, *117*, 4409–4410.
81. Uppuluri, S.; Keinath, S. E.; Tomalia, D. A.; Dvornic, P. R. *Macromolecules* **1998**, *31*, 4498–4510.
82. Farrington, P. J.; Hawker, C. J.; Fréchet, J. M. J.; Mackay, M. E. *Macromolecules* **1998**, *31*, 5043–5050.
83. Miller, T. M.; Neenan, T. X.; Zayas, R.; Bair, H. E. *J. Am. Chem. Soc.* **1992**, *114*, 1018–1025.
84. Wooley, K. L.; Fréchet, J. M. J.; Hawker, C. J. *Polymer* **1994**, *35*, 4489–4495.
85. De Brabander, E. M. M.; Brackman, J.; Mure-Mak, M.; de Man, H.; Hogeweg, M.; Keulen, J.; Scherrenberg, R.; Coussens, B.; Mengerink, Y.; van der Wal, S. *Macromol. Symp.* **1996**, *102*, 9–17.

86. Hawker, C. J.; Wooley, K. L.; Fréchet, J. M. J. *J. Am. Chem. Soc.* **1993**, *115*, 4375–4376.
87. Kamlet, M. J.; Abboud, J. M.; Abraham, M. H.; Taft, R. W. *J. Org. Chem.* **1983**, *48*, 2877–2887.
88. Zimmerman, S. C.; Wang, Y.; Bharathi, P.; Moore, J. S. *J. Am. Chem. Soc.* **1998**, *120*, 2172–2173.
89. Devadoss, C.; Bharathi, P.; Moore, J. S. *Angew. Chem., Int. Ed. Engl.* **1997**, *36*, 1633–1635.
90. Put, E. J. H.; Clays, K.; Persoons, A.; Biemans, H. A. M.; Jansen, J. F. G. A.; Kurvers, R.; Luijkx, C. P. M.; Meijer, E. W. *S.P.I.E. Int. Soc. Opt. Eng.* **1996**, *2852*, 122–131. Put, E. J. H.; Clays, K.; Persoons, A.; Biemans, H. A. M.; Luijkx, C. P. M.; Meijer, E. W. *Chem. Phys. Lett.* **1996**, *260*, 136–141.
91. Tomoyose, Y. T.; Jiang, D.-L.; Jin, R.-H.; Aida, T.; Yamashita, T.; Horie, K.; Yashima, E.; Okamoto, Y. *Macromolecules* **1996**, *29*, 5236–5238. Jiang, D.L.; Aida, T. *J. Am. Chem. Soc.* **1998**, *120*, 10895–10901.
92. Jiang, D. L.; Aida, T. *Nature* **1997**, *388*, 454–456.
93. Van Hest, J. C. M.; Delnoye, D. A. P.; Baars, M. W. P. L.; van Genderen, M. H. P.; Meijer, E. W. *Science* **1995**, *268*, 1592–1595. Van Hest, J. C. M.; Delnoye, D. A. P.; Baars, M. W. P. L.; Elissen-Román, C.; van Genderen, M. H. P.; Meijer, E. W. *Chem. Eur. J.* **1996**, *12*, 1616–1625.
94. Israelachvili, J. N.; Mitchell, D. J.; Ninham, B. W. *J. Chem. Soc., Faraday Trans. 2* **1976**, *72*, 1525–1567.
95. Newkome, G. R.; Yao, Z.-Q.; Baker, G. R.; Gupta, V. K.; Russo, P. S.; Saunders, M. J. *J. Am. Chem. Soc.* **1986**, *108*, 849–850.
96. Jackson, C. L.; Chanzy, H. D.; Booy, F. P.; Drake, B. J.; Tomalia, D. A.; Bauer, B. J.; Amis, E. J. *Macromolecules* **1998**, *31*, 6259–6265.
97. Slaney, M.; Bardají, M.; Casanove, M.-J.; Caminade, A.-M.; Majoral, J.-P.; Chaudret, B. *J. Am. Chem. Soc.* **1995**, *117*, 9764–9765.
98. Van Veggel, F. C. J. M.; Huck, W. T. S., Reinhoudt, D. N. *Macromol. Symp.* **1998**, *131*, 165–173.
99. Sheiko, S. S.; Muzafarov, A. M.; Winkler, R. G.; Getmanova, E. V.; Eckert, G.; Reineker, P. *Langmuir* **1997**, *13*, 4172–4181.
100. Tsukruk, V. V.; Rinderspacher, F.; Bliznyuk, V. N. *Langmuir* **1997**, *13*, 2171–2176. Tsukruk, V. T. *Adv. Mater.* **1998**, *10*, 253–257.
101. Bliznyuk, V. N.; Rinderspacher, F.; Tsukruk, V. V. *Polymer* **1998**, *39*, 5249–5252.
102. Esumi, K.; Goino, M. *Langmuir* **1998**, *14*, 4466–4470.
103. Watanabe, S.; Regen, S. L. *J. Am. Chem. Soc.* **1994**, *116*, 8855–8856.
104. Mansfield, M. L. *Polymer* **1996**, *37*, 3835–3841.
105. Zhao, M.; Tokuhisa, H.; Crooks, R. M. *Angew. Chem., Int Ed. Engl.* **1997**, *36*, 2596–2598. Tokuhisa, H.; Zhao, M.; Baker, L. A.; Phan, V. T.; Dermody, D. L.; Garcia, M. E.; Peez, R. F.; Crooks, R. M.; Mayer, T. M. *J. Am. Chem. Soc.* **1998**, *120*, 4492–4501.
106. Hierlemann, A.; Campbell, J. K.; Baker, L. A.; Crooks, R. M.; Ricco, A. J. *J. Am. Chem. Soc.* **1998**, *120*, 5323–5324.
107. Saville, P. M.; White, J. W.; Hawker, C. J.; Wooley, K. L.; Fréchet, J. M. J. *J. Phys. Chem.* **1993**, *97*, 293–294.
108. Saville, P. M.; Reynolds, P. A.; White, J. W.; Hawker, C. J.; Fréchet, J. M. J.; Wooley, K. L.; Penfold, J.; Webster, J. R. P. *J. Phys. Chem.* **1995**, *99*, 8283–8289.
109. Kampf, J. P.; Frank, C. W.; Malmström, E. E.; Hawker, C. J. *Langmuir* **1999**, *15*, 227–233. Kampf, J. P.; Frank, C. W.; Malmström, E. E.; Hawker, C. J. *Science* **1999**, *282*, 1730–1733.
110. Schenning, A. P. H. J.; Elissen-Román, C.; Weener, J.-W.; Baars, M. W. P. L.; van der Gaast, S. J.; Meijer, E. W. *J. Am. Chem. Soc.* **1998**, *120*, 8199–8208.
111. Sayed-Sweet, Y.; Hedstrand, D. M.; Spinder, R.; Tomalia, D. A. *J. Mater. Chem.* **1997**, *7*, 1199–1205.
112. Lorenz, K.; Hölter, D.; Stühn, B.; Müllhaupt, R.; Frey, H. *Adv. Mater.* **1996**, *8*, 414–416.
113. Cameron, J. H.; Facher, A.; Lattermann, G.; Diele, S. *Adv. Mater.* **1997**, *9*, 398–403.
114. Baars, M. W.; Söntjens, S. H. M.; Fischer, H. M.; Peerlings, H. W. I.; Meijer, E. W. *Chem. Eur. J.* **1998**, *4*, 2456–2466.
115. Buchko, C. J.; Wilson, P. M.; Xu, Z.; Zhang, J.; Moore, J. S.; Martin, D. C. *Polymer*, **1995**, *35*, 1817–1825.
116. Pesak, D. J.; Moore, J. S. *Angew. Chem., Int. Ed. Engl.* **1997**, *36*, 1636–1639.
117. Meier, H.; Lehmann, M. *Angew. Chem., Int. Ed. Engl.* **1998**, *37*, 643–645.

118. For some excellent reviews, see: Issberner, J.; Moors, R.; Vögtle, F. *Angew. Chem., Int. Ed.* **1994**, *33*, 2413-2420. Hobson, L. J.; Harrison, R. M. *Curr. Opin. Solid State Mat. Sci.* **1997**, *2*, 683-692. Zeng, F.; Zimmerman, S. C. *Chem Rev.* **1997**, *97*, 1681-1712. Matthews, O. A.; Shipway, A. N.; Stoddart, J. F. *Prog. Polym. Sci.* **1998**, *23*, 1-56. Smith, D. K.; Diederich, F. *Chem. Eur. J.* **1998**, *4*, 1353-1361. Archut, A.; Vögtle, F. *Chem. Soc. Rev.* **1998**, *27*, 233-240. Chow, H.-F.; Mong, T. K.-K.; Nongrum, M. F.; Wan, C.-W. *Tetrahedron* **1998**, *54*, 8543-8660. *Topics in Current Chemistry*; Springer-Verlag: Berlin, 1998; Vol. 197. Janssen, H. M.; Meijer, E. W. In *Synthesis of Polymers*; Schlüter, A.-D., Ed.; Material Science and Technology, Vol. 20; Cahn, R. W., Haasen, P. Kramer, E. J., Eds.; Wiley-VCH: Weinheim, 1999; pp. 403-458. Majoral, J.-P.; Caminade , A.-M. *Chem. Rev.* **1999**, *99*, 845–880. Fischer, M.; Vögtle, F. *Angew. Chem., Int. Ed. Engl.* **1999**, *38*, 884-905.

Soft-Core Dense-Shell Dendrimers*

2

Abstract: *The encapsulation of two different functional molecules in the dendritic box (DAB-dendr-(NH-t-BOC-L-Phe)$_{64}$) is described. Encapsulation of 7,7,8,8-tetracyano-quinodimethane (TCNQ) leads to a charge transfer complex with the polyamine interior of the poly(propylene imine) dendrimer. The resulting radical anion ($TCNQ^{\bullet-}$) is then physically trapped as a dimer, as evidenced with UV/vis and EPR spectroscopy. Encapsulation of the photosensitizer pheophorbide a, results in a chemical modification of pheophorbide a due to the basic interior. The resulting dye, chlorin e_6, shows reduced mobility in time-resolved fluorescence anisotropy as a consequence of encapsulation. Encapsulation in the dendritic box does not hamper singlet oxygen generation, opening the way to use these systems in photodynamical therapy (PDT). In order to obtain a dendritic box with a less congested shell, the preparation and hydrogen bonding properties of a series of fully functionalized poly(propylene imine) dendrimers (DAB-dendr-$(NH_2)_n$; n = 4, 8, 16, 32, 64) with N-t-BOC-glycine residues is described. The presence of intramolecular H-bonding between the N-t-BOC-glycine end groups is reflected in the X-ray structure of a first generation functionalized dendrimer (n = 4). NMR and infrared studies in dichloromethane of all dendrimer generations show that intramolecular H-bonding also occurs in solution. Moreover, there is a steady increase in H-bonding with generation because of the higher local concentration of end groups. Comparing DAB-dendr-(NH-t-BOC-Gly)$_{64}$ with the dendritic box, reveals that the degree of H-bonding is higher for the latter. The decrease in congestion of the shell in DAB-dendr-(NH-t-BOC-Gly)$_{64}$ is subscribed by 2D NOESY spectroscopy and size selective encapsulation of an aldol condensation product.*

* Part of this work has been published: Bosman, A. W.; Jansen, J. F. G. A.; Janssen, R. A. J.; Meijer; E. W. *Proc. ACS. PMSE.*, **1995**, *73*, 340-341. Bosman, A. W.; Bruining, M. J.; Kooijman, H.; Spek, A. L.; Janssen, R. A. J.; Meijer, E. W. *J. Am. Chem. Soc.*, **1998**, *120*, 8547-8584.

2.1 Introduction

The concept of "topological trapping" of guests by core–shell molecules has been introduced by Maciejewski as early as 1982.[1] It refers to the binding of guest molecules in internal and confined cavities of a host system. First indications for the presence of cavities in dendrimers come from studies of Tomalia et al.[2] They observed a decrease in spin–lattice relaxation times for guest like 2,4-dichlorophenoxyacetic acid and acetylsalicylic acid in the presence of carbomethoxy-terminated PAMAMs in deuterated chloroform solution. The validity of Maciejewski's concept has been shown experimentally by Jansen et al.[3,4] and has been confirmed theoretically later on.[5,6] In this system the soft-core, hard-shell framework of modified poly(propylene imine) dendrimers is used to encapsulate guest molecules. These structures are also called "dendritic box" and are constructed by end group functionalization of a fifth generation poly(propylene imine) dendrimer (DAB-*dendr*-$(NH_2)_{64}$) with bulky substituents like *t*-BOC-L-Phe.[3] The rigidity of the shell is reflected in the NMR relaxation behavior of the carbon atoms,[3] ^{1}H NMR data,[3] and chiroptical data.[7-9] These experimental findings show that intramolecular hydrogen bonding interactions between the *t*-BOC-L-Phe-moieties are stronger for the higher generation functionalized poly(propylene imine) dendrimers and, therefore, it is believed that these hydrogen bonds add to the solid phase character of the shell.

The encapsulation of molecules is performed by reaction of DAB-*dendr*-$(NH_2)_{64}$ with an activated ester of *N*-*t*-BOC-L-Phe in the presence of guest molecules with some affinity for the tertiary amine functions in the interior of the dendrimer (Scheme 2.1). Excess guest molecules and molecules adhered to the surface of the box can conveniently be removed by a dialysis procedure. Liberation of guests in the dendritic box is only possible after destruction, i.e., hydrolysis, of the shell.[10] Lower generation poly(propylene imine) dendrimers cannot be used as boxes, since the shells in these systems are not dense enough to trap guest molecules: aqueous work-up will release all adhered molecules.

The encapsulation of dye molecules in general, and of Rose Bengal in particular, has been studied in detail.[11] The features of the guest molecules can change upon capturing, obviously as a result of the changed micro environment. For example, Rose Bengal@DAB-*dendr*-(NH-*t*-BOC-L-Phe)$_{64}$[12] displays strong fluorescence at λ_{max} = 600 nm in chloroform, whereas the fluorescence of free Rose Bengal is quenched in this wavelength region. Induced chirality upon encapsulation has also been found for Rose Bengal. When one molecule of Rose Bengal—an achiral compound—is trapped, a CD spectrum is found which, on basis of UV/vis spectrum, has to be attributed to Rose Bengal.[13] When four molecules are trapped, an exciton-coupled Cotton effect is

observed, indicating the close proximity of chromophores. The CD experiments suggest that the cavities in the dendritic box must have retained some chiral features, although the shells of the box do not display significant optical activity. The close proximity of trapped guest molecules has been confirmed in EPR spectroscopy measurements on dendritic boxes containing 3-carboxy-PROXYL radicals as guests. Ferro-magnetic interactions are observed between the radical species present in one dendritic host molecule.[14]

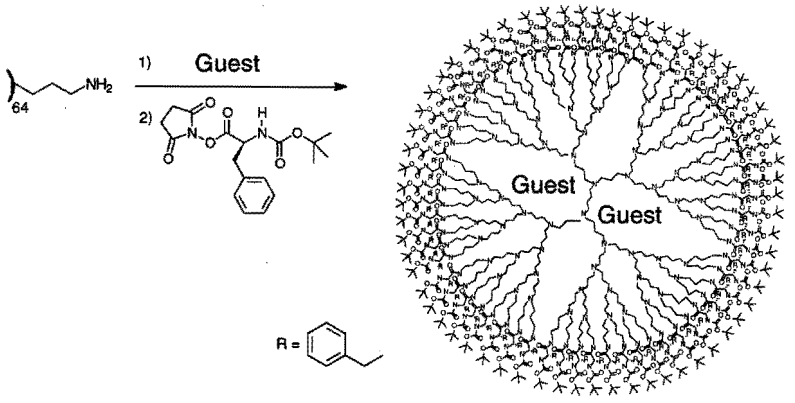

Scheme 2.1: *Construction of dendritic box in presence of guest molecules.*

In this chapter two other examples of encapsulation are given, resulting in a charge transfer complex and a photoactive species capable of producing singlet oxygen. Both encapsulated functionalities show unique properties due to the micro-environment imposed by the dendrimer. Then, functionalization of poly(propylene imine) dendrimers with the smaller *t*-BOC-Gly end group is addressed, in order to obtain a core–shell topology with a less sterically congested shell. The resulting "perforated dendritic box" has been investigated on its use as catalyst in aldol condensations.

2.2 Topological Trapping of Functionalities in the Dendritic Box

2.2.1 Charge Transfer with the Dendritic Box

Previously, evidence has been put forward that 7,7,8,8-tetracyanoquinodimethane (TCNQ, Figure 2.1) gives a charge transfer (CT) complex with a dendritic box.[3] This paragraph describes the encapsulation of TCNQ in more detail. As a result of the large electron affinity (E_A = 2.48 eV),[15] TCNQ forms stable CT complexes with various organic and inorganic donors; well known is the CT complex of TCNQ with triethylamine

(TEA).[16] Since the inside of the dendritic box contains many (62) tertiary amines, an electron transfer between TCNQ and the dendrimer is likely to occur. The ability of the dendritic box to donate electrons has also been shown in the photoinduced electron transfer to buckminsterfullerene.[17] Recently, intramolecular charge transfer has been observed in a dendrimer from tetrathiafulvalene to anthraquinone units which are both covalently linked to the same aromatic polyester dendrimer.[18]

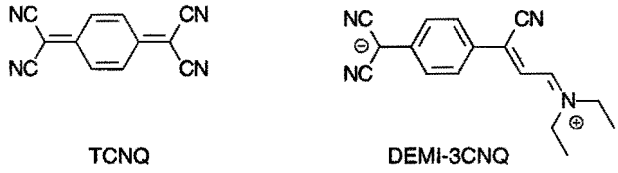

Figure 2.1: *TCNQ and DEMI-3CNQ.*

TCNQ with dendritic box. Reaction of TCNQ with increasing amounts of empty dendritic box produced an intense green color and new absorption bands at λ_{max} = 670, 750 and 850 nm were observed (Figure 2.2), with an associated loss of the TCNQ bands at 400 nm. The new absorptions are readily attributed to the TCNQ radical anion.[16]

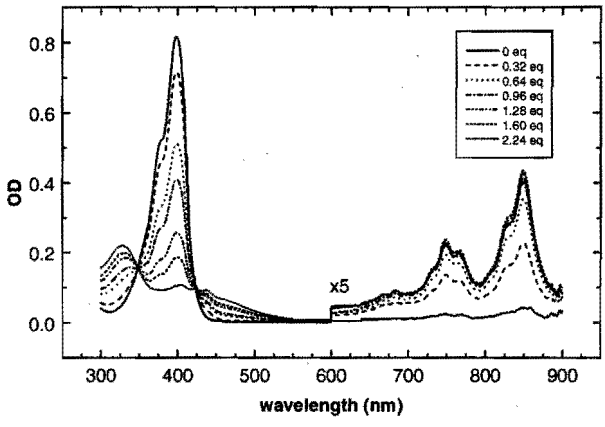

Figure 2.2: *UV/vis-spectra of TCNQ with different amounts of dendritic box, recorded in dichloromethane.*

Direct spectral evidence for charge transfer has been obtained using EPR spectroscopy which revealed the well-resolved hyperfine couplings (a_N = 1.00 G and a_H = 1.42 G) associated with $TCNQ^{\bullet-}$ (Figure 2.3a). These results subscribe that electron transfer from the inside of the dendritic box occurs to TCNQ. The nitrogen based radical cation of the dendrimer is not observed, probably due to disproportionation giving

ammonium and iminium ions stabilized by the free electron pairs of the remaining tertiary amines.

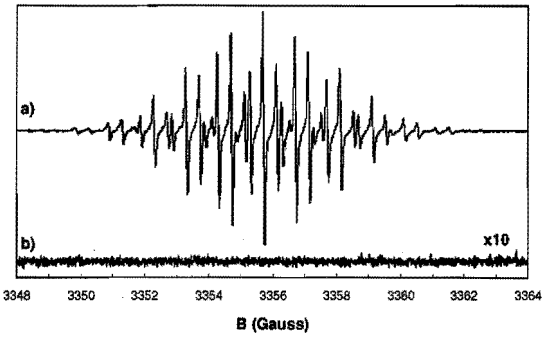

Figure 2.3: *EPR spectra of TCNQ with empty dendritic box (a) and TCNQ@DAB-dendr-(NH-t-BOC-L-Phe)$_{64}$ (b, 10 times magnified), recorded in dichloromethane.*

TCNQ in dendritic box. On addition of TCNQ to a solution of a DAB-*dendr*-$(NH_2)_{64}$ in dichloromethane, the same absorption bands were observed as found for the mixture of TCNQ with empty dendritic box (Figure 2.4) together with the corresponding $TCNQ^{\bullet-}$ EPR signal. Subsequently, encapsulation of TCNQ was accomplished by the construction of the dense outer shell, via endcapping the dendrimer with the *N*-hydroxy-succinimide ester of *t*-BOC-L-phenylalanine. The resulting reaction mixture was washed thoroughly to remove non-encapsulated TCNQ-molecules. After washing, a decrease of the relative intensities of the absorption bands at λ_{max} = 750 and 850 nm is observed as compared to the band at 670 nm, indicating the partial loss of $TCNQ^{\bullet-}$. Rigorous purification of the box from adhered molecules was attained by dialysing the sample in an acetone/water mixture (95/5 by volume) using a regenerated cellulose membrane. Dialysis was possible because of the large dimensions of the dendritic box (r_g = 18 Å, based on DLS and SAXS measurements).[4] After dialysis only absorption bands at λ_{max} = 615 and 663 nm remained (Figure 2.4), while the bands of $TCNQ^{\bullet-}$ at λ_{max} = 750 and 850 nm were completely lost together with the EPR signal (Figure 2.3b).

These results demonstrate that the species associated with the 750 and 850 nm absorptions, i.e. $TCNQ^{\bullet-}$, is not encapsulated in the dendritic box. However, the encapsulated molecules (TCNQ@DAB-*dendr*-(NH-*t*-BOC-L-Phe)$_{64}$) are associated with the 615 en 663 nm absorptions and are attributed to a dimer of the TCNQ radical anion in the box. This kind of π–π dimer has also been observed in aqueous solutions by Boyd et al.[19] exhibiting a λ_{max} of 643 nm. The equilibrium constant associated with the dimerization: $2TCNQ^{\bullet-} \rightleftharpoons TCNQ_2^{2-}$ is $2.5 \cdot 10^3$ M^{-1} in water at 298 K and lowers when the solution is made less polar by the addition of ethanol.[20]

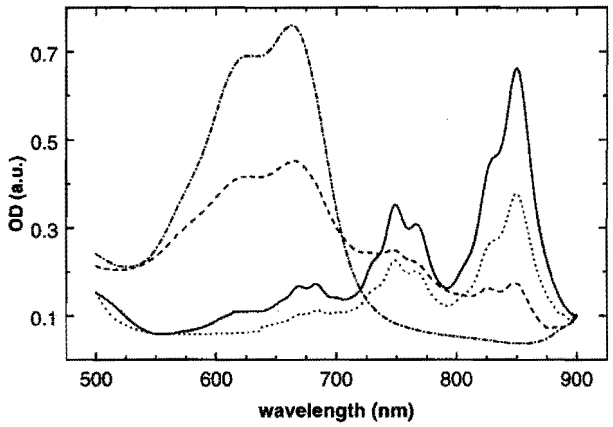

Figure 2.4: *Vis spectra of the reaction mixture on encapsulating TCNQ; TCNQ with DAB-dendr-(NH$_2$)$_{64}$ (···), TCNQ with DAB-dendr-(NH$_2$)$_{64}$ after addition of the active ester (—), TCNQ@DAB-dendr-(NH-t-BOC-L-Phe)$_{64}$ after washing the reaction mixture (- - -), and TCNQ@DAB-dendr-(NH-t-BOC-L-Phe)$_{64}$ after dialysis (-·-·-).*

Enhancement in formation of the π–π dimers in aqueous solution has been found in the presence of γ-cyclodextrine by complexing dimers in the cyclodextrine cavity.[21] Dimerization in pure organic solvents has never been observed before. The disappearance of the EPR signal is in agreement with the proposed dimerization, because pairing of the two unpaired electrons in the dimer will result in a diamagnetic product, as was found for γ-cyclodextrine complexation. Even heating dimers encapsulated in the dendritic box to 140°C in 1,2 dichlorobenzene, does not result in a recovery of the EPR spectrum, indicative for a high association constant. Assuming that the extinction coefficient for the TCNQ$^{\bullet-}$ dimer in the box is comparable to that in aqueous solution ($\varepsilon_{643} = 3.36 \cdot 10^4$ M^{-1}cm^{-1}),[19] a loading of approximately 0.3 dimer per dendritic box is obtained.

Recently, it has been shown that TCNQ reacts with TEA, resulting in a zwitterionic adduct of TCNQ (DEMI-3CNQ).[22] Hence, the difference in vis absorption bands between free and encapsulated TCNQ, could result from a reaction of TCNQ with the polyamine dendrimer involving the formation of covalent bonds. In order to eliminate the possibility that TCNQ has reacted similarly with the tertiary amines in the box, we exposed the polyamine dendrimer and TCNQ to the same reaction conditions as described for the synthesis of DEMI-3CNQ (reflux in chloroform for three days). However, only unreacted species were found together with an insoluble black tar. To check that TCNQ does not react with the primary amines of the poly(propylene imine) dendrimer under the reaction conditions of encapsulation, *n*-propylamine has been used as a probe. On mixing TCNQ with *n*-propylamine in dichloromethane, the CT

bands at 750 and 850 nm were observed, as has been found for the dendrimer. However after adding of *N*-hydroxy-succinimide ester of *t*-BOC-L-phenylalanine, the CT bands disappeared and only one absorption at 400 nm remained, belonging to TCNQ. More recently, amine terminated PAMAM dendrimers have been reacted with TCNQ under similar reaction conditions, however, this resulted only in intractable, hardly soluble material.[23] In order to obtain additional evidence for the absence of DEMI-3CNQ like derivatives in case of encapsulation of TCNQ, we encapsulated DEMI-3CNQ. On encapsulation the absorption bands of this molecule undergo a dramatic blue shift (~200 nm). This blue shift also occurs when TEA is added to DEMI-3CNQ, attributed to a reduction of the molecule.[24] Therefore, the formation of DEMI-3CNQ upon encapsulation of TCNQ can be completely ruled out.

In conclusion, both the synthesis as well as the optical data show that no reaction involving covalent bonds has occurred between TCNQ and the poly(propylene imine) dendrimers. Therefore, the TCNQ radical anions are trapped physically as π–π dimers in the dendritic box. The radical anions are formed via charge transfer with the dendritic polyamine, whereupon these anions combine to a dimer in the dendritic core. Probably, this dendritic core stabilizes the dimeric form of the TCNQ radical anion. In this way it is possible to generate the dimer in organic media, exemplifying the use of dendrimers as a tool to create a micro-environment.

2.2.2 Photosensitizer in the Dendritic Box

The presence of a typical micro-environment inside the dendrimer has inspired several research groups to prepare dendrimers with specific functionalities at the core.[25] Thus, molecular systems are created in which a certain functionality is surrounded by a particular, sterically congested structure. Especially porphyrin based dendrimers have attracted a lot of attention in this research field, in order to create substrate selectivity in catalysis,[26] to prevent quenching of the photoactive core,[27] to modify redox-potentials,[28] and to protect the porphyrin core from aggregation and chemical degradation when used as O_2-carriers.[29]

Prevention of aggregation of dye molecules is of utmost importance in photodynamic therapy (PDT) of cancer. PDT is based on the selective accumulation of a photosensitizer in tumor tissue and on the production of singlet oxygen by irradiation of the sensitizer-enriched tumor with visible light.[30] The resulting formation of cytotoxic singlet oxygen causes cell death and often total tumor necrosis. Effective candidates for PDT are distinguished by low self aggregation in water, as this results in a decrease in singlet oxygen production, and an lipophilic character. The presence of hydrophobic

sites is important for incorporation in cell membranes and uptake by low-density lipoproteins (LDL).[31] Tumor cells show enhanced uptake of LDLs.[32]

In this paragraph a model system for PDT–agents is described in which a photosensitizer is encapsulated in the dendritic box. Embedding the PDT–agent in the dendritic surroundings prevents aggregation of the photosensitizer dye used, i.e. pheophorbide a (pheo, Scheme 2.2). This dye is sensitized at the red end of the visible spectrum, where human tissue has the highest transmittance. Although the dendritic box is not water soluble, the structure can easily be modified to be soluble in aqueous solvent by attaching poly(ethylene)glycol chains at the periphery,[33] thereby remaining partly hydrophobic. Therefore, these structures will be promising candidates for a carrier system of a photoactive drug in PDT. These studies have been initiated by Prof. B. Rheiner of the Humboldt University in Berlin, and performed in a collaborative program with her group.

Encapsulation of Pheophorbide a. Construction of the dense shell around the poly(propylene imine) dendrimer in the presence of pheo resulted in encapsulation of the dye in the dendritic box. Adhered dye-molecules were removed via exhaustive dialysis with a regenerated cellulose membrane. The validity of this way of purification has been tested by mixing empty dendritic box with pheo followed by dialysis. This resulted in complete removal of the dye from the dendrimer as evidenced with UV/vis spectroscopy.

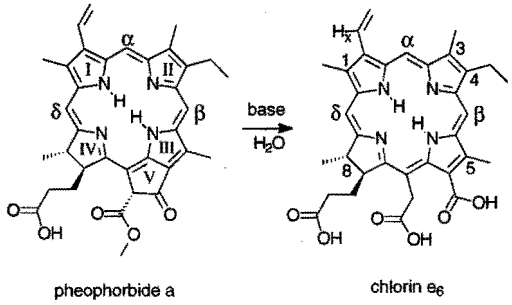

Scheme 2.2: *Ring opening of pheophorbide a under basic conditions.*

Compared to the native dye, the low field ^{1}H NMR signals belonging to the methine protons (α, β, and δ) of the encapsulated dye have shifted. To get more insight into these shifts, a first generation dendrimer with four primary amine end groups has been mixed with pheophorbide a. After work up, the ^{1}H NMR spectrum shows that no reaction with pheo has taken place. This indicates that the primary amines of the unfunctionalized dendrimer do not react with pheo during the encapsulation procedure.[34] A possible explanation for the changes in the ^{1}H NMR spectrum, can be

found in a chemical modification of pheo due to the basic environment inside the box.[35] The ring V of pheo is known to open under basic conditions resulting in chlorine e_6 (Scheme 2.2),[36] having comparable ^{1}H NMR resonances to the dye in the box.[37,38] Additional information came from a 2D NOESY spectrum (Figure 2.5). The methine protons showed negative cross-peaks with sharp signals which are otherwise masked by the dendritic box resonances. The observed through–space interactions are in agreement with a chlorin e_6 structure. In contrast, the non-encapsulated dye is NOE–silent in a 2D NOESY experiment. This can be explained by the intermediate molecular weight of the dye.[39] Thus, the dye has virtually gained weight by the encapsulation procedure resulting in a slower motion of chlorin e_6. No NOEs were found between dye and dendritic box, probably the signal intensities of the dye are too small.

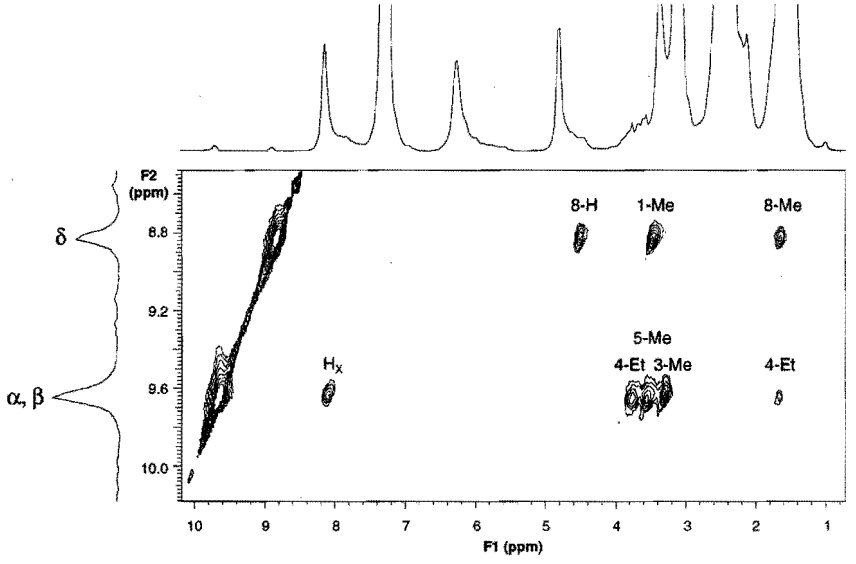

Figure 2.5: *NOE-interactions for dye resonances in chlorin e_6@DAB-dendr-(NH-t-BOC-L-Phe)$_{64}$, assignment of chlorin e_6 signals follows from Scheme 2.2.*

The loading of the dendritic box with chlorin e_6 was determined with both UV/vis and ^{1}H NMR spectroscopy. Using the extinction coefficient of the Q_y(0-0) band and the integrals of the methine protons in ^{1}H NMR, the dye–loadings of the dendritic box were calculated to be proportional to the amount of dye offered. Assuming that the extinction coefficient did not change upon encapsulation, the efficiency of encapsulation was 23 ± 2 %. The same number was found comparing the integrals of dye with dendrimer in ^{1}H NMR (Figure 2.6). A maximum number of 1.2 chlorin e_6 per dendritic box was reached, no saturation could be obtained as found for rose bengal.[11]

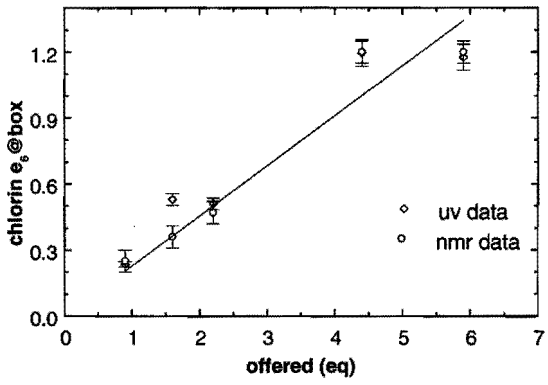

Figure 2.6: *Loading of dendritic box with chlorin e_6 as function of amount of guest offered. The loadings were determined with both ^1H NMR (open circles) and UV/vis spectroscopy (open diamonds), slope of the line is 0.23 ± 0.2.*

Photophysical Characterization. Upon encapsulation of pheo in the dendritic box, the photophysical behavior changes profoundly as expected when formation of chlorin e_6 takes place (Figure 2.7). Compared to pheo, the Soret and the Q-bands all shift hypsochromicly in ethanol. The Soret band becomes sharper and the intensities of the $Q_y(0,1)$, $Q_y(0,0)$ and the $Q_x(0,0)$-band decrease significantly. The fluorescence spectrum of chlorin e_6@DAB-*dendr*-(NH-*t*-BOC-L-Phe)$_{64}$ in ethanol is hypsochromicly shifted next to a decrease in intensity of the $Q_y(1,0)$ emission band, when compared to that of pheo. These spectral changes are in agreement with the proposed ring opening of pheo. Moreover the spectra of chlorin e_6@DAB-*dendr*-(NH-*t*-BOC-L-Phe)$_{64}$ can be almost completely reproduced by dissolving pheo in ethanol containing sodiumhydroxide, resulting in a spectrum analogous to the reported spectrum of chlorin e_6 in dioxane.[38] In order to get more structural information on the encapsulated dye, the circular dichroism (CD) spectrum of chlorin e_6@DAB-*dendr*-(NH-*t*-BOC-L-Phe)$_{64}$ was recorded in dioxane (Figure 2.7, top). The CD spectrum has the same features as the native dye, indicating that the chirality of the dye is hardly affected by the chiral shell of the dendritic box. However, the resolution of the spectrum obtained did not make it possible to discriminate between pheo and chlorin e_6, as the spectral features of both dyes only slightly differ.[40]

The reduced motion of the dye caused by the embedding in a polymeric structure, as found with NMR, was subscribed by a slower rotational fluorescence anisotropy decay. Pheo has a fast single exponential decay time of 0.22 ± 0.05 ns in ethanol. For the encapsulated species, however, a double exponential decay has been observed in ethanol. Both decay times (φ_1 and φ_2) are longer than those for the corresponding free dye. For chlorin e_6@DAB-*dendr*-(NH-*t*-BOC-L-Phe)$_{64}$ decay times of 1.1 ± 0.2 ns and

7 ± 2 ns were observed (Figure 2.8). The double exponential decay can be attributed to the presence of two different motions for the dye-dendrimer complexes, a possible explanation would be the motion of dye in the box and motion of the box itself.

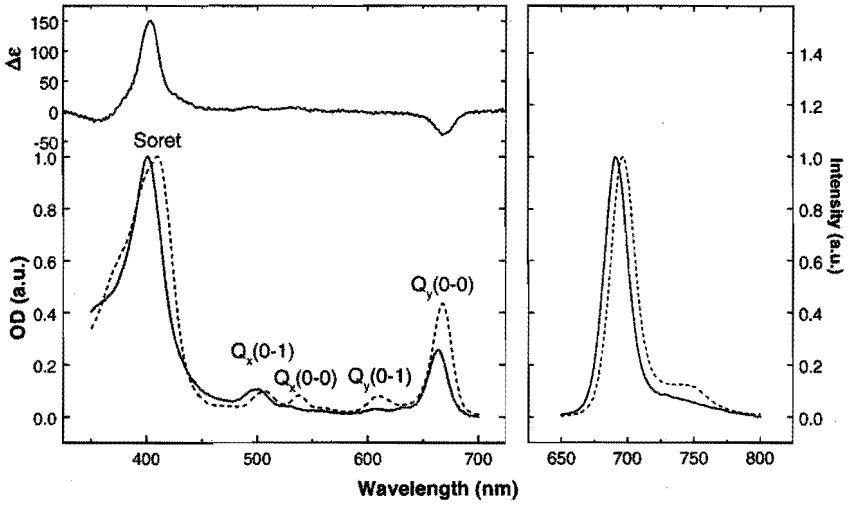

Figure 2.7: *UV/vis (left) and fluorescence (right) spectra of pheo (—) and chlorin e_6@DAB-dendr-(NH-t-BOC-L-Phe)$_{64}$ (- - -), recorded in ethanol. CD spectrum of chlorin e_6@DAB-dendr-(NH-t-BOC-L-Phe)$_{64}$ recorded in dioxane is shown on top.*

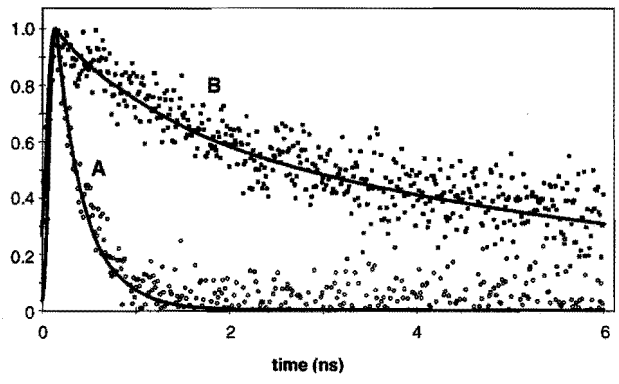

Figure 2.8: *Normalized decay in rotational fluorescence anisotropy for pheo (A) and chlorin e_6@DAB-dendr-(NH-t-BOC-L-Phe)$_{64}$ (B).*

Singlet Oxygen Generation. The photosensitized generation of singlet oxygen with pheo in ethanol results in a singlet oxygen lifetime of 14.7 μs. A small decrease in lifetime was observed when the dye is encapsulated in the dendritic box (13.9 μs). The observed quenching is ascribed to the interaction of singlet oxygen with the *t*-BOC-L-

Phe-modified dendrimer. This is supported by the dynamic quenching that takes place when "empty" dendritic boxes are added to a solution of pheo in ethanol, as a linear Stern-Volmer plot is obtained. However the quantum yield of the singlet oxygen is not affected by the encapsulation of pheo, in both cases this value is 0.52 ± 0.05.

In conclusion, encapsulation of pheophorbide a in the dendritic box results in small differences in absorption and emission spectra due to the basic micro-environment caused by the presence of the polyamine structure inside the dendrimer. This micro-environment results probably in a chemical modification of pheophorbide a giving chlorin e_6. Interestingly, in vivo PDT activity has been found for chlorin e_6.[41] The dye-dendrimer complex shows a double exponential decay in the fluorescence anisotropy, reflecting the presence of two different mobilities. Encapsulating pheo has no negative effect on the photoinduced generation of singlet oxygen. Only a small reduction in the lifetime of the singlet oxygen luminescence signal has been observed, which can be assigned to quenching by the dendritic framework. However, the same dendritic framework limits aggregation of dyes in different "boxes", suggesting the feasibility of the concept of compartmentalization.[1] Therefore, this system has the potential to be used as PDT–drug. Moreover, it is noteworthy that for both PAMAM[42] and lysine dendrimers[43] no immunogenicity has been found. However, more detailed investigations have to be performed to optimize the chemical structures of both the dendrimer and the photosensitizing dye before moving to investigations on biological systems

2.2.3 Concluding Remarks

Both the encapsulation of TCNQ and pheophorbide a show that topological trapping of functional molecules in the dendritic framework is possible. Moreover, the encapsulation procedure provides a way to alter the characteristics of the functionalities due to the typical micro-environment of the dendrimer. In this way molecules can be forced to be together ($TCNQ^{\bullet-}$), or they can be prevented from being close together (pheo). However, the constraints of the dendritic box system are the dependency on (unselective) acid–base interactions, and the irreversibility of encapsulation.

2.3 Perforated Dendritic Box

In the previous paragraph the irreversible encapsulation of guest molecules is described. Liberation of these molecules is only possible after chemically removing the shell.[10] Reversible binding of guests inside the dendrimer has been investigated by several research groups. The first indications (NMR relaxation data) of reversible

interactions between dendrimer and guest molecules come from Tomalia et al., who used the acid-base interaction between organic acids and PAMAMs in $CDCl_3$.[2] Also unimolecular micelles have frequently been employed as host systems for guest molecules. In these systems hydrophobic interactions are responsible for encapsulation of apolar guests like phenol blue and diphenylhexatriene[44] or pyrene[45] in aqueous solution.

Other hosts are based on a hydrophilic dendrimer modified with hydrophobic alkyl chains on the periphery.[46,47] The resulting structure behaves as an inverted unimolecular micelle in organic solvents. Poly(propylene imine) dendrimers with palmitoyl end groups can extract several anionic xanthene dyes from the water layer to the organic phase.[48] The amount of guests per dendrimer is directly related to the number of tertiary amines in the interior. The efficiency of the extraction is related to the pK_a and the hydrophobicity of the guest, and the pH of the water layer. DeSimone et al. have prepared poly(propylene imine) dendrimers with hexafluoropropylene oxide chains to obtain dendritic surfactants that are soluble in supercritical CO_2.[49] Indeed, the "CO_2–philic" amphiphiles are able to extract methyl orange, a CO_2–insoluble guest, from water to supercritical CO_2.

Dendrimers with specific receptors in the interior have been reported by Diederich et al.[50] These structures are composed of a cyclophane core modified with pendant poly(ether amide) dendrimers. The employed cyclophane cores bind flat aromatic substrates or steroids as determined with ^{1}H NMR and fluorescence studies in water and aqueous methanol.

Previously, flexibility in the dendritic box has been introduced by placing alkyl–chain spacers between the end of the branching of the dendrimer and the *t*-BOC-L-Phe end groups.[8,9] Here, the dendritic box has been made more flexible using a sterically less demanding end group then *t*-BOC-L-Phe. Therefore, the synthesis and characterization of the different generations poly(propylene imine) dendrimers with pendant t-BOC-Gly groups is described. Comparing DAB-dendr-(NH-*t*-BOC-Gly)$_{64}$ with the dendritic box, reveals that the degree of H-bonding is higher for the dendritic box. Moreover, the shell is less congested in DAB-dendr-(NH-*t*-BOC-Gly)$_{64}$ as shown by 2D NOESY and a "ship in the bottle" experiment.

2.3.1 Preparation of DAB-*dendr*-(NH-*t*-BOC-Gly)$_n$

The different generations of *N*-*t*-BOC protected glycine functionalized dendrimers **3a-e** (DAB-*dendr*-(NH-*t*-BOC-Gly)$_n$; n = 4, 8, 16, 32, and 64; Figure 2.9) were prepared in analogy to the synthesis of the dendritic box,[3] by the reaction of the *N*-hydroxy succinimidyl ester of *N*-*t*-BOC glycine with the poly(propylene imine) dendrimers.

Reference compounds **1** and **2** were synthesized from *n*-propylamine and 3,3'-diamino-*N*-methyldipropylamine, respectively. These compounds were fully characterized with NMR and IR measurements. Complete functionalization of the dendritic polyamines was also subscribed by MALDI-TOF mass analysis, showing the molecular ions and ions resulting from fragmentation of the dendritic framework (Figure 2.10).[51] The two highest generations also showed tailing to lower masses of which the origin is not yet clear. It might originate from the presence of defect structures in the native poly(propylene imine) dendrimers.

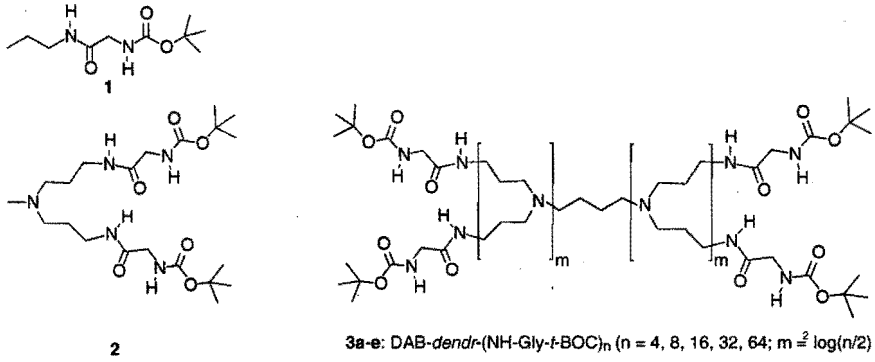

Figure 2.9: *Synthesized t-BOC-Gly-functionalized poly(propylene imine) dendrimers* ***3a-e*** *(n = 4, 8, 16, 32, 64), and reference structures* ***1*** *and* ***2****.*

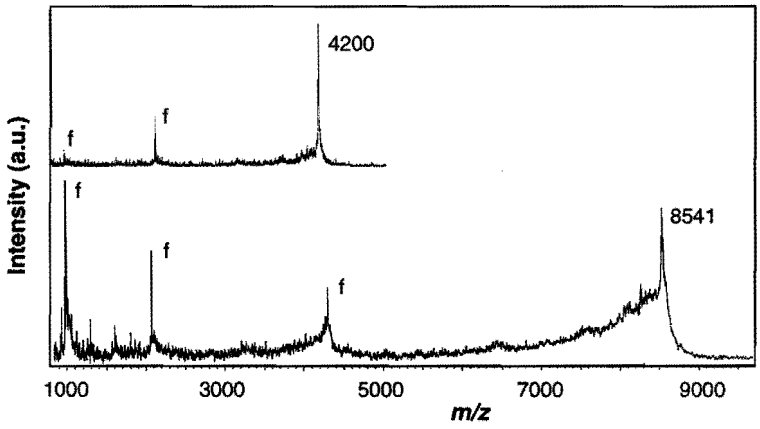

Figure 2.10: *MALDI-TOF mass spectra of* ***3c*** *(n = 16, top) and* ***3d*** *(n = 32, bottom) showing the molecular ion peaks at 4200 and 8541 respectively, peaks due to fragmentation of dendritic framework are labeled with f.*

2.3.2 Hydrogen Bonding in Solid State

Since single crystals of **3a** were obtained from dichloromethane, the hydrogen bonding motif could be investigated in the crystal structure. First generation dendrimer **3a** adopts a globular structure in the solid state (Figure 2.11), with four C_2 symmetric molecules **3a** and eight molecules dichloromethane in the unit cell. All H-bond donors of the end group are involved in the H-bonding with the acceptor sites within the amido-carbamate end group of the same or neighboring molecule. As a result, the end groups are assembled on one side of the structure and the core atoms are positioned at the other side. Two linear and two bifurcated intramolecular H-bonds are accompanied by four bifurcated intermolecular H-bonds per molecule (Table 2.1). All of the secondary interactions are located between carbonyls and N–H functions of different branches, while no interactions are found involving nearest neighbor groups (C5 or C7)[52] or tertiary amines. These findings are in sharp contrast to the X-ray structures of the Fréchet type dendrons[53] or the carbosilane dendrimers,[54] in which no end group interactions are present and there, the end groups are positioned away from each other as far as possible. The intermolecular hydrogen bonds link the molecules into an infinite two dimensional network in the *b-c* plane, as can be seen in Figure 2.12. Interestingly, all molecules are oriented in the same way.

Table 2.1: *Hydrogen bonding data of* ***3a****. Suffix n denotes symmetry operation -x, ½ -y, -½ + z, estimated standard deviations in parentheses.*

H-bonding type	atoms [a]	distance[b]	angle[c]
Intramolecular:	N102-O104	2.830(4)	144.7(2)
	N102-N103	2.782(5)	108.2(2)
	N104-O105	2.924(4)	161.6(2)
Intermolecular:	N103-O101n	2.993(4)	157.2(2)
	N105-O101n	2.893(4)	159.9(2)

a) for atom numbering see Figure 2.11. b) distance donor–acceptor (Å). c) angle N–H···A (°).

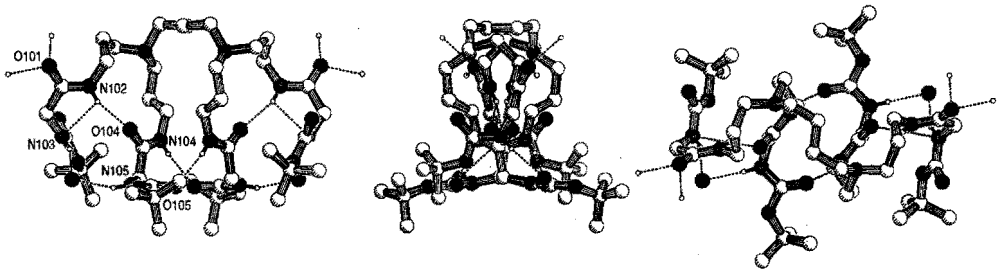

Figure 2.11: *PLUTON representations of the crystal structure of* ***3a****, projections along* ***a****,* ***b****, and* ***c****-axis, respectively. Hydrogen bonds are shown by dotted lines, only protons involved in hydrogen bonding are shown for clarity. Acceptor atom O101 [-x, ½ - y, -½ + z] as well as the donating hydrogen atoms of other neighboring molecules have been included to provide a complete scheme of all hydrogen bonding interactions.*

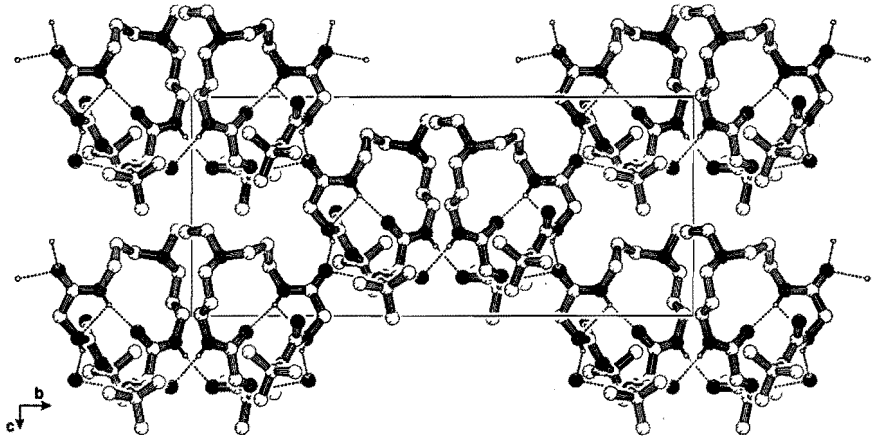

Figure 2.12: *PLUTON representation of intermolecular orientation of* ***3a*** *in the crystal structure. Hydrogen bonds are shown by dotted lines, only protons involved in hydrogen bonding are shown for clarity. Rectangular shows orthorhombic unit cell .*

2.3.3 Hydrogen Bonding in Solution

IR studies. The X-ray structure of **3a** supports the dense shell motif in the dendritic box having all end groups interacting intramolecularly. In order to confirm this proposal, all molecules were studied in solution. IR spectroscopy of **1–3** in dichloromethane (1 mM) showed both one absorption at 3435 cm^{-1} for the non H-bonded amide and carbamate N–H stretching vibrations and one broad absorption at approximately 3320 cm^{-1} for the H-bonded amide and carbamate N–H stretching vibrations (Figure 2.13).[52,55] Integration of the 3435 cm^{-1} absorptions and relating them

to that of compound **1**, yields the relative amount of H-bonded species (Table 2.2).[56] There is an increase in the amount of intramolecular H-bonding when going to dendrimers of higher generation, attributed to an increase in the local concentration of end groups, that are forced in closer proximity.[2] From the data a K_{eq} is estimated of 1.6 ± 0.1 (K_{eq} = [H-bonded]/[non H-bonded]) for model compound **2**, which is comparable to bipeptide systems reported before.[56] These H-bond interactions are only intramolecular, since the ratio of both peaks is not changed upon dilution of the starting solution.[57] Probably there is no significant difference in H-bonding for both the amide and carbamate functions, as they have comparable extinction coefficients.[58] The trend of increasing intramolecular H-bonding is also reflected in the carbonyl stretch region, the amide I peak shifts from 1680 cm^{-1} for **1** to 1665 cm^{-1} for **3e**. The latter resonance is also found for γ-turns in proteins.[59] An increase in intramolecular H-bonding with generation is subscribed by molecular dynamics calculations of DAB-*dendr*-(NH-*t*-BOC-L-Phe)$_n$,[6] although the amount of H-bonding is much smaller (7 % for n = 4 and 15% for n = 64).

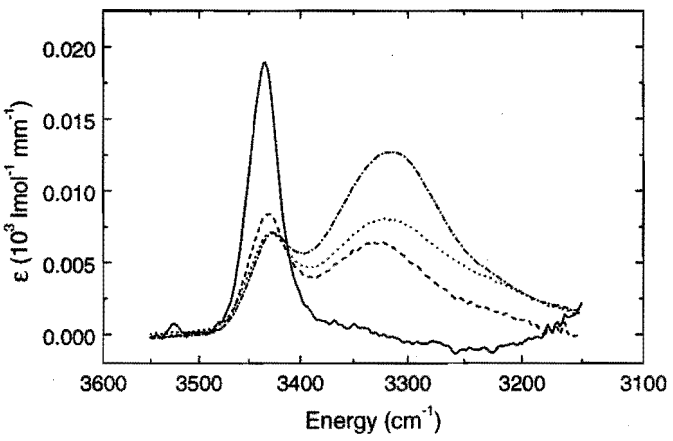

Figure 2.13: *N–H stretch IR spectra of* ***1*** *(—),* ***3a*** *(- - -),* ***3c*** *(···)* ***3e*** *(-·-·-) in CH_2Cl_2 at 298 K. Spectra are normalized to 1 mM end group.*

^{1}H NMR studies. To discriminate between the N–H resonances of the amide and the carbamate, proton NMR studies were performed in deuterated dichloromethane. However, due to the fast exchange of H-bonding with respect to the NMR time scale, the H-bonded and non H-bonded states are not visible separately. Both the amide as the carbamate N–H resonances shift to lower field by going to higher generations (Table 2.2). Comparable shifts have been found for poly(propylene imine) dendrimers functionalized with amide groups only.[46,60] Following the methods developed by Gellman

et al.[55] to establish the equilibrium constants of the intramolecular bonding in **2**, we estimate $K_{eq} = 0.8$ for the amide and $K_{eq} = 0.3$ for the carbamate, using the limiting chemical shifts as obtained from dimerization studies of **1** ($\delta_{non\text{-}bonded} = 5.94$ ppm, $\delta_{H\text{-}bonded} = 8.29$ ppm, and $K_{dim} = 0.22\ M^{-1}$ for amide NH, and $\delta_{non\text{-}bonded} = 5.04$ ppm, $\delta_{H\text{-}bonded} = 7.14$ ppm, and $K_{dim} = 0.21\ M^{-1}$ for carbamate NH). The calculated K_{eq} are in good agreement with the IR data. Measurements of the reduced temperature coefficients ($\Delta\delta/\Delta T$) show that there is almost no difference in temperature dependency for the different generations. This confirms that the observed differences in H-bonding originate from the closer proximity of the end groups.

Table 2.2: *Solution hydrogen bonding data of 1–3 and dendritic box.* [a]

			DAB-*dendr*-(NH-*t*-BOC-Gly)$_n$					dendritic
	1	**2**	**3a**	**3b**	**3c**	**3d**	**3e**	box[c]
amount of H-bonding[b]	0	0.61	0.67	0.70	0.77	0.79	0.80	0.87
amide I (cm^{-1})	1679	1671	1671	1670	1671	1667	1666	1654
δ sec. amide (ppm)	6.06	6.98	7.03	7.24	7.33	7.46	7.54	7.99
δ carbamate (ppm)	5.08	5.55	5.62	5.82	5.92	6.11	6.13	6.14
Δδ/ΔT sec. amide (ppb/K)	–3.4	–5.1	–7.8	–8.3	–8.0	–7.4	–6.4	–6.5
Δδ/ΔT carbamate (ppb/K)	–2.1	–5.4	–6.1	–7.7	–7.9	–6.6	–6.8	–5.2

a) FT IR measurements performed in dichloromethane, NMR measurements in deuterated dichloromethane, all measurements performed in 0.5 – 3.2 mM concentration regime. b) values obtained from FT IR spectra after subtraction of solvent spectrum and deconvolution of peaks, using $\varepsilon = 1.32 \cdot 10^3\ mm^{-1}M^{-1}$ for 3435 cm^{-1} absorption in absence of H-bonding (see text). c) N–H chemical shifts for *t*-BOC-L-Phe–NH–propyl are 5.86 and 5.00 ppm.

2.3.4 Host–Guest Interactions of DAB-*dendr*-(NH-*t*-BOC-Gly)$_{64}$ versus DAB-*dendr*-(NH-*t*-BOC-L-Phe)$_{64}$

Comparing the IR data of **3e** in solution with those of the dendritic box, a small increase in hydrogen bonding is observed for the latter (Table 2.2). This is subscribed by the larger changes in chemical shifts for the N–H resonances in the dendritic box. Moreover, the mode of H-bonding is different for the L-Phe-series when compared with the DAB-*dendr*-(NH-*t*-BOC-Gly)$_n$. This is reflected in the IR absorptions of both the N-H as the C=O stretch regions (Figure 2.14). In the dendritic box structure the extinction coefficient of the H-bonded amide frequencies is significant higher, and the carbonyl absorptions are shifted 13–21 cm^{-1} to lower energy relative to **3e**. These changes can probably be attributed to participation in H-bonding by the phenyl group of L-Phe.[61] Weak H-bonds between benzene rings and H-donors are known to play a role in nature, additional to conventional H-bridging systems.[62] Differences are also found on

macroscopic scale, as the glass transition temperature (T_g) of the dendritic box is 16°C higher then that of **3e** (T_g = 39°C and 23°C respectively). The higher T_g of the dendritic box reflects the presence of a more rigid structure. Therefore, changing the end group from *t*-BOC-L-Phe to *t*-BOC-Gly suggests a decrease in packing density of the shell, indeed.

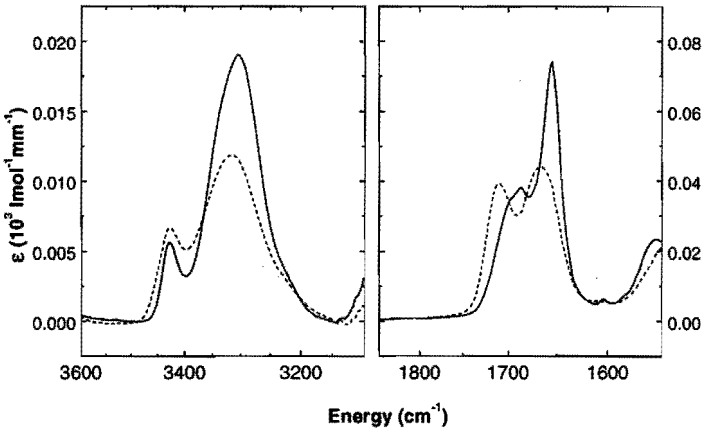

Figure 2.14: *N–H and C=O stretch regions in infrared of DAB-dendr-(NH-t-BOC-L-Phe)$_{64}$ (—), and DAB-dendr-(NH-t-BOC-Gly)$_{64}$ (- - -).*

Whether the difference in size—a proton instead of a benzylic group—does result in size selectivity, was first investigated with 2D NOESY NMR. As probe molecule benzoic acid was chosen because of its affinity for the basic interior of the poly(propylene imine) dendrimers. Adding benzoic acid (5 eq.) to both fifth generations dendrimers resulted in an additional dendrimer signal at 2.7 ppm attributed to methylene protons next to protonated tertiary amines. The signals of benzoic acid shifted to higher field ($\Delta\delta$ = 0.1 ppm), indicative of protonation of the dendrimer by the benzoic acid. The 2D NOESY spectrum of benzoic acid with **3e** is shown in Figure 2.15. Clearly visible are the cross-peaks between benzoic acid and the dendrimer signals, indicating that both species are close together. In contrast, the 2D NOESY spectrum of the dendritic box with benzoic acid revealed unresolved cross-peaks of lower intensity in the 1–3 ppm region, suggesting that the amount of host–guest interactions is lower in the dendritic box system.

To get more information on the rigidity of these systems, the dendrimers were used as base–catalyst in the aldol condensation of *p*-nitrobenzaldehyde with acetone. The polyamine interior of the functionalized poly(propylene imine) dendrimers results in a basic micro-environment inside the dendrimer (p*K* ~ 10), as evidenced by natural abundance ^{15}N NMR studies.[35] Upon dissolving the dendritic box or **3e** in acetone in the

presence of *p*-nitrobenzaldehyde, an orange-yellow solution was obtained. GC-MS analysis revealed the formation of 4-hydroxy-4-methyl-2-pentanone and condensation product **4** (Figure 2.16) in both cases. This shows that the basic interior is accessible, no matter which end group is used, in agreement with the deprotonation of benzoic acid found in NMR. However, when the resulting reaction mixtures were exhaustively dialyzed, differences were found between the two different systems. UV/vis spectroscopy showed the unchanged spectrum of the dendritic box after dialysis, whereas, in the case of **3e**, a residual absorption was observed attributed to the condensation product **4**. Therefore, it is proposed that all reactants are able to diffuse into **3e** where they react. Consequently, the size of **4** prevents it from diffusing out of the dendrimer. This ship in the bottle concept is also known to take place in supramolecular host–guest systems,[63,64] zeolites,[65] and dendrimer–copper nanocomposite.[66]

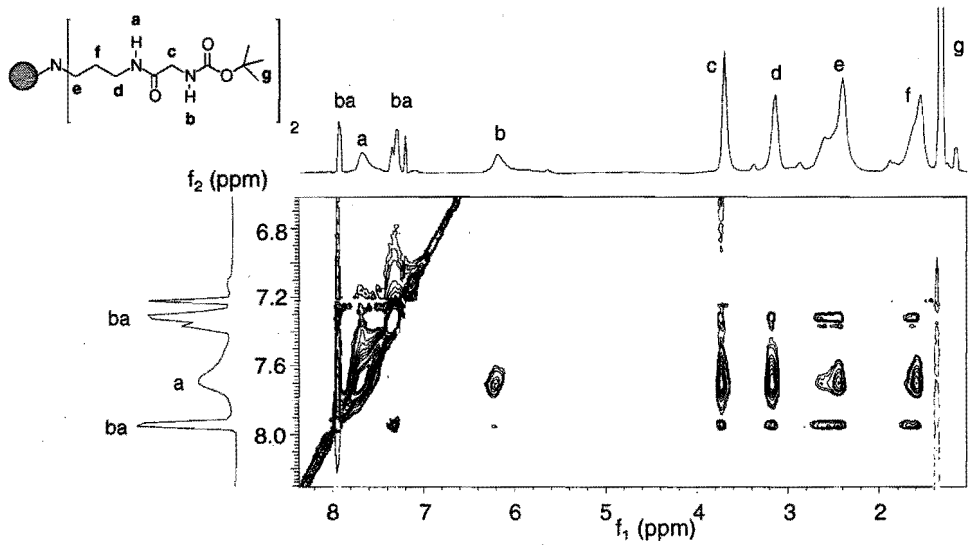

Figure 2.15: *2D NOESY spectrum of **3e** with benzoic acid. Signals belonging to benzoic acid are labeled with ba, labeling dendrimer signals is shown in upper left corner.*

2.3.5 Concluding Remarks

In conclusion the X-ray structure of **3a** shows multiple interactions between the different end groups of the dendrimer, modeling the shell of a higher generation dendrimer. Spectroscopic results from solutions of dendrimers of all generations confirm this close proximity of end groups due to the presence of secondary interactions. Moreover, changing the size of the end group, i.e., *t*-BOC-Gly instead of *t*-BOC-L-Phe,

leads to a less dense packing of the end groups on the dendrimer periphery. Consequently, the dendrimer core becomes more accessible.

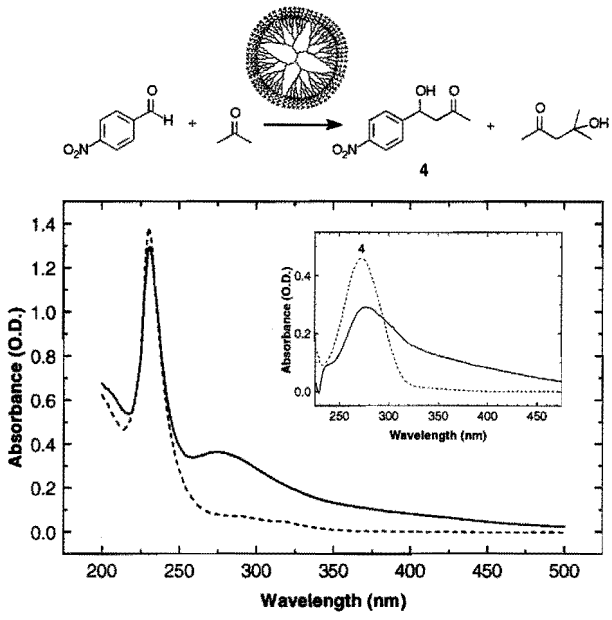

Figure 2.16: *UV/vis spectra* ***3e*** *(—) and* ***3e*** *(- - -) after dialysis, inset shows difference spectrum (—) and spectrum of* ***4*** *(- - -).*

2.4 Overall Conclusions

The localization of the end groups in dendritic systems is an issue of debate and a subject of many theoretical and experimental studies (see Chapter 1). The position of the end groups is of relevance, since many of the proposed uses of dendrimers rely on the availability of the large amount of neighboring end groups. The flexible nature of most known dendrimers usually implies that the end groups are found throughout the dendrimer volume. Thus, the voids inside the dendrimer are filled up to a certain extent. However, when the end groups can communicate with each other via secondary interactions, the dendritic termini will assemble at the periphery, thereby precluding backfolding.

In the fifth generation poly(propylene imine) dendrimer modified with *N*-*t*-BOC protected L-phenylalanine, the "dendritic box", this communication takes place via H-bonding between the amide and carbamate functions present in the outer tier. In combination with the steric bulky *N*-*t*-BOC-L-Phe end group, this results in a rigid shell

around the soft-core interior. As a result, it is possible to encapsulate different functionalities in the dendritic framework. In this way, the physical properties of the dendritic system can be altered in a rather broad range, resulting in for example radical dimer or photosensitizer containing dendrimers. The only restriction for encapsulation is some affinity of the guest for the polar basic interior.

Using sterically less demanding end groups (*N*-*t*-BOC-Gly instead of *N*-*t*-BOC-L-Phe), results in a more open ("perforated") shell and consequently a more flexible system, as reflected in a lower T_g and lesser amount of hydrogen bonding. Also the host–guest properties are biased by the size of the end group. For the fifth generation *N*-*t*-BOC-Gly functionalized dendrimer there is interaction possible between guests and the polyamine interior, whereas these interactions are much weaker in the dendritic box species.

2.5 Experimental Section

General Methods and Materials

Poly(propylene imine) dendrimers were kindly provided by DSM, The Netherlands. The *N*-hydroxy succinimide esters of *N*-*t*-BOC-L-phenylalanine and *N*-*t*-BOC-glycine were used as received (Sigma). Tetracyanoquinodimethane and 3,3'-diamino-*N*-methyldipropylamine were used without further purification (Aldrich). DEMI-3CNQ was kindly provided by Dr. G. H. Cross. Pheophorbide a was provided by Prof. B. Rheiner. All solvents were of p.a. quality except dichloromethane which was purified and dried following standard procedures. Merck silica gel 60 (particle size 0.063-0.200 mm) was used for column chromatography. UV/vis measurements were performed on a Perkin Elmer Lambda 3B UV/vis spectrophotometer or an UV/vis/NIR Perkin Elmer Lambda 900 spectrophotometer. CD-spectra were taken on a JASCO J-600 spectropolarimeter. GC-MS was performed on a Shimadzu GCMS-QP5000 equipped with a WCOT fused silica column (length 15 m, ID = 0.25 mm, coated with CP-sil 8 CB, DF = 0.10 μm). Differential scanning calorimetry (DSC) measurements were performed using a Perkin Elmer Pyris 1 DSC with a heating rate of 20 $Kmin^{-1}$. EI-MS spectra were obtained using the direct insert probe on the GCMS-QP5000. MALDI-TOF MS spectra were performed at the Max Planck Institute for Polymer Research in Mainz using a dithranol matrix.

EPR Spectroscopy

EPR spectra were recorded using a Bruker ER200D SRC spectrometer, operating with an X-band standard cavity and interfaced to a Bruker Aspect 3000 data system. Temperature was controlled by a Bruker ER4111 variable temperature unit between 100 and 400 K. Samples were flushed with He to remove molecular oxygen and kept under constant He atmosphere during measurements. Simulations were performed with NIEHS WinSim EPR, version 0.95.

NMR Spectroscopy

^1H and ^{13}C NMR spectra were recorded on a Bruker AM-400, a Varian Gemini equipped with a variable temperature unit, and a Varian Mercury 400 spectrometer operating at proton frequencies of 400 MHz, 300 MHz, and 400 MHz, respectively. Chemical shifts are given in ppm (δ) relative to TMS. NOESY spectra were recorded on a Varian Mercury 400 with mixing times of 100 ms.

IR Spectroscopy

Infrared spectra were recorded on a Perkin Elmer 1605 IR spectrophotometer operating between 4400 and 450 cm^{-1} using KBr pellets or a 1 mm cell with NaCl windows. Extinction-coefficients were obtained after subtracting of solvent-spectrum by integration of a fitted Gaussian curve.

X-Ray Crystallography

The X-ray diffraction pattern was taken using Mo Kα radiation and a multi-wire area detector X-1000 coupled with a graphite monochromator. Crystal data for **1a**: $C_{44}H_{84}N_{10}O_{12}.2CH_2Cl_2$, colorless crystals with orthorhombic spacegroup *Aba*2 (no. 41) with a = 22.942(4), b = 24.674(11), c = 10.775(4) Å, V = 6099(4) Å^3, Z = 4, 13406 reflections measured, (150 K, Mo Kα radiation, 0.89° < θ < 27.5°) of which 3413 are independent. The structure was solved by automated direct methods (SHELXS96). Refinement on F^2 (SHELXL-97), 331 parameters, with H-atoms at calculated positions. $wR2$ = 0.1384, $R1$ = 0.0546 for 2856 $I > 2\sigma(I)$, S = 1.046, $w = 1/[\sigma^2(F^2) + (0.0658P)^2 + 4.35P]$, with $P = (\mathrm{Max}(F_o^2, 0) + 2F_c^2)/3$. No residual density was found outside -0.50 and 0.47 e Å^{-3}.

Time-Resolved Fluorescence Spectroscopy and Singlet Oxygen Luminescence

Time-resolved spectroscopy and singlet oxygen luminescence[67] have been measured at Humboldt University in Berlin. For the measurement of time resolved fluorescence and rotational fluorescence anisotropy the aperture for time-correlated single photon counting (TCSPC) was used.[68] All measurements have been performed at concentrations of 10^{-5} – 10^{-6} mol/l to reach an OD of 0.2 at the excitation wavelength of 668 nm. The luminescence intensity I of singlet oxygen is given by:

$$I = \gamma * k_r * \tau_\Delta * \Phi_\Delta * (1-10^{-OD}) * I_{ex}$$

where k_r is the rate constant of radiative transitions, I_{ex} is the intensity of excitation, γ is a constant factor of the equipment, τ_Δ is the lifetime of singlet oxygen, OD is the optical density at excitation wavelength and Φ_Δ is the calculated quantum yield . Two different methods have been used to determine Φ_Δ, in method a the amplitude of the singlet oxygen luminescence signal, obtained by time resolved luminescence measurement, is compared with the amplitude of a reference sample with known singlet oxygen quantum yield. In method b the quotient of the steady state singlet oxygen signal and of the singlet oxygen decay time is compared with the quotient of a sample with known quantum yield. An ethanolic solution of TPP was used as reference.

Preparation

TCNQ@DAB-*dendr*-(NH-*t*-BOC-L-Phe)$_{64}$

To a stirred solution of 118 mg ($1.65\cdot10^{-5}$ mol) DAB-*dendr*-$(NH_2)_{64}$ and 0.1 mL triethylamine in 10 mL dichloromethane was added 14 mg of tetracyanoquinodimethane ($6.9\cdot10^{-5}$ mol, 4.2 equiv.). After 1 hour, 1.01 equivalents (386 mg, 1.07 mmol) of *N*-t-BOC-L-phenylalanine hydroxy succinimide ester was added to the turbid greenish reaction mixture. The reaction was stirred overnight and the resulting clear green solution was washed with water (3x) and subsequently with saturated aqueous Na_2CO_3 solution (3x). Adhered $TCNQ^{\bullet-}$ was removed from the dendritic box by dialyzing the sample in an acetone/water mixture (95/5 by volume). Yield: 160 mg (42%). ^{1}H NMR ($CDCl_3$, 400 MHz) δ 8.0 (64H, N*H*COCHPh), 7.1 (320 H, Phenyl), 6.0 (64H, N*H*COO), 4.6 (64 H, COC*H*NH), 3.3 (128 H, CH_2CH_2NHCO), 3.0 (128H, $CHCH_2Ph$), 2.4-2.0 (376 H, $N(CH_2)_3$), 1.5 (252H, CH_2CH_2NH), 1.3 (570H, $C(CH_3)_3$). UV/vis (CH_2Cl_2, nm (log ε)): λ_{max} 315 (4.28), 615 (3.96), 663 (4.00) nm. IR (KBr,cm^{-1}): ν 3323 (NH), 2977, 2185 (CN), 2128 (CN), 1709 (C=O).

DEMI-3CNQ@DAB-*dendr*-(NH-*t*-BOC-L-Phe)$_{64}$

To a stirred solution of 185 mg ($2.59\cdot10^{-5}$ mol) DAB-*dendr*-$(NH_2)_{64}$ and 0.1 mL triethylamine in 10 mL dichloromethane was added 7 mg of DEMI-3CNQ ($2.5\cdot10^{-5}$ mol, 1.4 equiv.). After 1 hour, 1.01 equivalents (423 mg, 1.17 mmol) of *N*-t-BOC-L-phenylalanine hydroxy succinimide ester was added to the red reaction mixture. The reaction was stirred overnight and the resulting red solution was washed with water (3x) and subsequently with saturated aqueous Na_2CO_3 solution (3x). Yield after dialysis with acetone/water mixture (95/5 v/v): 353 mg. ^{1}H NMR ($CDCl_3$, 400 MHz) δ 8.0 (64H, N*H*COCHPh), 7.1 (320 H, Phenyl), 6.0 (64H, N*H*COO), 4.6 (64 H, COC*H*NH), 3.3 (128 H, CH_2CH_2NHCO), 3.0 (128H, $CHCH_2Ph$), 2.4-2.0 (376 H, $N(CH_2)_3$), 1.5 (252H, CH_2CH_2NH), 1.3 (570H, $C(CH_3)_3$). UV/vis (CH_2Cl_2, nm (log ε)): λ_{max} 488 (3.59) nm.

Chlorin e_6@DAB-*dendr*-(NH-*t*-BOC-L-Phe)$_{64}$

In a typical procedure, 77 mg ($1.1\cdot10^{-5}$ mol) fifth generation poly(propylene imine) dendrimer in a dichloromethane/methanol mixture (4/1 v/v) was added to a stirred solution of 14 mg pheophorbide a ($2.4\cdot10^{-5}$ mol; 2.2 equivalents). After 30 minutes, 280 mg *N*-t-BOC-L-phenylalanine hydroxy succinimide ester (0.69 mmol; 1.01 eq) was added. The reaction was stirred for 6 hours and subsequently washed with 1N aqueous NaOH, saturated aqueous Na_2CO_3 solution (2x) and water. After drying in vacuo, the organic fraction was redissolved in 5 mL DMF and three times dialysed against 500 mL DMF. The contents of the

dialysis bag was dried in vacuo, redissolved in 5 mL methanol and two times dialyzed against 500 mL methanol. Evaporating of the solvent, redissolving in dichloromethane and drying over anhydrous Na_2SO_4 followed by drying in vacuo, resulted in 60 mg (24%) of a green glass. ^{1}H NMR ($CDCl_3$, 400 MHz) δ 8.0 (64H, N*H*COCHPh), 7.1 (320 H, Phenyl), 6.0 (64H, N*H*COO), 4.6 (64 H, COC*H*NH), 3.3 (128 H, CH_2CH_2NHCO), 3.0 (128H, $CHCH_2Ph$), 2.4-2.0 (376 H, $N(CH_2)_3$), 1.5 (252H, CH_2CH_2NH), 1.3 (570H, $C(CH_3)_3$). Signals belonging to encapsulated dye: δ 9.6 and 8.8 (methine protons), 3.7, 3.6, 3.5, -1.65 and -1.85 (NH). UV/vis (CH_2Cl_2, nm): λ_{max} 406, 504, 668 nm. IR: (KBr, cm^{-1}): ν 3309 (NH), 1698 (C=O), 1655 (C=O) 1654, 1526 (CONH). The dendritic boxes were obtained with different loads of pheo, depending on the ratio of dye to dendrimer, see Table 2.3.

Table 2.3: *Loadings of dendritic boxes with chlorin e6.*

Batch	equivalents offered	equivalents encapsulated	
		NMR[a]	vis[b]
A	0.9	0.25	0.24
B	1.6	0.36	0.54
C	2.2	0.47	0.52
D	4.4	1.20	1.22
E	5.9	1.20	1.20

a) based on comparing integrals of methine-protons with those of the *t*-BOC-L-Phe-endgroup; b) based on extinction coefficient $Q_y(0,0)$ band (668 nm).

Separation mixture DAB-*dendr*-(NH-*t*-BOC-L-Phe)$_{64}$ with pheo.

To a stirred solution of 45 mg DAB-*dendr*-(NH-*t*-BOC-L-Phe)$_{64}$ in a dichloromethane/methanol mixture (4/1 v/v) was added 2 mg pheo (1.8 equivalents). After stirring for 4 hours the reaction was worked up as described for the encapsulation of pheo. UV/vis recorded in dichloromethane showed absorptions belonging to dendritic box only.

DAB-*dendr*-$(NH_2)_4$ with pheo

To a stirred solution of 4 mg DAB-*dendr*-$(NH_2)_4$ ($1.3 \cdot 10^{-5}$ mol) in a dichloromethane/methanol mixture (4/1 v/v) was added 29 mg pheo ($5.0 \cdot 10^{-5}$ mol, 4 equivalents). After stirring for 12 hours the reaction mixture was dried in vacuo followed by dissolving in dichloromethane and washing with aqueous saturated ammoniumchloride solution (2x), and brine (1x). All water fractions were colorless, the organic fraction was evaporated to dryness. ^{1}H NMR ($CDCl_3$, 400 MHz) showed spectrum belonging to pheo.[69]

General Procedure for 1-3

The *N*-*t*-BOC-glycine functionalized poly(propylene imine) dendrimers were obtained by the reaction of the polyamines with 1.01 equivalent of the *N*-*t*-BOC-glycine *N*-hydroxy succinimide ester in dichloromethane. After 12 h an aqueous solution of 1 N sodium hydroxide was added and the two phase system was stirred for an hour to hydrolyze the excess of activated ester, followed by a base extraction with a saturated aqueous sodium carbonate solution and a washing with water. The organic phase was dried (Na_2SO_4) and concentrated in vacuo, resulting in white glasses for each generation.

Propylcarbamoylmethyl-carbamic acid *t*-butyl ester, 1[70]

Chemical yield: 72%. ^{1}H NMR ($CDCl_3$, 300 MHz): δ 6.53 (1, br.t., CH_2NHCO), 5.48 (1, br.t., N*H*COO), 3.72 (2H, m, $COCH_2NH$), 3.15 (2H, m, CH_2CH_2NH), 1.48 (2H, m, CH_3CH_2), 1.37 (9, s, $C(CH_3)_3$), 0.82 (3H, t, CH_3CH_2). ^{13}C NMR ($CDCl_3$, 75 MHz): δ 169.5, 158.4, 79.9, 44.2, 41.0, 28.2, 24.8, 22.6. IR (CH_2Cl_2,cm^{-1}): ν 3435w (NH), 1711s,b (C=O), 1673s,b (C=O), 1513s,b, 1368m, 1165s. EI-MS: *m/z* 216 $[M^+]^+$.

Bis-(*N*-propylcarbamoylmethyl-carbamic acid *t*-butyl ester)-methylamine, 2

Chemical yield: 90%. ^{1}H NMR ($CDCl_3$, 300 MHz): δ 7.2 (2H, br.t., $NHCOCH_2$), 5.7 (2H, br.t. N*H*COO), 3.7 (4H, br.t., $COCH_2NH$), 3.3 (4H, br.t., $CH_2NHCOCH_2$), 2.3 (4H, t, CH_3NCH_2), 2.1 (3H, s CH_3N), 1.6 (4H, m, $NCH_2CH_2CH_2N$), 1.3 (18H, s, $C(CH_3)_3$). ^{13}C NMR ($CDCl_3$, 75 MHz): δ 170.4, 156.8, 80.3, 56.2, 44.8, 42.2, 38.6, 28.8, 27.0. IR (CH_2Cl_2,cm^{-1}): ν 3435w (NH), 3320w (NH), 1711s,b (C=O), 1673s,b (C=O), 1513s,b, 1368m, 1165s. EI-MS: *m/z* 459 $[M^+]^+$.

DAB-*dendr*-(NH-*t*-BOC-glycine)$_4$, 3a
Chemical yield: 75%. ^{1}H NMR ($CDCl_3$, 300 MHz): δ 7.3 (4H, br.t., N*H*COCH$_2$), 5.8 (4H, br.t. N*H*COO), 3.8 (8H, m, COC*H*$_2$NH), 3.3 (8H, br.t., C*H*$_2$NHCOCH$_2$), 2.4 (12H, br.t., N(C*H*$_2$)$_3$), 1.6 (12H, m, NCH$_2$C*H*$_2$CH$_2$NH, NCH$_2$C*H*$_2$CH$_2$N, NCH$_2$C*H*$_2$C*H*$_2$CH$_2$N), 1.3 (36H, br.s., C(C*H*$_3$)$_3$). ^{13}C NMR ($CDCl_3$, 75 MHz): δ 169.7, 155.6, 79.3, 53 - 50, 43.8, 37.7, 28.0, 26.4, 24.2. IR (CH_2Cl_2,cm^{-1}): ν 3435w (NH), 3320w (NH), 1711s,b (C=O), 1673s,b (C=O), 1513s,b, 1368m, 1165s. MALDI-MS: *m/z* 946 [M+H]$^+$.

DAB-*dendr*-(NH-*t*-BOC-glycine)$_8$, 3b
Chemical yield: 90%. ^{1}H NMR ($CDCl_3$, 300 MHz): δ 7.4 (8H, br.t., N*H*COCH$_2$), 5.9 (8H, br.t. N*H*COO), 3.8 (16H, m, COC*H*$_2$NH), 3.2 (16H, br.t., C*H*$_2$NHCOCH$_2$), 2.3 (36H, br.t., N(C*H*$_2$)$_3$), 1.5 (28H, m, NCH$_2$C*H*$_2$CH$_2$NH, NCH$_2$C*H*$_2$CH$_2$N, NCH$_2$C*H*$_2$C*H*$_2$CH$_2$N), 1.3 (72H, br.s., C(C*H*$_3$)$_3$). ^{13}C NMR ($CDCl_3$, 75 MHz): δ 169.9, 156.2, 79.7, 53 - 50, 44.1, 37.8, 28.3, 26.7, 24.9. IR (CH_2Cl_2,cm^{-1}): ν 3435w (NH), 3320w (NH), 1711s,b (C=O), 1673s,b (C=O), 1513s,b, 1368m, 1165s. MALDI-MS: *m/z* 2031 [M+H]$^+$.

DAB-*dendr*-(NH-*t*-BOC-glycine)$_{16}$, 3c
Chemical yield: 88%. ^{1}H NMR ($CDCl_3$, 300 MHz) δ 7.5 (16H, br.t., N*H*COCH$_2$), 5.9 (16H, br.t. N*H*COO), 3.7 (32H, m, COC*H*$_2$NH), 3.2 (32H, br.t., C*H*$_2$NHCOCH$_2$), 2.4 (168H, br.t., N(C*H*$_2$)$_3$), 1.5 (60H, m, NCH$_2$C*H*$_2$CH$_2$NH, NCH$_2$C*H*$_2$CH$_2$N, NCH$_2$C*H*$_2$C*H*$_2$CH$_2$N), 1.3 (144H, br.s., C(C*H*$_3$)$_3$). ^{13}C NMR ($CDCl_3$, 75 MHz) δ 169.9 (NH*C*OCH$_2$), 156.1 (NH*C*OO), 79.5 (*C*(CH$_3$)$_3$), 53 - 50 (N(*C*H$_2$)$_3$), 43.1 (COCH$_2$NH), 37.5 (CH$_2$NHCOCH$_2$), 28.4 (C(*C*H$_3$)$_3$), 26.6 (NCH$_2$CH$_2$CH$_2$NHCO), 22.9 (NCH$_2$CH$_2$CH$_2$N, NCH$_2$CH$_2$CH$_2$CH$_2$N). IR (CH_2Cl_2,cm^{-1}): ν 3435w (NH), 3320w (NH), 1711s,b (C=O), 1673s,b (C=O), 1513s,b, 1368m, 1165s. MALDI-MS: *m/z* 4200 [M+H]$^+$, 2129.

DAB-*dendr*-(NH-*t*-BOC-glycine)$_{32}$, 3d
Chemical yield: 91%. ^{1}H NMR ($CDCl_3$, 300 MHz) δ 7.5 (32H, br.t., N*H*COCH$_2$), 6.1 (32H, br.t. N*H*COO), 3.7 (64H, m, COC*H*$_2$NH), 3.2 (64H, br.t., C*H*$_2$NHCOCH$_2$), 2.3 (180H, br.t., N(C*H*$_2$)$_3$), 1.5 (126H, m, NCH$_2$C*H*$_2$CH$_2$NH, NCH$_2$C*H*$_2$CH$_2$N, NCH$_2$C*H*$_2$C*H*$_2$CH$_2$N), 1.3 (288H, br.s., C(C*H*$_3$)$_3$). ^{13}C NMR ($CDCl_3$, 75 MHz) δ 169.9 (NH*C*OCH$_2$), 156.1 (NH*C*OO), 79.5 (*C*(CH$_3$)$_3$), 53 - 50 (N(*C*H$_2$)$_3$), 43.9 (COCH$_2$NH), 37.6 (CH$_2$NHCOCH$_2$), 29.2 (C(*C*H$_3$)$_3$), 26.6 (NCH$_2$CH$_2$CH$_2$NHCO), 24.1 (NCH$_2$CH$_2$CH$_2$N, NCH$_2$CH$_2$CH$_2$CH$_2$N). IR(CH_2Cl_2,cm^{-1}): ν 3435w (NH), 3320w (NH), 1711s,b (C=O), 1673s,b (C=O), 1513s,b, 1368m, 1165s. MALDI-MS: *m/z* 8541 [M+H]$^+$, 4298, 2074, 989.

DAB-*dendr*-(NH-*t*-BOC-glycine)$_{64}$, 3e
Chemical yield: 70%. ^{1}H NMR ($CDCl_3$, 300 MHz) δ 7.6 (64H, br.t., N*H*COCH$_2$), 6.2 (64H, br.t. N*H*COO), 3.8 (128H, m, COC*H*$_2$NH), 3.2 (64H, br.t., CH$_2$NHCOCH$_2$), 2.4 (360H, br.t., N(C*H*$_2$)$_3$), 1.5 (252H, m, NCH$_2$C*H*$_2$CH$_2$NH, NCH$_2$C*H*$_2$CH$_2$N, NCH$_2$C*H*$_2$C*H*$_2$CH$_2$N), 1.3 (570H, br.s., C(C*H*$_3$)$_3$). ^{13}C NMR ($CDCl_3$, 75 MHz) δ 171.1 (NH*C*OCH$_2$), 156.2 (NH*C*OO), 79.4 (*C*(CH$_3$)$_3$), 53 - 50 (N(*C*H$_2$)$_3$), 45.3 (COCH$_2$NH), 38.3 (CH$_2$NHCOCH$_2$), 29.2 (C(CH3)3), 27.4 (NCH$_2$CH$_2$CH$_2$NHCO), 25.2 (NCH$_2$CH$_2$CH$_2$N, NCH$_2$CH$_2$CH$_2$CH$_2$N). IR(CH_2Cl_2,cm^{-1}): ν 3435w (NH), 3320w (NH), 1711s,b (C=O), 1673s,b (C=O), 1513s,b, 1368m, 1165s. MALDI-MS: *m/z* 17229 [M+H]$^+$with severe tailing to lower masses, 8497, 4246.

Aldol Condensations with Functionalized Dendrimers

In a typical procedure 14 mg ($8.1 \cdot 10^{-7}$ mol) **3e** was dissolved in 3 mL acetone. To the stirred reaction mixture 9 mg ($6.0 \cdot 10^{-5}$ mol) *p*-nitro benzaldehyde was added. After 24 h stirring at room temperature, the reaction mixture was dialysed against acetone/water (95/5 v/v) until no further differences in UV/vis were observed.

2.6 References and Notes

1. Maciejewski, M. *J. Macromol. Sci. —Chem.* **1982**, *17A*, 689–703.
2. Naylor, A. M.; Goddard, W. A., III; Kiefer, G. E.; Tomalia, D. A. *J. Am. Chem. Soc.* **1989**, *111*, 2339–2341. Tomalia, D. A.; Naylor, A. M.; Goddard, W. A., III; *Angew. Chem., Int. Ed. Engl.* **1990**, *29*, 138–175.

3. Jansen, J. F. G. A.; de Brabander-van den Berg, E. M. M.; Meijer, E. W. *Science* **1994**, *265*, 1226–1229.
4. Jansen, J. F. G. A.; de Brabander-van den Berg, E. M. M.; Meijer, E. W. *New molecular architectures and functions, Proceedings of the OUMS 1995*, Toyonaka, Osaka, Japan 2–5 June, 1995, Springer-Verlag, Berlin Heidelberg, **1996**.
5. Miklis, P.; Çagin, T.; Goddard III, W. A. *J. Am. Chem. Soc.* **1997**, *119*, 7458–7462.
6. Cavallo, L.; Fraternali, F. *Chem. Eur. J.* **1998**, *4*, 927–934.
7. Jansen, J. F. G. A.; Peerlings, H. W. I.; de Brabander-van den Berg, E. M. M.; Meijer, E. W. *Angew. Chem., Int. Ed. Engl.* **1995**, *34*, 1206–1209.
8. Peerlings, H. W. I.; Meijer, E. W. *Chem. Eur. J.* **1997**, *3*, 1563–1570.
9. Peerlings, H. W. I. *Ph.D. Thesis*, University of Technology Eindhoven, Sept. **1998**.
10. Jansen, J. F. G. A.; Meijer, E. W. *J. Am. Chem. Soc.* **1995**, *117*, 4417–4418.
11. Jansen, J. F. G. A.; Meijer, E. W. *Macromol. Symp.*, **1996**, *102*, 27–33.
12. Encapsulated species are specified by the @-symbol.
13. Jansen, J. F. G. A.; de Brabander-van den Berg, E. M. M.; Meijer, E. W. *Recl. Trav. Chim. Pays-Bas* **1995**, *114*, 225–230.
14. Jansen, J. F. G. A.; Janssen, R. A. J.; de Brabander-van den Berg, E. M. M.; Meijer, E. W. *Adv. Mater.* **1995**, *7*, 561–564.
15. Gutmann, F.; Lyons, L. E. *Organic Semiconductors*, Krieger Publishing Co.: Malabar, Florida, 1981, Part A, pp. 463.
16. Melby, L. R.; Harder, R. J.; Hertler, W. R.; Mahler, W.; Benson, R. E.; Mochel, W. E. *J. Am. Chem. Soc.* **1962**, *84*, 3374–3387.
17. Janssen, R. A. J.; Jansen, J. F. G. A.; van Haare, J. A. E. H.; Meijer, E. W. *Adv. Mater.* **1996**, *8*, 494–496.
18. Bryce, M. R.; de Miguel, P.; Devonport W. *Chem. Commun.* **1998**, 2565–2566.
19. Boyd, R. H.; Phillips, W. D. *J. Chem. Phys.* **1965**, *43*, 2927–2929.
20. Sakata, T.; Nakane, A. Tsubomura, H. *Bull. Chem. Soc. Japan* **1975**, *48*, 3391–3392.
21. Becket, J. L.; Hartzell, C. J.; Eastman, N. L.; Blake T.; Eastman, M. P. *J. Org. Chem.* **1992**, *57*, 4173–4179.
22. Szablewski, M. *J. Org. Chem.* **1994**, *59*, 954–956.
23. Thornton, A.; Bloor, D.; Cross, G. H.; Szablewski, M. *Macromolecules* **1997**, *30*, 7600–7603.
24. Szablewski, M.; Cross, G. H. *personal communication.*
25. Issberner, J.; Moors, R.; Vögtle, F. *Angew. Chem., Int. Ed.* **1994**, *33*, 2413–2420. Smith, D. K.; Diederich, F. *Chem. Eur. J.* **1998**, *4*, 1353–1361. Bosman, A. W.; Janssen, H. M.; Meijer, E. W. *Chem. Rev.* **1999**, accepted.
26. Bhyrappa, P.; Young, J. K.; Moore, J. S.; Suslick, K. S. *J. Am. Chem. Soc.* **1996**, *118*, 5708–5711.
27. Jin, R.-H.; Aida, T.; Inoue, S. *J. Chem. Soc., Chem. Commun.* **1993**, 1260–1262. Sadamoto, R.; Tomioka, N.; Aida, T. *J. Am. Chem. Soc.* **1996**, *118*, 3978–3979. Tomoyose, Y. T.; Jiang, D.-L.; Jin, R.-H.; Aida, T.; Yamashita, T.; Horie, K.; Yashima, E.; Okamoto, Y. *Macromolecules* **1996**, *29*, 5236–5238. Jiang, D.-L.; Aida, T. *J. Am. Chem. Soc.* **1998**, *120*, 10895–10901.
28. Dandliker, P. J.; Diederich, F.; Gross, M.; Knobler, C. B.; Louati, A.; Sanford, E. M., *Angew. Chem., Int. Ed. Engl.* **1994**, *33*, 1739–1742. Dandliker, P. J.; Diederich, F.; Gisselbrecht, J.-P.; C. B.; Louati, A.; Gross, M. *Angew. Chem., Int. Ed. Engl.* **1995**, *34*, 2725–2728. Dandliker, P. J.; Diederich, F.; Zingg, A.; Gisselbrecht, J.-P.; Gross, M.; Louati, A.; Sanford, E. *Helv. Chim. Acta* **1997**, *80*, 1773–1801.
29. Jiang, D.-L.; Aida, T. *Chem. Commun.* **1996**, 1523–1524. Jiang, D.-L.; Aida, T. *J. Mater. Sci. —Pure Appl. Chem.* **1997**, *A34*, 2047–2055. Collman, J. P.; Fu, L.; Zingg, A.; Diederich, F. *Chem. Commun.* **1997**, 193–194.
30. Dolphin, D. *Can. J. Chem.* **1993**, *72*, 1005–1013. Bonnet, R. *Chem. Soc. Rev.* **1995**, 19–33.
31. Shulok, J. R.; Wade, M. H.; Lin, C.-W. *Photochem. Photobiol.* **1990**, *51*, 451–457.
32. Allison, B. A.; Pritchard, P. H.; Levy, J. G. *Br. J. Cancer* **1994**, *69*, 833–839.
33. Janssen, J., Undergraduate report, University of Technology, Eindhoven, August 1995.
34. Amidation of the sp^3 carbon on ring V of pheo is described in: Weller, A.; Livingston, R. *J. Am. Chem. Soc.* **1954**, *76*, 1575–1578. Pennington, F. C.; Boyd, S. D.; Horton, H.; Taylor, S. W.; Wulf, D. G.; Katz, J. J.; Strain, H. H. *J. Am. Chem. Soc.* **1967**, *89*, 3871–3875.

35. Koper, G. J. M.; van Genderen, M. H. P.; Elissen-Román, C.; Baars, M. W. P. L.; Meijer, E. W; Borkovec, M. *J. Am. Chem. Soc.* **1997**, *119*, 6512–6521.
36. *The Porphyrins Part I*; Dolphin, D. ed.; London Acad. Press: London, 1978, pp. 324–327.
37. Inhoffen, H. H.; Klotmann, G.; Jeckel, G. *Ann. Chem.* **1966**, *695*, 112–132.
38. Falk, E. J. *Porphyrins and Metalloporphyrins*; Elsevier Sci. Publ.: Amsterdam, 1975.
39. Derome, A. E. in *Modern NMR Techniques for Chemistry Research*; Baldwin, J. E., Magnus, P. D., Eds.; Pergamon Press: Oxford, 1987; pp. 97–127.
40. Briat, B.; Schooley, D. A.; Records, R.; Bunnenberg, E.; Djerassi, C. *J. Am. Chem. Soc.* **1967**, *89*, 6170–6177.
41. Kostenich, G. A.; Zhuravkin, I. N.; Zhavrid, E. A. *J. Photochem. Photobiolog., B. Biol.* **1994**, *22*, 211–217.
42. Roberts, J. C.; Bhalgat, M. K.; Zera, R. T. *J. Biomed. Mater. Res.* **1996**, *30*, 53–65.
43. Posnett, D. N.; McGrath, H.; Tam, J. P. *J. Biol. Chem.* **1988**, *263*, 1719–1725.
44. Newkome, G. R.; Moorefield, C. N.; Baker, G. R.; Saunders, M. J.; Grossman, S. H. *Angew. Chem., Int. Ed. Engl.* **1991**, *30*, 1178–1181.
45. Hawker, C. J.; Wooley, K. L.; Fréchet, J. M. J. *J. Chem. Soc., Perkin Trans. I* **1993**, 1287–1297.
46. Stevelmans, S.; van Hest, J. C. M.; Jansen, J. F. G. A.; van Boxtel, D. A. F. J.; de Brabander-van den Berg, E. M. M.; Meijer, E. W. *J. Am. Chem. Soc.* **1996**, *118*, 7398–7399.
47. Sayed-Sweet, Y.; Hedstrand, D. M.; Spinder, R.; Tomalia, D. A. *J. Mater. Chem.* **1997**, *7*, 1199–1205.
48. Baars, M. W. P. L.; Froehling, P. E.; Meijer, E. W. *Chem. Commun.* **1997**, 1959–1960.
49. Cooper, A. I.; Londono, J. D.; Wignall, G.; McClain, J. B.; Samulski, E. T.; Lin, J. S.; Dobrynin, A.; Rubinstein, M.; Burke, A. L. C.; Fréchet, J. M. J.; DeSimone, J. M. *Nature* **1997**, *389*, 368–371.
50. Mattei, S.; Seiler, P.; Diederich, F.; Gramlich, V. *Helv. Chim. Acta.* **1995**, *78*, 1904–1912. Wallimann, P.; Seiler, P.; Diederich, F. *Helv. Chim. Acta.* **1996**, *79*, 779–788. Wallimann, P.; Seiler, P.; Diederich, F. *Helv. Chim. Acta.* **1996**, *79*, 779–788. Wallimann, P.; Mattei, S.; Seiler, P.; Diederich, F. *Helv. Chim. Acta.* **1997**, *80*, 2368–2390. Mattei, S.; Walliman, P.; Kenda, B.; Amrein, W.; Diederich, F. *Helv. Chim. Acta.* **1997**, *80*, 2391–2417.
51. Weener, J. W.; van Dongen, J. L. J.; Hummelen, J. C.; Meijer, E. W. *Proc. ACS. PMSE.*, **1997**, *77*, 147–148. Weener, J. W.; van Dongen, J. L. J.; Meijer, E. W. *submitted to J. Am. Chem. Soc.*
52. Néel, J. *Pure Appl. Chem.* **1972**, *31*, 201–225.
53. Ferguson, G.; Gallagher, J. F.; McKervey, M. A.; Madigan, E. *J. Chem. Soc., Perkin Trans. 1* **1996**, 599–602. Karakaya, B; Claussen, W.; Gessler, K.; Saenger, W.; Schlüter, A.-D. *J. Am. Chem. Soc.* **1997**, *119*, 3296–3301.
54. Seyferth, D.; Son, D. Y.; Rheingold, A. L.; Ostrander, R. L. *Organometallics* **1994**, *13*, 2682–2690. Sekiguchi, A.; Nanjo, M.; Kabuto, C.; Sakurai, H. *J. Am. Chem. Soc.* **1995**, *117*, 4195–4196. Jaffrès, P.-A.; Morris, R. E. *J. Chem. Soc., Dalton Trans.* **1998**, 2767–2770. Nanjo, M.; Sekiguchi, A. *Organometallics* **1998**, *17*, 492–494.
55. Gellman, S. H.; Dado, G. P.; Liang, G.-B.; Adams, B. R. *J. Am. Chem. Soc.* **1991**, *113*, 1164–1173.
56. For determination of amount of hydrogen bonding see: Gardner, R.R.; Gellman, S. H. *J. Am. Chem. Soc.* **1995**, *117*, 10411–10412.
57. Highly concentrated solution, however, showed a small increase of H-bonding, but only for the modelcompounds and the lower generations **3a-c**.
58. Katritzky, A. R.; Jones, R. A. *J. Chem. Soc.* **1959**, 2067–2071. *ibid.* **1960**, 676–679.
59. Bandekar, J. *Biochim. et Biophys. Acta* **1992**, *1120*, 123–143.
60. Put, E. J. H.; Clays, K.; Persoons, A.; Biemans, H. A. M.; Luijkx, C. P. M.; Meijer, E. W. *Chem. Phys. Lett.* **1996**, *269*, 136–141.
61. Levitt, M.; Perutz, M. *J. Mol. Biol.* **1988**, *201*, 751–754. Rodham, D. A.; Suzuki, S.; Suenram, R. D.; Lovas, F. J.; Dasgupta, S.; Goddard, W. A., III; Blake, G. A. *Nature*, **1993**, *362*, 735–737. Adams, H.; Harris, K. D. M.; Hembury, G. A.; Hunter, C. A.; Livingstone, D.; McCabe, J. F.; *Chem. Commun.* **1996**, 2531–2532.
62. Fong, T. M.; Cascieri, M. A.; Yu, H.; Bansal, A.; Swain, C.; Strader, C. D. *Nature* **1993**, *362*, 350–353. Mitchell, J. B. O.; Nandi, C. L.; Ali, S.; McDonald, I. K.; Thornton, J. M.; Price, S. L.; Singh, J. *Nature* **1993**, *366*, 413.
63. Cram, D.J.; Tanner, M. E.; Thomas, R. *Angew. Chem., Int. Ed. Engl.* **1991**, *30*, 1024–1027. Cram, D. J. *Nature* **1992**, *356*, 29–36.

64. Kusukawa, T.; Fujita, M. *J. Am. Chem. Soc.* **1999**, *121*, 1397–1398.
65. Lei, X.-G.; Doubleday, C. E., Jr.; Zimmt, M. B.; Turro, N. J. *J. Am. Chem. Soc.* **1986**, *108*, 2444–2445.
66. Balogh, L.; Tomalia, D. A. *J. Am. Chem. Soc.* **1998**, *120*, 7355-7356.
67. Spiller, W.; Kliesch, H.; Wöhrle; Hackbarth, S.; Röder, B.; Schnurpfeil, G. *J. Porphyrins Phthalocyanines* **1998**, *2*, 145–158.
68. Röder, B.; Zimmermann, C.; Herter, R. *S.P.I.E. Proc.* **1994**, *2325*, 80–91.
69. Closs, G. L.; Katz, J. J.; Pennington, F. C.; Thomas, M. R.; Strain, H. H. *J. Am. Chem. Soc.* **1963**, *83*, 3809–3821.
70. Synthesis is also described in: Tamiaki, H.; Kiyomori, A.; Maruyama, K. *Bull. Chem. Soc. Jpn.* **1993**, *66*, 1768–1772.

Nitroxyl-Functionalized Dendrimers*

3

Abstract: *The preparation and EPR spectroscopy of a series of fully functionalized poly(propylene imine) dendrimers (DAB-dendr-$(NH_2)_n$; n = 2, 4, 8, 16, 32, 64) with 3-carboxy-PROXYL radical end groups is described. The pendant nitroxyl end groups exhibit a strong exchange interaction. As a consequence, the EPR spectrum directly reveals the number of end groups from the splitting between the hyperfine transitions for the lower generations. For the higher generations an increasingly exchanged-narrowed EPR spectrum is observed. The temperature and solvent dependency of the exchange interaction is used to assess the dynamic behavior of the dendritic branches. IR spectroscopy shows that a hydrogen-bonded network between the amide functionalities is present, consistent with the observed solvent effect on the EPR spectra. Additionally, formation of intramolecular hydrogen bonding is investigated in a homologous series of bis-PROXYLs with different spacer lengths.*

* Part of this work has been published: Bosman, A.W.; Janssen, R. A. J.; Meijer, E.W. *Macromolecules* **1997**, *30*, 3606-3611.

3.1 Introduction

Combination of the globular structure of dendrimers with functional properties is one of the focal points of current research in dendritic molecules.[1] This interest is motivated by the recognition that the controlled branching of dendritic structures may provide a three-dimensional architecture that allows functional groups to be incorporated in a geometrically well-defined fashion. However, not only the architecture is important for understanding the properties of dendrimers, but also the interaction between the pendant functional groups at the exterior of the dendritic surface as well as their dynamic behavior.

An increasing number of dendrimers is being functionalized with stable organic radicals or redox active groups, aiming at molecules or materials with a wide variety of functional properties. Living radical polymerization of vinyl monomers has been performed with different generations of poly(benzyl ether) dendrons attached to a stable nitroxyl radical core.[2] High-spin molecules formed from organic radicals incorporated into a π-conjugated hyperbranched topology have been studied in relation to future organic magnetic materials.[3-5] In these molecules, dendritic branching is used to ensure a more robust intramolecular spin alignment than can be obtained in linear or branched structures. Electrical conductivity of PAMAM dendrimers with naphthalene diimide anion radical end groups, forming π–dimers or π–stacks, has been reported.[6] Arborol dendrimers peripherally modified with oligothiophenes also show π–dimerization upon oxidation to the cation radicals.[7] Redox active end groups such as tetrathiafulvenyl[8] and ferrocenyl[9,10] have been attached to the periphery of aromatic polyester and silicon dendrimers, respectively. In these cases, multi-electron oxidation to the corresponding cations could be accomplished, but no evidence was obtained for a significant interaction between the end groups. Although recently, intramolecular π–π interactions in oxidized tetrathiafulvenyl dendrimers based on glycol have been observed.[11]

EPR-spectroscopy has been applied to study the dynamic behavior of dendrimers using paramagnetic probes. PAMAMs containing carboxylate end groups have been probed with Cu(II),[12] Mn(II)[13] and TEMPO-derivatives[14] in aqueous solutions by Ottaviani et al. The authors rationalize their findings by assuming a high mobility of the complexes for the lower generations and a somewhat reduced motion for generations 4.5 and higher. This is explained by a more congested structure for the higher generations. The dynamics of PAMAMs modified at the periphery with the chelating group diethylenetriaminepentaacetic acid (DTPA), have been studied with EPR spectroscopy using vanadyl (VO^{2+}).[15] The dendritic vanadyl-chelate complexes indicate that the rotational correlation times of the end groups increase with generation and reflect the internal segmental motions of the dendrimer.

In analogy to their linear macromolecular counterparts,[16,17] the dynamic behavior of pendant end groups and their mutual interactions can also be probed using EPR spectroscopy when the functional groups are covalently attached stable radicals. In this way, intramolecular interactions can be probed and the possibility of an equilibrium between free and bound radical-probes is ruled out.

Here a first example of five generations of dendrimers with stable radical end groups is described.[18] A series of poly(propylene imine) dendrimers functionalized with 3-carboxy-PROXYL radicals, **3a-e,** and the mono- and biradical analogues **1** and **2** (see Figure 3.1), have been prepared and studied in detail using EPR spectroscopy. The individual nitroxyl radicals at the exterior of the DAB-*dendr*-(NH-3-CO-PROXYL)$_n$ dendrimers are found to exhibit a strong exchange interaction which depends on temperature and solvent, and reflects the dynamic behavior of dendritic branches. Additionally biradical series **4a-d** have been prepared to investigate the influence of spacer length on the exchange interaction.

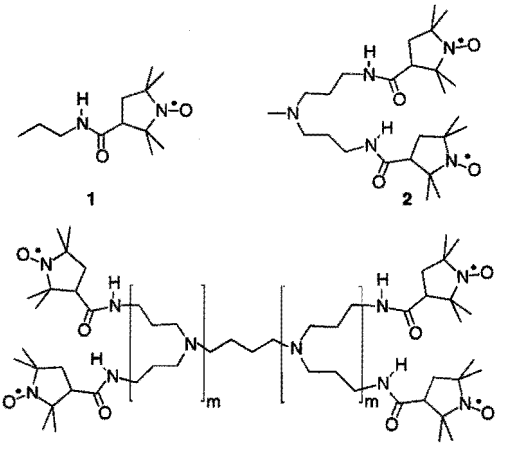

3a-e: DAB-*dendr*-(NH-CO-PROXYL)$_n$ (n = 4, 8, 16, 32, 64; m = ^{2}log(n/2))

Figure 3.1: *The different 3-carboxy-PROXYL-functionalized amines.*

3.2 Synthesis

The preparation of different generations of poly(propylene imine) dendrimers has been described elsewhere.[19] For end-group-functionalization 3-carboxy-2,2,5,5-tetramethyl-1-pyrrolidin-1-oxyl (3-carboxy-PROXYL) was first activated with *N*-hydroxysuccinimide in 1,2-dimethoxyethane in the presence of 1,3-dicyclohexylcarbodiimide. The DAB-*dendr*-(NH_2)$_n$ dendrimers were subsequently

functionalized by reaction with this activated ester in dichloromethane (Scheme 3.1, for n = 16). The resulting DAB-*dendr*-(NH-3-CO-PROXYL)$_n$ dendrimers (**3a-e**, Figure 3.1), with molecular weights up to 19 kgmol^{-1} for the fifth generation, were extensively purified from monoradical impurities using combinations of extraction, column chromatography, precipitation, and dialysis, depending on dendrimer generation. The absence of starting material was checked using IR, monitoring the absence of C=O stretch vibration of free 3-carboxy-PROXYL (1750 cm^{-1}) and its *N*-hydroxysuccinimide ester (1745 cm^{-1}), and checking the presence of the carbonamide vibration (1660 cm^{-1}). Simulation of the experimental EPR spectra (vide infra) demonstrated that after purification less than 3% monoradical was present for **3d**, and less than 1% for all other dendrimers.

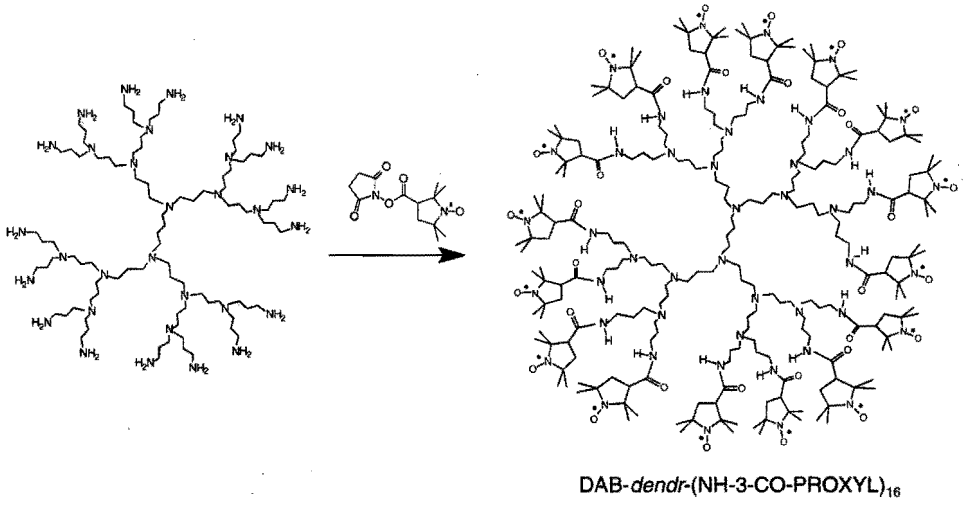

Scheme 3.1: *Synthesis of third generation PROXYL-functionalized poly(propylene imine) dendrimer (**3c**).*

The identity of the DAB-*dendr*-(NH-3-CO-PROXYL)$_n$ dendrimers was confirmed using MALDI-TOF mass spectrometry employing a dithranol matrix. In each case a small deviation between measured and calculated values has been observed. This difference is explained by the partial reduction of the nitroxyl groups to hydroxylamines during sample preparation or ionization, due to presence of electron donors in acidic medium.[20] Next to typical fragmentation products resulting from formation of pyrolidinium or azetidinium based fragments,[21] peaks at lower mass (m/z) values were also found for n = 8 and n = 16 (Figure 3.2) that are possibly due to incomplete product formation (n = 7 and n = 14, and 15, respectively) or post source fragmentation during

the measurement.[22] The two highest generation dendrimers (n = 32 and n = 64) gave signals at the calculated values, but strong tailing to lower masses occurred.

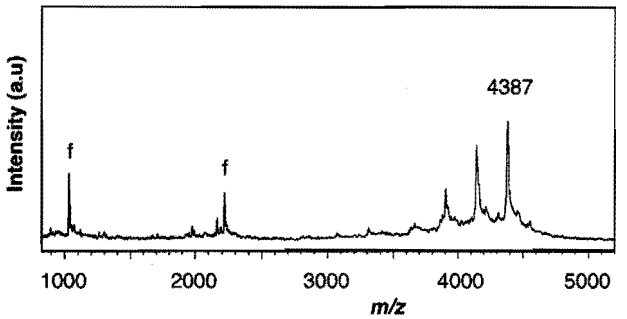

Figure 3.2: *MALDI-TOF mass spectrum of* ***3c*** *showing the partly reduced molecular ion peak at 4387 (see text), peaks due to fragmentation of dendritic framework are labeled with f.*

3.3 EPR Spectroscopy

The EPR spectra of **2** and DAB-*dendr*-(NH-3-CO-PROXYL)$_n$ (n = 4, 8, 16, 32, and 64) dendrimers recorded in oxygen-free *N,N*-dimethylacetamide at 298 and 378 K are shown in Figure 3.3. The EPR spectrum of these polyradicals in a non-viscous solvent can be described with a three-term Hamiltonian:

$$\hat{H} = g\mu_B B_0 \sum_{i=1}^{n} \hat{S}_z^{(i)} + a_N \sum_{i=1}^{n} \hat{I}_z^{(i)} \cdot \hat{S}_z^{(i)} - \sum_{i>j=1}^{n} 2J^{(ij)} \hat{S}^{(i)} \cdot \hat{S}^{(j)} \qquad (1)$$

describing the electron Zeeman interactions, hyperfine coupling a_N, and the exchange interaction J in the definition that when J is negative, the diamagnetic state is the lowest. An important aspect of these polyradicals in solution is the fact that the exchange integrals $J^{(ij)}$ are not constant but a function of the intramolecular conformation. Therefore, the spectrum depends on temperature, viscosity, and nature of the solvent. Before discussing the spectra of the higher generations, it is instructive to look in some detail at the spectral properties for biradical **2**.

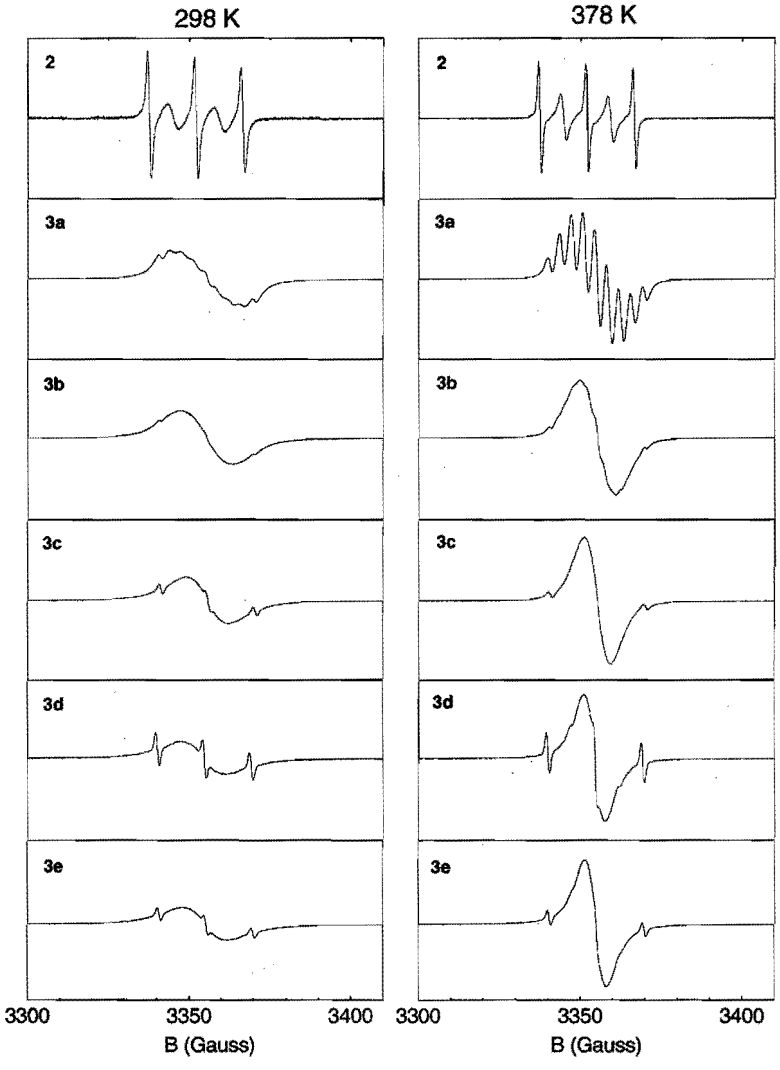

Figure 3.3: *EPR spectra of* ***2*** *and* ***3a-e*** *in N,N-dimethylacteamide recorded at 298 and 378 K.*

The EPR spectra of nitroxyl biradicals and the influence of the exchange interaction on these spectra have been described in detail theoretically.[23-26] Using Hamiltonian (1) and the usual singlet $|S\rangle$ and triplet states $|T_+\rangle$, $|T_0\rangle$, $|T_-\rangle$, the four energy levels for a symmetric nitroxyl biradical (**2**) in any nuclear spin state $|m_1 m_2\rangle$ are described by:

$$|1\rangle = |T_+\rangle \qquad E_1 = g\mu_B B_0 - \tfrac{1}{2}J + \tfrac{1}{2}a_N(m_1 + m_2) \qquad (2)$$

$$|2\rangle = \cos\theta|T_0\rangle + \sin\theta|S\rangle \qquad E_2 = -\tfrac{1}{2}J + \tfrac{1}{2}a_N(m_1 - m_2)\tan\theta$$

$$|3\rangle = -\sin\theta|T_0\rangle + \cos\theta|S\rangle \qquad E_3 = \tfrac{3}{2}J - \tfrac{1}{2}a_N(m_1 - m_2)\tan\theta$$

$$|4\rangle = |T_-\rangle \qquad E_4 = -g\mu_B B_0 - \tfrac{1}{2}J + \tfrac{1}{2}a_N(m_1 + m_2)$$

Where θ is given by:

$$\tan 2\theta = -a_N(m_1 + m_2)/2J \qquad (3)$$

The energies of the transitions, and their intensities, obtained by calculating the matrix elements of the $[\tfrac{1}{2}(\hat{S}^+ + \hat{S}^-)]^2$ operator, are listed in Table 3.1. From the transition energies and their intensities it can be seen that for $|J| << |a_N|$ the spectrum of the biradical is similar to that of two independent monoradicals exhibiting three lines separated by a_N with relative intensities 1:1:1. The other possibility that $|J| >> |a_N|$ gives rise to a five-line hyperfine pattern with a separation of $\tfrac{1}{2}a_N$ and relative intensities of 1:2:3:2:1. These five lines are conveniently labeled with the sum of m_i and m_j (given by M_I = +2, +1, 0, -1, -2). At intermediate values, where $|J| \approx |a_N|$, the spectra are more complex.

Table 3.1: *Transitions and intensities for a nitroxyl biradical.*

transition	energy[a]	intensity[a]
$\|1\rangle \leftrightarrow \|2\rangle$	$g\mu_B B_0 + \tfrac{1}{2}a_N(m_1 + m_2) - \tfrac{1}{2}a_N(m_1 - m_2)\tan\theta$	$\tfrac{1}{2}\cos^2\theta$
$\|1\rangle \leftrightarrow \|3\rangle$	$g\mu_B B_0 - 2J + \tfrac{1}{2}a_N(m_1 + m_2) + \tfrac{1}{2}a_N(m_1 - m_2)\tan\theta$	$\tfrac{1}{2}\sin^2\theta$
$\|2\rangle \leftrightarrow \|4\rangle$	$g\mu_B B_0 + \tfrac{1}{2}a_N(m_1 + m_2) + \tfrac{1}{2}a_N(m_1 - m_2)\tan\theta$	$\tfrac{1}{2}\cos^2\theta$
$\|3\rangle \leftrightarrow \|4\rangle$	$g\mu_B B_0 + 2J + \tfrac{1}{2}a_N(m_1 + m_2) - \tfrac{1}{2}a_N(m_1 - m_2)\tan\theta$	$\tfrac{1}{2}\sin^2\theta$

[a] θ is defined in equation 3

The experimental EPR spectrum of **2** recorded at 298 K (Figure 3.3) exhibits five lines, indicating that $|J| >> |a_N|$ The widths of the five hyperfine lines clearly alternate. The alternating line width at 298 K, and the changes in the spectrum when warming to 378 K, result from the modulation of the exchange interaction *J*, caused by conformational changes of the chain linking the two nitroxyl radicals. The alternating

line width and the changes in the spectrum with temperature can be rationalized (albeit in a somewhat naive model) by assuming the presence of at least two classes of conformers designated with A and B (Figure 3.4), characterized by strongly different exchange interactions. In the extended structure A, the exchange integral J is small compared to the ^{14}N hyperfine coupling ($|J_A| << |a_N|$), whereas in conformation B, with two proximate nitroxyl radicals, a strong exchange interaction is present ($|J_B| >> |a_N|$).

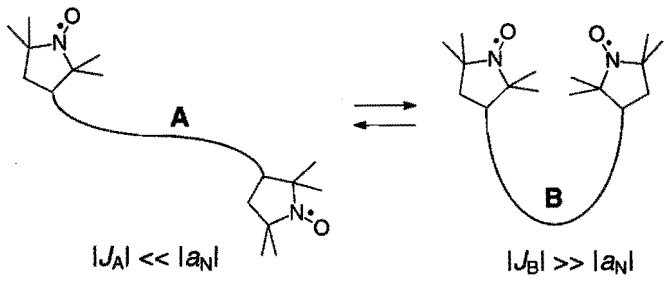

Figure 3.4: *Schematic representation of nitroxyl biradical with two conformations A and B having different exchange interactions J.*

In solution, both classes of conformers will exist and the actual EPR spectrum depends on the values of J_A and J_B and the rate of interconversion between A and B, expressed by the lifetimes τ_A and τ_B.[23–25] When the exchange interaction is rapidly modulated, the broadening of the line widths due to modulation of J in time is given by:[23]

$$T_2^{-1} = \frac{a_N^2 j(2\bar{J})}{16\bar{J}^2}[m_1 - m_2]^2 \qquad (4)$$

where $j(2\bar{J})$ is the spectral density and $\bar{J} = (\tau_A J_A + \tau_B J_B)/(\tau_A + \tau_B)$. This expression shows that of the total of nine nuclear spin functions in a nitroxyl biradical, the three lines corresponding to $m_1 = m_2$ (i.e. $M_I = \pm 2, 0$) are not affected by the modulation of J. In contrast, the widths of the six remaining transitions, for which $m_1 \neq m_2$, are increased. The spectrum exhibits two broader lines for $M_I = \pm 1$ together with a central $M_I = 0$ line (overlapping the sharp central transition) which is broadened by an additional factor of four. The spectra of **2** clearly correspond to this situation as is demonstrated by simulation of the spectra at 298 and 378 K, using this model with a_N = 14.58 Gauss (Figure 3.5). Because the line widths of the $M_I = \pm 1$ transitions decrease with increasing temperature it can be concluded that the modulation of the exchange interaction is fast. If the spectrum at 298 K would correspond to a situation of

slow modulation of exchange interaction, the spectrum would be a superposition of the spectra of the individual conformations A and B, and hence an increase in temperature would affect the line widths much less. Moreover, the ratio of the doubly integrated intensities in the experimental spectra is very close to 1:2:3:2:1, confirming the conclusion of fast modulation of exchange interaction.

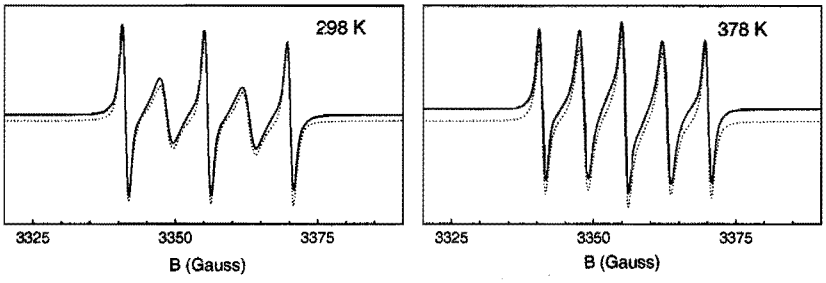

Figure 3.5: *Experimental (solid line) and simulated (dotted line, offset for clarity) EPR spectra of* **2**.

The spectra of the higher generations and their temperature dependence (Figure 3.3) show a similar behavior as compared to the biradical. Apart from the polyradical signals, a characteristic nitroxyl 1:1:1 triplet signal of variable intensity is present in each of the spectra. This is attributed to a residual amount of monoradical impurity. Spectral simulation as well as double integration reveals that the amount of nitroxyl monoradicals is less than 3% for n = 32, and less than 1% for all other generations. In each case the broadening which is present at room temperature decreases considerably when the temperature is increased to 378 K. For n = 4 the spectrum recorded at 378 K clearly shows the expected 9 lines separated by $a_N/4$. For n = 8 it is possible to discern a number of shoulders, separated by $a_N/8$. For n = 16, 32, and 64 the spectral resolution does not allow the observation of the ever decreasing spacing between the various hyperfine transitions, and the number of nitroxyl radicals can no longer be determined directly from the spectrum. The continuously decreasing peak-to-peak line width (ΔB_{pp}) observed for n = 16, 32, and 64, is consistent with the increasing number of nitroxyl end groups. The EPR spectra of these higher generations agree well with spectral simulations for n nuclei with I = 1 (n = 16, 32, and 64) having a hyperfine coupling of a_N/n and an EPR line width that is identical to that of the monoradical measured under similar conditions.

The EPR spectra of the DAB-*dendr*-(NH-3-CO-PROXYL)$_n$ dendrimers also depend on the nature of the solvent as shown in (Figure 3.6) for n = 4 and n = 64. In general, the line widths are smaller in polar solvents such as methanol (ε = 33.6) and acetonitrile (ε = 37.5) than in more apolar solvents such as toluene (ε = 2.4) and

dichloromethane ($\varepsilon = 9.1$). The fact that the spectrum in *N,N*-dimethylacteamide is broader than expected from its high dielectric constant ($\varepsilon = 37.8$), is rationalized by the significantly higher viscosity of this solvent at room temperature ($\eta = 2.14$ mPa·s) as compared to the other solvents ($\eta = 0.3$–0.6 mPa·s). Clearly, the higher viscosity will slow down intramolecular motion and hence the modulation of the exchange interaction. In all solvents investigated, the EPR spectra exhibit a smaller line width at higher temperatures, similar to the behavior shown in Figure 3.3.

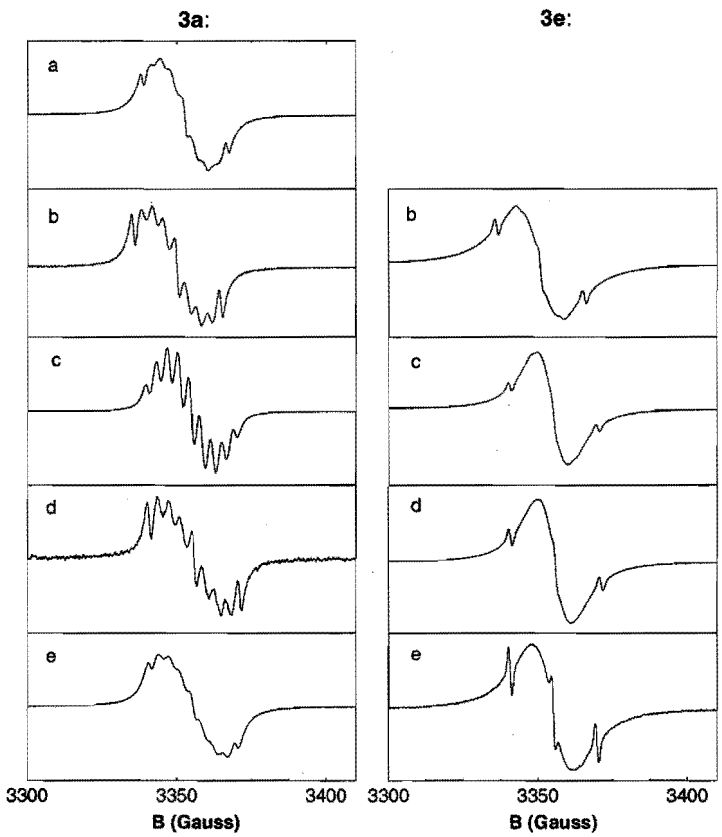

Figure 3.6: *EPR spectra of **3a** and **3e**, recorded at room temperature in (a) toluene, (b) dichloromethane, (c) acetonitrile, (d) methanol, and (e) N,N-dimethylacetamide. No EPR spectrum for **3e** in toluene could be recorded because of poor solubility.*

At lower temperatures, the spectra of all dendritic polyradicals continue to broaden. The resulting spectrum for $n = 64$ in dichloromethane at 120 K is shown in Figure 3.7 as an example and consists of a single and essentially "isotropic line" with a width of $\Delta B_{pp} = 21$ Gauss. Under these conditions a $|\Delta m_s| = 2$ transition at half field is

observed for each generation, which gives direct evidence of the presence of a high-spin state, exhibiting a zero-field splitting (D). No $|\Delta m_s| = 3$ or other lower-field transitions could be observed. Their absence is in accordance with the fact that the intensity of the $|\Delta m_s| = 1$, 2, and 3 transitions are expected in the ratio $1 : (D/B_0)^2 : (D/B_0)^4$.[27] Therefore the $|\Delta m_s| \geq 3$ transitions will go undetected, except when D is large.

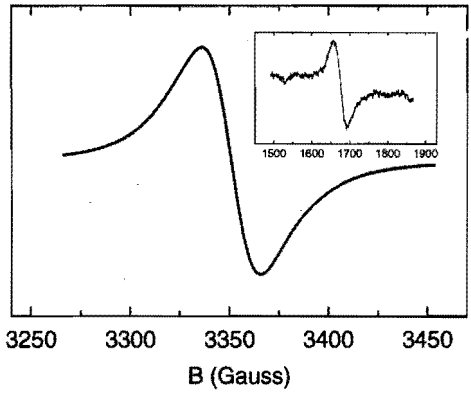

Figure 3.7: *EPR spectrum of DAB-dendr-(NH-3-CO-PROXYL)$_{64}$ in dichloromethane, recorded at 120 K. Inset shows the $|\Delta m_s| = 2$ transition at half field.*

3.4 IR Spectroscopy

The increased flexibility of the dendritic polyradicals in more polar solvents suggests that electric-dipole interactions play a role in the dynamic conformational changes. This observation is consistent with the presence of an intramolecular hydrogen bonded network for poly(propylene imine) dendrimers where functional end groups are attached via an amide bond.[28,29] This is schematically shown for the PROXYL-functionalized dendrimers in Figure 3.8. The presence of intramolecular hydrogen bonds in the PROXYL-systems has been inferred from IR spectroscopy. The IR spectra of the N–H-stretch region for 0.5–1.5 mM samples of DAB-*dendr*-(NH-3-CO-PROXYL)$_n$ in dichloromethane have been recorded and are shown in Figure 3.8 for n = 4, 16 and 64 together with the spectrum for monoradical **1**.

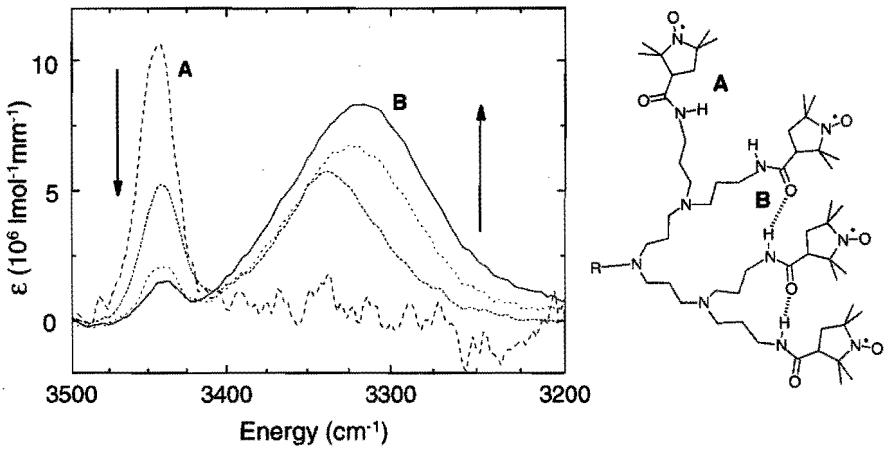

Figure 3.8: *N–H stretch IR spectra of* ***1*** *(- - -),* ***3a*** *(···),* ***3c*** *(···)* ***3e*** *(—) in CH_2Cl_2 at 298 K. Spectra are normalized to 1 mM end group. Schematic view of the hydrogen bonded network is shown on the right.*

The dendrimers give rise to two bands; a narrow band at 3441 cm^{-1} arises from free N–H and a broad band at 3300–3350 cm^{-1} due to N–H hydrogen bonded to an amide carbonyl.[30] The IR spectrum of **1** shows a single N–H stretch at 3441 cm^{-1}, indicating that at the concentrations employed no intermolecular hydrogen bonding occurs. For higher dendrimer generations the band at 3300–3350 cm^{-1}, assigned to intramolecular hydrogen-bonded N–H, increases with respect to the band at 3441 cm^{-1} from non-hydrogen-bonded N–H. Indicating the progressive formation of an intramolecular hydrogen-bonded network at the periphery of the dendrimers for higher generations, formed by organization of the amide functionalities. Also the maximum of the low-energy band shifts to lower wavenumbers (Figure 3.9), reflecting an increment in strength of the H-bond with dendrimer generation. In addition the amide I peak shifts from 1677 cm^{-1} for **1** to 1659 cm^{-1} for **3e**. Quantification of the degree of hydrogen bonding for the different generations as done for the DAB-*dendr*-(NH-*t*-BOC-Gly)$_n$ series (Chapter 2),[29] shows that the same trend is observed for H-bonding, although the increase in hydrogen bonding is somewhat higher for the PROXYL-series.

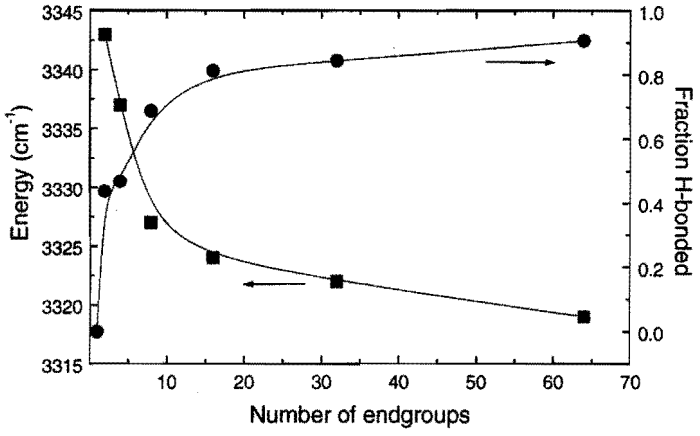

Figure 3.9: *Energy of in H-bonded amide absorption (■, left axis) and amount of H-bonding (●, right axis) as function of end groups for* ***1-3****.*

3.5 Influence of Spacer Length on Biradicals

From the results described above, it is clear that intramolecular hydrogen bonding within the dendrimers plays an important role in the dynamics of the molecules. In order to obtain more insight into the influence of spacer length on the dynamic behavior of biradicals, bis-nitroxide series **4a-d** (Scheme 3.2) has been synthesized starting from the corresponding diamines. Double-label EPR spectroscopy has also been used as a tool to get information on secondary structures of proteins,[31] as it provides information on the relative distances between the labels.

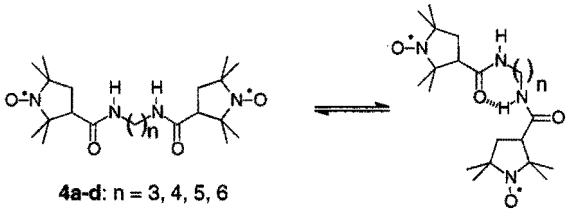

Scheme 3.2: *Investigated biradicals and proposed mode of intramolecular H-bonding.*

The EPR spectra of all these bis-PROXYL derivatives show the typical five line pattern in various solvents (toluene, dichloromethane, methanol) as observed for **2**. However, the modulation of the exchange interaction differs significantly for the different biradicals in the series. Surprisingly, this deviation is not linearly related to

the distance of the radical centers, but shows anomalous behavior for **4b** as can be inferred from Figure 3.10.

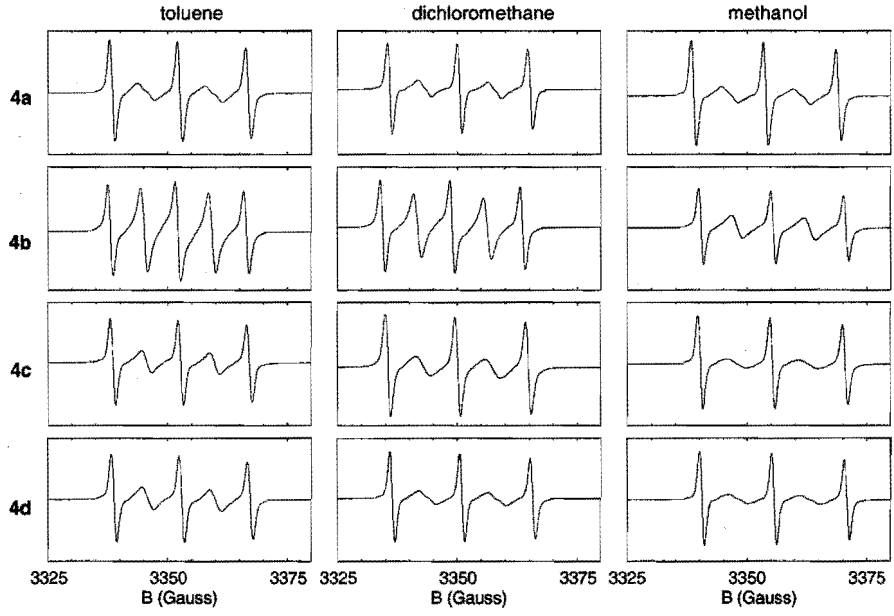

Figure 3.10: *EPR spectra **4a-d** in different solvents.*

Moreover, the exceptional behavior of **4b** is more pronounced in an apolar solvent (toluene, dichloromethane) than in a polar solvent (methanol). This suggests that hydrogen bonding plays an important role in the dynamic behavior of these biradicals as seen before for dendrititic polyradicals. This is described by the IR spectra of **4a-d** recorded in dichloromethane (Figure 3.11). Although all biradicals shows comparable amounts of hydrogen bonding, the nature of the H-bond is different for **4b** as its absorption is shifted to lower energy reflecting a stronger H-bonding mode.

An explanation of this behavior can be found, if the studies on protein folding with model compounds are taken into account. Deviant behavior within homologous series of linear diamides has also been found when these have been functionalized with *N-t*-BOC-L-phenylalanine.[32] The pentamethylene derivative shows different chiroptical features compared to the others in the series. This difference is attributed to favorable intramolecular H-bonding for the pentamethylene derivative, as inferred from ^{1}H NMR and IR studies. Gellman et al. have observed anomalous behavior concerning intramolecular hydrogen bonding in homologous series of diamides based on dicarboxylic acids.[30] ^{1}H NMR and IR data show that the derivative containing the

tetramethylene spacer is more intramolecularly H-bonded. They rationalize their findings by addressing the difference in steric interactions present in the different cyclic structures.

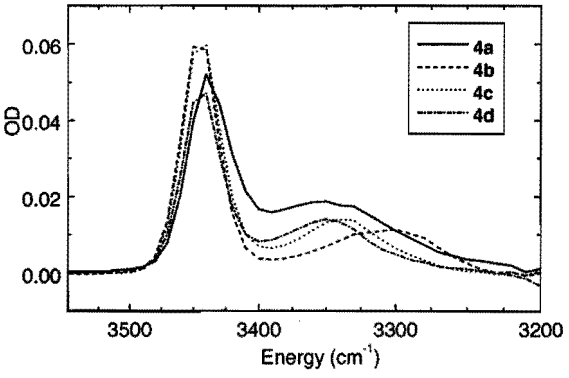

Figure 3.11: *N–H stretch vibrations* ***4a-d*** *in dichloromethane.*

3.6 Conclusion

The first five generations of poly(propylene imine) dendrimers have been functionalized with pendant nitroxyl radicals. The nitroxyl radicals at the periphery of the dendrimers exhibit a strong exchange interaction resulting in thermally populated high-spin states. For the lower generations (**2, 3a** and **3b**), the number of transitions in the EPR spectrum and their spacing can be directly related to the number of end groups, confirming the proposed structures. For the higher generations, such an analysis is hampered by the decreasing value of the splitting (a_N/n) and the increasing number of lines ($2n + 1$). In these cases, however, the EPR spectrum gives direct spectral evidence for interaction between the end groups from the progressive exchange narrowing. This result is in contrast with previous studies on dendrimers with paramagnetic end groups in which no interaction[8–10] or formation of a diamagnetic state was observed.[6]

An interesting aspect of the exchange interaction is the fact that it is modulated by the dynamic behavior of the dendritic branches, since they probe conformations with strongly different values of J in time. Since this modulation of the exchange interaction can be influenced by the temperature and the nature of the solvent, the EPR spectra give evidence of the dynamic behavior of the dendritic branches. IR spectroscopy has revealed that a hydrogen-bonded network is formed between the amide functionalities of the end groups, consistent with the observed solvent effect on the EPR spectra.

Moreover an increase in amount and strength of hydrogen bonding is observed with increasing generation.

In an homologous series of linear diamines (3 through 6 bridging methylene units) functionalized with 3-carboxy-PROXYL, anomalous behavior is observed in spin exchange interactions and N–H infrared absorptions. These anomalies can be directly related to the favorable formation of a intramolecular hydrogen bonded nine-ring.

3.7 Experimental Section

General Methods and Materials

Commercial grade reagents were used without further purification. All solvents were of p.a. quality except dichloromethane and toluene which were purified and dried following standard procedures. For a general section concerning spectroscopic techniques: see Chapter 2. Infrared spectra of compounds **4a-d** were recorded on a UV/vis/NIR Perkin Elmer Lambda 900 spectrophotometer using 5 mm quartz cells.

Preparation

***N*-succinimidyl 3-carbonylate-2,2,5,5-tetramethylpyrrolidin-1-oxyl[33]**

To a solution of 3-carboxy-PROXYL (Aldrich, 203 mg, 1.09 mmol) in 1 mL 1,2-dimethoxyethane, *N*-hydroxysuccinimide (126 mg, 1.09 mmol) and 1,3-dicyclohexylcarbodiimide (247 mg, 1.20 mmol) were added upon cooling with an ice-bath. After one hour the reaction mixture was brought to room temperature and was allowed to react for an additional 12 hours and subsequently filtered. The filtrate was evaporated to dryness under reduced pressure followed by two washings with hot cyclohexane (5 mL). After drying in vacuo, the ester was obtained as a yellow viscous oil (281 mg, 91%). IR (CH_2Cl_2, cm^{-1}): ν 1814 (C=O), 1788 (C=O), 1744 (C=O), 1364 ($R_2NO\cdot$). EPR (CH_2Cl_2, G): 14.49 (a_N), 9.7 (a_{C1}), 5.9 (a_{C2}). GC-MS yielded one peak with a molecular mass of 283 $(M^{\bullet})^+$.

General Procedure for 1-4

The 3-carboxy-PROXYL functionalized amines were obtained by the reaction with 1.01 equivalent of the *N*-succinimidyl ester per end group in dichloromethane in the presence of triethylamine. After the reaction was completed, an aqueous solution of 1 N sodium hydroxide was added and the two phase system was stirred for one hour to hydrolyze the excess of activated ester, followed by a base extraction with a saturated aqueous sodium carbonate solution and a washing with water. The organic phase was dried (Na_2SO_4) and concentrated in vacuo, resulting in yellow glasses for each generation.

3-((*N*-propylamino)carbonyl)-2,2,5,5-tetramethylpyrrolidin-1-oxyl), 1

Yellow needles were obtained after recrystallization in hexane (50 mg, 88%). IR (CH_2Cl_2, cm^{-1}): ν 3444 (Amide A, $\varepsilon = 3.2\cdot10^2$ $mm^{-1}M^{-1}$), 1677 (Amide I), 1515 (Amide II), 1364 ($R_2NO\cdot$). EPR (CH_2Cl_2, G): = 14.49 (a_N), 9.7 (a_{C1}), 5.9 (a_{C2}). GC-MS yielded one peak with a molecular mass of 227 $(M^{\bullet})^+$.

4-Methyl-1,7-bis-(1-oxy-2,2,5,5-tetramethyl-3-pyrrolidinyl-carbonylamino)-4-aza-heptane, 2

Biradical **2** was purified using column chromatography (SiO_2, eluent: methanol), redissolved in dichloromethane and subsequently filtered and dried in vacuo (65 mg, 42%). IR (CH_2Cl_2, cm^{-1}): ν 3444 (Amide A), 3343 (H-bonded amide), 1665 (Amide I), 1514 (Amide II), 1364 ($R_2NO\cdot$). EI-MS: m/z 481 $(M^{\bullet})^+$.

DAB-*dendr*-(NH-3-CO-PROXYL)$_4$, 3a

DAB-*dendr*-(NH-3-CO-PROXYL)$_4$ was purified using column chromatography (SiO_2, eluent: methanol), redissolved in dichloromethane and subsequently filtered and dried in vacuo (83 mg, 51%). IR (CH_2Cl_2, cm^{-1}): ν 3441 (Amide A), 3337 (H-bonded amide), 1666 (Amide I), 1518 (Amide II), 1364 ($R_2NO\cdot$). MALDI-MS: m/z 992.3 $(M+3H)^+$.

DAB-*dendr*-(NH-3-CO-PROXYL)$_8$, 3b
The second generation PROXYL functionalized dendrimer was purified by extraction from dichloromethane into an aqueous solution of 1 N hydrogenchloride. The aqueous layer was brought to pH > 10 and extracted with dichloromethane. The organic phase was dried (Na_2SO_4) and concentrated in vacuo (45 mg, 35%). IR (CH_2Cl_2, cm^{-1}): ν 3441 (Amide A), 3327 (H-bonded amide), 1661 (Amide I), 1519 (Amide II), 1364 ($R_2NO\cdot$). MALDI-MS: *m/z* 2123.9 $(M+5H)^+$, 1955.4 $(M+4H-[3\text{-CO-PROXYL}])^+$, 1911.8, 1898.3, 1883.8, 1786.9 $(M+4H-[3\text{-CO-PROXYL}]_2)^+$, 1089.8, 1035.4.

DAB-*dendr*-(NH-3-CO-PROXYL)$_{16}$, 3c
DAB-*dendr*-(NH-3-CO-PROXYL)$_{16}$ was purified in a similar way as **3b** (57 mg, 38%). IR (CH_2Cl_2, cm^{-1}): ν 3441 (Amide A), 3324 (H-bonded amide), 1660 (Amide I), 1520 (Amide II), 1364 ($R_2NO\cdot$). MALDI- MS: *m/z* 4386.9 $(M+9H)^+$, 4146.9, 3906.9, 2221.1, and 1035.8.

DAB-*dendr*-(NH-3-CO-PROXYL)$_{32}$, 3d
DAB-*dendr*-(NH-3-CO-PROXYL)$_{32}$ was purified by precipitation in hexane (34 mg, 28%). IR (CH_2Cl_2, cm^{-1}): ν 3441 (Amide A), 3322 (H-bonded amide), 1657 (Amide I), 1530 (Amide II), 1364 ($R_2NO\cdot$). MALDI-MS: *m/z* 8910 $(M+13H)^+$, 8669, 8409 with broad tail, 4485, 2166, and 1105.

DAB-*dendr*-(NH-3-CO-PROXYL)$_{64}$, 3e
DAB-*dendr*-(NH-3-CO-PROXYL)$_{64}$ was purified by dialysis (regenerated cellulose 24 Å) with dimethylformamide. Dialysis was continued until no further decrease in the EPR signal belonging to free 3-carboxy-PROXYL radicals compared to the broad signal of the functionalized dendrimer was observed. After removing the solvent, the functionalized dendrimer was obtained (59 mg, 42%). IR (CH_2Cl_2, cm^{-1}): ν 3441 (Amide A), 3322 (H-bonded amide), 1659 (Amide I), 1514 (Amide II), 1364 ($R_2NO\cdot$). MALDI-MS: *m/z* broad peak around 17618 with severe tailing to lower masses (M_{calc} = 17934 g/mol).

1,3-bis-(1-oxy-2,2,5,5-tetramethyl-3-pyrrolidinyl-carbonylamino)-propane, 4a
Biradical **4a** was obtained after precipitation in hexane (90 mg, 70%). IR (CH_2Cl_2, cm^{-1}): ν 3438 (Amide A), 3366 (H-bonded amide), 1670 (Amide I), 1518 (Amide II), 1364 ($R_2NO\cdot$). EI-MS: *m/z* 410 $(M^\bullet)^+$.

1,4-bis-(1-oxy-2,2,5,5-tetramethyl-3-pyrrolidinyl-carbonylamino)-butane, 4b
Biradical **4b** was obtained without further purification (120 mg, 84%). IR (CH_2Cl_2, cm^{-1}): ν 3443 (Amide A), 3307 (H-bonded amide), 1676 (Amide I), 1515 (Amide II), 1364 ($R_2NO\cdot$). EI-MS: *m/z* 424 $(M^\bullet)^+$, MALDI-MS: *m/z* 427.2 $(M+3H)^+$.

1,5-bis-(1-oxy-2,2,5,5-tetramethyl-3-pyrrolidinyl-carbonylamino)-pentane, 4c
Biradical **4c** was obtained after precipitation in hexane (103 mg, 62%). IR (CH_2Cl_2, cm^{-1}): ν 3443 (Amide A), 3342 (H-bonded amide), 1675 (Amide I), 1516 (Amide II), 1364 ($R_2NO\cdot$). EI-MS: *m/z* 438 $(M^\bullet)^+$.

1,6-bis-(1-oxy-2,2,5,5-tetramethyl-3-pyrrolidinyl-carbonylamino)-hexane, 4d
Biradical **4d** was obtained after precipitation in hexane (92 mg, 58%). IR (CH_2Cl_2, cm^{-1}): ν 3443 (Amide A), 3354 (H-bonded amide), 1675 (Amide I), 1516 (Amide II), 1364 ($R_2NO\cdot$). EI-MS: *m/z* 452 $(M^\bullet)^+$.

3.8 References and Notes

1. Newkome, G. R.; Moorefield, C. N.; Vögtle, F. Dendritic Molecules: Concepts, Synthesis, Perspectives; VCH: Weinheim, 1996. Tomalia, D. A.; Naylor, M. A.; Goddard III, W. A. *Angew. Chem., Int. Ed. Engl.* **1990**, *29*, 138–175. Fréchet, J. M. J. *Sience* **1994**, *263*, 1710–1715.
2. Matyjaszewski, K.; Shigemoto, T.; Fréchet, J. M. J.; Leduc, M. *Macromolecules*, **1996**, *29*, 4167–4171.
3. Racja, A.; Utamapanya, S.; Thayumanavan, S. *J. Am. Chem. Soc.* **1992**, *114*, 1884–1885. Racja, A.; Utamapanya, S. *J. Am. Chem. Soc.* **1993**, *115*, 2396–2401. Racja, A.; Utamapanya, S. *J. Am. Chem. Soc.* **1993**, *115*, 10688–10694. Racja, A. *Chem. Rev.*, **1994**, *94*, 871–893. Racja, A. *Adv. Mater.* **1994**, *6*, 605. Rajca, A.; Wongsriratanakul, J.; Rajca, S.; Cerny, R. *Angew. Chem., Int. Ed.* **1998**, *37*, 1229–1232.

4. Veciana, J.; Rovira, C.; Crespo, M. I.; Armet, O.; Domingo, V. M.; Palacio, F. *J. Am. Chem. Soc.* **1991**, *113*, 2552–2561. Veciana, J.; Rovira, C.; Ventosa, N.; Crespo, M. I.; Palacio, F. *J. Am. Chem. Soc.* **1993**, *115*, 57–64. Ventosa, N.; Ruiz, D.; Rovira, C.; Veciana, J. *Mol. Cryst. Liq. Cryst. Sect. A.* **1993**, *232*, 333–342. Veciana, J.; Rovira, C. In *Magnetic Molecular Materials*; Gattechi, D., Kahn, O., Miller, J. S., Palacio, F., Eds.; Kluwer: Dordrecht, 1991, p 121.
5. Nakamura, N.; Inoue, K.; Iwamura, H.; Fujioka, T.; Sawaki, Y. *J. Am. Chem. Soc.* **1992**, *114*, 1484–1485. Nakamura, N.; Inoue, K.; Iwamura, H. *Angew. Chem., Int. Ed. Engl.* **1993**, *32*, 872–874. Matsuda, K.; Nakamura, N.; Inoue, K.; Koga, N.; Iwamura, H. *Chem. Eur. J.* **1996**, *2*, 259–263. Matsuda, K.; Nakamura, N.; Inoue, K.; Koga, N.; Iwamura, H. *Bull. Chem. Soc. Jpn.* **1996**, *69*, 1483–1494.
6. Miller, L. L.; Hashimoto, T.; Tabakovic, I.; Swanson, D. R.; Tomalia, D. A. *Chem. Mater.* **1995**, *7*, 9–11. Duan, R. G.; Miller, L. L.; Tomalia, D. A. *J. Am. Chem. Soc.* **1995**, *117*, 10783–10784.
7. Miller, L. L.; Kunugi, Y.; Canavesi, A.; Rigaut, S.; Moorefield, C. N.; Newkome, G. R. *Chem. Mater.* **1998**, *10*, 1751–1754.
8. Bryce, M. R.; Devonport, W.; Moore, A. J. *Angew. Chem., Int. Ed. Engl.* **1994**, *33*, 1761–1764. Bryce, M. R.; Devonport, W.; Goldenberg, L. M. *Chem. Commun.* **1998**, 945–951.
9. Fillaut, J.-L.; Linares, J.; Astruc, D. *Angew. Chem., Int. Ed. Engl.* **1994**, *33*, 2460–2462. Moulines, F.; Djakovitch, L. Boese, R.; Gloaguen, B.; Thiel, W.; Fillaut, J.-L.; Deville, M.-H.; Astruc, D. *Angew. Chem., Int. Ed. Engl.* **1993**, *32*, 1075–1077.
10. Alonso, B.; Morán, N.; Casado, C. M.; Lobete, P.; Losada, J.; Cuadrado, I. *Chem. Mater.* **1995**, *7*, 1440–1442.
11. Christensen, C. A., Goldenberg, L. M.; Bryce, M. B.; Becher, J. *Chem. Commun.*, **1998**, 509–510.
12. Ottaviani, M. F.; Bossmann, S.; Turro, N. J.; Tomalia, D. A. *J. Am. Chem. Soc.* **1994**, *116*, 661–671.
13. Ottaviani, M. F.; Montalti, F.; Romanelli, M; Turro, N. J.; Tomalia, D. A. *J. Phys. Chem.* **1996**, *100*, 11033–11042.
14. Ottaviani, M. F.; Cossu, E.; Turro, N. J.; Tomalia, D. A. *J. Am. Chem. Soc.* **1995**, *117*, 4387–4398. Ottaviani, M. F.; Turro, C.; Turro, N. J.; Bossmann, S.; Tomalia, D. A. *J. Phys. Chem.* **1996**, *100*, 13667–13674. Ottaviani, M.F.; Andechaga, P.; Turro, N. J.; Tomalia, D.A. *J. Phys. Chem. B* **1997**, *101*, 6057–6065.
15. Wiener, E. C.; Auteri, F. P.; Chen, J. W., Brechbiel, M. W.; Gansow, O. A.; Schneider, D. S.; Belford, R. L.; Clarkson, R. B.; Lauterbur, P. C. *J. Am. Chem. Soc.* **1996**, *118*, 7774–7782.
16. Pilar, J.; Horák, D.; Labský, J.; Švec, F. *Polymer* **1988**, *29*, 500–506. Wielema, T. A.; Engberts, J. B. F. N. *Eur. Polym. J.* **1988**, *24*, 647–650. Tsay, F. D.; Gupta, A. *J. Polym. Sci. B, Polym. Phys.* **1987**, *25*, 855–881. Rånby B. G.; Rabek, B. F. *ESR Spectroscopy in Polymer Research*; Springer, Berlin, 1977.
17. Ferruti, P.; Gill, D.; Klein, M. P.; Wang, H. H.; Entine, G.; Calvin, M. *J. Am. Chem. Soc.* **1970**, *92*, 3704–3713. Vlietstra, E. J.; Nolte, R. J. M.; Zwikker, J. W.; Drenth, W.; Meijer, E. W. *Macromolecules* **1990**, *23*, 946–948. Hanson, P.; Millhauser, G.; Formaggio, F.; Crisma, M.; Toniolo, C. *J. Am. Chem. Soc.* **1996**, *118*, 7618–7625.
18. PAMAMs functinalized with 1–2 nitroxide radicals per dendrimer have been described recently: Ottaviani, M. F.; Matteini, P.; Brustolon, M.; Turro, N. J.; Jockusch, S.; Tomalia, D. A. *J. Phys. Chem.* **1998**, *102*, 6029–6039.
19. De Brabander-van den Berg, E. M. M.; Meijer, E. W. *Angew. Chem., Int. Ed. Engl.* **1993**, *32*, 1308–1311.
20. Rozantsev, E. G. In *Free Nitroxyl Radicals*; Ulrich, H., Ed.; Plenum Press: New York, 1970, chapter 4.
21. Weener, J. W.; van Dongen, J. L. J.; Hummelen, J. C.; Meijer, E. W. *Proc. ACS. PMSE.*, **1997**, *77*, 147–148. Weener, J.-W.; van Dongen, J. L. J.; Meijer, E. W. *submitted to J. Am. Chem. Soc.*
22. Brown, R. S.; Carr, B. L.; Lennon, J. J. *J. Am. Soc. Mass. Spectrom.* **1996**, *7*, 225–232.
23. Luckhurst, G. R. *Mol. Phys.* **1966**, *10*, 543–550. Luckhurst, G. R.; Pedulli, G. F. *J. Am. Chem. Soc.* **1970**, *92*, 4738–4739. Luckhurst, G. R. In *Spin Labeling Theory and Applications*; Berliner, L. J., Ed.; Academic Press: New York, 1976, p 133.
24. Glarum, S. H.; Marshall, J. H. *J. Chem. Phys.* **1967**, *47*, 1374–1378.
25. Parmon, V. N.; Zhidomirov, G. M. *Mol. Phys.* **1974**, *27*, 367–375. Parmon, V. N.; Kokorin, A. I.; Zhidomirov, G. M.; Zamaraev, K. I. *Mol. Phys.* **1975**, *30*, 695–701.

26. Avdievich, N. I.; Forbes, M. D. E. *J. Phys. Chem.* **1995**, *99*, 9960–9667.
27. Slichter, C. P. *Principles of Magnetic Resonance*, Harper and Row: New York, 1963.
28. Jansen, J. F. G. A.; Peerlings, H. W. I.; de Brabander-van den Berg, E. M. M.; Meijer, E. W. *Angew. Chem., Int. Ed. Engl.* **1995**, *34*, 1206–1209. Stevelmans, S.; van Hest, J. C. M.; Jansen, J. F. G. A.; van Boxtel, D. A. F. J.; de Brabander-van den Berg, E. M. M.; Meijer, E. W. *J. Am. Chem. Soc.* **1996**, *118*, 7398–7399. Put, E. J. H.; Clays, K.; Persoons, A.; Biemans, H. A. M.; Luijkx, C. P. M.; Meijer, E. W. *Chem. Phys. Lett.* **1996**, *260*, 136–141.
29. Bosman, A. W.; Bruining, M. J.; Kooijman, H.; Spek, A. L.; Janssen, R. A. J.; Meijer, E. W. *J. Am. Chem. Soc.* **1998**, *120*, 8547–8548.
30. Gardner, R. R.; Gellman, S. H. *J. Am. Chem. Soc.* **1995**, *117*, 10411–10412. Gellman, S. H.; Dado, G. P.; Liang, G.-B.; Adams, B. R. *J. Am. Chem. Soc.* **1991**, *113*, 1164–1173.
31. Miick, S. M.; Martinez, G. V.; Fiori, W. R.; Todd, A. P.; Millhausen, G. L. *Nature*, **1992**, *359*, 653–655. Smythe, M. L.; Nakaie, C. R.; Marshall, G. R. *J. Am. Chem. Soc.* **1995**, *117*, 10555–10562.; Hanson, P.; Martinez, G.; Millhauser, G.; Formaggio, F.; Crisma, M.; Toniolo, C.; Vita, C. *J. Am. Chem. Soc.* **1996**, *118*, 271–272.
32. Peerlings, H. W. I. *Ph. D. Thesis*, University of Technology Eindhoven, Sept. 1998, chapter 3.
33. For another synthesis route see: Degrand, C.; Limoges, B.; Blankespoor, R. L.; *J. Org. Chem.* **1993**, *58*, 2573–2577.

Metallodendrimers*

4

Abstract: *Different generations poly(propylene imine) dendrimers DAB-dendr-$(NH_2)_n$ (n = 4, 8, 16, 32, and 64) are used as multifunctional ligands for the transition metals Cu(II), Zn(II), and Ni(II). Complexation takes place by the dipropylenetriamine (dpt) end groups. Therefore, metallodendrimers are formed with 2, 4, 8, 16, or 32 metal sites per molecule, as shown with UV/vis and EPR spectroscopy, ESI-MS spectrometry, and X-ray crystallography. Guests like azide can be reversibly bound by the Cu(II) containing dendrimer, whereas the Zn(II)-dendrimers exhibit catalytic activity towards p-nitrophenol esters that increases with generation. The large size of the fifth generation poly(propylene imine) dendrimer (3–4 nm) makes it possible to use membrane separation techniques. Here, the dendrimers have been applied in a hemodialyzer set up, resulting in continuous extraction of Cu(II) from aqueous solution, sensing of azide, and continuous catalysis in a membrane reactor.*

* Part of this work has been published: Bosman, A. W.; Schenning, A. P. H. J.; Janssen, R. A. J.; Meijer, E. W. *Chem. Ber./Receuil* **1997**, *130*, 725-728.

4.1 Introduction

Metal containing architectures in the range of 1–10 nm are thought to create new materials with promising electronic[1] and catalytic[2] properties. Polymers with metal coordinating side groups[3,4] or amphiphilic assemblies[5] are most commonly used in this field. Polymers, however, show polydispersity while amphiphilic aggregates are dynamic systems, making both structures less defined. In contrast, dendrimers combine the attractive properties of polymers (size and large number of functionalities) with those of classic organic molecules (highly defined structure). This makes dendrimers well suited for nanoscopic materials, e.g., in complexation of metals.

From an architectural point of view, metal containing dendrimers can be divided into three groups. In the first group, metals are located in the core, especially metalloporphyrins have attracted a lot of attention.[6–11] Additionally, metals are placed in the dendrimer core to assemble the different wedges,[12–15] or to add a functionality.[16,17] Second, metals are used as assembly points in the dendrimer branches. Metals that have been used as connectors are: Ru(II),[18,19] Pt(II),[20] and Pd(II).[21] Finally, dendrimers have been functionalized at the periphery with a manifold of metals, resulting amongst others in end groups containing Au(I),[22,23] Gd(III),[24] Ni(II),[25] Ru(II),[26,27] Pd(II),[28,29] and ferrocene.[30,31] For a complete overview, the reader is referred to some excellent reviews.[32]

Catalysis seems to be a research area in which promising applications for metallodendrimers may be developed. Dendrimers have nanoscopic dimensions and can be molecularly dissolved. This combination of features makes dendrimers suited to close the gap between homo- and heterogeneous catalysis, in other words, dendrimers will combine the advantages of homo- and heterogeneous catalysts, if soluble dendrimers with defined catalytic sites are developed that can be removed from homogeneous reaction mixtures by simple separation techniques (i.e., ultrafiltration or dialysis).[33]

Several metallodendrimers with the metal site in the core have been applied as catalyst aimed at improved characteristics due to site isolation. However, in all cases investigated, no significant improvements were observed concerning regioselectivity,[11] or enantioselectivity.[34,35] In some cases the dendritic framework even hampered the reactions leading to deteriorations in enantioselectivity[36] and activity.[37,38]

The first metallodendrimer with multiple catalytic sites at the periphery has been reported by van Koten et al.[25] Inspired by the idea of anchoring catalytic sites to soluble polymer supports, the authors have used the Ni(II)-containing dendrimer as catalyst for the Kharasch addition of tetrachloromethane to methyl methacrylate. This first generation dendritic catalyst has turnover frequencies that are 30% lower than those

observed for monomeric or polymer bound analogues.[39] Recently, this metallodendrimer has been applied in a continuous membrane reactor.[40]

Following van Koten's initial approach, Reetz et al. have produced third generation poly(propylene imine) dendrimers with peripheral biphenylphosphine ligands.[28] These dendrimers complexate $PdCl_2$, $Pd(CH_3)_2$, $Ir(cod)BF_4$, or $Rh(cod)BF_4$. The Pd(II)-containing dendrimer catalyzes the Heck reaction of bromobenzene and styrene. A 4-fold increase in turnover number has been observed for the Pd(II)-dendrimer as compared to a mono-palladium analogue. This has been ascribed to the higher thermal stability of the dendritic catalyst. Hydroformylation of 1-octene is possible with the Rh(I) dendrimer, although a monomeric analogue shows a comparable turnover frequency. Up to date, no catalyst regeneration via filtration has been reported.

Marquardt and Lüning have prepared a second generation aromatic ether dendrimer with six pendant concave pyridine moieties that are able to catalyze the acylation of alcohols with diphenylketene.[41] In contrast to analogues coupled to a linear polymer or to a Merrifield resin, the dendritic systems do not show a decrease in selectivity toward primary, secondary, or tertiary alcohols. Recovery of the catalyst by nanofiltration is possible in fair yields (70–90%).

Several examples of enantioselective catalysis with peripherally functionalized dendrimers have been reported. However, a drop in enantiomeric excess (ee) with generation is observed.[42,43] Possibly, the packed end groups at the periphery of higher generation dendrimers do not allow proper three-point interactions. Interestingly, Togni et al. have synthesized low generation dendrimers which hardly show a decrease in ee.[44] Moreover, the dendrimers can be separated from the reaction mixtures by applying a nanofiltration membrane.

A new approach towards catalysis and metallodendrimers is the dendrimer-templated synthesis of metal nanoclusters.[45] Both the groups of Tomalia[46] and Crooks[47] reported on stable nanocomposites consisting of hydroxyl-terminated PAMAMs with Cu-particles in the range of 2–4 nm. These structures were obtained by mixing the dendrimers with the appropriate Cu(II)-salt, followed by chemical reduction. In addition, dendrimer nanocomposites have been constructed containing CdS,[48] and zero-valent silver and gold clusters.[49] The use of metal-dendrimer composites in catalysis has recently been shown by Crooks et al. using dendrimer-encapsulated Pd and Pt nanoparticles.[50] The resulting noble metal entities show catalytic activity towards hydrogenation of alkenes in water or O_2 reduction in 1M aqueous sulfuric acid.

In this chapter the propensity of the different generations poly(propylene imine) dendrimers to act as multifunctional ligand for the transition metals Cu(II), Zn(II) and Ni(II) is investigated. The copper dendrimers show reversible binding of azide, whereas

the zinc analogues catalyze the ester hydrolysis of *p*-nitro phenol esters. Finally, the fifth generation poly(propylene imine) dendrimer has been applied in a membrane reactor, giving the possibility to continuously extract Cu(II) from aqueous solutions, probe for azide, and to do catalysis.

4.2 Poly(propylene imine) Dendrimers as Polyvalent Ligands

The end groups in poly(propylene imine) dendrimers consist of a dipropylenetriamine (dpt) unit, known from X-ray studies to act as a tridentate ligand for a number of transition metals (Scheme 4.1).[51-54] Therefore, the possibility of site specific metal inclusion in the poly(propylene imine) dendrimers is investigated in this paragraph.

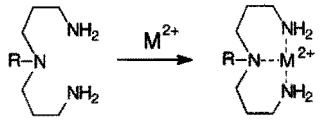

Scheme 4.1: *Complexation of transition metals by dpt-unit.*

4.2.1 Cu(II)-complexes

UV/vis Spectroscopy. The addition of $CuCl_2$ to the different generations poly(propylene imine) dendrimers in methanol immediately resulted in a deep blue color from a broad absorption band at $\lambda_{max} = 620$ nm belonging to the copper *d-d* transition, indicative of the formation of a complex between the two species. The metal complexation of Cu(II) was followed with UV/vis spectroscopy by monitoring the increase in absorption at $\lambda_{max} = 620$ nm upon titration of the polyamines with $CuCl_2$ in methanol. All generations form a 1:2 complex between Cu(II) and the NH_2-functions (Figure 4.1), indicating the presence of multiple Cu(II)dpt complexes within one dendrimer, leading to molecules with 2, 4, 8, 16 or 32 copper sites. A linear increase in extinction coefficient with number of end groups is found when going from the first to the fifth generation (inset Figure 4.1). From the shape of the titration curves it can be concluded that Cu(II) is strongly complexated by all dendrimer generations as is found for the complexation of Cu(II) with dpt, having a p*K* of 14.[55] When dendrimers were used in which the primary amines had been converted into amides,[56] or when nitrile end capped poly(propylene imine) dendrimers were used, no complexation was observed. These results clearly show that no complexation takes place with the inner

tertiary amines. In contrast to the findings for PAMAM dendrimers, which show also coordination of Cu(II) inside the dendrimer.[57]

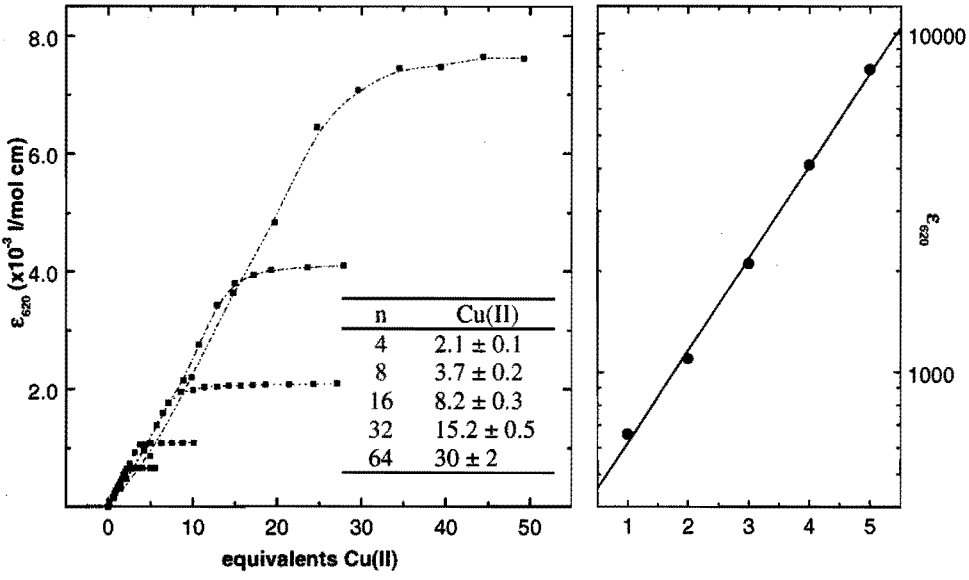

Figure 4.1: *Titration curves for DAB-dendr-$(NH_2)_n$ (n = 4, 8, 16, 32, 64) with $CuCl_2$ in methanol, table shows the determined amount of Cu(II) per dendrimer. Graph on the right shows the extinction coefficients for the fully occupied dendrimers of different generations.*

EPR Spectroscopy. The complexation of copper with the poly(propylene imine) dendrimers could also be followed with EPR spectroscopy. When less than one Cu(II) cation is present per dendrimer, the EPR spectrum shows an isotropic 4-line pattern (g_{iso} = 2.11, Figure 4.2a). As soon as the number of Cu(II) ions per dendrimer exceeds one, a single unresolved signal is observed probably caused by exchange interactions between the copper centers mediated by bridging chloride ligands. Consequently, no exchange narrowing was observed when a non-coordinating anion like perchlorate was used. Further increase of the Cu/NH_2-ratio to a value of 0.5, produces the signal of free $CuCl_2$ in methanol, indicating that all complexation sites are occupied. The anisotropic g-values for the copper complexes were determined in a methanol matrix at 130 K (0.4 equivalent Cu(II), Figure 4.2b), giving an axial Cu(II)-spectrum with $g_{//} = 2.223$, $g_{\perp} = 2.048$, and $A_{//} = 175 \cdot 10^{-4}$ cm^{-1}.

The EPR parameters indicate the formation of a Cu(II)-complex involving three nitrogen nuclei.[58] Moreover, the UV/vis data are typical for a five-coordinated species with a square-pyramidal or trigonal bipyramidal ligand field.[59] Therefore, a

coordination geometry between trigonal bipyramidal and square-based pyramidal is proposed for the dendrimer Cu(II) complex, analogueous to the X-ray structure of the copper(II)chloride complex with N,N,N',N'-tetrakis(3-aminopropyl)-1,5-diamino-3-oxapentane.[52]

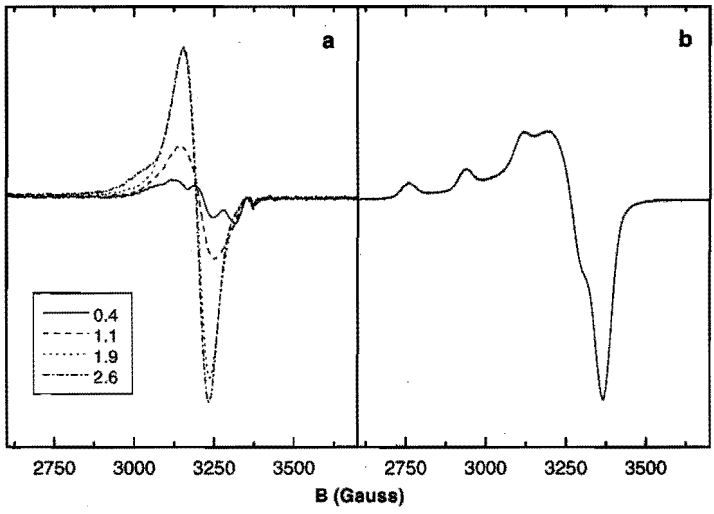

Figure 4.2: *a) EPR spectra of DAB-dendr-$(NH_2)_4$ upon titration with $CuCl_2$ in methanol, legends shows equivalents of Cu(II) added; b) EPR spectrum of DAB-dendr-$(NH_2)_4$ with 0.4 equivalent Cu(II) in methanol at 130 K.*

ESI-MS Spectrometry. Further characterization of the metal complexes was achieved with electrospray ionization mass spectrometry (ESI-MS). This technique is well suited for organometallic compounds, since these species are easily charged by the loss of labile anions.[60] Therefore, the complexes of $Cu(ClO_4)_2$ with DAB-*dendr*-$(NH_2)_n$ (n = 4, 8, 16) obtained by precipitation in diethylether, have been subjected to mass analysis. The ESI-MS spectrum of a first generation poly(propylene imine) dendrimers loaded with $Cu(ClO_4)_2$ is shown in Figure 4.3. Next to the peak belonging to the native complex minus one perchlorate ion (739 amu), peaks are observed, attributed to doubly charged species and copper complexes in which perchlorate has been replaced by hydroxide combined with a solvent molecule (methanol or acetonitrile). Interestingly, peaks were also observed displaying subsequent loss of perchloric acid. Although these losses may be attributed to proton transfer from the ligand to the anion,[61] this seems highly unlikely because of the low basicity of perchlorate. A more convenient explanation would be reduction of Cu(II) to Cu(I) by the ligand followed by the loss of perchloric acid.

The collision-induced dissociation (CID) of Cu(II)-complexes accompanied by reduction of the metal in electrospray conditions, has been observed before whereby solvent molecules or ligands act as electron donors.[62-64] Consequently, reduction of Cu(II) to Cu(I) during ESI leads to a mixed valence species (Cu(II)Cu(I)) and fully reduced species ($Cu(I)_2$) for the first generation dendrimer. Moreover, this reduction is tunable by the orifice voltage (Figure 4.3), indicating that CID-processes are operative, and the proposed structures were subscribed by the observed isotope patterns.

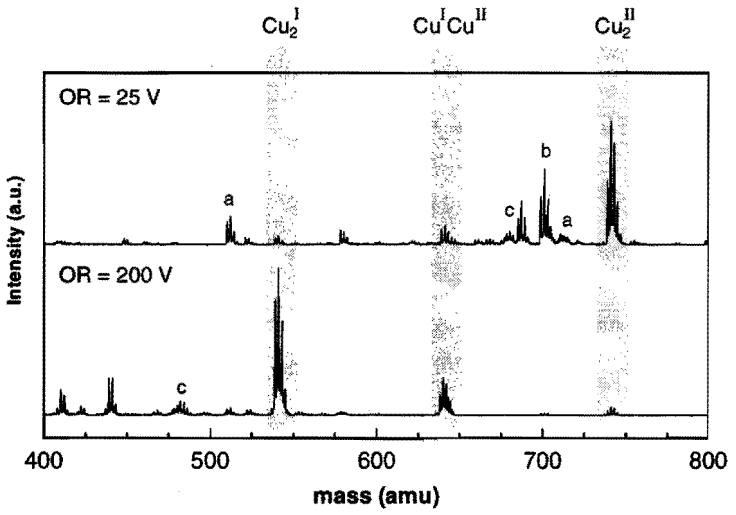

Figure 4.3: *ESI-MS spectra $[Cu_2DAB\text{-}dendr\text{-}(NH_2)_4](ClO_4)_4$ at low orifice voltage (25 V, top) and high orifice voltage (100 V, bottom). Labels on peaks show oxidation state of copper sites, peaks belonging to ions in which ClO_4^- is exchanged for OH^- and solvent molecule (S) are labeled with: a (S = MeOH), b (S = MeCN), and c (S = H_2O).*

The same behavior was found for the second generation Cu(II)-dendrimer, leading to five peaks for the different mixed valence species (Figure 4.4, OR = 100 V). The isotope patterns of these five signals were in agreement with the proposed structures as shown for the $Cu(I)Cu(II)_3$-dendrimer in Figure 4.4. Again the relative intensities of the peaks could be tuned by changing the orifice voltage. For the higher generations no signals belonging to molecular ions were obtained (ESI or MALDI-TOF). This can be rationalized by the increase of complexity of the systems and the limited mass range of the ESI mass spectrometer. Indeed, nine different redox-states are possible for the third generation Cu(II)-dendrimer. Moreover, the isotope-pattern for the corresponding $Cu(II)_8$-species (3 675 amu) ranges over 27 mass units.

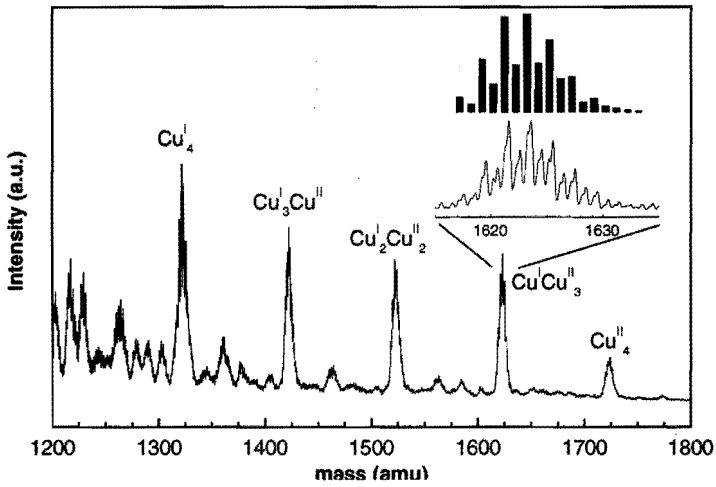

Figure 4.4: *ESI-MS spectrum [Cu4DAB-dendr-(NH2)8](ClO4)8 in acetonitrile displaying the five possible oxidation states of the four copper centers. Graph in the right upper corner shows isotope pattern (top: simulated, bottom: measured) for [Cu(I)Cu(II)3DAB-dendr-(NH2)8](ClO4)6.*

X-ray Crystallography. The tridentate binding by the dpt-unit was subscribed by the X-ray structure obtained from a first generation poly(propylene imine) dendrimer containing a $Cu_4(\mu_4\text{-}CO_3)(\mu\text{-}Cl)_2$ site (Figure 4.5). The crystals were grown in aqueous solution in the presence of chloride and perchlorate ions. Carbonate has been generated by fixation of atmospheric CO_2, a process known to take place for metal complexes in slightly basic aqueous solutions.[65,66] The structure of the tetranuclear unit consists of four copper atoms placed at the corners of a rectangular with a μ_4-carbonato ligand in the center (disordered). This tetranuclear binding mode for the carbonate is also found in similar compounds with dpt as organic ligand,[66] and in the mineral malachite ($Cu_2(OH)_2(CO_3)$).[67] The bridging chlorides are in the plane of the rectangle perpendicular to the short edges. The dpt ligand-unit is *mer* coordinated to the copper, resulting in a five-coordinated complex. Due to the disorder in the carbonato-ligand, two different coordination spheres are present for the copper. Both are best described as irregular square pyramid (*SP*) with the chloro ligand apical. For selected bond lengths see Table 4.1. Residual electron density through the crystal structure is attributed to the presence of unresolved perchlorate anions. IR spectroscopy supports the presence of non-coordinating perchlorates. The DAB-*dendr*-$(NH_2)_4$, Cu(II), carbonato, and chloro ligands form a two-dimensional infinite array in the *b*,*c*-plane as shown in Figure 4.5 and Figure 4.6. Due to this packing channels are formed through the crystal structure, probably the location where the perchlorate anions are resorting.

Table 4.1: *Selected bond-lengths for* $[(\mu_4\text{-}CO_3)(\mu\text{-}Cl)_2\{Cu_4(DAB\text{-}dendr\text{-}(NH_2)_4)_2\}](ClO_4)_4$.

atoms	distance (Å)	atoms	distance (Å)
Cu(11)-Cl(11)	2.4961(18)	Cu(21)-Cl(11)	2.5124(18)
Cu(11)-O(11)	2.094(5)	Cu(21)-O(12)	2.087(5)
Cu(11)-N(101)	2.005(4)	Cu(21)-N(104)	1.990(4)
Cu(11)-N(102)	2.068(4)	Cu(21)-N(105)	2.073(4)
Cu(11)-N(103)	1.992(4)	Cu(21)-N(106)	1.987(4)
Cu(11)-O(10)	2.051(5)	Cu(21)-O(10)	2.087(5)
Cu(11)-Cu(21)	3.6744(8)		

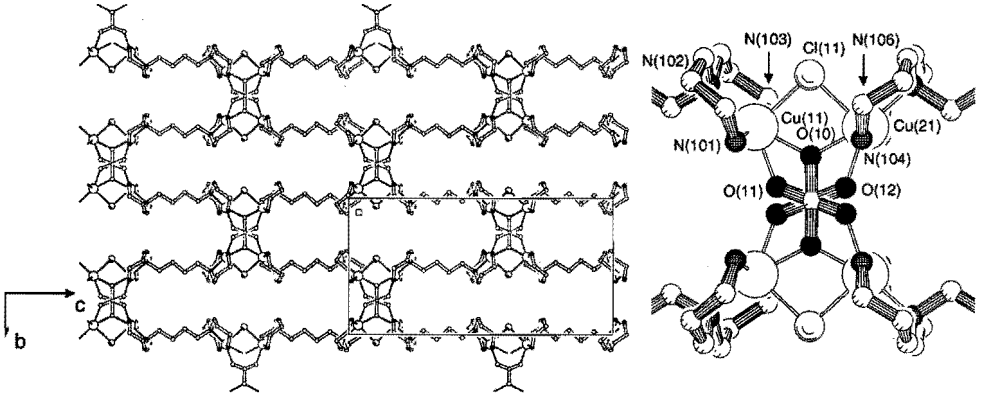

Figure 4.5: *PLUTON representations of* $[(\mu_4\text{-}CO_3)(\mu\text{-}Cl)_2\{Cu_4(DAB\text{-}dendr\text{-}(NH_2)_4)_2\}](ClO_4)_4$, *crystal packing in b,c-plane with unit cell on the left, tetranuclear unit is enlarged on the right showing the disorder of the carbonate group.*

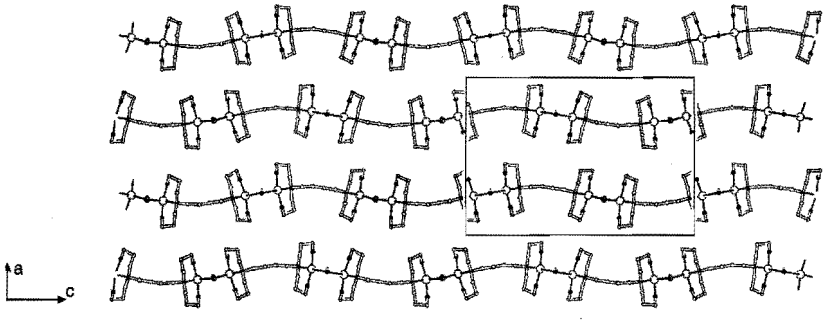

Figure 4.6: *PLUTON representations of intermolecular orientation of* $[(\mu_4\text{-}CO_3)(\mu\text{-}Cl)_2\{Cu_4(DAB\text{-}dendr\text{-}(NH_2)_4)_2\}](ClO_4)_4$, *viewed along b-axis.*

4.2.2 Zn(II)-complexes

^{1}H NMR spectroscopy. To investigate the metal complexating abilities of the dendritic polyamines with ^{1}H NMR spectroscopy, Zn(II) was used. Upon titration the dendrimer with $ZnCl_2$ in deuterated methanol a downfield shift is observed for the protons present in the outer tier (Figure 4.7), caused by the complexation of the zinc cation. This indicates that complexation of Zn(II) occurs exclusively at the periphery of the dendrimers via the primary amines and the tertiary amines of the penultimate generation. Moreover, when the ratio of Zn(II)/NH_2 exceeds 0.5, no further shifting of the proton resonances is observed, consistent with the complexation of one Zn(II) per two end groups. The presence of a three-nitrogen coordinated Zn(II) was subscribed by ^{13}C NMR and COSY measurements and is in agreement with the X-ray structure of a Zn(II)dpt complex.[53]

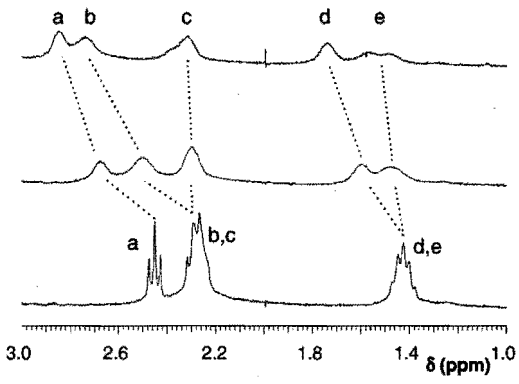

Figure 4.7: *^{1}H NMR spectra of DAB-dendr-$(NH_2)_{32}$ upon titration with $ZnCl_2$ in deuterated methanol, a: protons α to primary amines; b: protons γ to primary amines; c: protons α to all tertiary amines except those in the outer tier; d: protons β to primary amines; e: protons β to all tertiary amines except those in the outer tier.*

4.2.3 Ni(II)-complexes

UV/vis Spectroscopy. Complexation of $NiCl_2$ with the poly(propylene imine) dendrimers revealed a somewhat different behavior as compared to $CuCl_2$ and $ZnCl_2$. Although the first generation dendrimer shows the same 1:2 ratio for complexation of Ni(II) to NH_2 end groups, all higher generations exhibit 1:4 complexation when the Ni(II) concentration is low compared to that of the polyamine. At higher Ni(II) concentrations, 1:2 complexation is found between Ni(II) and the NH_2 end groups as evidenced from a reverse titration experiment in which aliquots of poly(propylene imine) dendrimers were added to a $NiCl_2$ solution (Figure 4.8). By monitoring the *d-d*

absorption at λ_{max} = 640 nm,[59,68] a singularity is observed at a Ni/NH_2 ratio of 1:2, while the absorption at λ_{max} = 680 nm exhibits a singularity at a ratio of 1:4.

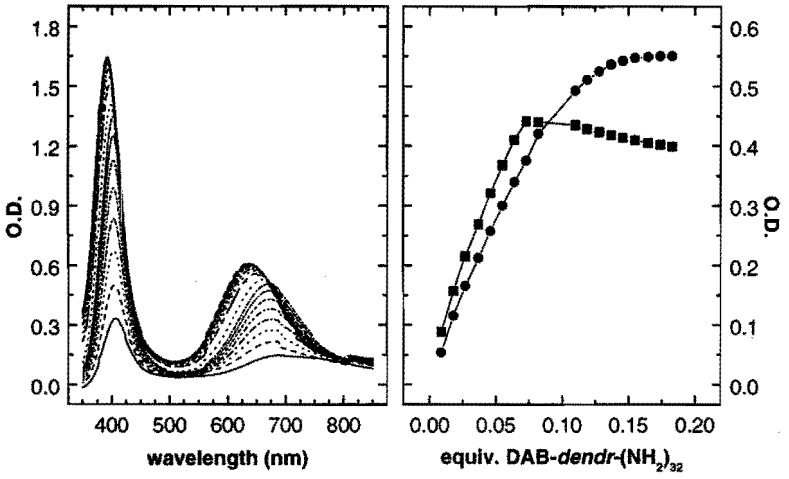

Figure 4.8: *Change in UV/vis spectra upon addition of DAB-dendr-(NH_2)$_{32}$ to $NiCl_2$ in methanol (left), corresponding changes in optical density for absorptions at λ_{max} = 640 nm (-■-) and 680 nm (-●-) (right).*

In agreement with the fact that two different coordination spheres have been found in complexes of Ni(II) with dpt,[55] it is proposed that first a site with six coordinating nitrogens is formed, followed by a site with three coordinating nitrogens when the ratio of Ni(II) to dendrimer is increased (Scheme 4.2). The complex with six coordinating nitrogens is attributed to octahedrally surrounded Ni(II) (two ligand units).[59,68] Such a structure is known from the X-ray structure of Ni(dpt)$_2$(ClO_4)$_4$.[54] In the second complex Ni(II) is only coordinated by three nitrogens. Probably, this structure is comparable to the Cu(II)-complexes. The fact that the first generation dendrimer does not show an octahedral coordination sphere can be rationalized by steric factors.

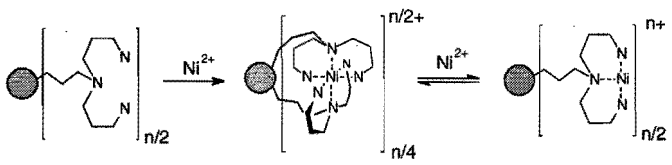

Scheme 4.2: *Schematic representation of the different binding modes for Ni(II) in DAB-dendr-(NH_2)$_n$ (n = 8, 16, 32, 64), filled circle represents dendritic framework.*

4.3 Catalysis

4.3.1 Azide-binding by Cu(II)-dendrimers

In order to probe the accessibility of the different generations metal-functionalized poly(propylene imine) dendrimers, the binding of azide to the Cu(II)-sites in the dendrimer was investigated. As this azide binding is accompanied by ligand to metal charge transfer (LMCT) bands in the visible or near-UV region and produces changes in the EPR spectra, this probe method has been widely employed to obtain information on the metal sites in copper proteins.[69]

Addition of sodium azide to a solution of $[Cu_{n/2}DAB\text{-}dendr\text{-}(NH_2)_n]Cl_n$ (n = 4, 8, 16, 32, and 64) in methanol resulted in the formation of a LMCT-band at 371 nm for every generation (Figure 4.9). From the titration curve in the inset of Figure 4.9 it is clear that there is an equilibrium between bound and non-bound azide. Assuming that every Cu(II)-site binds one azide and has no interaction with other Cu(II)-sites in the dendrimer, the equilibrium constants for the different generations was obtained. The value dropped from $4.4 \cdot 10^4$ M^{-1} for the first generation to $1.9 \cdot 10^4$ M^{-1} for the fifth generation (Table 4.2), probably due to increased steric constraints in the dendrimers.

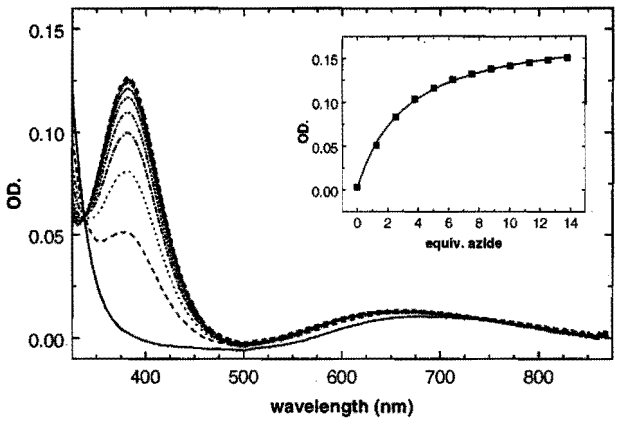

Figure 4.9: *Spectral changes upon addition of NaN_3 to $[Cu_4DAB\text{-}dendr\text{-}(NH_2)_8]Cl_8$ in methanol. Inset shows increase in 371 nm absorption against equivalents azide.*

Following the titrations with EPR in frozen methanol solutions, revealed a decrease in signal intensity with increasing azide concentration. This can be rationalized assuming that the azide is bridging between two coppers in a μ-1,3 mode, since these complexes are known to be anti-ferromagnetic.[70] In contrast, only a small

change in *g*-values and signal intensity was observed when a mononuclear analogue, [CuMedpt)]Cl_2 (Medpt = bis(propylamine) methylamine), was titrated with azide. Moreover, the LMCT-band of the corresponding azide complex is shifted to the red (λ_{max} = 382 nm) and displayed an azide stretch vibration at higher energy in the IR spectrum, when compared to the dendrimer systems. All these spectroscopic data are in agreement with a bridged azide between the Cu(II)-sites in the dendrimers in a μ-1,3 binding mode,[71] reflecting the accessibility and dynamics of these metal loaded systems.

Table 4.2: *Kinetic data azide-binding[a] and PNPP-ester hydrolysis[b] for the different generations metal-loaded poly(propylene imine) dendrimers .*

		PNPP-ester hydrolysis		
Generation[c]	K_{azide} (10^3 M^{-1})	k_{obs} (10^{-3} s^{-1})	K_{PNPP} (M^{-1})	k_c (10^{-2} s^{-1})
0	15 ± 1	0.86 ± 0.01	-	-
1	44 ± 3	0.90 ± 0.01	510 ± 30	2.4 ± 0.1
2	34 ± 3	1.09 ± 0.01	-	-
3	21 ± 1	1.48 ± 0.01	-	-
4	21 ± 1	2.71 ± 0.02	-	-
5	19 ± 1	3.90 ± 0.02	322 ± 10	16 ± 1

a) Dendrimers containing $CuCl_2$ in methanol. b) Dendrimers containing $Zn(ClO_4)_2$ in 0.05 M HEPES buffer at 35°C, pH = 7.2. c) Generation 0 consists of metal salt with Medpt as ligand.

4.3.2 Ester hydrolysis with Zn(II)-dendrimers

Zn(II)-amine complexes have been widely investigated on their activity in hydrolytic reactions. These investigations are motivated by the fact that Zn(II) plays an essential role in hydrolytic metalloenzymes like carboxypeptidase A (CPA), carbonic anhydrase (CA), and alkaline phosphatase (AP).[72] In low-molecular model systems, the cleavage of carboxylic and phosphoric esters have been thoroughly investigated. Three different roles have been attributed to the metal. It serves as a template to assemble substrate and nucleophile, the metal activates the substrate (i.e. carbonyl or phosphoryl bond) and it activates the nucleophile (i.e. metal-bound hydroxide ion).[73-76]

In order to get more insight into the use of dendrimers in catalysis, the poly(propylene imine) dendrimers loaded with zinc(II)perchlorate have been investigated on their catalytic activity towards hydrolysis of *p*-nitrophenyl picolinate (PNPP, Scheme 4.3). The reaction was followed by observing the release of *p*-nitrophenolate spectrophotometrically (400 nm). Pseudo first-order rate constants were determined in the presence of excess catalyst (20 equiv.) in a buffered solution of pH = 7.2 (HEPES) at 35 °C. First generation dendrimer containing 2 Zn(II)-ions, showed

comparable catalytic activity when compared to [ZnMedpt](ClO$_4$)$_2$ or other mono-zinc compounds.[75,77] However, when going to higher generations dendrimers, a steady increase of activity per Zn(II)-site with generation was observed (Table 4.2). The turn-over behavior of the fifth generation Zn(II)-dendrimer was tested by adding 5 equivalents of PNPP per Zn(II)-ion. Release of *p*-nitrophenolate was quantitive, indicative of a rapid regeneration of catalyst.

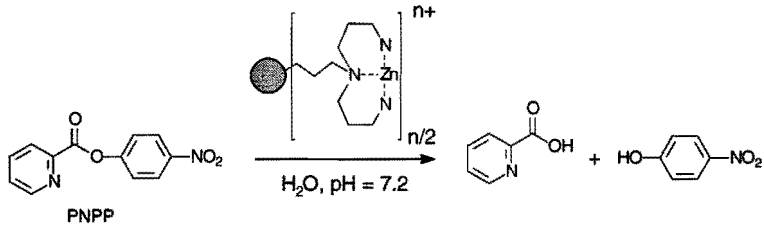

Scheme 4.3: *PNPP-ester hydrolysis with Zn(II)-dendrimers.*

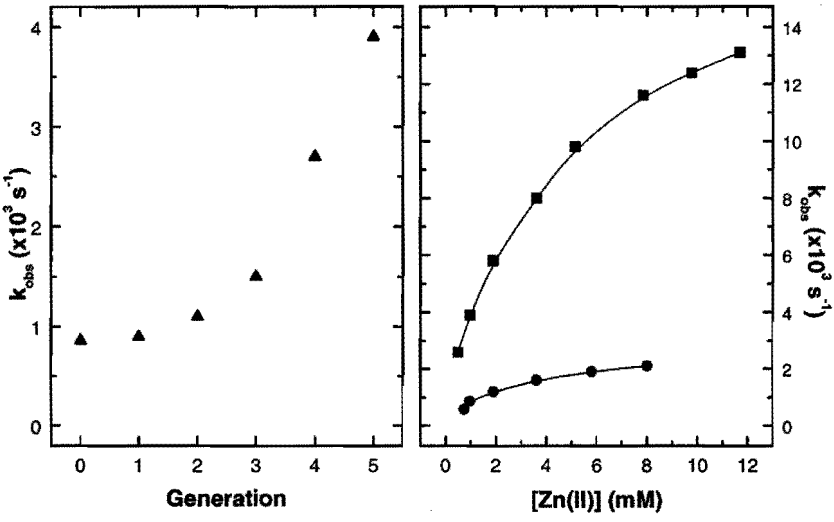

Figure 4.10: *Pseudo first-order rate constants for the hydrolysis of PNPP as function of dendrimer generation ([Zn(II)] = 1 mM, left), and as function of the Zn(II)-concentration for first (-●-) and fifth (-■-) generation Zn(II)-functionalized poly(propylene imine) dendrimers (right), at pH = 7.2 and 35°C, [PNPP] = 0.05 mM.*

For a better understanding of the ester hydrolysis mediated by the Zn(II)-loaded poly(propylene imine) dendrimers, the rate of hydrolysis was investigated as function of the catalyst concentration for a first generation (n = 4) and a fifth generation (n = 64) poly(propylene imine) dendrimer loaded with Zn(II). In both cases saturation kinetics was observed, indicative of strong affinity of PNPP for both Zn(II)-species. Assuming a

rapid reversible formation of a Zn(II)dendrimer-substrate complex followed by a rate determining hydrolysis, the corresponding association constant K and catalytic rate constant k_c (Scheme 4.4) can be determined.[75]

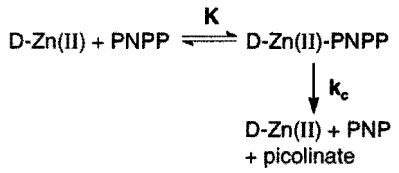

Scheme 4.4: *Proposed reaction mechanism for dendrimer-catalyzed ester-hydrolysis, D represents poly(propylene imine) dendrimer.*

The values found for the first generation catalyst are comparable to those found for Zn(II) metallosurfactants in micellar systems (Table 4.2).[75] The lower value found for K in the case of the fifth generation, can be attributed to an increase in steric crowding, making the metal site less attainable for substrate. In accordance with the observed decrease in K for azide-binding when going to higher generations. The increase in catalytic rate with generation is unprecedented, and is probably best understood when compared with the rate increments observed for micellar systems. In the latter systems, rate accelerations upon incorporation in micelles is rationalized by binding of substrate to the micellar surface and high local concentration of cations, resulting in enhanced electrophilicity of the metal and lowering of the pK_a of metal-bound water.[75–78] To what extent these effects are also present in the dendritic systems remains unclear. However, it is obvious that the high local concentration of metal-sites will lead to different features when compared to a monomeric system.

4.4 Separation based on Nanoscopic Size

As stated in the introduction, the combination of nanoscopic size and catalytic activity would make dendrimers well suited for use in a membrane reactor.[33] The size of a fifth generation poly(propylene imine) dendrimer is in the range of 3–4 nm as measured with SANS[79–81] and viscosimetry measurements.[81] The Cu(II) complexes of the fifth generation poly(propylene imine) dendrimer could be visualized using transmission electron microscopy. The micrographs showed the presence of spherical structures with a diameter of 5 nm with almost no size distribution (Figure 4.11). Therefore, it can be concluded that unimolecular nanoscopic structures are formed.

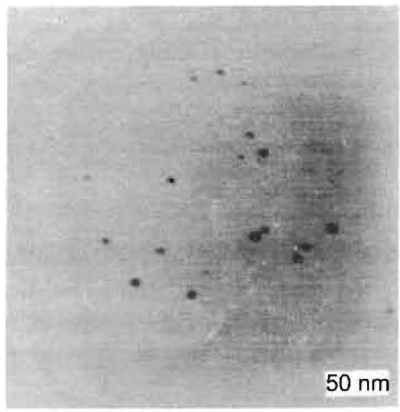

Figure 4.11: *TEM-micrograph of [Cu_{32}DAB-dendr-$(NH_2)_{64}$]Cl_{64} as developed from an aqueous solution (10^{-4} M).*

4.4.1 Nanofiltration

Since the dimensions of fifth generation poly(propylene imine) dendrimers are in the nanometer regime, the molecules can be separated using membrane techniques. Dialysis bags consisting of regenerated cellulose have been used previously to purify functionalized poly(propylene imine) dendrimers.[82] Here, a commercially hemodialyzer ("artificial kidney", Figure 4.12) is used to separate the metallodendrimers from the bulk solution, using the same regenerated cellulose membranes. However, because the hemodialyzer consists of many microtubili, the surface over which exchange takes place is much larger than in case of the dialysis bag (1.5 m^2 compared to 50 cm^2).[83]

The applicability of the hemodialyzer was tested with a solution containing [Cu_{32}DAB-*dendr*-$(NH_2)_{64}$]$(ClO_4)_{32}$ in HEPES/methanol (1/1 v/v). When this solution was dialyzed against the same solvent combination without the Cu(II)-dendrimer, a small signal attributed to a Cu(II)-amine complex was observed in the dialyzate with EPR spectroscopy (Figure 4.13). Double integration of this signal revealed that 1% of the Cu(II) had leached through the membrane. As in a second run no more Cu(II) was observed, this leaching is attributed to the presence of low molecular defect structures present in fifth generation poly(propylene imine) dendrimers.[84]

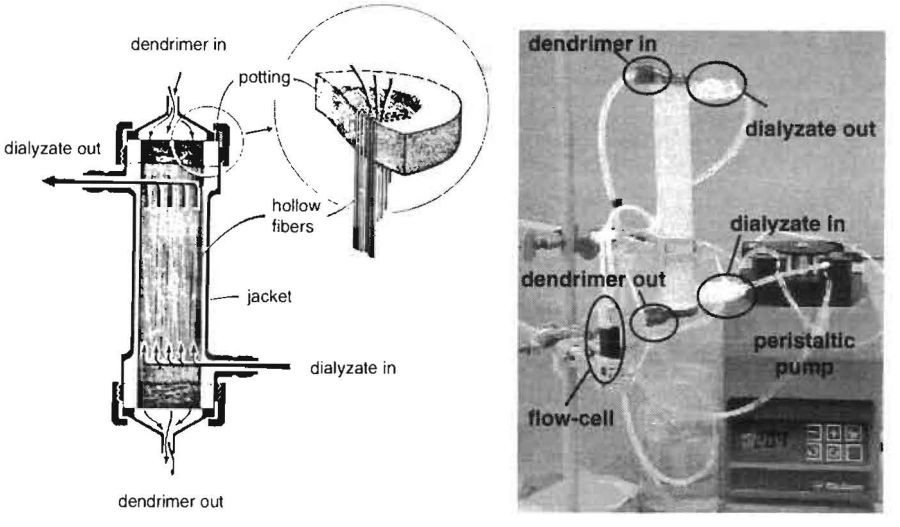

Figure 4.12: *Schematic diagram of hollow fiber dialyzer,*[83] *experimental setup shown on the right.*

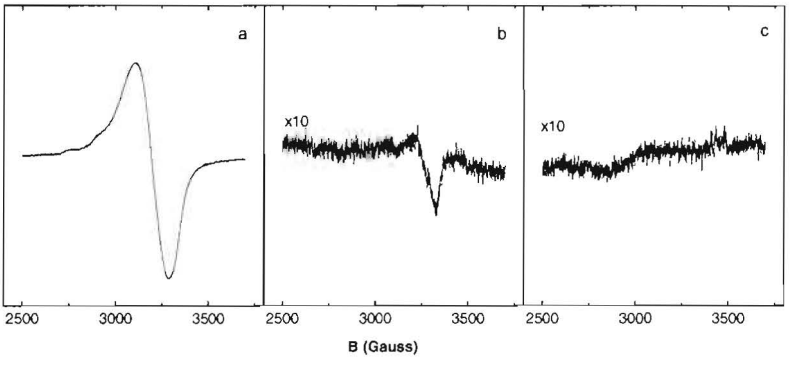

Figure 4.13: *Performance hemodialyzer in retention of* $[Cu_{32}DAB\text{-}dendr\text{-}(NH_2)_{64}](ClO_4)_{32}$ *followed with EPR; a: dendrimer-containing solution, b: dialyzate first run, c: dialyzate second run.*

4.4.2 Metal Absorption

In order to remove metals from dilute aqueous solutions, water soluble polymeric supports containing metal-complexating sites (polychelatogens) have been developed.[85,86] Although polymer resins are used a lot for this purpose,[87] the major drawbacks of these systems are the lack of chemical definition, and slow exchange rate

due to the heterogeneous nature of the extraction. Therefore, the use of soluble polymeric chelating agents in combination with membrane separation has attracted considerable attention.[88] Requirements for such systems are water solubility, large number of functional groups and high molecular weight. Consequently, branched poly(ethylene imine), PEI, has been widely used as it is commercially available, water soluble and contains 1°, 2°, and 3° amino groups in the polymer chain capable of metal binding.[86,88] Poly(propylene imine) dendrimers can be viewed as the dendritic analogues of PEI, they are soluble in water and are large enough to use in a membrane reactor (fifth generation). In contrast, they have a lower intrinsic viscosity, a very low dispersity (1.0018),[84] and contain chemical defined complexating units having affinity for metals like Cu(II), Zn(II), Ni(II). Hence, the fifth generation poly(propylene imine) dendrimer has been tested to extract metals from water streams using the hemodialyzer setup. The hemodialyzer was first loaded with DAB-*dendr*-$(NH_2)_{64}$ and subsequently flushed with aqueous solution containing 2.4 mM $Cu(ClO_4)_2$. Almost immediately a blue color evolved in the hemodialyzer, indicative of the complexation of Cu(II) by the dendrimer. Monitoring the dendrimer-containing stream with UV/vis in time, revealed a growing signal belonging to a Cu(II)-poly(propylene imine) dendrimer complex (λ_{max} = 610 nm, Figure 4.14). Moreover, after 3000 s, there was no further increase in the 610 nm absorption, exhibiting that the dendrimer is fully loaded with Cu(II). Simultaneously monitoring the copper contents in the filtrate, shows that there is a sudden rise in [Cu(II)] coinciding with the leveling off observed for the dendrimer solution (Figure 4.14). In addition, the UV/vis spectrum of the filtrate is typical for an aqueous copper containing solution (λ_{max} = 720 nm), subscribing that the limiting capacity of the dendrimer is reached. From the extinction coefficient of the dendrimer solution a loading of 29 mol copper per dendrimer was determined, equivalent to a capacity of 4.1 mmol Cu(II) per gram. This is higher than for branched PEI with M_w = 30 000–40 000 (2.4 mmol/g, Polymin P, BASF)[85] reflecting the higher density of endgroups in a dendrimer compared to a branched polymer. Recycling of the dendrimer solution was performed by flushing with acidified water (pH = 1), as all copper was removed from the dendrimer.

In conclusion, a fifth generation poly(propylene imine) dendrimer is effective in extracting Cu(II)-ions from aqueous solution using a hemodialyzer in a continious flow system. This makes it possible to apply high flow rates and large volumes, which is attractive for highly diluted metal salt solutions. Compared to branched PEI, a higher Cu(II)-loading is possible. Moreover, the poly(propylene imine) dendrimers are easily modified with selective metal-complexating ligands, opening the way to use these systems for specific metal-extractions.

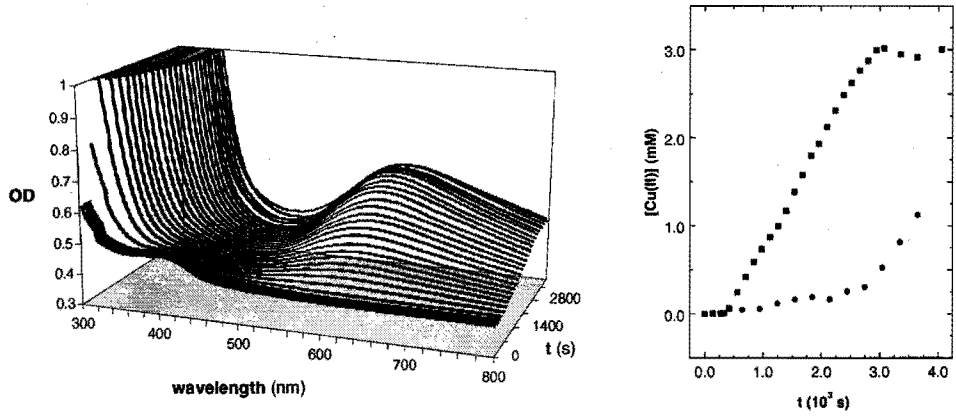

Figure 4.14: *Cu(II)-absorption by fifth generation poly(propylene imine) dendrimer in hemodialyzer. UV/vis spectral changes in dendrimer-stream are shown on the left, changes in [Cu(II)] for dendrimer-stream (–■–) and waterstream (–●–) are shown on the right, based on UV/vis absorption at λ_{max} = 610 and 260 nm respectively; [DAB-dendr-$(NH_2)_{64}$] = 0.11 mM in end group, [Cu(II)] = 2.4 mM, flow rate 15 mL/min .*

4.4.3 Reversible Azide-Binding

The possibility of reversible binding of guests using the hemodialyzer, was investigated with the Cu(II)-dendrimer azide system described in paragraph 4.3.[89] Adding NaN_3 to the feed solution results immediately in an increase in the 400 nm absorption in the dendrimer stream (Figure 4.15) attributed to the formation of a copper-azide complex. Subsequent flushing of the hemodialyzer with NaN_3-free aqueous solution leads to decomplexation of the azide from the Cu(II)-center ($K_{aqua} = 2.2 \cdot 10^2\ M^{-1}$) as apparent from the disappearance of the 400 nm absorption. A second run gave similar results, subscribing the reversibility of the system.

These experiments illustrate the possible use of poly(propylene imine) dendrimers as sensor materials, since rapid response on the presence of azide takes place and the binding is reversible. Dendrimers in films have been used as sensors for volatile organic compounds[90] and sulfurdioxide.[91] However, these sensors are heterogeneous as volatile compounds interact with solid substrates (dendrimer-films). Here, sensor and probe molecule are both in the same aqueous phase, only separated by a size-selective membrane. Moreover, the dialyzer set up makes it possible to monitor aqueous streams continuously.

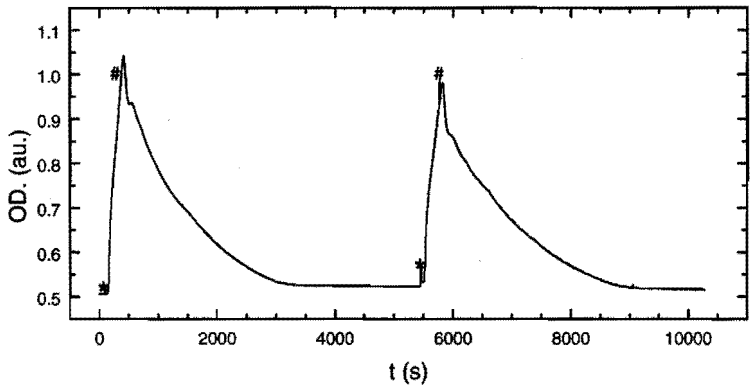

Figure 4.15: *Changes in optical density of Cu(II)-dendrimer solution at $\lambda = 400$ nm in presence and absence of azide; * denotes addition of NaN_3 to feed, # denotes beginning of azide-free feed. [Cu(II)] = 5.7 mM; [N_3^-] = 0.86 mM; flow rate = 6 mL/min.*

4.4.4 Ester Hydrolysis in Membrane Reactor

The possibility of using functionalized fifth generation poly(propylene imine) dendrimers as catalyst in a membrane reactor, was investigated with a Zn(II)-containing dendrimer as catalyst for ester hydrolysis. In a first attempt, a dialysis bag was used to separate the dendrimer from the bulk solution. Adding *p*-nitrophenol acetate to the solution, resulted first in a yellowing of the contents of the dialysis bag. Where upon the complete solution turned yellow, caused by the release of *p*-nitrophenolate. Repeating this procedure after refreshing of the bulk solution gave similar results, showing that the catalyst is retained by the membrane. Figure 4.16c-g shows the reproductivity up to five sequential runs. In contrast, when [ZnMedpt]$(ClO_4)_2$ was used as catalyst, refreshing of bulk solution resulted in a drop in reaction rate (Figure 4.16b). What is expected for a catalytic species that is small enough to diffuse through the dialysis membrane.

An even better way to perform ester hydrolysis with a membrane reactor was found when a stirred cell was used. In this case separation of catalyst and products only takes place batch wise after a certain period of time by pressing the solution through a membrane (polymer supported regenerated cellulose). Consequently, a better mixing exists between catalyst and substrate, resulting in almost quantitative hydrolysis of the ester after 1 hour. Then, the reaction mixture was pressed through the membrane, leaving the fifth generation Zn(II)-dendrimer almost completely stripped from reaction products in the reactor. In the two sequential runs, the same catalyst solution did not show a decrease in catalytic activity, subscribing the validity of this approach.

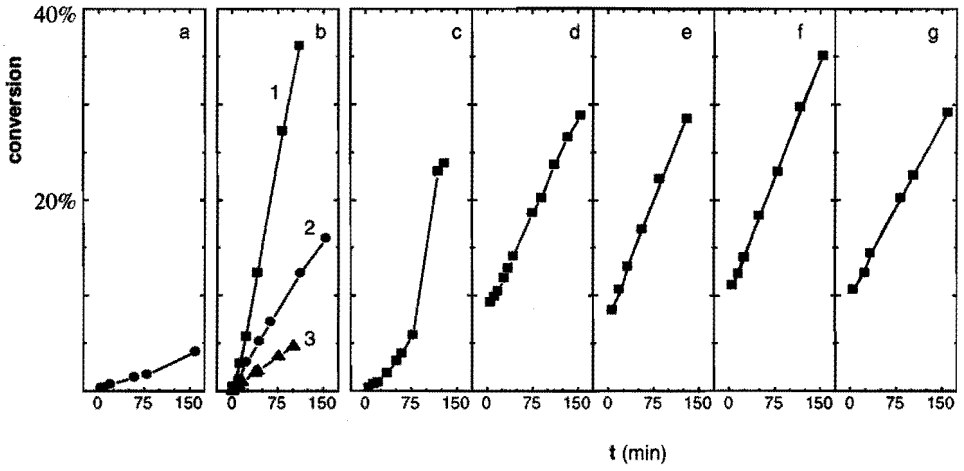

Figure 4.16: *Hydrolysis of p-nitrophenol acetate in membrane reactor consisting of dialysis bag; a: no catalyst present, b: three sequential runs with [ZnMedpt](ClO_4) as catalyst, c-g: five sequential runs with [Zn_{32}DAB-dendr-(NH_2)$_{64}$](ClO_4)$_{64}$ as catalyst. HEPES / MeOH (1 / 1 v / v), pH = 7.2, 35°C.*

Changing the dialysis bag for the hemodialyzer, made it possible to do the reaction continuously. Monitoring the release of *p*-nitro phenol in time, revealed a steadily increase in product formation followed by a gradual leveling off at 5% conversion. This low conversion is probably caused by a combination of the short residence time in the dialyzer (11.5 min.) and slow diffusion through the membrane.

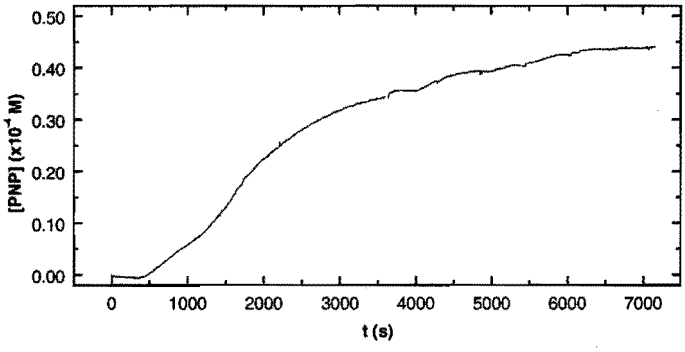

Figure 4.17: *Ester hydrolysis with Zn(II)-dendrimer in hemodialyzer, [Zn(II)] = 5.8 mM, [PNP] = 0.8 mM, flow rate is 2.6 mL / min. Corrected for non-catalyzed reaction.*

4.5 Conclusions

In conclusion we have shown that the poly(propylene imine) dendrimers can be used as polydentate ligands for Cu(II), Ni(II), and Zn(II). Site selective metal-complexation takes place by the dpt end group. Therefore, the construction of metal containing assemblies of defined structure and size is possible. The peripheral metal-sites are accessible for guest-molecules (azides), and capable of catalyzing ester hydrolysis. Due to their large size, the fifth generation metal loaded dendrimers can be separated from solution using regenerated cellulose membranes. As a consequence, these dendrimers combine the advantages of homo- and heterogeneous systems used for metal-extraction, sensoring, and catalysis.

Thus, this study has shown that it is possible to use dendrimers in homogeneous catalysis and separate them via filtration techniques. However, in line with other studies,[11,25,34–44] attaching catalytic sites to a dendritic molecule does not result in dramatic beneficial effects in catalytic activity, when compared to monomeric analogues. As the added value of the dendritic systems is only coming from the large size of the dendrimer, this field of research can be regarded as a revisitation of the research on polymer-supported catalysts. Ultimately, a more tailored design of dendritic catalysts can have a great future when systems are created in which multiple interactions favor the reaction under investigation, or in which the dendritic framework provides a beneficial micro-environment.[92]

4.6 Experimental Section

General Methods and Materials

Commercial grade reagents were used without further purification. All solvents were of p.a. quality. $Cu(ClO_4)_2.6H_2O$, $Zn(ClO_4)_2.6H_2O$, and 4-nitrophenyl acetate were purchased from Aldrich. *N*-[2-hydroxyethyl)piperazine-*N'*-[2-ethanesulfonic acid] (HEPES) was purchased from Sigma. In all cases HEPES used, the buffered solutions consisted of 50 mM HEPES in water adjusted to a pH of 7.2. *p*-Nitrophenyl-picolinate was prepared according to literature methods, *m.p.* 148–152 °C (lit. 144–146 °C).[93] pH-measurements were performed with a Sentron 1001 pH system calibrated between pH = 7 and 10. The stirred cell was received from Schleicher and Schuell equipped with an Ultran RC membrane having a cut off of 10 kD. The hemodialyzer (COBE Centrysystem) was kindly provided by Prof. J. T. F. Keurentjes. The hemodialyzer was connected to a Minipuls 3 Peristaltic Pump (Gilson) using PVC tubing, the flow range was in between 0 and 26 mL/min. For a general section concerning spectroscopic techniques: see Chapter 2.

Warning! Although the perchlorate salts described here were not found to be shock sensitive, care should be taken in handling these compounds.[94]

X-Ray Crystallography

Crystal data for of $[(\mu_4\text{-}CO_3)(\mu\text{-}Cl)_2\{Cu_4(DAB\text{-}dendr\text{-}(NH_2)_4)_2\}](ClO_4)_4$: $C_{33}H_{80}Cl_2Cu_4N_{12}O_3$, Mr = 1018.19, blue, block-shaped crystal (0.15 x 0.15 x 0.30 mm), orthorombic spacegroup Pnma (no. 62) with a = 17.8337(18), b = 13.2938(12), c = 25.857(3) Å, V = 6130.1(10) Å^3, Z = 4, D_x = 1.103 gcm^{-3}, F(000) = 2144, μ(Mo Kα) = 1.5 mm^{-1}. All data, where relevant, are given without disordered solvent contribution (*vide*

infra). 96063 Reflections measured, 5808 independent reflections, R_{int} = 0.134, 1.6° < θ < 25.25°, T = 150 K, Mo Kα radiation, graphite monochromator, λ = 0.71073 Å). and 259 parameters. Data were collected on an Enraf-Nonius KappaCCD area detector on rotating anode. The structure was solved by Patterson methods (SHELXS86) and refined on F^2 using SHELXL-97-2. Channels, with a total volume of 2151 Å^3 per unit cell were found to be filled with disordered counterions (ClO_4^-) and solvent molecules, probably water and methanol. No satisfactory model could be refined. This disordered density was taken into account with the SQUEEZE procedure, as implemented in PLATON. A total electron count of 1088 per unit cell was found and corrected for. Hydrogen atoms were included in the refinement on calculated positions riding on their carrier atoms. All non-hydrogen atoms were refined with anisotropic thermal parameters; hydrogen atoms were refined with a fixed isotropic thermal parameter related to the value of the equivalent isotropic displacement parameter of their carrier atoms by a factor of 1.2. Final $wR2$ = 0.1534, $R1$ = 0.0686 (for 5221 $I > 2\sigma(I)$), $w = 1/[\sigma^2(F^2) + (0.0515P)^2 + 20.78P]$, with $P = (\mathrm{Max}(F_o^2, 0) + 2F_c^2)/3$, S = 1.140, $-1.13 < \Delta\rho < 0.51$ e Å^{-3}.

UV/vis Titrations

Stock solutions of 10^{-2} M metal salt in methanol were added in aliquots of 10–40 μL to a 10^{-3} M (end group) solution of poly(propylene imine) dendrimer of a known volume (2–3 mL) in a quartz cell. Spectra were recorded after vigorous stirring and corrected for dilution. Azide titrations were performed by adding aliquots (40–50 μL) of NaN_3 dissolved in methanol (10^{-3} M) to a methanol solution containing the $CuCl_2$-loaded dendrimers (10^{-5} M in copper) of known volume (2 mL). Binding constants were evaluated by fitting the data with a nonlinear least squares fitting procedure (Origin 4.1).[95]

EPR Titrations

To a 10^{-2} M (end group) methanolic solution of DAB-*dendr*-$(NH_2)_n$ in a quartz EPR-tube (300–400 μL) aliquots (20–40 μL) were added of 10^{-2} M Cu(II) in methanol. The solution was mixed by bubbling helium through it. In case of low temperature measurements (130 K), samples were quenched in liquid nitrogen prior to measurements.

NMR Titrations

In a typical titration, 7.2 mg DAB-*dendr*-$(NH_2)_8$ was directly weighed into a NMR-tube and dissolved in 1 mL deuterated methanol. Aliquots of 20 uL (0.7 equiv.) $ZnCl_2$ solution in CD_3OD were added portion-wise added. Spectra were recorded after vigorous stirring and short heating of the sample.

ESI-MS Spectrometry

ESI-MS spectra were recorded on a API 300 MS/MS mass spectrometer (PE-Sciex) with a mass range of 3000. The sample solutions were delivered to the ES-mass spectrometer by a syringe pump (Harvard Apparatus) at a flow rate of ca. 5 μLmin^{-1} in MeOH/MeCN mixtures containing ~1 mM [Cu(II)]. Orifice voltages ranged between 25 and 200 V. Spectral simulations were performed with IsoPro 3.0.

Kinetic Studies

In a typical run a cell was filled 2 mL HEPES-buffer, 30 μL dendrimer solution (66 mM in dpt-end group, HEPES), and 34 μL $Zn(ClO_4)_2$ (58 mM, H_2O). The cell was placed in a thermostated cell-holder at 35 °C and continuously stirred. The kinetic run was initiated by injecting a 12 μL sample of 8.2 mM PNPP in acetonitrile. Liberation of PNP was monitored at 400 nm for at least 8 half-lives. Linear first-order plots were always obtained for at least 2 half-lives.

Experiment using the dialysis bag were performed in HEPES/methanol (1/1 v/v). In a typical experiment, a dialysis bag containing 5 mL of Zn(II)-dendrimer solution ([Zn(II)] = 30 mM) was placed in the solution (20 mL) which was thermostated at 35 °C. Catalytic runs were started by addition of 6.5 mg ($3.6 \cdot 10^{-5}$ mol) *p*-nitrophenol acetate. For subsequent runs, the dialysis bag was not changed, whereas the contents of the reaction vessel was refreshed.

The stirred cell experiments were performed in 60 mL HEPES/methanol (1/1 v/v) containing DAB-*dendr*-$(NH_2)_{64}$ with 32 equivalents $Zn(ClO_4)_2$ ([Zn(II) = 4 mM) which was first dialyzed with an equal amount of solvent. Reactions were performed at room temperature and initiated by adition of 17 mg ($9.4 \cdot 10^{-5}$ mol) *p*-nitrophenol acetate.

Hemodialyzer Experiments

Retention of $[Cu_{32}DAB\text{-}dendr\text{-}(NH_2)_{64}](ClO_4)_{32}$ was tested with a solution of 50 mL HEPES/MeOH (1/1 v/v) containing 44 mg DAB-*dendr*-$(NH_2)_{64}$ with 32 equiv. $Cu(ClO_4)_2$ ([Cu(II)] = 4 mM). This was dialyzed (2x) against 50 mL of the same solvent combination, every run lasted for 4 h at a rate of 20 mL/min. The [Cu(II)] in the dialyzate was determined with EPR and amounted to 1% of that of the dendrimer solution in the first run and unmeasurable small in the second run. In the subsequent experiments, the hemodialyzer loaded with fifth generation poly(propylene imine) dendrimer was first dialyzed against HEPES to remove low molecular weight impurities before the actual experiment was started.

The extraction of Cu(II) from the dialyzate was performed by dialyzing 0.11 mM DAB-*dendr*-$(NH_2)_{64}$ in 30 mL HEPES against 2.4 mM $Cu(ClO_4)_2$-solution in HEPES at aflow rate of 15 mL/min. The [Cu(II)] in the dendrimer stream was followed on line with UV/vis spectroscopy, whereas the [Cu(II)] in the dialyzant was determined periodically by measuring the absorption at 260 nm.

Reversible azide-binding was probed with a solution of DAB-*dendr*-$(NH_2)_{64}$ with 32 equivalents $Cu(ClO_4)_2$ in 30 mL HEPES ([Cu(II)] = 5.7 mM), which was dialyzed against a 0.86 mM NaN_3 solution in HEPES, or azide-free HEPES solution, at a flow rate of 6 mL/min. The formation of a Cu(II)-N_3 complex was on line followed spectrophotometrically by monitoring the optical density at λ = 400 nm.

Ester hydrolysis was performed with a 30 mL solution of DAB-*dendr*-$(NH_2)_{64}$ with 32 equivalents $Zn(ClO_4)_2$ ([Zn(II)] = 5.8 mM) in HEPES/MeOH (1/1 v/v). This was dialyzed against *p*-nitrophenol acetate (0.8 mM) in the same solvent combination at a flow rate of 2.6 mL/min. The release of *p*-nitrophenol (PNP) in the dialyzate was spectrophotometrically monitored on line at λ = 400 nm. The concentration of PNP was determined by callibration with a PNP stock solution. The non-catalyzed release of PNP was determined by performing the dialysis-procedure without the presence of Zn(II)-dendrimer.

4.7 References and Notes

1. Steigerwald, M.; Brus, L. *Acc. Chem. Res.* **1990**, *23*, 183–188. Weller, H. *Adv. Mater.* **1993**, *5*, 88–95. Weller, H. *Angew. Chem. Int. Ed. Engl.* **1993**, *32*, 41–53. Alivisatos, A. P. *Science* **1996**, *271*, 933–937.
2. Schmid, G. *Chem. Rev.* **1992**, *92*, 1709–1727. Lewis, L. N. *Chem. Rev.* **1993**, *93*, 2693–2730.
3. Kaneko, M.; Tsuchida, E. *J. Polym. Sci., Macromol. Rev.*, **1981**, *16*, 397–522.
4. Biswas, M.; Mukherjee, A. *Adv. Polym. Sci.*, **1994**, *115*, 91–123.
5. Feiters, M. C. In *Supramolecular Catalysis*; Reinhoudt, D. N., Ed.; Comprehensive Supramolecular Chemistry 10; Lehn, J.-M. Ed.; Pergamon Press: Elmsford, NY, 1995; pp. 267-360.
6. Tomoyose, Y. T.; Jiang, D.-L.; Jin, R.-H.; Aida, T.; Yamashita, T.; Horie, K.; Yashima, E.; Okamoto, Y. *Macromolecules* **1996**, *29*, 5236–5238. Sadamoto, R.; Tomioka, N.; Aida, T. *J. Am. Chem. Soc.* **1996**, *118*, 3978–3979.
7. Dandliker, P. J.; Diederich, F.; Gross, M.; Knobler, C. B.; Louati, A.; Sanford, E. M., *Angew. Chem., Int. Ed. Engl.* **1994**, *33*, 1739–1742.
8. Pollak, K. W.; Leon, J. W.; Fréchet, J. M. J.; Maskus, M.; Abruña, H. D. *Chem. Mater.* **1998**, *10*, 30–38.
9. Dandliker, P. J.; Diederich, F.; Gisselbrecht, J.-P.; C. B.; Louati, A.; Gross, M. *Angew. Chem., Int. Ed. Engl.* **1995**, *34*, 2725–2728. Dandliker, P. J.; Diederich, F.; Zingg, A.; Gisselbrecht, J.-P.; Gross, M.; Louati, A.; Sanford, E. *Helv. Chim. Acta* **1997**, *80*, 1773–1801. Collman, J. P.; Fu, L.; Zingg, A.; Diederich, F. *Chem. Commun.* **1997**, 193–194.
10. Jiang, D.-L.; Aida, T. *Chem. Commun.* **1996**, 1523–1524. Jiang, D.-L.; Aida, T. *J. Mater. Sci. —Pure Appl. Chem.* **1997**, *A34*, 2047–2055.
11. Bhyrappa, P.; Young, J. K.; Moore, J. S.; Suslick, K. S. *J. Am. Chem. Soc.* **1996**, *118*, 5708–5711. Bhyrappa, P.; Young, J. K.; Moore, J. S.; Suslick, K. S. *J. Mol. Cat. A.* **1996**, *113*, 109–116.

12. Gorman, C. B.; Parkhurst, B. L.; Su, W. Y.; Chen, K.-Y. *J. Am. Chem. Soc.* **1997**, *119*, 1141–1142. Gorman, C. B. *Adv. Mater.* **1997**, *9*, 1117–1119. Gorman, C. B.; Hager, M. W.; Parkhurst, B. L.; Smith, J. C. *Macromolecules* **1998**, *31*, 815–822.
13. Chow, H.-F.; Chan, I. Y. K.; Chan, D. T.; Kwok, R. W. *Chem. Eur. J.* **1996**, *2*, 1085–1091.
14. Pollak, K. W.; Leon, J. W.; Fréchet, J. M. J.; Maskus, M.; Abruña, H. D. *Chem. Mater.* **1998**, *10*, 30–38.
15. Issberner, J.; Vögtle, F.; De Cola, L.; Balzani, V. *Chem. Eur. J.* **1997**, *3*, 706–712.
16. Mak, C. C.; Chow, H.-F. *Macromolecules* **1997**, *30*, 1228–1230. Chow, H.-F.; Mak, C.C. *J. Org. Chem.* **1997**, *62*, 5116–5127.
17. Rheiner, P. B.; Sellner, H.; Seebach, D. *Helv. Chim. Acta* **1997**, *80*, 2027–2032.
18. Campagna, S.; Denti, G.; Serroni, S.; Ciano, M.; Juris, A.; Balzani, V. *Inorg. Chem.* **1992**, *31*, 2982–2984. Denti, G.; Campagna, S.; Serroni, S.; Ciano, M.; Balzani, V. *J. Am. Chem. Soc.* **1992**, *114*, 2944–2950.
19. Newkome, G. R.; Cardullo, F.; Constable, E. C.; Moorefield, C. N.; Thompson, A. M. W. C. *J. Chem. Soc., Chem. Commun.* **1993**, 925–927. Newkome, G. R.; Güther, R.; Moorefield, C. N.; Cardullo, F.; Echegoyen, L.; Pérez-Cordero E.; Luftmann, H. *Angew. Chem., Int Ed. Engl.* **1995**, *34*, 2023–2026.
20. Achar S.; Puddephatt, R.J. *Angew. Chem., Int Ed. Engl.* **1994**, *33*, 847–849.
21. Huck, W. T. S.; van Veggel, F. C. J. M.; Reinhoudt, D. N. *Angew. Chem.*, **1996**, 35, 1213–1215. Huck, W. T. S.; Prins, L.J.; Fokkens, R. H.; Nibbering, N. M. M.; van Veggel, F. C. J. M.; Reinhoudt, D. N. *J. Am. Chem. Soc.* **1998**, *120*, 6240–6246.
22. Slany, M.; Bardají, M.; Casanove, M.-J.; Caminade, A.-M.; Majoral, J. P.; Chaudret, B. *J. Am. Chem. Soc.*, **1995**, *117*, 9764–9765.
23. Lange, P.; Schier; A.; Schmidbauer, H. *Inorg. Chem.* **1996**, *35*, 637–642.
24. Wiener, E. C.; Brechbiel, M. W.; Brothers, H.; Magin, R. L.; Gansow, O. A.; Tomalia, D. A.; Lauterbur, P. C. *Magn. Reson. Med.* **1994**, *31*, 1–8.
25. Knapen, J. W. J.; van der Made, A. W.; de Wilde, J. C.; van Leeuwen, P. W. M.; Wijkens, P.; Grove, D. M.; van Koten, G. *Nature* **1994**, *372*, 659–663.
26. Lia, Y.-H.; Moss, J. R. *Organometallics*, **1996**, *14*, 2130–2132. Lia, Y.-H.; Moss, J. R. *Organometallics*, **1996**, *15*, 4307–4316.
27. Bardaji, M.; Caminade, A.-M.; Majoral, J.-P.; Chaudret, B. *Organometallics* **1997**, *16*, 3489–3497.
28. Reetz, M. T.; Lohmer, G.; Schwickardi, R. *Angew. Chem., Int. Ed. Engl.* **1997**, *36*, 1526–1529.
29. Bardaji, M.; Kustos, M.; Caminade, A.-M.; Majoral, J.-P.; Chaudret, B. *Organometallics* **1997**, *16*, 403–410
30. Cuadrado, I.; Morán, M. Casado, C. M.; Alonso, B.; Lobete, F.; Garcia, B.; Ibisate, M.; Losada, J. *Organometallics*, **1996**, *15*, 5278–5280. Takada, K.; Diaz, D.; Abruña, H. D.; Cuadrado, I.; Casado, C.; Alonso, B.; Morán, M.; Losada, J. *J. Am. Chem. Soc.* **1997**, *119*, 10763–10773.
31. Valério, C.; Fillaut, J.-L.; Ruiz, J.; Guittard, J.; Blais, J.-C.; Astruc. D. *J. Am. Chem. Soc.* **1997**, *119*, 2588–2589.
32. Zeng, F.; Zimmerman, S. C. *Chem Rev.* **1997**, *97*, 1681–1712. Gorman, C. *Adv. Mater.* **1998**, *10*, 295–309. Archut, A.; Vögtle, F. *Chem. Soc. Rev.* **1998**, *27*, 233–240. Smith, D. K.; Diederich, F. *Chem. Eur. J.* **1998**, *4*, 1353–1361. Hearshaw, M. A.; Moss J. R. *Chem. Commun.* **1999**, 1–9.
33. Tomalia, D. A.; Dvornic, P. R. *Nature* **1994**, 617–618.
34. Bolm, C; Derrien, N.; Seger, A. *Synlett* **1996**, 387–388.
35. Rheiner, P. B.; Sellner, H.; Seebach, D. *Helv. Chim. Acta* **1997**, *80*, 2027–2032.
36. Brunner, H. *J. Organomet. Chem.* **1995**, *500*, 39–46. Brunner, H.; Altmann, S. *Chem. Ber.* **1994**, *127*, 2285–2296. Brunner, H.; Fürst, J. *Tetrahedron* **1994**, *50*, 4303–4310.
37. Morao, I.; Cossío, P. *Tetrahedron Lett.* **1997**, *38*, 6461–6464.
38. Mak, C.C.; Chow, H.-F. *Macromolecules* **1997**, *30*, 1228–1230. Chow, H.-F.; Mak, C.C. *J. Org. Chem.* **1997**, *62*, 5116–5127.
39. van de Kuil, L. A.; Grove, D. M.; Zwikker, J. W.; Jenneskens, L. W.; Drenth, W.; van Koten, G. *Chem. Mater.* **1994**, *6*, 1675–1683.
40. Hovestadt, N. J.; Eggeling, E. B.; Heidbuchel, H. J.; Jastrzebski, J. T. B. H.; Kragl, U.; Keim, W.; Vogt, D.; van Koten, G. *Abstract of Papers*, 1st Dutch Dendrimer Meeting, Eindhoven, The Netherlands, February 1999.
41. Marquardt, T.; Lüning, U. *Chem. Commun.* **1997**, 1681–1682.

42. Suzuki, T.; Hirokawa, Y.; Ohtake, K.; Shibata, T.; Soai, K. *Tetrahedron Asymm.* **1997**, *8*, 4033–4040.
43. Peerlings, H. W. I.; Meijer, E. W. *Chem. Eur. J.* **1997**, *3*, 1563–1570. Peerlings, H. W. I. *Ph.D. Thesis*, University of Technology Eindhoven, Sept. 1998.
44. Köllner, C.; Pugin, B.; Togni, A. *J. Am. Chem. Soc.* **1998**, *120*, 10274–10275.
45. Dagani, R. *Chem. Eng. News* **1999**, *77(6)*, 33-36.
46. Balogh, L.; Tomalia, D. A. *J. Am. Chem. Soc.* **1998**, *120*, 7355–7356.
47. Zhao, M.; Sun, L.; Crooks, R. M. *J. Am. Chem. Soc.* **1998**, *120*, 4877–4878.
48. Sooklal, K.; Hanus, L. H.; Ploehn, H. J.; Murphy, C. J. *Adv. Mater.* **1998**, *10*, 1083–1087. Beck Tan, N. C.; Balogh, L.; Trevino, S. F.; Tomalia, D. A.; Lin, J. S. *Polymer* **1999**, *40*, 2537–2545.
49. Balogh, L.; Valluzzi, R.; Laverdure, K. S.; Gido, S. P.; Hagnauer, G. L.; Tomalia, D. A. *J. Nanoparticle Res.* **1999**, in press.
50. Zhao, M.; Crooks, R. M. *Angew. Chem., Int. Ed. Engl.* **1999**, *38*, 364–366, Zhao, M.; Crooks, R. M. *Adv. Mat.* **1999**, *11*, 217–220 .
51. Barefield, E. K.; Carrier, A. M.; VanDerveer, D. G. *Inorg. Chim. Acta*, **1980**, *42*, 271–275. Cannas, M.; Cristini, A.; Marongin, G. *Acta Cryst. A*, **1978**, *34*, 139S. House D. A.; Robinson, W. I. *Inorg. Chim. Acta*, **1988**, *141*, 211–220. Harada, K. *Bull. Chem. Soc. Jpn.*, **1993**, *66*, 2889–2899.
52. Adams, H.; Bailey, N. A.; Carlisle, W. D.; Fenton D. E. *Acta Cryst. C*, **1990**, *46*, 1439–1441.
53. Itoh, T.; Fujii, Y.; Tada, T.; Yoshikawa, Y.; Hisada, H. *Bull. Chem. Soc. Jpn.*, **1996** *69*, 1265–1274.
54. Biagini, S.; Cannas, M. *J. Chem. Soc. (A)*, **1970**, 2398–2408.
55. Vacca, A.; Arenare, D.; Paoletti, P. *Inorg. Chem.* **1966**, *5*, 1384–1389.
56. Stevelmans, S.; van Hest, J. C. M.; Jansen, J. F. G. A.; van Boxtel, D. A. F. J.; de Brabander-van den Berg, E. M. M.; Meijer, E. W. *J. Am. Chem. Soc.* **1996**, *118*, 7398–7399.
57. Ottaviani, M. F.; Bossmann, S.; Turro, N. J.; Tomalia, D. A. *J. Am. Chem. Soc.* **1994**, *116*, 661–671. Ottaviani, M. F.; Montalti, F.; Turro, N. J.; Tomalia, D. A. *J. Phys. Chem. B* **1997**, *101*, 158–166.
58. Barbucci, R.; Campbell, M. J. M. *Inorg. Chim. Acta*, **1976**, *16*, 113.
59. Lever, A. B. P. In *Inorganic Electronic Spectroscopy*, 2nd ed.; Studies in Physical and Theoretical Chemistry 33; Elsevier: Amsterdam, 1984.
60. Colton, R.; D'Agostino, A.; Traeger, J. C. *Mass Spectrom. Rev.* **1995**, *14*, 79–106.
61. Chu, I. K.; Lau, T.-C.; Siu, K. W. M. *J. Mass Spectrom.* **1998**, *33*, 811–818.
62. Gatlin, C. L.; Tureček, F.; Vaisar, T. *J. Am. Chem. Soc.* **1995**, *117*, 3637–3638. Vaisar, T.; Gatlin, C. L.; Tureček, F. *Int. J. Mass Spectrom. Ion Proc.* **1997**, *162*, 77–87.
63. Kohler, M.; Leary, J. A. *J. Am. Soc. Mass Spectrom.* **1997**, *8*, 1124–1133.
64. Lavanant, H.; Virelizier, H.; Hoppiliard, Y. *J. Am. Soc. Mass Spectrom.* **1998**, *9*, 1217–1221.
65. Curtis, N. F.; Hay, R. W.; Curtis, Y. M. *J. Chem. Soc. A* **1968**, 182–187.
66. Einstein, F. W. B.; Willis, A. C. *Inorg. Chem.* **1981**, *20*, 609–614. Escuer, A.; Peñalba, E.; Vicente, R.; Solans, X.; Font-Bardía, M. *J. Chem. Soc. Dalton Trans.I*, **1997**, 2315–2319.
67. Süsse, P. *Acta Crystallogr.* **1967**, *22*, 146–148.
68. Drago, R. S.; Meek, D. W.; Longhi, R.; Joesten, M. D. *Inorg. Chem.*, **1963**, *2*, 1056–1060.
69. Solomon, E. I. In *Copper Proteins*; Spiro, T. G., Ed.; Wiley: New York, 1981; Vol. 3, pp. 41–108. *Copper Coordination Chemistry: Biochemical & Inorganic Perspectives;* Karlin, K. D., Zubieta, J., Eds.; Adenine: Guilderland, NY, 1983.
70. Comarmond, J.; Plumeré, P.; Lehn, J.-M.; Agnus, Y.; Louis, R.; Weiss, R.; Kahn, O.; Morgenstern-Badarau, I. *J. Am. Chem. Soc.* **1982**, *104*, 6330–6340.
71. McKee, V.; Zvagulis, M.; Dagdigian, J. V.; Patch, M. G.; Reed, C. A. *J. Am. Chem. Soc.* **1984**, *106*, 4765–4772. Pate, J. E.; Ross, P. K.; Thamann, T. J.; Reed, C. A.; Karlin, K. D.; Sorrell, T. N.; Solomon, E. I. *J. Am. Chem. Soc.* **1989**, *111*, 5198–5209.
72. Dugas, H.; Penney, C. In *Bioorganic Chemistry*; Springer Advanced Texts in Chemistry, Cantor, C. R. Ed., Springer-Verlag: New York, 1981. Kimura, E. In *Progress in Inorganic Chemistry*; Karlin, K. D., Ed.; John Wiley & Sons: New York, 1994; Vol. 41, pp 443–491.
73. Sigman, D. S.; Jorgensen, C. T. *J. Am. Chem. Soc.* **1972**, *94*, 1724–1730.
74. Fife, T. H.; Przystas, T. J. *J. Am. Chem. Soc.* **1985**, *107*, 1041–1047.
75. Weijnen, J. G. J.; Koudijs, A.; Engbersen, J. F. J. *J. Chem. Soc., Perkin Trans. 2* **1991**, 1121–1126. Weijnen, J. G. J.; Koudijs, A.; Schellekens, G. A.; Engbersen, J. F. J. *J. Chem. Soc., Perkin Trans. 2* **1992**, 829–834.
76. Kimura, E.; Hashimoto, H.; Koike, T. *J. Am. Chem. Soc.* **1996**, *118*, 10963–10970.

77. Fornasier, R.; Scrimin, P.; Tecilla, P.; Tonellato, U. *J. Am. Chem. Soc.* **1989**, *111*, 224–229.
78. Menger, F. M.; Gan, L. H.; Johnson, E.; Durst, D. H. *J. Am. Chem. Soc.* **1987**, *109*, 2800–2803.
79. Prosa, T. J.; Bauer, B. J.; Amis, E. J.; Tomalia, D.A.; Scherrenberg, R. *J. Polym. Sc. B* **1997**, *35*, 2913–2924.
80. De Brabander, E. M. M.; Brackman, J.; Mure-Mak, M.; de Man, H.; Hogeweg, M.; Keulen, J.; Scherrenberg, R.; Coussens, B.; Mengerink, Y.; van der Wal, S. *Macromol. Symp.* **1996**, *102*, 9–17.
81. Scherrenberg, R.; Coussens, B.; van Vliet, P.; Edouard, G.; Brackman, J.; de Brabander, E.; Mortensen, K. *Macromolecules* **1998**, *31*, 456–461.
82. Bosman, A. W.; Jansen, J. F. G. A.; Janssen, R. A. J.; Meijer; E. W. *Proc. ACS. PMSE.*, **1995**, *73*, 340–341. Bosman, A. W.; Janssen, R. A. J.; Meijer, E. W. *Macromolecules* **1997**, *30*, 3606–3611. Klein Gebbink, R. J. M.; Bosman, A. W.; Feiters, M. C.; Meijer, E. W.; Nolte, R. J. M. *Chem. Eur. J.* **1998**, *5*, 65–69.
83. Kesting, R. E. In *Synthetic Polymeric Membranes*; McGraw-Hill: New York, 1971. Jonsson, G. In: *Synthetic Membranes*; Bungay, P.M., Lonsdale, H. K., Pinho, de, M.N., Eds.; NATO ASI Series C 181, D. Reidel Publishing: Dordrecht (The Netherlands), 1986, pp. 625–646.
84. Hummelen, J. C.; van Dongen, J. L. J.; Meijer, E. W. *Chem. Eur. J.* **1997**, *3*, 1489–1493.
85. Geckeler, K.; Lange, G.; Eberhardt, H.; Bayer, E. *Pure Appl. Chem.* **1980**, *52*, 1883–1905.
86. Rivas, B.; Geckeler, K. E. *Adv. Polym. Sci.* **1992**, *102*, 171–188.
87. Lindsay, D.; Sherrington, D. C.; Greig, J. A.; Hancock, R. D. *React. Polym.* **1990**, *12*, 59–73. Lindsay, D.; Sherrington, D. C.; Greig, J. A.; Hancock, R. D. *React. Polym.* **1990**, *12*, 75–82.
88. Spivakov, B. Y.; Geckeler, K.; Bayer, E. *Nature* **1985**, *315*, 313–315. Geckeler, K.; Volchek, K. *Envir. Sci. Techn.* **1996**, *30*, 725–734.
89. Fabbrizzi, L.; Pallavicini, P.; Parodi, L.; Taglietti, A. *Inorg. Chim. Acta* **1995**, *238*, 5–8. Fabbrizzi, L.; Faravelli, I.; Francese, G.; Licchelli, M. Perotti, A.; Taglietti, A. *Chem. Commun.* **1998**, 971–972.
90. Wels, M.; Crooks, R. M. *J. Am. Chem. Soc.* **1996**, *118*, 3988–3989. Ricco, A. J.; Crooks, R. M.; Osburn, G. C. *Acc. Chem. Res.* **1998**, *31*, 289.
91. Albrecht, M.; Gossage, R. A.; Spek, A. L.; van Koten, *Chem. Comm.* **1998**, 1003–1004. Albrecht, M.; van Koten, G. *Adv. Mater.* **1999**, *11*, 171–174.
92. Piotti, M.; Hawker, C.; Fréchet, J. M. J.; Rivera, F.; Dao, J.; Bond, R. *Polym. Preprints* **1999**, *40*, 410-411.
93. Sigman, D. S.; Jorgensen, C. T. *J. Am. Chem. Soc.* **1972**, *94*, 1724–1730.
94. Wolsey, W. C., *J. Chem. Ed.* **1973**, *50*, A335.
95. For the equation used, see ref. 10 in: Deans, R.; Cooke, G.; Rotello, V. M. *J. Org. Chem.* **1997**, *62*, 836–839.

Biomimicry with Dendrimers*

5

Abstract: *Functionalized poly(propylene imine) dendrimers are used to mimic the multivalency present in many biological systems resulting from the highly branched architecture of dendrimers. First, four subsequent generations of poly(propylene imine) dendrimers, DAB-dendr-$(NH_2)_n$ with n = 4, 8, 16, and 32 have been functionalized by a high-pressure reaction with 2-vinyl pyridine to give bis[2-(2-pyridyl)ethyl]amine or PY2 ligands as peripheral end groups of the dendrimer. Quantitative coordination of one Cu(II) or Zn(II) ion per PY2 group takes place for every generation. The fourth generation dendrimer DAB-dendr-$(PY2)_{32}$ binds approximately 30 Cu(I) ions. Low temperature (-85 °C) UV/vis spectroscopy of this complex in dichloromethane in the presence of dioxygen shows that 70–75 % of the copper centers are involved in dioxygen binding, corresponding to 11–12 molecules of dioxygen per dendrimer molecule. This complex is a model for hemocyanin, the copper containing oxygen transport protein of molluscs and arthropods. Second, the poly(propylene imine) dendrimers are used as a scaffold to assemble multiple porphyrins, both in a covalent and non-covalent way. In the non-covalent approach, two different Zn(II)-porphyrins are assembled around the dendrimers via coordination to the primary amine end groups. The number of assembled porphyrins ranges from 2 to 33, depending on dendrimer generation and porphyrin used. In the covalent approach, assemblies with 4, 8, 16, and 64 porphyrins have been obtained by attaching an acid-functionalized porphyrin to the dendrimer periphery. The covalent assemblies show intramolecular electronic interactions between the porphyrin end groups in the excited state as measured with time-resolved fluorescence anisotropy measurements at 77 K. Thereby mimicking the light harvesting of the natural LH2 system, which is responsible for capturing and storing light-energy in photosynthetic bacteria.*

* Part of this work has been published: Klein Gebbink, R. J. M.; Bosman, A. W.; Feiters, M. C.; Meijer, E. W.; Nolte, R. J. M. *Chem. Eur. J.* **1998**, *5*, 65-69. Reek, J. N. H.; Schenning, A. P. H. J.; Bosman, A. W.; Meijer, E. W.; Crossley, M. J. *Chem. Commun.* **1998**, 11-12.

5.1 Introduction

Already in the early years of dendrimer chemistry, it was proposed that dendrimers can mimic many of the functions that are present in different proteins.[1] This because several characteristic properties of proteins, i.e., the presence of endo- and exo-receptors, globular structure and nanoscopic size, can be found in many dendritic molecules.[2] However, since proteins are much more sophisticated entities than the covalently and polymerically constructed dendrimers, until now only few properties of proteins have been, only partly, mimicked.

Endo-receptors are buried inside a sterically congested protein structure, implying a typical micro-environment at the receptor. This site-isolation has been mimicked in several dendritic structures, since the dendritic core is—at least to some extent—shielded from the medium. In this way several dendritic models for electron-transfer proteins (i.e. cytochrome *c*, iron-sulfur proteins) have been synthesized. They are based on an electroactive core, metalloporphyrin[3] or Fe_4S_4-cluster,[4] surrounded by dendritic wedges. Indeed, large shifts in redox-potentials have been found depending on dendrimer-type and generation. Other examples of endo-receptor mimicking in dendrimers are the myoglobin models based on dendrimers with an iron porphyrin core.[5,6] The dendrimers show reversible oxygen binding in toluene and diminished sensitivity towards water as a result of the dendritic surroundings. Recently, dendrimers containing a Cu(I) complex of *N*-substituted 1,4,7-triazacyclononane in the core, dimerized on addition of oxygen at low temperatures, resulting in a bis(μ-oxo)-dicopper species which can be seen as a mimic for multinuclear metalloproteins.[7]

In many biological systems interactions take place through simultaneous binding of multiple ligands on one biological entity to multiple receptors on other species.[8] This results, amongst others, in enhanced substrate binding originating from either statistical or cooperativity effects. The combination of discrete numbers of functionalities in one molecule and high local densities of active groups, makes dendritic molecules therefore very well suited to act as a synthetic multivalent ligand in biological systems. An example of multivalency in biology can be found in carbohydrate-protein interactions (this specific cooperativity effect is known as the glycoside cluster effect).[9] Consequently, many research groups have been inspired to prepare carbohydrate containing dendrimers, also called 'glycodendrimers'.[10] Indeed several glycodendrimers show enhanced binding properties towards relevant biological macromolecules as tested in several in vitro studies.[11-14] Other biological applications in which the multivalency of dendritic molecules have been successfully applied are the generation of antibodies with dendrimers containing multiple antigen peptides,[15] and dendrimers as gene-transfer agent.[16]

In this chapter two examples of biomimetic dendrimers will be addressed, both based on the multivalency present in these synthetic highly-branched structures. In the first part of the chapter, a multi-O_2 complex derived from a Cu(I)-functionalized poly(propylene imine) dendrimer is described. This complex can be seen as a model for hemocyanine, the copper containing oxygen transport protein of molluscs and arthropods.[17] These studies have been performed in a collaborative program with the group of Prof. R. J. M. Nolte.[18] In the second part, the poly(propylene imine) dendrimers have been used as scaffolds to assemble porphyrins, both in a covalent and non-covalent way, together with the group of Dr. J. N. H. Reek and Prof. M. J. Crossley. Intramolecular electronic interactions are observed between the porphyrin end groups in the excited state.

5.2 Multi-Copper Hemocyanine Model

The remarkable oxygen-binding properties of the binuclear copper protein hemocyanin (Hc) have stimulated many groups to develop biomimetic copper complexes displaying various Cu:O_2 stoichiometries and different binding modes for the O_2-ligand.[17] In particular the complexes reported by Karlin[17] and by Kitajima[17,19] have been very helpful in predicting the μ–η^2:η^2 peroxo binding mode for the O_2-ligand in oxy-Hc. Hc molecules are known to assemble into large aggregates under the influence of protons and of certain alkali and earth alkali metal ions.[20] In this way a multi-metal complex is formed which binds many molecules of O_2. Inspired by this behavior of Hc, a multi-copper complex is designed which is similarly capable of binding a large number of O_2 molecules. In this paragraph the synthesis and metal-binding properties of four generations of dendrimers possessing 4, 8, 16, and 32 bis[2-(2-pyridyl)ethyl]amine (PY2) ligands at their peripheries (**1a-d** respectively, see Figure 5.1) is described. Additionally, pyridine dendrimer **1d** is used to bind approximately 30 Cu(I) ions in its PY2 groups, and the $Cu(I)_{30}$ complex, in turn, can bind 11 or more molecules of O_2.

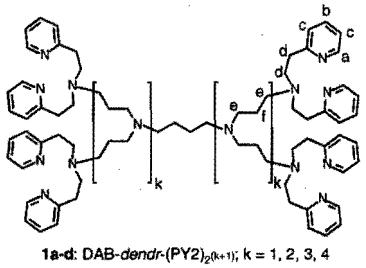

1a-d: DAB-*dendr*-$(PY2)_{2(k+1)}$; k = 1, 2, 3, 4

Figure 5.1: *Newly synthesized PY2-functionalized poly(propylene imine) dendrimers.*

5.2.1 Synthesis and Metal-Binding Properties DAB-dendr-(PY2)$_n$

Synthesis of DAB-*dendr*-(PY2)$_n$. To obtain a multi-ligand system designed to complex Cu(I) ions, the primary amines of the poly(propylene imine) dendrimers were transformed into PY2 groups. Under a pressure of 15 kbar, at 50 °C, and with acetic acid as a catalyst (Scheme 5.1), the dendrimers DAB-*dendr*-(NH_2)$_n$ with n = 4, 8, 16, and 32 were completely converted within sixteen hours into the desired pyridine compound DAB-*dendr*-(PY2)$_n$ (**1a-d**).[21] The resulting viscous orange-brown oils were purified by column chromatography for **1a**, precipitation for **1b** and **1c**, and by dialysis for **1d**.

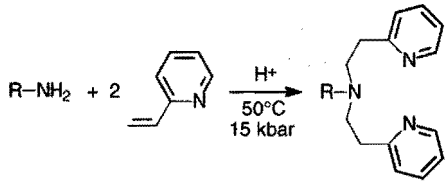

Scheme 5.1: *Synthesis of **1a-d**, R = different generations poly(propylene imine) dendrimers.*

IR and ^{13}C NMR analysis showed that all primary amine groups had reacted under the reaction conditions applied, moreover the relative intensities of the signals in ^1H NMR spectroscopy were in agreement with the expected polypyridine dendrimer structures. For **1a-c**, ESI-MS spectra confirmed the complete functionalization of the dendrimers. Next to the peaks at the expected $[M+H]^+$ positions (1 158, 2 456, and 5 052, respectively), peaks were found at $[M-105]^+$ attributed to retro-Michael reactions resulting in the loss of one vinylpyridine. Moreover, all spectra showed minor peaks originating from fragmentation of the dendritic core[22] and from defects present in the native poly(propylene imine) dendrimers.[23] Peaks at higher masses then the $[M+H]^+$-peak, showed the presence of non-covalent assemblies with vinylpyridine and formic acid, the latter is added to protonate the dendrimers. A typical ESI massaspectrum of compound **1c** is shown in Figure 5.2. ESI and MALDI-TOF mass analysis revealed a very broad ion cluster of low intensity between 7 500–10 500 Da for **1d**. This range corresponds to the calculated molecular mass of the monocation of a completely reacted polyamine, i.e., 10 242 Da. The origin of the broadening of the peak is not clear, but it may be caused by retro-Michael reactions of the PY2 end groups or by fragmentation of the dendritic framework during mass analysis.

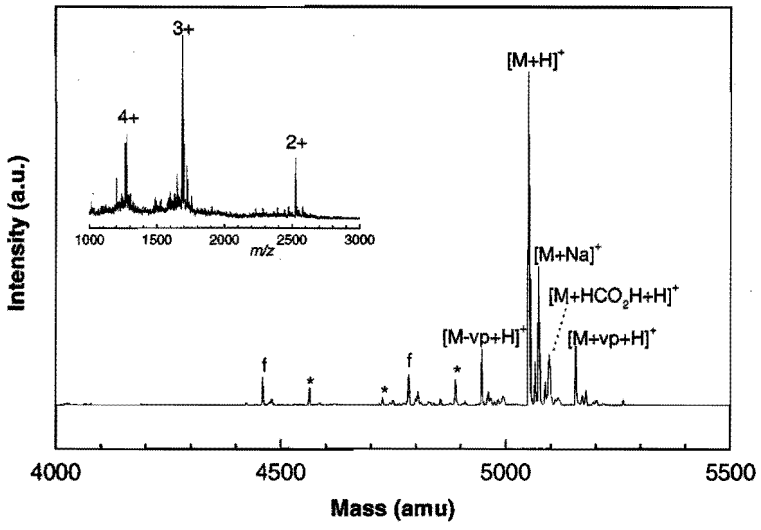

Figure 5.2: *Experimental (inset) and deconvoluted ESI-MS data of* ***1c*** *with molecular ion at 5052; peaks due to fragmentation of dendritic framework are labeled with f, peaks originating from defects in native dendrimer DAB-dendr-$(NH_2)_{16}$ are labeled with an asterisk (vp = vinylpyridine).*

Zn(II) and Cu(II) complexes of DAB-*dendr*-(PY2)$_n$. The number of Cu(II) ions that is complexed by **1a** was investigated by performing a UV/vis titration with $Cu(ClO_4)_2$ in methanol. The titration curve in which the increase in the *d-d* absorption band of the resulting complex at $\lambda = 664$ nm was plotted against the number of Cu(II) ions per ligand revealed the uptake of 4 Cu(II) ions per molecule of **1a**. To get more structural information, a ^{1}H NMR titration of **1a** with $Zn(II)(ClO_4)_2$ in a mixture of deuterated methanol and acetonitrile was carried out. This yielded a number of bound Zn(II) ions identical to that found for Cu(II) in the UV/vis titration, viz. 4 Zn(II) ions. Addition of Zn(II) to **1a** resulted in a new set of pyridine signals at lower field (Figure 5.3) indicating the coordination of the PY2 donor centers to a transition metal. Downfield shifts were also observed for protons belonging to the ethylene spacer and for some of the methylene protons next to tertiary amine nitrogen atoms of **1a**. On the other hand, no shifts were observed for the β-methylene protons in the dendrimer core. Addition of more than 4 equivalents of Zn(II) to **1a** did not result in any additional changes in the ^{1}H NMR spectrum.

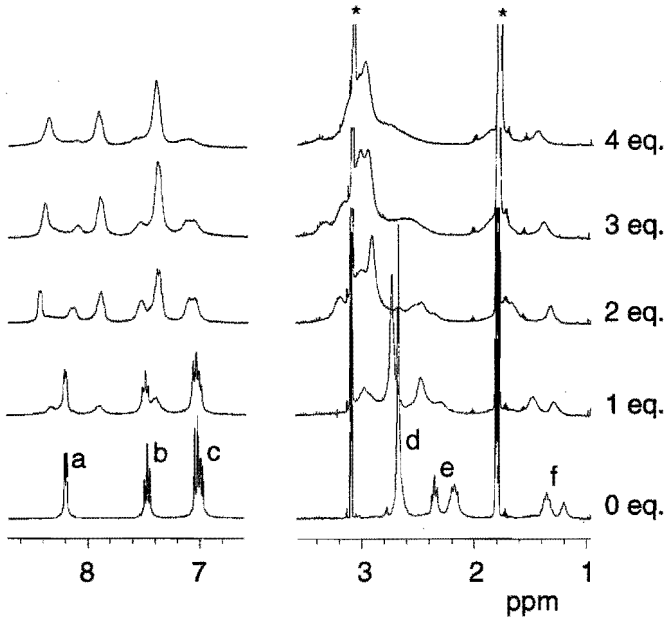

Figure 5.3: *^{1}H NMR titration of **1a** with $Zn(ClO_4)_2$. For peak-assignment see Figure 5.1, asterisk denotes solvent peak.*

The tetranuclear copper complex [**1a**(Cu(II)$_4$](ClO$_4$)$_8$ was obtained in 42 % yield by simply adding a methanol solution of the appropriate amount of Cu(II)(ClO$_4$)$_2$·6H$_2$O to a stirred solution of **1a** in methanol, followed by warming to reflux temperature, and precipitation upon subsequent cooling. MALDI-TOF mass analysis showed a parent peak at 1 710 Da corresponding to a single charged cationic species composed of ligand **1a**, four Cu(I) ions,[24] and three perchlorate counter ions. In its main fragmentation pattern this cation looses the copper and the perchlorate counter ions in consecutive pair-wise steps. In methanol solution this complex behaved as an 8:1 electrolyte, Λ_m = 1 116 Scm^{2}mol^{-1}, indicative of the complete dissociation of the perchlorate counter ions. IR analysis confirmed that also in the solid state the perchlorate is non-coordinating (ν (ClO$_4^-$) = 1 097 and 623 cm^{-1}). A frozen methanol solution of the complex at 130 K displayed a typical axial EPR spectrum ($g_\perp$ = 2.07, $g_{//}$ = 2.25, $A_{//}$ = 170 G), which might be explained by the weak axial coordination of solvent molecules to the copper centers. The EPR line width is small and there is no indication of the presence of more than a single type of copper center. Together with the NMR data and the mass analysis these observations point to the formation of tetranuclear complexes in which the metal centers are complexed by the PY2-ligands and are further weakly coordinated

by solvent molecules. There is no evidence for participation of the tertiary amine nitrogens of the dendritic backbone in the complexation.

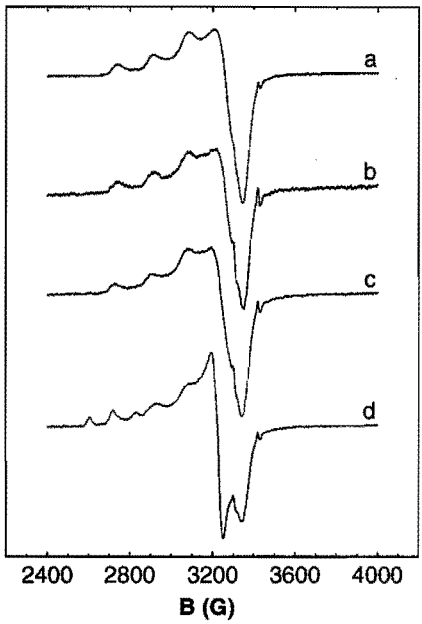

Figure 5.4: *EPR titration of* **1d** *with* $Cu(ClO_4)_2 \cdot 6H_2O$ *in methanol; a) 8 eq. of Cu(II), b) 12 eq. of Cu(II), c) 24 eq. of Cu(II), and d) 32 eq. of Cu(II).*

UV/vis and EPR titrations showed that the newly synthesized pyridine dendrimers **1b**, **1c**, and **1d** readily bind copper ions as well. The UV/vis titration curves of **1b**, **1c**, and **1d** with $Cu(II)(ClO_4)_2 \cdot 6H_2O$ in a 1/1 (v/v) $MeOH/CH_3CN$ mixture revealed inflection points at roughly 8, 16, and 32 copper ions per dendrimer, respectively. The EPR spectra of different mixtures of **1d** and $Cu(II)(ClO_4)_2 \cdot 6H_2O$ in pure methanol are presented in Figure 5.4. A typical axial spectrum, resembling the spectrum recorded for the tetranuclear complex derived from **1a**, was obtained for the 8:1 mixture of $Cu(II)(ClO_4)_2$ and **1d** ($g_\perp = 2.07$, $g_{//} = 2.25$, $A_{//} = 185$ G). Further addition of Cu(II) initially did not change the spectrum much; only after 32 equivalents of Cu(II) had been added, signals belonging to free Cu(II) in solution emerged. During this titration neither the *g*-tensor values nor the copper hyperfine coupling constant underwent large changes, implying a large homogenity of the copper centers. Dendrimer **1d** was also investigated with ^1H NMR by adding different amounts of $Zn(ClO_4)_2$ in a 1/1 (v/v) CD_3OD/CD_3CN mixture. Comparable shifts were obtained as for **1a** with Zn(II). The results of both the UV/vis, EPR and NMR titrations indicate that the fourth generation

dendrimer **1d** was completely functionalized with PY2 ligands, and that the expected number of Cu(II) ions could be bound.

5.2.2 Binding of Cu(I) and O_2 by DAB-*dendr*-(PY2)$_{32}$.

Cu(I)-complexation. To investigate whether the dendritic ligand **1d** behaved in a comparable way towards Cu(I) ions, a UV/vis titration was performed by adding $[Cu(I)(CH_3CN)_4](ClO_4)$ in acetonitrile to a solution of **1d** in dichloromethane under oxygen-free conditions (see Figure 5.5). This titration revealed the uptake of approximately 30 Cu(I) ions per molecule of **1d**, which resembles the number of Cu(II) ions that is bound by this fourth generation dendrimer.

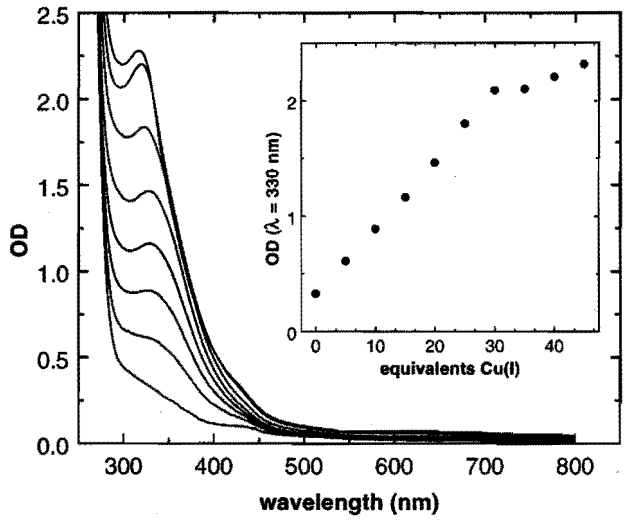

Figure 5.5: *UV/vis titration curve of* ***1d*** *with* $[Cu(I)(CH_3CN)_4](ClO_4)$ *in an acetonitrile-dichloromethane mixture.*

Complex $[\mathbf{1d}(Cu(I))_{30}](ClO_4)_{30}$ was synthesized by simply mixing solid $[Cu(I)(CH_3CN)_4]ClO_4$ with a solution of the pyridine dendrimer **1d** in CH_2Cl_2. The perchlorate counter ion is expected to result in highly reactive, three-coordinate Cu(I) complexes, which are known to be formed from PY2-based ligands and $[Cu(I)(CH_3CN)_4]ClO_4$.[25] Characterization of the complex $[\mathbf{1d}(Cu(I))_{30}](ClO_4)_{30}$ was performed by NMR and UV/vis spectroscopy. Shifts in down-field direction were observed for the pyridine protons and for the methylene protons next to some of the tertiary amine nitrogen atoms of **1d**, indicating the coordination of the PY2 donor centers to a transition metal. No shifts were observed for the β-methylene protons in the dendrimer backbone. The UV/vis spectrum showed no absorptions corresponding to

Cu(II) *d-d* transitions, but instead displayed a very strong feature at $\lambda = 340$ nm (see Figure 5.6). This spectrum strongly resembles the spectra of other Cu(I) complexes in which the copper ion is coordinated by the PY2 unit.[21,25] The extinction coefficient of the 340 nm band amounts to approximately $\varepsilon = 3.47 \cdot 10^3$ $M^{-1}cm^{-1}$ per copper. This value corresponds well to that reported by Karlin and co-workers for $[Cu(I)_2N4](ClO_4)_2$, a Cu(I) complex derived from a tetramethylene linked bis-PY2 ligand,[25] and to those reported by Klein Gebbink et al.[21] for related molecular host complexes ($\varepsilon = 1.75 \cdot 10^3$ $M^{-1}cm^{-1}$ and $2.5 \cdot 10^3$–$3.0 \cdot 10^3$ $M^{-1}cm^{-1}$ per Cu(I)-PY2 unit, respectively). These observations indicate that the copper ions are coordinated at the dendrimer periphery only, and that the amine functions in the inside the dendrimer are not involved in the Cu(I) coordination.

O_2-binding of Cu(I)-modified dendrimer. The ability of $[\mathbf{1d}(Cu(I))_{30}](ClO_4)_{30}$ to bind dioxygen was studied by low-temperature UV/vis spectroscopy. At -85 °C pre-dried dioxygen was bubbled through a dichloromethane solution of this complex, which resulted in the formation of a strong absorption band at $\lambda = 360$ nm (see Figure 5.6). This band is indicative of the formation of dioxygen complexes in which the dioxygen molecule is bound as a bent μ–η^2:η^2 peroxo ligand between two Cu(II)-centers,[25] comparable to the binding mode in oxy-Hc.[20] The absence of additional absorption features around $\lambda = 430$ nm excludes the formation of bis μ-oxo species.[26] The extinction coefficient of the 360 nm band amounted to $1.45 \cdot 10^5$ $M^{-1}cm^{-1}$ per $(Cu)_{30}$-complex. This number corresponds to $\varepsilon = 9.7 \cdot 10^3$ $M^{-1}cm^{-1}$ per Cu_2O_2 unit, assuming that all copper ions are involved in O_2-binding. For the O_2-complex formed by Karlin's $[Cu(I)_2N4](ClO_4)_2$ complex the extinction coefficient of the 360 nm band is $1.4 \cdot 10^4$ $M^{-1}cm^{-1}$.[25] The same band has values $\varepsilon = 1.3 \cdot 10^4$ $M^{-1}cm^{-1}$ in the O_2-complexes of the molecular host compounds previously reported by Klein Gebbink et al.[21] Given these numbers it appears likely, therefore, that approximately 70–75% of all copper centers of $[\mathbf{1d}(Cu(I))_{30}](ClO_4)_{30}$ are involved in dioxygen binding, which corresponds to a total number of 11–12 molecules of dioxygen per Cu(I) dendrimer **1d**. The fact that not all copper ions are involved in dioxygen binding may be the result of restrictions placed on the structure of the complex by the highly branched nature of the dendrimer backbone. Another explanation would be that 15 dioxygen molecules are bound, involving all copper ions of the dendritic complex, but that the individual Cu_2O_2 moieties in the resulting complex have a relatively low extinction coefficient, viz. $\varepsilon = 9.7 \cdot 10^3$ $M^{-1}cm^{-1}$. In any case, this dendritic dioxygen complex may be regarded as a "hot" species as it contains at least approximately 11–12 highly activated dioxygen molecules at its copper-covered periphery, resulting in a high local concentration of oxygenating equivalents. On standing at low temperature and upon warming to room temperature

green Cu(II) complexes were formed (Figure 5.6), showing that no additional stabilization of the copper dioxygen species in the dendritic complex occurred.

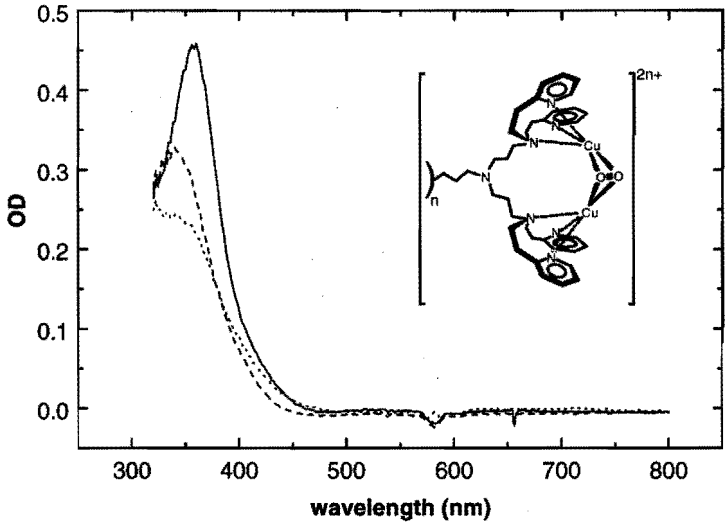

Figure 5.6: *UV/vis spectra in dichloromethane of the Cu(I)ClO$_4$ complex of* **1d** *(···), its O$_2$-complex (—), and the O$_2$-complex after warming to ambient temperature (- - -). Inset shows proposed μ-η^2:η^2 peroxo binding mode between two Cu(II)-centers, only one of the possible dendrimer conformations is depicted.*

5.2.3 Concluding Remarks

The high pressure reaction with 2-vinylpyridine results in quantitative conversion of DAB-*dendr*-(NH$_2$)$_n$ (n = 4, 8, 16, and 32) to the DAB-*dendr*-(PY2)$_n$ analogues, and these molecules can bind one Zn(II) or Cu(II) ion per PY2 group. DAB-*dendr*-(PY2)$_{32}$ (**1d**) binds approximately 30 Cu(I) ions per molecule and this complex can bind 11-12 dioxygen molecules at low temperature in dichloromethane. The resulting dendritic multivalent dioxygen complex may, therefore, be seen as a mimic for the oxygen binding by hemocyanine-assemblies.

5.3 Non-Covalent and Covalent Dendritic Multi-Porphyrin Arrays

The light-harvesting system present in plants, algea, and photosynthetic bacteria is able to convert light into chemical energy very efficiently, supplying the earth's biosphere with energy from sunlight.[27] In this natural antenna system the photophysical properties are determined by the spatial arrangement and orientation of

the chromophores, which is controlled by non-covalent interactions within a protein scaffold. Recently, the crystal structure of the light-harvesting antenna LH2 of a purple bacterium has been resolved. The LH2 system is capable of capturing light and store it by a multi-step energy transfer process untill this light-energy is passed to another light-harvesting complex (LH1) which leads to the conversion of light-energy to chemical energy in the photosynthetic reaction center (RC).[27] LH2 consists of two sets of rings containing 27 bacteriochlorophyll and 9 carotenoid chromophores held in place without stacking by the assembly of 18 helical protein subunits forming a hollow cylinder with a radius of 18Å.[28] This architecture makes the LH2-system well suited to harvest light due to the favorable energetical interactions between the different chlorophylls in one ring.

The biological photoconversion system of the purple bacteria has inspired many research groups to construct mimics consisting of cylindrical arrays of porphyrins.[29] However, a dendrimer as template to assemble chromophores has had little attention up till now. The synthesis of dendrimers with porphyrins at the periphery has only been reported for low generation dendrimers (first and second).[30–34] Still, in none of these systems unconventional photophysical behavior has been found resulting from interaction between the porphyrin end groups in the dendrimer. In fact, the only multiporphyrin system that actually uses the dendritic framework is introduced by Sanders et al.,[34] who constructed a metalloporphyrin system that shows cooperative binding towards a diamine.

In this paragraph a covalent and non-covalent method is described to construct spherical porphyrin arrays using the different generations poly(propylene imine) dendrimers. First, the dendrimers are applied as a template to construct porphyrin assemblies in a non-covalent approach. Second, the porphyrins are covalently attached to the dendrimers, thus leading to more defined and stable structures. Importantly, the porphyrins are prevented from stacking by attaching bulky *t*-butyl groups at the *meso*-position of the porphyrins. The resulting porphyrin dendrimers have nanosize dimensions and, moreover, the covalent assemblies show intramolecular electronic interactions between the porphyrin end groups in the excited state, as measured with time-resolved fluorescence anisotropy measurements at 77 K. Thereby mimicking the light harvesting of the natural LH2 system.

5.3.1 Non-Covalent Multi-Porphyrin Assemblies

Zn(II)porphyrin. Amino groups are known to be good ligands for zinc porphyrins and this metal-to-ligand interaction has been used in the construction of porphyrin assemblies and in host-guest complexation.[29,34,35] In the non-covalent approach, the

complexation of zinc(II) porphyrin **2** (Figure 5.7) towards the different generations of poly(propylene imine) dendrimers is used in order to form large well organized porphyrin arrays.

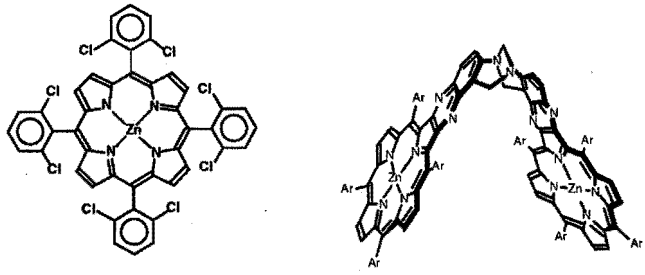

2 **3**

Figure 5.7: *Zinc(II)porphyrin **2** and Tröger's base bis-porphyrin receptor **3** used in the non-covalent approach.*

Binding studies were conducted using UV/vis spectroscopy, following the characteristic bands of the porphyrin chromophores upon the addition of the dendrimer. From the inflection point of the titration curve, the ratio of porphyrin to dendrimer could be estimated. This method showed that upon full complexation of the DAB-*dendr*-$(NH_2)_n$ to the zinc atom of **2** roughly a 1:1 ratio between the zinc porphyrin and each amino end group of the dendrimer was found in the case of the first three generations (n = 4, 8, and 16). Thus, around the DAB-*dendr*-$(NH_2)_4$ core 4 porphyrins were assembled, and around the second and third generation this number is approximately 8 and 16, respectively. In the case of the DAB-*dendr*-$(NH_2)_4$-core the titration curve obtained could be fitted, assuming that all binding constants were equal, giving a binding constant of approximately $7 \cdot 10^4$ M^{-1} (per porphyrin-amine interaction). This value is in the range of the binding constant of hexylamine to zinc porphyrin ($5.1 \cdot 10^4$ M^{-1}).[36] For the higher generations the fitting procedure did not converge, indicating that the assumption of equal equilibrium constants was no longer valid. However, it was clear that the average binding constant of **2** to the amino groups of DAB-*dendr*-$(NH_2)_n$ drops with higher generations. This is very likely to be due to the increasing steric interactions between bound porphyrins. For the same reason the fourth and fifth generations bind to **2** in less than a 1:1 ratio.

Tröger's base bis-porphyrin. Earlier studies have shown that ditopic ligands are bound much stronger in a rigid Tröger's base bis-porphyrin receptor molecule such as **3**,[37] compared with the above described monotopic ligandation (at least by a factor of 1000).[36] Therefore the assembly of **3** around the different generations of the poly(propylene imine) dendrimers was also studied, expecting that more porphyrin

units with a different geometry would assemble around the dendrimers. The complexation of **3** around the first generation poly(propylene imine) dendrimer was studied using both ^{1}H NMR and UV/vis titrations. The spectrophotometric titration revealed two inflection points upon addition of dendrimer to the bis-porphyrin receptor in toluene. These inflection points are attributed to a 1:2 complex and a 1:1 complex (DAB-*dendr*-$(NH_2)_4$:**3**), respectively. In the 1:2 complex all Zn-atoms of the porphyrin units are bound to the primary amines of one DAB-*dendr*-$(NH_2)_4$. Therefore, a molecular capsule is formed as schematically depicted in Figure 5.8, as subscribed by NMR titrations in deuterated chloroform. The formation of a 1:2 complex led to significant upfield shifts for all protons present in DAB-*dendr*-$(NH_2)_4$ due to the presence of the porphyrin rings (differences in chemical shifts ranged from -1.8 ppm for β-CH_2 protons to -5.9 ppm for NH_2 protons). Both UV/vis and NMR titrations did not show the presence of 1:4 complexes in the presence of excess **3**, indicating that the 1:2 complex is relative stable, which is in agreement with earlier work.[37]

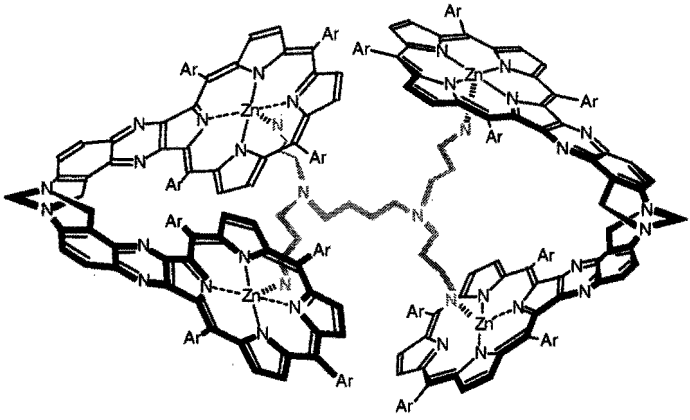

Figure 5.8: *Schematic view of molecular capsule based on 3.*

In the case of the higher generations of the dendrimers more inflection points could be expected, however, they were not clearly observed. During the titration both the absorption of the free receptor (616 or 572 nm) and that of the complexed receptor (632 and 582 nm) were monitored. The curves of these different absorptions as function of the concentration of dendrimer gave clearly two different inflection points. From the inflection point of the disappearance of the Q-band assigned to the free receptor, i.e. λ = 616 or 572 nm, a good estimation of the maximum number of receptor molecules **2** assembled around the dendrimer core could be made. In the case of DAB-*dendr*-$(NH_2)_{16}$ for example (Figure 5.9), the absorptions at λ = 616 and λ = 572 nm did not change after the addition of 0.06 equivalents of dendrimer to the receptor **3** solution, indicating that

the maximum number of molecules of **3** around the dendrimer is about 16. In this case the ratio of **3**-NH_2 is 1:1, indicating that each receptor is bound only monotopically.

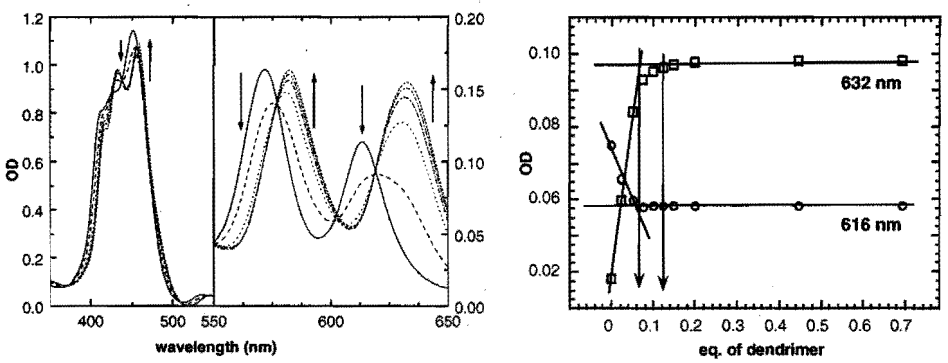

Figure 5.9: *UV/vis spectra (left) and titration curves (right) of receptor DAB-*dendr-*$(NH_2)_{16}$ added to **3** in dichloromethane. The disappearance of the absorption assigned to free **3** (616 nm) gives the number of maximum monotopically bound receptors around DAB-*dendr-*$(NH_2)_{16}$ and the increase in the absorption assigned to complex (632 nm) gives the maximum number of ditopically bound receptors (see text).*

Plotting the absorptions of the complex (632 and 582 nm) against the equivalents of dendrimer, a second inflection point at higher dendrimer concentrations was observed. In contrast to the first inflection point at 0.06 equivalents, the second inflection point is less defined and the experimental error is significant higher here. Adding more than 0.06 equivalents of dendrimer resulted in a further increase (up to approximately 0.12 equivalents) of the bands belonging to the complexed receptor, i.e. $\lambda = 632$ and $\lambda = 582$ nm, indicating that the assembly of porphyrins rearranged into a dendrimer complexed with about 8 receptor molecules **3** (Figure 5.9). The receptor molecules **3** can now be bound ditopically, since the ratio of **3**-NH_2 is 1:2. Thus, dependent on the ratio of receptor to dendrimer, a maximum of 8 receptor molecules **3** were assembled around the core in a ditopic way, and a maximum of 16 porphyrins in a monotopic way (see also Figure 5.13). For the other generations these observed maxima are given in Table 5.1. The maximum numbers of receptors **3** bound ditopically to the different generations of dendrimers is close to the expected maximum numbers, i.e. $n/2$, for all generations. Assembling more receptors **3** around the DAB-*dendr*-$(NH_2)_8$ and DAB-*dendr*-$(NH_2)_{16}$ led to the expected number of 8 and 16, respectively, which means that to each amino group of the dendrimer one molecule **3** is bound. For the higher generations this number was smaller than the theoretical maximum, presumably due to steric hindrance. The maximum number of receptor molecules **3** that can be assembled around the DAB-*dendr*-$(NH_2)_{32}$ appears to be 21 and around the DAB-*dendr*-$(NH_2)_{64}$

core only 33 receptors. Thus, in the non-covalent approach different number of porphyrin compounds can be assembled around the dendritic templates by using simple metal to ligand interactions.

Table 5.1: *The maximum number of receptor molecules* ***3*** *that can be assembled either mono- or ditopically around the different dendrimer generations.*

Dendrimer	Maximum number of **3** assembled around dendrimer	
	2nd inflection point (monotopically)	1st inflection point (ditopically)
DAB-*dendr*-$(NH_2)_4$	-[a]	2
DAB-*dendr*-$(NH_2)_8$	8	4
DAB-*dendr*-$(NH_2)_{16}$	16	8
DAB-*dendr*-$(NH_2)_{32}$	21	14
DAB-*dendr*-$(NH_2)_{64}$	-[b]	33

[a] Upon the addition of an excess of **3** no higher complexes (4:1) were observed, showing that the 2:1 complex was more stable. [b] Not more than 33 receptor molecules **3** were found to complex to this generation.

5.3.2 Covalent Multi-porphyrin Assemblies

In order to obtain more defined and stable structures, porphyrins were covalently attached to the poly(propylene imine) dendrimers. The resulting porphyrin functionalized dendrimers **5a-d** (DAB-*dendr*-(NH–CO–C_2H_4–CO–NH-porphyrin)$_n$; n = 4, 8, 16, and 64) were prepared by coupling the *N*-hydroxy succinimidyl ester of **4a** to the different generations of dendritic polyamines (Scheme 5.3). The compounds were purified by intensive washing, and extraction and finally by precipitation from dichloromethane and methanol. According to TLC analysis, IR and ^{1}H NMR spectroscopy, the compounds obtained were pure and no starting materials were detected.

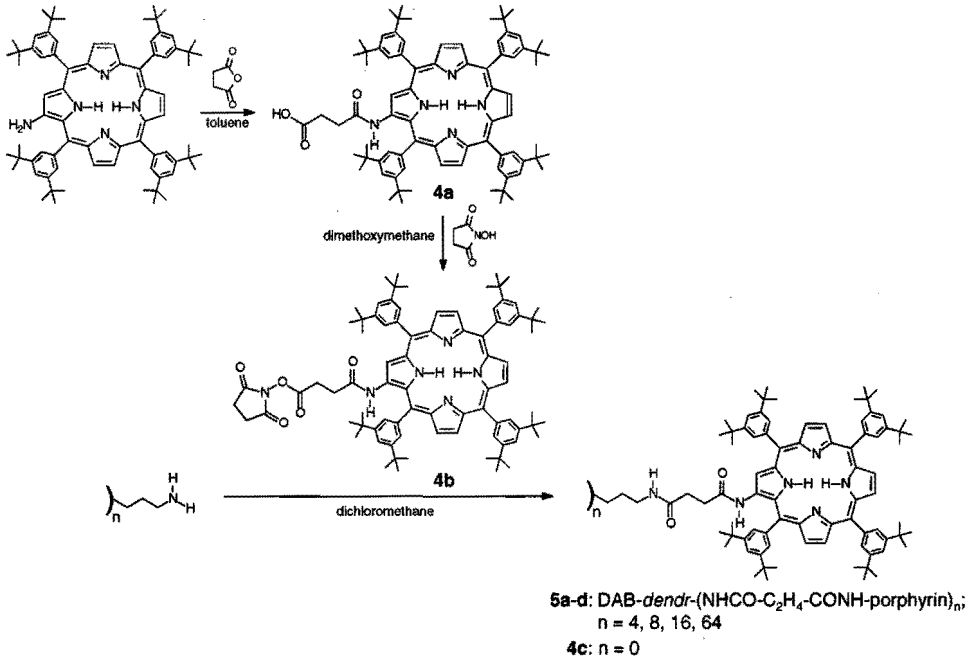

Scheme 5.3: *Synthesis of the different generations of the porphyrin functionalized poly(propylene imine) dendrimers* ***5a-d*** *and monofunctional compound* ***4c****.*

The peaks in the ^{1}H NMR spectrum of the first generation dendrimer **5a**, bearing four end groups were sharp and could easily be assigned. Shifts were observed for the spacer CH_2 protons in the products as compared with respect to the resonances found for the porphyrin ester **4b**. Integration of the dendrimer and the porphyrin resonances revealed that they had reacted in the expected 1:4 ratio. The resonance of the amide proton attached to the dendritic core was shifted 0.5 ppm down field when compared to monomeric analogue **4c**, indicative of the formation of intramolecular hydrogen bonds between the amide functions. The ^{1}H NMR spectrum of the higher generations **5b-d** were significantly broadened due to diminished molecular motion and overlapping resonances of the dendrimer core (between 1.5 and 3.3 ppm). Moreover, an incremental downfield shift of the amide protons attached to the dendritic core was observed (resp. 0.1, 0.2, and 0.6 ppm compared to **5a**), as expected for a progressive formation of an intramolecular H-bonded network of the amides at the periphery of the dendrimers for the higher generations.[38-40] Moreover, small upfield shifts for the porphyrin resonances were found (0.06 ppm for **5c** and 0.08–0.17 ppm for **5d**) indicating that these porphyrin rings are closer to each other. Additional evidence for H-bonding was found in the IR spectra of the dendrimers (1 mM in dichloromethane), which showed a decrease in

signal intensity for the free amide N–H (3 439 cm^{-1}) in favor of the broad peak belonging to the hydrogen bonded amides (3 320 cm^{-1}) when going to higher generations.

The functionalized dendrimers were further analyzed with mass spectroscopy. Compound **5a** gave peaks at the expected $[M+H]^+$ in both FAB-MS and MALDI-TOF (4 959 and 4 961 Da, respectively). The mass spectra also showed several post-source fragmentation peaks with intensities depending on laser power used,[41,42] indicating that these compounds were not stable under the conditions of analysis. These fragmentation peaks were found at $[M-1178]^+$ and $[M-2x1178]^+$, reflecting the loss of one and two butanoic acid porphyrins, respectively. Compounds **5b** and **5c** gave signals at the expected $[M+H]^+$ positions (10 063 and 20 243 Da, respectively). These molecules not only showed the same fragmentation pattern as for **5a**, i.e., subsequential loss of acid porphyrin moieties, but also fragmentation of the aminodendrimer core.[22] Consequently, the signals for the degraded compounds were relatively more intense. A typical MALDI-TOF spectrum of compound **5c** is shown in Figure 5.10. Compound **5d** did not give any results with MALDI-TOF nor ESI-MS, probably due to strong fragmentation and the relatively high molecular weight of **5d** (MW = 81 408).

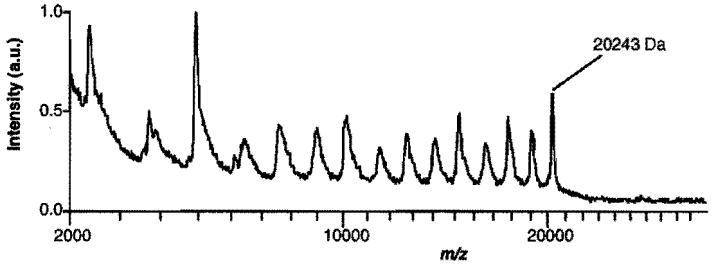

Figure 5.10: *MALDI-TOF mass spectrum of **5c** showing the molecular mass peak (20 243) and fragmentation peaks.*

The first three generations of functionalized dendrimers **5a-c** gave UV/vis and fluorescence spectra which were virtually the same (Figure 5.11a, λ_{max} = 424 nm and FWHM[43] = 21 nm), suggesting that the ground state interaction between the porphyrins is negligible. The extinction coefficients of the compounds increased linearly with the number of porphyrins, as expected for fully functionalized dendrimers (inset Figure 5.11). Fifth Generation dendrimer **5d** showed a small broadening of the Soret band (λ_{max} = 423 nm, FWHM = 25 nm). Furthermore, the relative fluorescence quantum yield of **5d** (per porphyrin unit) was found to be only 85 % of the quantum yields of the lower generations (Figure 5.11b). Together with the ^1H NMR and IR data, these results

indicate that in compound **5d** the porphyrins are forced in close proximity in a face-to-face[44] manner due to the dendritic architecture of the compound.

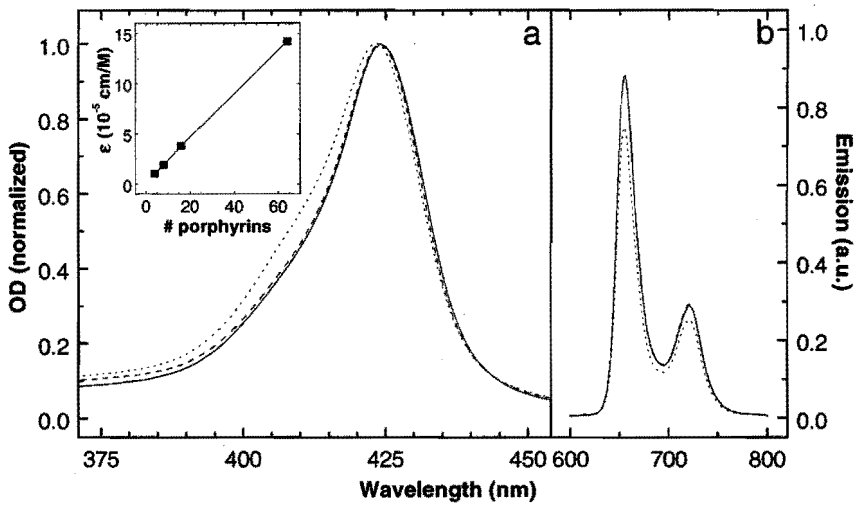

Figure 5.11: *a) Normalized (per porphyrin unit) UV/vis spectra of* ***5a*** *(—),* ***5b*** *(- - -) and* ***5c*** *(···); b) fluorescence emission spectra when excited at 424 nm (curves for* ***5a*** *and* ***5b*** *partly coincide). Inset shows ε as function of theoretical number of end groups.*

To investigate possible electronic interactions between the porphyrin end groups in the excited state, time-resolved fluorescence polarization measurements were performed in an ethanol-pentane-ether (2:5:5) glass at 77 K. The porphyrin functionalized dendrimers **5a** and **5c** showed a fast depolarization of the fluorescence as compared to monofunctional reference compound **4c** (Figure 5.12). This difference between the dendrimers **5a** and **5c** and monofunctional compound **4c** indicates that energy migration takes place between the chromophores within the dendrimer. Remarkably, both the first and third generation dendrimers **5a** and **5c** have similar rates of anisotropy decay.[45] Apparently, the end groups are already close to each other in **5a**, probably assisted by the hydrogen bonding between the amides, which is promoted by the polarity of the solvent and the low temperature used. Close proximity of the end groups due to the presence of secondary interactions in first generation amide-functionalized poly(propylene imine) dendrimers, have also been found in the solid state,[40] and at low temperatures.[39]

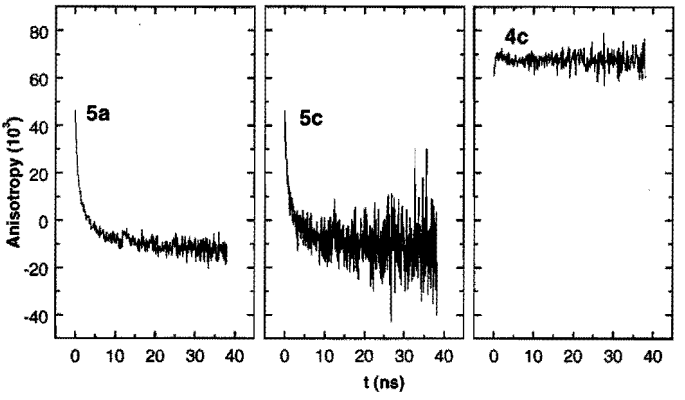

Figure 5.12: *Time-resolved fluorescence anisotropy curves of dendrimers* ***5a, 5c,*** *and monomeric reference compound* ***4c.***[45]

5.3.3 Concluding remarks

Metal-to-ligand interactions can be used to assemble multiple porphyrin molecules **2** and bis-porphyrin molecules **3** around the different generations of the poly(propylene imine) dendrimers. The number of assembled porphyrins ranges from 2 to 33, depending on dendrimer generation and porphyrin used. In the covalent approach, 4, 8, 16, and 64 porphyrins have been attached to the different generations poly(propylene imine) dendrimers using the activated ester synthesis. Both approaches are schematically outlined in Figure 5.13. Only the fifth generation porphyrin functionalized dendrimer **5d** shows indications of ground-state interactions between the chromophores. In contrast, both first and third generation dendrimers **1** and **3** show fast energy migration between these chromophoric units in the nanosecond regime.

5.4 Conclusions

The use of the multivalency present in dendrimers, has resulted in two different mimics of multivalent structures known from biology. These biomimics show some of the features present in the natural occuring systems, but are far away from the degree of sophistication present in nature. This relates to both structure and function.

A major conceptual difference in structure with Nature is the method of construction. In contrast to the synthesized structures described in this chapter, many biological systems are built up by assembling different functional subunits into one non-covalent entity that is particularly equipped for its function. This assembly results for example in the formation of complex aggregates of hemocyanines in order to effectively

bind dioxygen, or in the typical orientation of porphyrins in the light harvesting system resulting in an effective photoconversion. Assemblage as construction method creates the possibility to build many different functional structures with a relative small amount of building blocks. This is a major advantage compared to the covalent constructed dendritic biomimics described in this chapter.

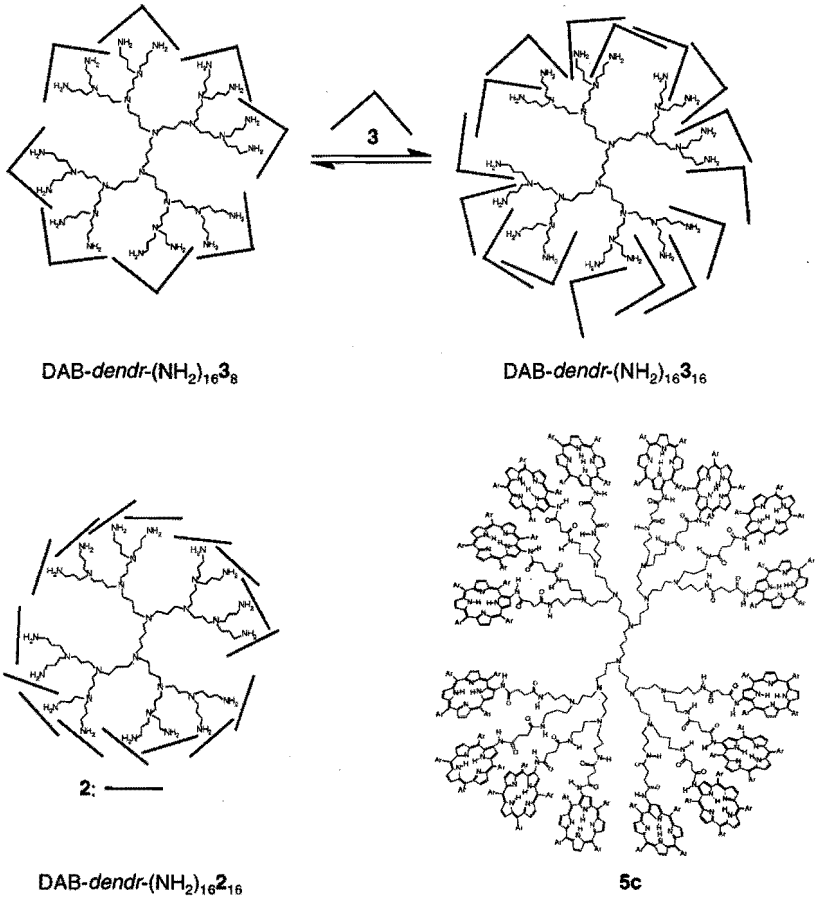

Figure 5.13: *Schematic representations of the different ways to construct porphyrin arrays around a third generation poly(propylene imine) dendrimer. Switching from 8:1 to 16:1 ratio with bis-porphyrin* **3** *(above), assembling of porphyrin* **2** *and a porphyrin-functionalized dendrimer* **5c** *(below).*

The other main difference of the dendritic biomimics with their biological archetypes can be found in the complexity of the interactions with the surroundings. In biological systems the overall performance is the sum of an interplay of many different interactions, instead of the only few modes of interaction present in dendrimers. This gives biological systems the possibility to tune their characteristics, in order to be able

to react to different environmental conditions. A feature that is almost completely absent in their dendritic analogues.

Although there are many drawbacks present in the dendritic biomimics, the possibilities for the dendritic systems in this field are numerous. Since dendrimers do have the potency to possess site-isolation and multivalency, and since they are also used for assembly processes,[46] it is probably only a matter of time until these three features are combined into one structure. This will, eventually, result in more complex systems that will be closer to Nature. Moreover, the constraints imposed on the biomimics are usually much lower than those imposed on biosystems by living organisms. As we are mostly interested to use the biomimic for limited function only.

5.5 Experimental Section

General methods and Materials

$[Cu(I)(CH_3CN)_4]ClO_4$ was synthesized according to Kubas.[47] 2-Vinylpyridine was purified before use by flash chromatography over Silica 60 using diethyl ether as the eluent. Porphyrin 2[48] was kindly provided by Dr. A. P. H. J. Schenning, and bis-porhyrin 3,[37] and 2-amino-5,10,15,20-tetrakis(3,5-di-*tert*-butylphenyl)porphyrin[49] were kindly provided by Prof. M. J. Crossley. All other chemicals were purchased commercially and used as received. Solvents were dried and distilled prior to use, except methanol which was of HPLC-grade and used as received. Diethyl ether was distilled from sodium/benzophenone. Dichloromethane and acetonitrile were distilled from calcium hydride. Dichloromethane used in the handling of the Cu(I)-complexes was stirred with concentrated sulfuric acid for 2 days, and neutralized by washings with ammonia and water prior to destillation. Preparation of the air-sensitive Cu(I) samples was carried out using standard Schlenk techiques. Solvents were deoxygenated by repeated freeze-thaw cycles or by bubbling dinitrogen through them (20 min.). Flash chromatography was carried out using neutral alumium oxide 70-200 mesh (Acros) brought to activity III,[50] or Merck silica gel 60 (particle size 0.063-0.200 mm). Dialysis was performed using regenerated cellulose dialysis tubing (pore size 24 Å), which was swollen in water for 1 h. For remaining general procedures, see Chapter 2.

Mass spectrometry

MALDI-TOF-MS spectrometry was performed on a PerSeptive Biosystems Voyager-DE-RP MALDI-TOF mass spectrometer with a dihydroxybenzoic acid matrix at the Institute for Mass-Spectrometry at the University of Amsterdam (PY2-containing products), and an IR-MALDI using a Er-YAG laser emitting at 2.94 μm and a thiourea matrix at the Institute für Medizinische Physik un Biophysik at the Westfälische Wilhelms-university of Münster (porphyrin-systems). ESI-MS spectra were recorded on a API 300 MS/MS mass spectrometer (PE-Sciex) with a mass range of 3000. The sample solutions were delivered to the ESI-mass spectrometer by a syringe pump (Harvard Apparatus) at a flow rate of ca. 5 $\mu L min^{-1}$ in MeOH/MeCN mixtures containing ~1 % formic acid. HR FAB MS measurements have been performed on a Fisons Instruments ZAB-2SEQ mass spectrometer using a cesium ion gun operating at 30kV at the Research School of Chemistry, Australian National University. The matrix used was *meta*-nitrobenzyl alcohol. The mass resolution was 10,000, cesium iodide was used as an external reference and the mass range scanned from 10% below to 10% above the required mass using voltage scanning. Abbreviations used: vp = vinylpyridine; pa = propylamine.

UV/vis spectroscopy

UV/vis spectra were recorded on a Perkin-Elmer Lambda 900 spectrophotometer with path lengths of 10 mm. Titration-experiments were carried out under magnetic stirring. For Cu(I) titration, Cu(I)-containing solution was added via a gas-tight Hamilton syringe through a teflon-lined septum sealing the cell. Low-temperature UV/vis spectra were obtained on a Hewlett Packard 8452A diode array spectrophotometer

driven by a Compaq Deskpro 386S computer using a software system written by On-Line Instrument Systems, Inc. The spectrophotometer was equipped with a Kontes KM-611772 variable temperature UV/vis Dewar cell with quartz windows. The low temperature inside the Dewar assembly was achieved by putting a copper tubing coil inside the methanol-filled Dewar-cell. Through the coil cold methanol was circulated by an external cooling unit (Neslab CC-100II cryocool immersion cooler, an Agitainer A with circulation pump). The cell assembly consisted of a quartz cell fused to one end of a glass tube. The other end was attached to a high-vacuum-stopcock and a 14/20 ground glass joint. The temperature inside the Dewar assembly was monitored by an Omega Model 651 resistance thermometer probe. The spectrum of the solvent was also recorded for each set of experiments. After placing a solution of $[1d(Cu(I))_{30}](ClO_4)_{30}$ in dichloromethane in the Dewar assembly, the temperature was allowed to equilibrate for 10 min. and the spectrum was subsequently recorded. The cell assembly had been previously calibrated for volume vs. height in the tube, and the height of the solution in the cell assembly at low temperature was noted for the purpose of concentration determination. Oxygenation of the chilled solutions was effected by direct bubbling of dry, pre-cooled dioxygen using a syringe needle. The spectra were recorded at set intervals. After warming to room temperature, the spectra were recorded again.

Time-resolved fluorescence anisotropy

Time-resolved fluorescence anisotropy measurements were carried out as described previously[53] using a synchronously mode-locked dye laser as the excitation source and time-correlated single photon counting detection. The excitation wavelength was 595 nm and the emission monitored at 655 nm. The samples were studied in an ethanol-pentane-ether (2:5:5) glass at 77 K in an Oxford Instruments Optistat DN cryostat.

Preparation

General procedure for 1a-d

A teflon high-pressure capsule was filled with a solution of poly(propylene imine) dendrimer (typical 1–4 mmol in end group), 4 equivalents 2-vinylpyridine, and 2 equivalents of acetic acid in methanol (total volume 15 mL) and kept at 50 °C and 15 kbar for 16 hrs. The resulting reddish solution was dissolved in CH_2Cl_2 and this solution was washed twice with an equal amount of aqueous 15% NaOH and once with an equal amount of water. The organic layer was dried over Na_2SO_4 and the solvent removed in vacuo. The excess vinylpyridine was removed by leaving the resulting brown oil under vacuum on a rotary evaporator for several hours.

DAB-*dendr*-(PY2)$_4$, 1a

Purification of **1a** was performed portionwise by means of column chromatography (neutral alumina (act. III), CH_2Cl_2/MeOH = 97/3, v/v). Typically, 209 mg (64 %) of the yellowish oil **1** was obtained from 400 mg of the crude oil. ^{1}H NMR ($CDCl_3$, 400 MHz): δ = 1.35 (m, 4H), 1.56 (m, 8H), 2.33 (t, 12H, J = 7.2 Hz), 2.54 (t, 8H, J = 7.4 Hz), 2.91 (s, 12 H), 7.06 (ddd, 8H, J = 1.1, 4.8, 7.3 Hz), 7.09 (d, 8H, J = 7.7 Hz), 7.52 (dt, 8H, J = 2.3, 9.9 Hz), 8.49 (ddd, 8H, J = 1.0, 4.8 Hz). ^{13}C NMR ($CDCl_3$, 100 MHz): δ = 25.5, 25.7, 36.6, 52.7, 52.8, 54.6, 121.6, 124.0, 136.8, 149.8, 161.4. IR (KBr, cm^{-1}) = 3067, 3007 (ArH), 1591, 1568, 1473, 1434 (C=C, C=N), 1302, 1248, 1211 (C–N), 749 (Ar). ESI-MS: m/z 1158 [M+H]$^+$, 1053 [M-vp+H]$^+$, 890[M-(pa+2vp)+H]$^+$, 606, 552. Analysis Calcd. for $C_{72}H_{98}N_{14}$·MeOH: C, 73.70; H, 8.47; N, 16.48. Found: C, 73.64; H, 8.19; N, 16.10.

DAB-*dendr*-(PY2)$_8$, 1b

Purification of **1b** was achieved by precipitation of a concentrated dichloromethane solution of the crude product in hexane. This procedure yielded 922 mg (87 %) of **1b** as a brownish orange oil. ^{1}H NMR ($CDCl_3$, 400 MHz): δ = 1.35 (m, 4H), 1.52 (m (br), 24H), 2.32 (t, 20 H), 2.35 (m (br), 16H), 2.53 (t, 16H), 2.86 (s, 64H), 7.05 (m, 32H), 7.50 (m, 16H), 8.47 (m, 16H). ^{13}C NMR ($CDCl_3$, 100 MHz): δ = 25.2, 25.4, 36.7, 52.7, 52.9, 54.1, 54.7, 121.7, 124.0, 136.8, 149.9, 161.4. IR (KBr, cm^{-1}) ν = 3067, 3007 (ArH), 1590, 1568, 1474, 1434 (C=C, C=N), 1365–1250 (C–N), 749 (Ar). ESI-MS: m/z 2456 [M+H]$^+$, 2351 [M-vp+H]$^+$, 2189 [M-(pa+2vp)+H]$^+$, 1864.

DAB-*dendr*-(PY2)$_{16}$, 1c

Purification of **1c** was achieved by precipitation of a concentrated dichloromethane solution of the crude product in hexane. This procedure yielded 1.02 g (91 %) of **1c** as a brownish orange oil. ^{1}H NMR ($CDCl_3$, 400 MHz): δ = 1.35 (m (br), 4H), 1.52 (m (br), 56H), 2.32 (t (br), 52 H), 2.35 (m (br), 32H), 2.51 (t, 32H), 2.87 (s, 128H), 7.05 (m, 64H), 7.47 (m, 32H), 8.46 (m, 32H). ^{13}C NMR ($CDCl_3$, 100 MHz): δ = 25.0, 25.5, 36.7, 52.6, 52.8, 52.9, 53.2, 54.1, 54.6, 121.6, 124.0, 136.8, 149.8, 161.4. IR (KBr, cm^{-1}) ν = 3067, 3007 (ArH), 1590, 1568, 1474, 1434 (C=C, C=N), 1365–1250 (C–N), 749 (Ar); ESI-MS: *m/z* 5052 [M+H]$^+$, 4947 [M-vp+H]$^+$, 4888, 4784 [M-(pa+2vp)+H]$^+$, 4565, 4460 [M-2(pa+2vp)+H]$^+$.

DAB-*dendr*-(PY2)$_{32}$, 1d

Purification of **1d** was achieved by means of three subsequent dialysis runs against 500 mL methanol/water (95/5 v/v). This procedure yielded 330 mg (100 %) of **1d** as a brownish orange oil. ^{1}H NMR ($CDCl_3$, 400 MHz): δ = 1.3 (br, 4H), 1.52 (m (br), 124H), 2.30 (t (br), 64H), 2.37 (m (br), 116H), 2.49 (t (br), 64H), 2.85 (s (br), 256H), 7.02 (m (br), 128H), 7.46 (m (br), 64H), 8.44 (m (br), 64H). ^{13}C NMR ($CDCl_3$, 100 MHz): δ = 24.8, 25.3, 36.5, 52.5, 52.8, 53.1, 54.5, 121.7, 124.0, 136.8, 149.7, 161.3. IR (KBr, cm^{-1}) ν = 3067, 3007 (ArH), 1590, 1568, 1474, 1434 (C=C, C=N), 1365–1250 (C–N), 749 (Ar). MALDI-TOF-MS: *m/z* 7,500-10,500 (Calcd. 10,242.8). Analysis Calcd. for $C_{632}H_{880}N_{126}$·MeOH: C, 74.00; H, 8.67; N, 17.18. Found: C, 74.42; H, 8.58; N, 16.85.

[1a(Cu(II))$_4$](ClO$_4$)$_8$

To a solution of 45 mg (0.039 mmol) of ligand **1a** in 10 mL of MeOH was added dropwise a solution of 57.6 mg (0.156 mmol) of $Cu(ClO_4)_2.6H_2O$ in 1 mL of MeOH. A dark green precipitate formed immediately upon addition of the copper salt. After the addition was completed, the reaction mixture was shortly heated to reflux, which resulted in a clear, dark green solution. The solution was set aside and allowed to come to room temperature upon which a dark green precipitate formed. The precipitate was collected by filtration: after drying *in vacuo* 36 mg (42 %) of a pale, dark green powder was obtained. Mp. 168 °C (dec.). Λ_m: 1116 S·cm^2·mol^{-1} (solvent acetonitrile). UV/vis (acetonitrile, nm (ε, M^{-1}·cm^{-1})): λ_{max} 261 (26,300), 307 (sh, 13,700), 390 (sh, 3640), 664 (750). IR (KBr, cm^{-1}) ν = 3474 (H_2O), 3084 (ArH), 1612, 1572, 1489, 1448 (C=C, C=N), 1320 (C–N), 1097, 623 (non-coord. ClO_4^-), 769 (Ar); MALDI TOF-MS *m/z* 1710 [M+4Cu+3ClO$_4$]$^+$, 1546 [M+3Cu+2ClO$_4$]$^+$, 1383 [M+2Cu+ClO$_4$]$^+$, 1221 [M+Cu]$^+$. Anal. Calcd. for $C_{72}H_{96}N_{14}Cu_4Cl_8O_{32}$·4$H_2O$: C, 37.94; H, 4.60; N, 8.60. Found: C, 37.72; H, 4.89; N, 8.53.

[1d(Cu(I))$_{30}$](ClO$_4$)$_{30}$

To 50.2 mg of solid $Cu(I)(CH_3CN)_4ClO_4$ (0.156 mmol, 32 equivalents) was added dropwise a solution of 49.1 mg of **1d** in 35 mL of CH_2Cl_2 under continuous stirring. After 2 hours the resulting orange solution had turned somewhat cloudy. Filtration yielded an orange powder, which was discarded, and a clear orange solution. This solution was concentrated in vacuo and an excess of diethyl ether was added to induce precipitation of an orange brown powder. After storage at -20 °C overnight the supernatant was decanted and the precipitate dried in vacuo. Isolation of the pale yellow brown product was achieved after another precipitation. The yield of the product was not determined. ^{1}H NMR (CD_3NO_2, 300 MHz): δ = 1.59 (s (br), 124H), 2.30–2.70 (m (br), 244H), 2.89 (s (br), 256H), 7.33 (s (br), 128H), 7.81 (s (br), 64H), 8.59 (s (br), 64H). UV/vis (CH_2Cl_2): λ_{max} 340 nm (ε = 104,600 M^{-1}·cm^{-1}).

4-{Amino-2-[5,10,15,20-tetrakis(3,5-di-*tert*-butylphenyl)-porphyrinyl]}-4-oxo-butanoic acid, 3a

A mixture of 2-amino-5,10,15,20-tetrakis(3,5-di-*tert*-butylphenyl)porphyrin (580 mg, 0.54 mmol) and succinic anhydride (240 mg, 2.39 mmol) in dry toluene (50 ml) was heated at reflux for 16 h under nitrogen. Dichloromethane (100 ml) was added and the organic layer was washed with water (2 x 50 ml), dried over anhydrous sodium sulfate and filtered. The solvent was removed and the crude product was purified by column chromatography over silica (dichloromethane-methanol; 98:2) and recrystallized from chloroform-methanol to yield **3a** (509 mg, 80%) as a dark brown microcrystalline solid, m.p. > 320 °C. IR (CH_2Cl_2, cm^{-1}): ν ($CHCl_3$) 3402br w (NH), 2963s, 2905m, 2869m, 1710m (C=O), 1592m, 1515m, 1477m, 1426w, 1363m, 1247m, 918m, 860. UV/vis ($CHCl_3$, nm (log ε)): λ_{max} 425 (5.56), 488 (3.62), 520 (4.33), 554 (3.83), 5.93 (3.80), 648 (3.62) nm. ^{1}H NMR (400 MHz; $CDCl_3$) δ -2.60 (2 H, br s, inner NH), 1.50–1.53 (72 H, m, *t*-butyl H), 2.28 (2 H, t, *J* 7.0 Hz, $\underline{CH_2}CO_2H$), 2.72 (2 H, t, *J* 7.0 Hz, $\underline{CH_2}CONH$), 7.77 (3 H, m, aryl H), 7.97–8.02 and 8.02–8.10 (9 H, m, aryl H), 8.64 (1 H, d, *J* 4.5 Hz β-pyrrolic H), 8.80–8.94 (6 H, m, β-pyrrolic H), 9.44 (1 H, s, $CH_2CO\underline{NH}$). MS (EI) 1178 [M$^+$].

4-{Amino-2-[5,10,15,20-tetrakis(3,5-di-*tert*-butylphenyl)-porphyrinyl]}-4-oxo-butyric acid 2,5-dioxo-pyrrolidin-1-yl ester, 3b

To a solution of 3a (420 mg, 0.36 mmol) in dimethoxyethane (3 ml) cooled in an ice bath, *N*-hydroxysuccinimide (40 mg) and 1,3-dicyclohexylcarbodiimide (80 mg) was added. The reaction mixture was stirred for 16 h and the precipitate was filtered and washed with additional dimethoxyethane. The solution was evaporated to dryness, dissolved in dichloromethane (2 ml) and recrystallized at 0 °C with isopropanol yielding **3b** (386 mg, 85%). This compound was directly used for further reactions with the dendrimers. IR (CH_2Cl_2, cm^{-1}): ν 3392 s (NH), 1815w (C=O), 1788 w (C=O), 1744 s (C=O), 1591s 1513s, 1477m, 1364m. ^1H NMR (300 MHz; $CDCl_3$) δ -2.72 (2 H, br s, inner NH), 1.50–1.53 (72 H, m, *t*-butyl H), 2.38 (2 H, t, J = 7.0 Hz, $\underline{CH_2}CO_2Suc$), 3.03 (2 H, t, J = 7.0 Hz, $\underline{CH_2}CONH$), 7.77 (3 H, m, aryl H), 7.97–8.02 and 8.02–8.10 (9 H, m, aryl H), 8.64 (1 H, d, J 4.5 Hz β-pyrrolic H), 8.80–8.94 (6 H, m, β-pyrrolic H), 9.44 (1 H, s, $CH_2CO\underline{NH}$).

4-{Amino-2-[5,10,15,20-tetrakis(3,5-di-*tert*-butylphenyl)-porphyrinyl]}-4-oxo-N-propyl-butyramide, 3c

To a solution of **3b** (39 mg, $3 \cdot 10^{-5}$ mol) in dichloromethane (2 ml) 4 drops of *n*-propylamine were added. The reaction mixture was stirred for 12 h, aqueous sodium hydroxide solution (1 N, 3 ml) was added and the mixture stirred for another 3 h. Dichloromethane (10 ml) was added and the organic layer was washed with water, sodium carbonate (10%, 2 times), water and dried over anhydrous sodium sulfate. The solution was filtered and the solvent was evaporated to dryness. The compound was further purified by column chromatography over silica (dichloromethane-methanol; 98:2) to yield **3c** (21 mg, 57%) as a dark brown microcrystalline solid. IR (CH_2Cl_2, cm^{-1}): ν 3439, 3396s, 3333, 3309 (NH 1675m,b (C=O), 1591s, 1513s, 1477m, 1363m. ^1H NMR (400 MHz; $CDCl_3$) δ -2.78 (2 H, br s, inner NH), 0.90 (3H, t, $CH_2CH_2\underline{CH_3}$), 1.45–1.55 and 1.60 (72 H, m, *t*-butyl-H and 2 H $CH_3\underline{CH_2}CH_2N$), 2.28 (2 H, t, $\underline{CH_2}CONH$–porphyrin), 2.52 (2 H, t, $\underline{CH_2}CONHCH_2$), 3.22 (2 H, q, $\underline{CH_2}CONHCH_2CH_2CONH$), 6.30 (1 H, br, $CH_2CO\underline{NH}CH_2$), 7.71 and 7.76 (3 H, m, aryl H), 7.94 and 8.04–8.10 (9 H, m, aryl H), 8.61 (1 H, d, J 4.5 Hz, β-pyrrolic H), 8.80–8.90 (6 H, m, β-pyrrolic H), 9.41 (1 H, s, $CH_2CO\underline{NH}$).

General procedure for 5a-d

To a solution of **3b** (80 mg, 0.06 mmol) in dry dichloromethane (2 ml) 0.95 equivalents of DAB-*dendr*-NH_2 (about 5 mg) was added. The reaction mixture was stirred for 20 h, aqueous sodium hydroxide solution (1 N, 3 ml) was added and the mixture stirred for another 3 h. Dichloromethane (20 ml) was added and the organic layer was washed with water, sodium carbonate (10%, 2 times), water (5 times) and dried over anhydrous sodium sulfate (DO NOT use $MgSO_4$). The solution was filtered and the solvent was evaporated to dryness. The compound was further purified by adding a few drops of methanol to a dichloromethane solution of porphyrin functionalized dendrimer, the compound precipitated and was immediately filtered off.

DAB-*dendr*-(NH–CO–C_2H_4–CO–NH-porphyrin)$_4$, 5a

5a was obtained in a yield of 62 mg (83 %). IR (CH_2Cl_2, cm^{-1}): ν 3438w (NH), 3396m (NH), 3320w,b (NH), 1666m,b (C=O), 1591s, 1513s, 1477m, 1364m. UV/vis (CH_2Cl_2, nm (log ε)): λ_{max} 424 (6.00), 520 (3.87), 553 (3.36), 594 (3.33), 649 (3.14) nm. ^1H NMR (400 MHz; $CDCl_3$) δ -2.78 (8 H, br s, inner NH), 1.45–1.55 and 1.60 (288 H, m, *t*-butyl H and 12 $CH_2\underline{CH_2}CH_2N$ dendrimer-H), 2.25 (8 H, m, $\underline{CH_2}CONHCH_2$), 2.38 (4 H, br, $\underline{CH_2}NCH_2$), 2.41 (8 H, br, $CH_2N\underline{CH_2}$), 2.47 (8 H, m, $\underline{CH_2}CONH$-porphyrin), 3.24 (8 H, m, $\underline{CH_2}CONHCH_2CH_2CONH$), 6.72 (4 H, m, $CH_2CO\underline{NH}CH_2$), 7.71 and 7.76 (12 H, m, aryl H), 7.94 and 8.04–8.10 (36 H, m, aryl H), 8.61 (4 H, d, J 4.5 Hz, β-pyrrolic H), 8.80–8.90 (24 H, m, β-pyrrolic H), 9.41 (4 H, s, $CH_2CO\underline{NH}$). MALDI-TOF MS: m/z 4959 $[M+H]^+$, 3781 $[M-3a+H]^+$, 2603 $[M-(3a)_2+H]^+$. HR-FAB-MS: m/z 4956.53 $[C_{336}H_{429}N_{26}O_8]^+$, 4957.53 $[C_{335}{}^{13}C_1H_{429}N_{26}O_8]^+$, 4958.53 $[C_{334}{}^{13}C_2H_{429}N_{26}O_8]^+$, 4959.54 $[C_{333}{}^{13}C_3H_{429}N_{26}O_8]^+$, 4960.54 $[C_{332}{}^{13}C_4H_{429}N_{26}O_8]^+$, 4961.54 $[C_{331}{}^{13}C_5H_{429}N_{26}O_8]^+$.

DAB-*dendr*-(NH–CO–C_2H_4–CO–NH-porphyrin)$_8$, 5b

5b was obtained in a yield of 57 mg (72 %). IR (CH_2Cl_2, cm^{-1}): ν 3438w (NH), 3396m (NH), 3320w (NH), 1666m,b (C=O), 1591s, 1513s,1477m, 1364m. UV/vis (CH_2Cl_2, nm (log ε)): λ_{max} 424 (6.28), 520 (4.14), 553 (3.64), 594 (3.60), 649 (3.42) nm. ^1H NMR (400 MHz; $CDCl_3$) δ -2.77 (16 H, br s, inner NH), 1.42–1.55 and 1.60–1.80 (576 H, m, *t*-butyl H and 48 H, br, dendrimer-H), 2.26 (16 H, br s, $\underline{CH_2}CONHCH_2$), 2.50–2.60 (16 H, br, dendrimer-H and $\underline{CH_2}CONH$-porphyrin), 3.30 (16 H, m, $\underline{CH_2}CONHCH_2CH_2CONH$), 6.83 (8 H, m,

$CH_2CO\underline{NH}CH_2$), 7.69 and 7.76 (24 H, m, aryl H), 7.93 and 8.04–8.10 (72 H, m, aryl H), 8.60 (8 H, d, *J* 4.5 Hz, β-pyrrolic H), 8.83 (48 H, br m, β-pyrrolic H), 9.42 (8 H, s, $CH_2CO\underline{NH}$). MALDI-TOF MS: *m/z* 10063 $[M+H]^+$.

DAB-*dendr*-(NH–CO–C_2H_4–CO-NH-porphyrin)$_{16}$, 5c

5c was obtained in a yield of 69 mg (68 %). IR (CH_2Cl_2, cm^{-1}): ν 3399m (NH), 3320m,b (NH), 1666m,b (C=O), 1591s, 1513s, 1477m, 1364m. UV/vis (CH_2Cl_2, nm (log ε)): λ_{max} 424 (6.58), 520 (4.44), 553 (3.94), 594 (3.91), 649 (3.71) nm. ^1H NMR (400 MHz; $CDCl_3$) δ -2.78 (32 H, br s, inner NH), 1.25–1.80 (1152 H, m, *t*-butyl H and 112 H, dendrimer-H), 2.25 (32 H, m, $\underline{CH_2}CONHCH_2$), 2.50 (64 H, br m, dendrimer-H and $\underline{CH_2}CONH$-porphyrin), 3.32 (32 H, br, $\underline{CH_2}CONHCH_2CH_2CONH$), 6.90 (16 H, br, $CH_2CO\underline{NH}CH_2$), 7.55–7.76 (48 H, 2 br m, aryl H), 7.90–8.10 (144 H, m, aryl H), 8.50–8.60 (16 H, br m, β-pyrrolic H), 8.70–8.90 (96 H, br m, β-pyrrolic H), 9.39 (16 H, br s, $CH_2CO\underline{NH}$). MALDI-TOF MS: *m/z* 20243 $[M+H]^+$, 19075, 17817, 16600, 15238, 14070, 12743, 11554, 10146, 8991, 7647, 6439, 4959, 3702, 2394 (see also Figure 5.10).

DAB-*dendr*-(NH–CO–C_2H_4–CO-NH-porphyrin)$_{64}$, 5d

5d was obtained in a yield of 48 mg (57 %). IR (CH_2Cl_2, cm^{-1}): ν 3398m (NH), 3320m,b (NH), 1666m,b (C=O), 1591s, 1513s, 1477m, 1364m. UV/vis (CH_2Cl_2, nm (log ε)): λ_{max} 424 (7.16), 520 (5.02), 553 (4.51), 594 (4.48), 649 (4.29) nm. ^1H NMR (400 MHz; $CDCl_3$) δ -2.78 (8 H, br s, inner NH), 1.10–1.80 (4608 H, m, *t*-butyl H and 496 H, $CH_2\underline{CH_2}CH_2N$ dendrimer-H), 2.25 (128 H, br, $\underline{CH_2}CONHCH_2$), 2.47 (256 H, br, $\underline{CH_2}CONH$-porphyrin and dendrimer-H), 3.27 (128 H, br, $\underline{CH_2}CONHCH_2CH_2CONH$), 7.2 (64 H, m, $CH_2CO\underline{NH}CH_2$), 7.60–8.20 (768 H, br, aryl H), 8.60–9.00 (448 H, br, β-pyrrolic H), 9.30–9.45 (64 H, br, $CH_2CO\underline{NH}$).

5.6 References and Notes

1. Tomalia, D. A.; Naylor, M. A.; Goddard III, W. A. *Angew. Chem., Int. Ed. Engl.* **1990**, *29*, 138-175. Tomalia, D. A. *Sci. Am.* **1995**, *272(5)*, 42-48.
2. Smith, D. K.; Diederich, F. *Chem. Eur. J.* **1998**, *4*, 1353-1361. Tomalia, D. A.; Brothers, H. M., II, In: *Biological Molecules in Nanotechnology*; IBC Library Series 1927, Southborough (MA), 1998; Chapter 10.
3. Dandliker, P. J.; Diederich, F.; Gross, M.; Knobler, C. B.; Louati, A.; Sanford, E. M., *Angew. Chem., Int. Ed. Engl.* **1994**, *33*, 1739-1742. Dandliker, P. J.; Diederich, F.; Gisselbrecht, J.-P.; C. B.; Louati, A.; Gross, M. *Angew. Chem., Int. Ed. Engl.* **1995**, *34*, 2725-2728. Dandliker, P. J.; Diederich, F.; Zingg, A.; Gisselbrecht, J.-P.; Gross, M.; Louati, A.; Sanford, E. *Helv. Chim. Acta* **1997**, *80*, 1773-1801.
4. Gorman, C. B.; Parkhurst, B. L.; Su, W. Y.; Chen, K.-Y. *J. Am. Chem. Soc.* **1997**, *119*, 1141-1142. Gorman, C. B. *Adv. Mater.* **1997**, *9*, 1117-1119.
5. Jiang, D.-L.; Aida, T. *Chem. Commun.* **1996**, 1523-1524. Jiang, D.-L.; Aida, T. *J. Mater. Sci. —Pure Appl. Chem.* **1997**, *A34*, 2047-2055.
6. Collman, J. P.; Fu, L.; Zingg, A.; Diederich, F. *Chem. Commun.* **1997**, 193-194.
7. Enomoto, M.; Aida, T. *J. Am. Chem. Soc.* **1999**, *121*, 874-875.
8. Mammen, M.; Choi, S.-K.; Whitesides, G. M. *Angew. Chem., Int. Ed. Engl.* **1998**, *37*, 2754-2794.
9. Lee, Y.C.; Lee, R.T.; Rice, K.; Ichikawa, Y.; Wong, T.-C. *Pure Appl. Chem.* **1991**, *63*, 499-506.
10. Recently, reviews on glycodendrimers have been published: Roy, R. *Curr. Opin. Struct. Biol.* **1996**, *6*, 692-702. Lindhorst, T.K. *Nachr. Chem. Tech. Lab.* **1996**, *44*, 1073-1079. Jayaraman, N.; Nepogodiev, S.A.; Stoddart, J.F. *Chem. Eur. J.* **1997**, *3*, 1193-1199.
11. Roy, R.; Zanini, D.; Meunier, S.J.; Romanowska, A. *J. Chem. Soc., Chem. Commun.* **1993**, 1869-1872. Roy, R. *Polym. News* **1996**, *21*, 226-232. Zanini, D.; Roy, R. *Bioconjugate Chem.* **1997**, *8*, 187-192. Pagé, D.; Zanini, D.; Roy, R. *Bioorg. Med. Chem.*, **1996**, *4*, 1949-1961. Zanini, D.; Roy, R. *J. Am. Chem. Soc.* **1997**, *119*, 2088-2095.
12. Ashton, P. R.; Hounsell, E. F.; Jayaraman, N.; Nilsen, T. M.; Spencer, N.; Stoddart, J. F.; Young, M. *J. Org. Chem.* **1998**, *63*, 3429-3437.
13. Aoi, K.; Itoh, K.; Okada, M. *Macromolecules* **1995**, *28*, 5391-5393.
14. Reuter, J. D.; Myc, A.; Hayes, M. M.; Gan, Z.; Roy, R.; Qin, D.; Yin, R.; Piehler, L. T.; Esfand, R.; Tomalia, D.; Baker, J. R., Jr. *Bioconjugate Chem.* **1999**, *10*, 271-278.

15. Tam, J. P. *Proc. Nat. Acad. Sci. U.S.A.* **1988**, *85*, 5409-5413. Posnett, D. N.; McGrath, H.; Tam, J. P. *J. Biol. Chem.* **1988**, *263*, 1719-1725.
16. Haensler, J.; Szoka, F. C., Jr. *Bioconjugate Chem.* **1993**, *4*, 372-379. Kukowska-Latallo, J.; Bielinska, A. U.; Johnson, J.; Spindler, R.; Tomalia, D. A.; Baker, J. R., Jr. *Proc. Natl. Acad. Sci. USA* **1996**, *93*, 4897-4902. Qin, L.; Pahud, D. R.; Ding, Y.; Bielinska, A. U.; Kukowska-Latallo, J. F.; Baker Jr., J. R.; Bromberg, J. S. *Hum. Gene Ther.* **1998**, *9*, 553-560.
17. For selected reviews see: Sorrell, T. N. *Tetrahedron* **1989**, *45*, 3-68. Kitajima, N. *Adv. Inorg. Chem.* **1992**, *39*, 1-77. Karlin, K. D.; Tyeklár, Z.; Zuberbühler A. D. In *Bioinorganic Catalysis*; Reedijk J., Ed.; Marcel Dekker: New York, 1993; pp. 261-315; Fox S.; Karlin K. D. In *Active Oxygen in Biochemistry*; Valentine, J. S.; Foote, C. S.; Greenberg, A.; Liebman, J. F., Eds.; Chapman & Hall: Glasgow, 1995; pp. 188-231.
18. Part of this work has also been described in: Klein Gebbink, B. *Ph.D. Thesis*, University of Nijmegen, Jan. 1998, Chapter 8.
19. Kitajima, N.; Fujisawa, K.; Fujimoto, C.; Moro-oka, Y.; Hashimoto, S.; Kitagawa, T.; Toriumi, K.; Tatsumi, K.; Nakamura, A. *J. Am. Chem. Soc.* **1992**, *114*, 1277-1291.
20. Magnus, K. A.; Ton-That, H.; Carpenter, J. E. *Chem. Rev.* **1994**, *94*, 727-735, and references cited therein.
21. Klein Gebbink, R. J. M.; Martens, C. F.; Feiters, M. C.; Karlin, K. D.; Nolte, R. J. M. *Chem. Commun.* **1997**, 389-390.
22. Weener, J. W.; van Dongen, J. L. J.; Hummelen, J. C.; Meijer, E. W. *Proc. ACS. PMSE.*, **1997**, *77*, 147–148. Weener, J. W.; van Dongen, J. L. J.; Meijer, E. W. *submitted to J. Am. Chem. Soc.*
23. Hummelen, J. C.; van Dongen, J. L. J.; Meijer, E. W. *Chem. Eur. J.* **1997**, *3*, 1489-1493.
24. Reduction of Cu(II) to Cu(I) is more often observed during mass analysis, see: Chapter 4, and refs 60–62 therein.
25. Karlin, K. D.; Tyeklár, Z.; Farooq, A.; Haka, M. S.; Ghosh, P. R.; Cruse, W.; Gultneh, Y.; Hayes, J. C.; Toscano, P. J.; Zubieta, J. *Inorg. Chem.* **1992**, *31*, 1436-1451.
26. S. Mahapatra, J. A. Halfen, E. C. Wilkinson, G. Pan, X. Wang, V. G. Young Jr., C. J. Cramer, L. Que, Jr, W. B. Tolman, *J. Am. Chem. Soc.* 1996, *118*, 11555-11574.
27. Pullerits, T.; Sunström, V. *Acc. Chem. Res.* **1996**, *29*, 381-389. van Grondelle, R.; Monshouwer, R.; Valkunas, L. *Pure Appl. Chem.* **1997**, *6*, 1211-1218.
28. McDermott, G.; Prince, S. M.; Freer, A. A.; Hawthornthwaite-Lawless, A. M.; Papiz, M. Z.; Cogdell, R. J.; Isaacs, N. W. *Nature* **1995**, *374*, 517-521.
29. For some selected reviews on synthetic multi chromophoric systems see: Wasielewski, M. R. *Chem. Rev.* **1992**, *92*, 435-461. Kurreck, H.; Huber, M. *Angew. Chem., Int. Ed. Engl.* **1995**, *34*, 849-866. Chen, T.-C. In *Supramolecular Reactivity and Transport: Bioinorganic Systems*; Suslick, K. S., Ed.; Supramolecular Chemistry 5; Lehn, J.-M., Ed., Pergamon Press: Elmsford, NY, 1996; pp. 91-140. Sanders, J. K. M. In *Templating, Self-Assembly, and Self-Organization*; Sauvage, J.-P.; Hosseini, M. W., Eds.; Supramolecular Chemistry 10; Lehn, J.-M. Ed., Pergamon Press: Elmsford, NY, 1996; pp. 131-164. Harriman, A.; Sauvage, J.-P. *Chem. Soc. Rev.* **1996**, *25*, 41-48. Ward, M. D. *Chem. Soc. Rev.* **1997**, *26*, 365-375.
30. Officer, D. L.; Burrel, A. K.; Reid, D. C. W. *Chem. Commun.* **1996**, 1657-1658.
31. Norsten, T.; Branda, N. *Chem. Commun.* **1998**, 1257-1258.
32. Mongin, O.; Papamicael, C.; Hoyler, N.; Gossauer, A. *J. Org. Chem.* **1998**, *63*, 5568-5580.
33. Huck, W. T. S.; Rohrer, A.; Anilkumar, A. T.; Fokkens, R. H.; Nibbering, N. M. M.; van Veggel, F. C. J. M.; Reinhoudt, D. N. *New J. Chem.* **1998**, 165-168.
34. Mak, C. C.; Bampos, N.; Sanders, J. K. M. *Angew. Chem., Int. Ed. Engl.* **1998**, *37*, 3020-3023.
35. Hunter, C. A.; Sarson, L. D.; *Angew. Chem., Int. Ed. Engl.* **1994**, *33*, 2313-2316. Anderson, S.; Anderson, H. L.; Bashall, A.; McPartlin, M.; Sanders, J. K. M. *Angew. Chem., Int. Ed. Engl.* **1995**, *34*, 1096-1099. Burrel, A. K.; Officer, D. L.; Reid, D. C. W.; Wild, K. Y. *Angew. Chem., Int. Ed. Engl.* **1998**, *37*, 114-117.
36. Crossley, M. J.; Hambley, T. W.; Mackay, L. G.; Try, A. C.; Walton, R. *J. Chem. Soc., Chem. Commun.* **1995**, 1077-1079.
37. Crossley, M. J.; Try, A. C.; Walton, R. *Tetrahedron* **1996**, *37*, 6807-6810.
38. Stevelmans, S.; van Hest, J. C. M.; Jansen, J. F. G. A.; van Boxtel, D. A. F. J.; de Brabander-van den Berg, E. M. M.; Meijer, E. W. *J. Am. Chem. Soc.* **1996**, *118*, 7398-7399.

39. Bosman, A. W.; Janssen, R. A. J.; Meijer, E. W. *Macromolecules* **1997**, *30*, 3606-3611.
40. Bosman, A. W.; Bruining, M. J.; Kooijman, H.; Spek, A. L.; Janssen, R. A. J.; Meijer, E. W. *J. Am. Chem. Soc.* **1998**, *120*, 8547-8548.
41. Fenyo, D.; Chait, B. T.; Johnson, T. E.; Lindsey, J. S. *J. Porphyrins Phthalocyanines* **1997**, *1*, 93-99.
42. Brown, R. S.; Carr, B. L.; Lennon, J. J. *J. Am. Soc. Mass. Spectrom.* **1996**, *7*, 225-232.
43. Full width at half-height of the maximum absorbance of the Soret band.
44. Kasha, M.; Rawls, H. R.; Ashraf El-Bayoumi, M. *Pure Appl. Chem.* **1965**, *11*, 371.
45. The anisotropy is defined as: $r(t) = (I_{//} - I_{\perp})/(I_{//} + 2I_{\perp})$, see also ref. 51.
46. Zeng, F.; Zimmerman, S. C. *Chem. Rev.* **1997**, *97*, 1681-1712, and references cited therein.
47. Kubas, G. J. *Inorg. Synth.* **1979**, *19*, 90.
48. Schenning, A. P. H. J.; Hubert, D. H. W.; Feiters, M. C.; Nolte, R. J. M. *Langmuir* **1996**, *12*, 1572-1577.
49. Baldwin, J. E.; Crossley, M. J.; DeBernardis, J.; *Tetrahedron*, **1981**, *38*, 685-692.
50. Brockman, H.; Schrodder, H. *Ber.* **1941**, *74B*, 73-78.
51. Ghiggino, K.P.; Smith, T. A. *Prog. Reac Kin.* **1993**, *19*, 375-436. Ghiggino, K.P.; Yeow, E.; Haines, D. J.; Scholes , G. D.; Smith, T. A. *J. Photochem. Photobiol. A: Chem.* **1996**, *102*, 81-86.

Summary

Dendrimers are highly branched macromolecules with a tree-like structure. As a consequence these molecules posses a large number of end groups (Figure 1). Moreover, the typical dendrimer-architecture forces the termini to be close together. The combination of these aberrant features and the high chemical definition of dendrimers has attracted the interest from many different disciplines of science. In this thesis the modification of poly(propylene imine) dendrimers with different functionalities is described, making use the unique features of the dendritic framework.

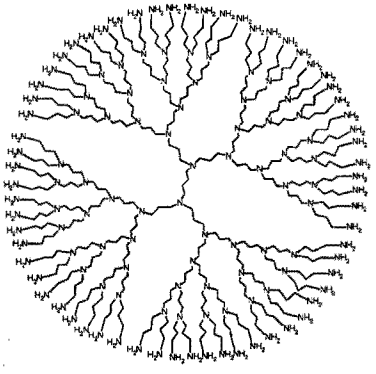

Figure 1: *Fifth generation poly(propylene imine) dendrimer (DAB-dendr-$(NH_2)_{64}$).*

Covering the flexible dendrimer with a dense shell makes it possible to physically entrap guest molecules in a dendrimer ("dendritic box"). This encapsulation procedure often leads to altered characteristics of the guests as a result of the typical micro-environment within the dendrimer. In this way molecules can be forced to be in close contact as shown for radical anions of tetracyanoquinodimethane ($TCNQ^{\bullet-}$). Or molecules can be prevented from self-aggregation, illustrated by the encapsulation of isolated photosensitizer dyes (pheophorbide a). The entrapped dye remains it ability to produce singlet oxygen, opening the way to use this system in photodynamical therapy (PDT) of cancer.

In addition, the structure of the shell has been modified to obtain a more flexible system. IR and NMR spectroscopy studies in solution and X-ray diffraction data indicate that the presence of hydrogen bonds between the end groups is of utmost

importance for the solid state character of the shell. EPR spectroscopy performed on dendrimers functionalized with pendant stable nitroxyl radicals subscribes the presence of a H-bonded network at the periphery of the molecule. The EPR data show that the flexibility of nitroxyl functionalized dendrimers is related to both temperature and nature of the solvent.

The end groups in poly(propylene imine) dendrimers consist of a dipropylenetriamine (dpt) unit capable of binding transition metal ions like Cu(II), Ni(II), and Zn(II) in a tridentate way. UV/vis, EPR, NMR spectroscopy, X-ray crystallography, and electrospray mass spectrometry, confirm this site specific metal inclusion in the poly(propylene imine) dendrimers. Consequently, the dendrimers are used as nano-scaffolds for several metal-ions. The highest (fifth) generation dendrimer binds up to 32 metal-ions, and has nanometer dimensions. This makes it possible to use membrane-filtration to isolate the metallodendrimers from solution. The versatility of this size selective recovery of metal containing species has been illustrated by using the poly(propylene imine) dendrimers for continuous metal extraction, sensor-applications and catalysis.

Finally, functionalized poly(propylene imine) dendrimers have been investigated on their propensity to mimic the multivalency present in many biological systems using the highly branched architecture of the dendrimers. The first example consists of a Cu(I)-modified dendrimer which is able to bind multiple molecules of dioxygen. Therefore, this multivalent dioxygen complex may be seen as a model for oxygen binding by hemocyanine assemblies, the oxygen-carriers in molluscs and arthropods. In the second example, the poly(propylene imine) dendrimers are used as scaffold to assemble multiple porphyrins, both in a covalent and noncovalent way. The covalent assemblies show intramolecular electronic interactions between the porphyrin end groups in the excited state, thereby mimicking the light harvesting of the natural LH2 system, which is responsible for capturing and storing light-energy in photosynthetic bacteria.

Samenvatting

Dendrimeren zijn sterk vertakte macromoleculen met een boomvormige struktuur (Figuur 1). Deze kenmerkende architectuur heeft tot gevolg dat dendrimeren veel eindgroepen bevatten die bovendien gedwongen worden om dicht bij elkaar te zitten. Samen met de hoge graad van chemische definitie, hebben deze eigenschappen er toe geleid dat dendrimeren de aandacht hebben getrokken van een breed scala aan wetenschappers. In dit proefschrift wordt de modificatie van poly(propylene imine) dendrimeren met verschillende functionaliteiten beschreven. In al deze modificaties is gebruik gemaakt van de typische kenmerken van het dendrimeer.

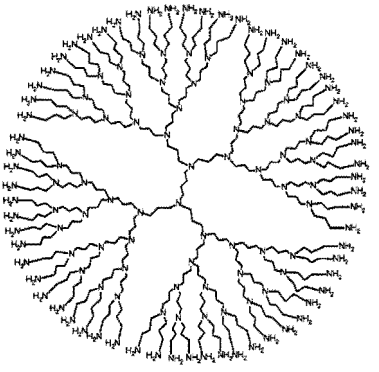

Figuur 1: *Een vijfde generatie poly(propylene imine) dendrimeer (DAB-dendr-$(NH_2)_{64}$).*

Door de buitenkant van de flexibele poly(propylene imine) dendrimeren te bedekken met een dicht gepakte schil is het mogelijk om gast moleculen fysisch op te sluiten in een dendrimeer ("het dendrimere doosje"). Deze opsluiting leidt vaak tot veranderingen in de eigenschappen van de gasten als gevolg van de micro-omgeving opgelegd door het dendrimeer. Op deze wijze is het mogelijk om moleculen te dwingen dicht bij elkaar te zitten, zoals aangetoond voor de radicaal-anionen van tetracyanoquinodimethaan ($TCNQ^{\bullet-}$). Ook kunnen moleculen van elkaar geïsoleerd worden, zodat er geen zelf-aggregatie meer op kan treden. Dit is geïllustreerd aan de hand van de opsluiting van de photo-sensitizer kleurstof pheophorbide a. De opgesloten kleurstof blijft zijn vermogen behouden om singlet-zuurstof te produceren, wat perspectieven biedt om dit systeem te gebruiken in de fotodynamische therapie (PDT) van kanker.

Ten einde een flexibeler systeem te verkrijgen, is de schil van het dendrimere doosje vervolgens opgebouwd met een kleinere eindgroep. Uit spectroscopische gegevens gemeten in oplossing (IR en NMR) en kristallografische informatie, blijkt dat de aanwezigheid van waterstof bruggen tussen de eindgroepen in een dendrimeer uitermate belangrijk is voor het vaste stof karakter van de dendrimere schil. Electron spin resonantie (ESR) spectroscopie metingen aan dendrimeren gefunctionaliseerd met stabiele nitroxide-radicalen als eind groep, bevestigen de aanwezigheid van een netwerk van H-bruggen in de periferie van het molecuul. Deze ESR-metingen laten zien dat de flexibiliteit van nitroxide-gefunktionaliseerde dendrimeren afhangt van zowel temperatuur als oplosmiddel.

De termini van de poly(propylene imine) dendrimeren bestaan uit een dipropyleen-triamine (dpt) eenheid, welke in staat is om de tweewaardige overgangsmetaalionen van koper, nikkel en zink tridentaat te binden. Deze specifieke metaalbinding door de dendrimere eindgroepen is aangetoond met UV/vis-, ESR- en NMR-spectroscopie, röntgenkristallografie en electrospray ionisatie massa-spectrometrie. De hoogste (vijfde) generatie poly(propylene imine) dendrimeer is in staat om 32 metaalionen te binden en heeft nanometer dimensies. Deze grootte maakt het mogelijk om membraan technieken te gebruiken voor de isolatie van de metallodendrimeren uit oplossing. De toepasbaarheid van deze scheiding op grootte is toegelicht aan de hand van het gebruik van poly(propylene imine) dendrimeren in continue metaalextractie, azide-meting en katalyse.

Tenslotte zijn gefunktionaliseerde poly(propylene imine) dendrimeren onderzocht op hun vermogen om de multivalentie na te bootsen zoals deze aanwezig is in vele biologische systemen. In de eerste benadering is een Cu(I)-bevattend dendrimeer gebruikt dat in staat is om meerdere moleculen zuurstof te binden. Deze complexen kunnen beschouwd worden als model voor de hemocyanine-assemblages die aanwezig zijn in weekdieren en geleedpotigen en daar het zuurstoftransport verzorgen. In de tweede benadering zijn de poly(propylene imine) dendrimeren gebruikt als verzamelpunt voor meerdere porfyrines. Deze multi-porfyrine assemblages zijn zowel op covalente als niet covalente wijze verkregen. De covalent gebonden strukturen vertonen intramoleculaire elektronische interakties tussen de geëxciteerde porfyrine-eindgroepen. Dit is vergelijkbaar met het verzamelen van lichtenergie in de natuur door het LH2-systeem dat de opname en opslag van lichtenergie reguleert in fotosynthetische bacteriën.

Curriculum Vitae

Tonny Bosman werd geboren op 25 augustus 1970 te Nijmegen. Na een VWO-opleiding aan het Dominicus College te Nijmegen werd in 1988 een aanvang genomen met de studie Scheikunde aan de Katholieke Universiteit Nijmegen, alwaar in 1989 het propadeutisch examen behaald werd. Het doctoraal examen werd in augustus 1994 afgesloten met als hoofdvak Fysisch Organische Chemie (Prof. Dr. R. J. M. Nolte) en als bijvak Polymeerchemie (Prof. Dr. E. W. Meijer, TU Eindhoven). Vanaf december 1994 tot januari 1999 was de schrijver in dienst van de Nederlands Organisatie voor Wetenschappelijk Onderzoek. Gedurende deze periode werkte hij bij de vakgroep Macromoleculaire en Organische Chemie van de Technische Universiteit Eindhoven onder leiding van Prof. Dr. E. W. Meijer en Dr. R. A. J. Janssen aan het in dit proefschrift beschreven onderzoek.

Tonny Bosman was born in Nijmegen, The Netherlands, on August 25th, 1970. In 1988 he obtained his high school degree at the "Dominicus College" in Nijmegen, the Netherlands. He continued with the study of Chemistry at the University of Nijmegen that same year, and graduated in August 1994. His major was "Physical Organic Chemistry" (Prof. Dr. R. J. M. Nolte) and his minor was "Polymer Chemistry" (Prof. Dr. E. W. Meijer, Eindhoven University of Technology, The Netherlands). The author of this thesis has been working for the Dutch Foundation for Scientific Research from December 1994 till January 1999. During this period he worked in the group of "Macromolecular and Organic Chemistry" of the Eindhoven University of Technology under the guidance of Prof. Dr. E. W. Meijer and Dr. R. A. J. Janssen. This thesis discusses the results of the investigations.

List of Publications

Van Nostrum, C. F.; Bosman, A. W.; Gelinck, G. H.; Picken, S. J.; Schouten, P. G.; Warman, J. M.; Schouten, A. J.; Nolte, R. J. M.: Evidence of a Chiral Superstructure in the Discotic Mesophase of an Optically-Active Phthalocyanine, *J. Chem. Soc. Chem. Commun.* **1993**, 1120-1122.

Van Nostrum, C. F.; Bosman, A. W.; Gelinck, G. H.; Schouten, P. G.; Warman, J. M.; Kentgens, A. P. M.; Devillers, M. A. C.; Meijerink, A.; Picken, S. J.; Sohling, U.; Schouten, A.-J.; Nolte R. J. M.: Supramolecular Structure, Physical Properties, and Langmuir-Blodgett Film Formation of an Optically Active Liquid-Crystalline Phthalocyanine, *Chem. Eur. J.* **1995**, ***1***, 171-182.

Bosman, A. W.; Jansen, J. F. G. A.; Janssen, R. A. J.; Meijer E. W.: Charge Transfer in the Dendritic Box, *Polym. Mater. Sci. Eng.* **1995**, *73*, 340-341.

Servens, E.; Löwik, D.; Bosman, A. W.; Nelissen, L.; Lemstra P. J.: Synthesis and Characterization of Poly[(2,6-dimethyl-1,4-phenylene oxide)-*block*-isoprene] Diblock Copolymers, *Macromol. Chem. Phys.* **1997**, *198*, 379-389.

Bosman, A. W.; Janssen, R. A. J.; Meijer, E. W.: Five Generations of Nitroxyl-Functionalized Dendrimers, *Macromolecules* **1997**, *30*, 3606-3611.

Bosman, A. W.; Schenning, A. P. H. J.; Janssen, R. A. J.; Meijer, E. W.: Well-Defined Metallodendrimers by Site-Specific Complexation, *Chem. Ber. / Receuil* **1997**, *130*, 725-728.

Bosman, A. W.; Schenning, A. P. H. J.; Janssen, R. A. J.; Meijer, E. W.: Probing the Structure and Dynamics of End-Group Functionalized Poly(propylene imine) Dendrimers, *Polym. Mater. Sci. Eng.* **1997**, *77*, 149-150.

Reek, J. N. H.; Schenning, A. P. H. J.; Bosman, A. W.; Meijer, E. W.; Crossley, M. J.: Templated Assembly of a Molecular Capsule, *Chem. Commun.* **1998**, 11-12.

Bosman, A. W.; Bruining, M. J.; Kooijman, H.; Spek, A. L.; Janssen, R. A. J.; Meijer, E. W.: Concerning the Localization of End Groups in Dendrimers, *J. Am. Chem. Soc. 1998*, ***120***, 8547-8584.

Klein Gebbink, R. J. M.; Bosman, A. W.; Feiters, M. C.; Meijer, E. W.; Nolte, R. J. M.: A Multi-O_2 Complex Derived from a Copper(I) Dendrimer, *Chem. Eur. J.* **1999**, *5*, 65-69.

Bosman, A. W.; Janssen, H. M.; Meijer, E. W.: About Dendrimers, *Chem. Rev.*, **1999**, *99, accepted.*

Dankwoord

Het belangrijkste van dit proefschrift, het dankwoord, heb ik tot het laatst bewaard. Wat is er immers mooier dan een promotie onderzoek af te sluiten met iedereen te bedanken die het mij mogelijk gemaakt heeft om dit verhaal op te schrijven.

De vrijheid die ik gekregen heb van mijn promotor Bert Meijer en co-promotor René Janssen is uitzonderlijk, en daarvoor ben ik jullie beiden ook zeer dankbaar. Bert, niet alleen heb jij mij veel nieuwe wetenschappelijke inzichten gegeven, maar zeker ook heb ik veel geleerd van jouw vermogen om mensen op allerlei wijzen te stimuleren. René, jouw uitgesproken kijk op vele zaken heeft mij altijd kunnen boeien. Het is echter denk ik niet voor niks dat Ajax en Anomientje allitereren.

Mijn eerste schreden op het onderzoekspad in Eindhoven zijn gedaan in het bijzijn van Emmanuelle Servense, Dennis Löwik, Jan van Hest en Johan Jansen. Jullie hebben er voor gezorgd dat ik dit pad ben blijven volgen. Een bijzonder belangrijk deel van het onderzoek beschreven in dit proefschrift is gebeurd in samenwerking met oud-Nijmegenaren afkomstig van Praktikumzaal VII, Albert (Hoofdstuk 4 en 5), Bert (Hoofdstuk 5) en Joost (Hoofdstuk 5), het is denk ik sprekend voor onze samenwerking dat de meeste ideeën ontstonden onder het genot van menig biertje. Henk Janssen wil ik bedanken voor zijn bijdrage aan "De Moeder" (Hoofdstuk 1), ik heb veel geleerd van jouw verhaalkunsten. Het is mooi dat we samen Meijel op wereldkaart hebben kunnen zetten.

Eén van de meest boeiende kanten van promoveren is het begeleiden van studenten. Monique, het is geweldig dat je het hebt aangedurfd om bij mij af te studeren, ik kan alleen maar hopen dat je net zo veel geleerd hebt van mij als ik van jou. Researchstagiaires Jan de Boer, Jeroen van Gestel en Ronald Ligthart ben ik zeer erkentelijk voor hun enthousiaste inzet. Mijn dank gaat ook uit naar de leden van de Dendrimeren-lunch. Rob, Cristina, Maurice, Jan Willem (wie kent hem niet), Kees, Jørn, Anil, AKB, Jef en Marcel, gelukkig hebben we regelmatig stevig van gedachten kunnen wisselen. Mijn kamergenoten waarmee ik door al die jaren heb samen geleefd, wil ik hier graag bedanken. Felix, Luc, en stiekem ook Brigitte, jullie hebben er voor gezorgd dat geen dag van mijn promotie hetzelfde was. Luc, ik hoop dat jij en Emiel snel een goede opvolger voor het, o zo succesvolle, SMO promoteam vinden. Speciale dank gaat uit naar Hanneke Veldhoen, Ingrid van de Boomen, Joost van Dongen, Henk

Eding, Hans Damen en Hanny van de Lee, jullie zijn de pilaren waarop deze vakgroep gebouwd is. Hanny, niet alleen heb jij fijn al die jaren mijn bureau opgeruimd, maar bovendien was jij één van de weinigen die mijn muzieksmaak kon waarderen. Joost, jou wil ik vooral bedanken omdat jij mij kennis hebt laten maken met de wereld die DIP heet. Alle (oud) leden van de vakgroep Macromoleculaire en Organische Chemie, helaas te veel om op te noemen, wil ik bedanken voor de gezelligheid binnen en buiten het lab. Ik zal jullie voortaan niet meer vervelen met mijn vele interpretaties van het Nederlandse Lied.

De dendrimeren-club van DSM, met name Ellen de Brabander, Manon Muré-Mak ("De Moeder aller Astramolen"), Peer Froehling en Remko Vreekamp, ben ik erkentelijk voor de vele grammen (kilo's ?) poly(propylene imine) dendrimeren.

I am gratefull to Dr. H. Räder (MPI-Mainz), Dr. S. Berkenkamp (Westfälische Wilhems-universität, Münster) and R. Fokkens (UvA), for performing several MALDI-TOF experiments. Prof. B. Röder und Steffen Hackbarth von der Humboldt Universität in Berlin, möchte ich gern danken für die Zusammenarbeit in dem Pheophorbide a Project. De prachtige kristalstructuren in Hoofdstuk 2 en 4 zijn opgelost door Dr. Huub Kooijman (RUU), hiervoor mijn dank. Prof. Jos Keurentjes van de vakgroep SPD ben ik erkentelijk voor het idee en gebruik van de kunstnier. In addition, I would like to acknowledge Prof. Max Crossley (University of Sydney), Prof. Ken Ghiggino, and Edwin Yeow (University of Melbourne) for the collaboration in the LH2-project.

De nodige relativering en ontspanning heb ik gevonden bij mijn vrienden, die mij gelukkig altijd in staat stelden om het doen van wetenschappelijk onderzoek in het juiste perspectief te zetten tijdens menig zeilweekend, squash-meeting, of stap-avond. Helaas waren de omstanders niet altijd even gecharmeerd van mijn retorica.

Mijn ouders hebben mij in staat gesteld om te studeren en mij altijd gesteund in mijn beslissingen, jullie hebben mij mede gemaakt tot wat ik ben. Mijn zus(je) wil ik bedanken voor de vele gezellige momenten, ik kan mij geen betere paranimf wensen.

Anke, jij was er altijd voor mij en bleef ook bij mij zelfs als ik in het weekend weer even een paar uurtjes naar het lab moest. Voor jou is geen bos rode rozen groot genoeg.

Vonnie

STELLINGEN

behorende bij het proefschrift

Dendrimers in Action

door

Anton W. Bosman

1. De vorm-selectiviteit waargenomen in de binding van amine-liganden door dendrimere metalloporfyrines heeft niets te maken met een 'dendrimeer-effekt', maar alles met het substitutiepatroon van het porfyrine.

   Bhyrappa, P.; Vaijayanthimala, G.; Suslick, K. S. *J. Am. Chem. Soc.* **1999**, *121*, 262.

2. De noodzakelijkheid van ozonolyse om holle nanobollen gebaseerd op een micel met een vernette schil te verkrijgen, maakt het vrijwel onmogelijk om deze strukturen te gebruiken voor de opsluiting van biologische actieve stoffen.

   Huang, H.; Remsen, E. E.; Kowalewski, T.; Wooley, K. L. *J. Am. Chem. Soc.* **1999**, *121*, 3805.

3. Het is opmerkelijk dat het bedekken van cellen met een laag van zouten zoveel aandacht krijgt, daar de basis voor de techniek meer dan 100 jaar geleden is gelegd.

   Mendelson, N. H. *Science* **1992**, *258*, 1633. Davis, S. A.; Burkett, S. L.; Mendelson, N. H.; Mann, S. *Nature* **1997**, *385*, 420. Harting, P. *Natuurk. Verh. der Koninkl. Academie* **1873**, *13*, 1.

4. Het beschrijven van dendrimere strukturen aan de hand van culinaire vergelijkingen (erwten, bloemkool, inktvis, zeester, zeeëgel en pannekoek), is niet alleen kenmerkend voor de ruime belevingswereld van onderzoekers in het dendrimeren veld, maar ook voor de vele verschijningsvormen die deze moleculen kunnen aannemen.

   Vögtle, F.; Weber, E. *Angew. Chem., Int. Ed. Engl.* **1974**, *13*, 814. Tomalia, D. A.; Durst, H. D. *Top. Curr. Chem.* **1993**, *165*, 193. Fréchet, J. M. J. *Science* **1994**, *263*, 1710. Balogh, L.; de Leuze-Jallouli, A.; Dvornic, P.; Kunugi, Y.; Blumstein, A.; Tomalia, D. A. *Macromolecules* **1999**, *32*, 1036. Bosman, A. W.; Janssen, H. M.; Meijer, E. W. *Chem. Rev.* **1999**, *99*, xxxx.

5. De ontdekkingen van de bulk commodities low-density polyethyleen (LDPE), high-density polyethyleen (HDPE), polyvinylchloride (PVC) en polyethyleen oxide (PEO) berusten op een hoge mate van serendipiteit, hetgeen aangeeft dat de beoordeling van onderzoeksprojecten op hun eventuele economische utiliteit uitermate hachelijk is.

   Swallow, J. C. In *Polythene—The Technology and Uses of Ethylene Polymers*; 2nd ed., Renfrew, A. Ed.; Iliffe and Sons: London, 1957. *Coordination Polymerization*; Chien, J. C. W., Ed.; Academic Press Inc.: New York, 1975; Chapter 1. *Degradation and Stabilization of PVC*; Owen, E. D., Ed.; Elsevier Appl. Sci. Publ.: London, 1984; Chapter 1. Myerly, R. C. *J. Chem. Ed.* **1980**, *57*, 437.

6. Regelmatig de afwas doen, kan leiden tot baanbrekende wetenschappelijke technieken en inzichten, echter het vuile vaatwerk laten staan ook.

   Pockels, A. *Nature* **1891**, *43*, 437. ibid., **1892**, *46*, 418. ibid., **1893**, *48*, 152. ibid., **1894**, *50*, 223. Maurois, A. *The Life of Sir Alexander Fleming*; Jonathan Cape Ltd.: Oxford, 1959. Hoofdstuk 2 en 4 in dit proefschrift.

7. Aangezien spermine, spermidine en putrescine (chemische motieven die voorkomen in polypropyleenimine dendrimeren) gevonden worden in bloemknoppen en humaan sperma, is het aannemelijk dat polypropyleenimine dendrimeren een vruchtbare toekomst tegemoet gaan.

   Van Leeuwenhoek, A. *Philos. Trans. R. Soc. London* **1687**, *12*, 1040. Evans, P. T.; Malmberg, R. L. *Annu. Rev. Plant Physiol. Plant Mol. Biol.* **1989**, *40*, 235.

8. In het voorgestelde belastingstelsel voor de 21e eeuw gaat de inkomstenbelasting wel omlaag, maar door de verhogingen van de BTW en energie heffingen, en het verdwijnen van de belastingen op vermogen, dividend en rente, zullen de verschillen in netto besteedbaar inkomen groter worden, ondanks invoering van de forfaitaire rendementsheffing.

   Belastingen in de 21e eeuw: een verkenning; Ministerie van Financiën: Den Haag, 1999; http://www.minfin.nl.

9. Een goede Margarita is meer dan de som der delen.

   Tequila, Cointreau, zumo de limón, hielo, sal.

10. Dat bezitters van rijbewijs B opnieuw een theorie examen moeten afleggen voor rijbewijs A, laat zien dat het CBR weinig vertrouwen heeft in de kennis van automobilisten inzake de verkeersregelgeving en dientengevolge ook in hun eigen toetsingskwaliteiten.

11. Don't solve problems that do not exist.

12. De top halen is niet genoeg, men moet ook kunnen terugkeren naar de basis.

    Mount Everest expeditie G. Mallory, 1924.

13. Soms is kunst Broodnodig.

    Gebouw Scheikundige Technologie van de Technische Universiteit Eindhoven.

14. Elvis leeft.